Multilevel Monte Carlo Approach for Estimating Reliability of Electric Distribution Systems

A. S. Nazmul Huda

Master of Science in Electrical and Electronic Engineering

Thesis submitted to the Faculty of Engineering, Computer and Mathematical Sciences in total to fulfillment of the requirements for the degree of

Doctor of Philosophy

School of Electrical and Electronic Engineering
The University of Adelaide
Australia

-September 2018-

Abstract

Most of the power outages experienced by the customers are due to the failures in the electric distribution systems. However, the ultimate goal of a distribution system is to meet customer electricity demand by maintaining a satisfactory level of reliability with less interruption frequency and duration as well as less outage costs. Quantitative evaluation of reliability is, therefore, a significant aspect of the decision-making process in planning and designing for future expansion of network or reinforcement.

Simulation approach of reliability evaluation is generally based on sequential Monte Carlo (MC) method which can consider the random nature of system components. Use of MC method for obtaining accurate estimates of the reliability can be computationally costly particularly when dealing with rare events (i.e. when high accuracy is required). This thesis proposes a simple and effective methodology for accelerating MC simulation in distribution systems reliability evaluation. The proposed method is based on a novel Multilevel Monte Carlo (MLMC) simulation approach.

MLMC approach is a variance reduction technique for MC simulation which can reduce the computational burden of the MC method dramatically while both sampling and discretisation errors are considered for converging to a controllable accuracy level. The idea of MLMC is to consider a hierarchy of computational meshes (levels) instead of using single time discretisation level in MC method. Most of the computational effort in MLMC method is transferred from the finest level to the coarsest one, leading to substantial computational saving. As the simulations are conducted using multiple approximations, therefore the less accurate estimate on the preceding coarse level can be sequentially corrected by averages of the differences of the estimations of two consecutive levels in the hierarchy. In this dissertation, we will find the answers to the following questions: can MLMC method be used for reliability evaluation? If so, how MLMC estimators for reliability evaluation are constructed? Finally, how much computational savings can we expect through MLMC method over MC method?

MLMC approach is implemented through solving the stochastic differential equations of random variables related to the reliability indices. The differential equations are solved using different discretisation schemes. In this work, the performance of two different

discretisation schemes, Euler-Maruyama and Milstein are investigated for this purpose. We use the benchmark Roy Billinton Test System as the test system. Based on the proposed MLMC method, a number of reliability studies of distribution systems have been carried out in this thesis including customer interruption frequency and duration based reliability assessment, cost/benefits estimation, reliability evaluation incorporating different time-varying factors such as weather-dependent failure rate and restoration time of components, time-varying load and cost models of supply points. The numerical results that demonstrate the computational performances of the proposed method are presented. The performances of the MLMC and MC methods are compared. The results prove that MLMC method is computationally efficient compared to those derived from standard MC method and it can retain an acceptable level of accuracy. The novel computational tool including examples presented in this thesis will help system planners and utility managers to provide useful information of reliability of distribution networks. With the help of such tool they can take necessary steps to speed up the decision-making process of reliability improvement.

Table of Contents

Statement of Originality

I certify that this work contains no material which has been accepted for the award of any other degree or diploma in my name in any university or other tertiary institution and, to the best of my knowledge and belief, contains no material previously published or written by another person, except where due reference has been made in the text. In addition, I certify that no part of this work will, in the future, be used in a submission in my name for any other degree or diploma in any university or other tertiary institution without the prior approval of The University of Adelaide and where applicable, any partner institution responsible for the joint award of this degree.

I give consent to this copy of my thesis when deposited in the University Library, being made available for loan and photocopying, subject to the provisions of the Copyright Act 1968.

The author acknowledges that copyright of published works contained within this thesis resides with the copyright holder(s) of those works.

I also give permission for the digital version of my thesis to be made available on the web, via the University's digital research repository, the Library Search and also through web search engines, unless permission has been granted by the University to restrict access for a period of time.

07.09.2018

A. S. Nazmul Huda Date

List of Publications

Journal Papers:

1. **A. S. Nazmul Huda** and Rastko Živanović (2018) Study effect of components availability on distribution system reliability through Multilevel Monte Carlo method, IEEE Transactions on Industrial informatics. Published (Early access)

2. **A. S. Nazmul Huda** and Rastko Živanović (2017) Accelerated distribution systems reliability evaluation by multilevel Monte Carlo simulation: Implementation of two discretisation schemes, IET Generation, Transmission & Distribution, 11(13), 3397-3405.

3. **A. S. Nazmul Huda** and R. Živanović (2019) An efficient method with tunable accuracy for estimating expected interruption cost of distribution systems, International Journal of Electrical Power & Energy Systems, 105, 98-109. [Elsevier]

4. **A.S.N. Huda** and Rastko Živanović (2017) Improving distribution system reliability calculation efficiency using multilevel Monte Carlo method, International Transactions on Electrical Energy Systems, 27(7), 1-12. [Wiley]

5. **A.S.N. Huda** and R. Živanović (2017) Large-scale penetration of distributed generation into distribution networks: Study objectives, review of models and computational tools, Renewable and Sustainable Energy Reviews, 76, 974-988. [Elsevier]

6. **A. S. Nazmul Huda** and Rastko Živanović (2018) Estimation of Expected Energy Not Supplied considering Time-Varying Load Models by Multilevel Monte Carlo method: Effect of different factors on computation variation, Electric Power Components and Systems. Submitted revision. [Taylor & Francis]

7. **A. S. Nazmul Huda** and R. Živanović (2018) Analysis effect of weather conditions on electric distribution system reliability evaluation through an efficient approach, Quality and Reliability Engineering International. Received feedback from reviewers. [Wiley]

Conference Papers:

1. **A. S. Nazmul Huda** and Rastko Živanović, Efficient estimation of interrupted energy with time varying load models for distribution systems planning studies, 9th Vienna International Conference on Mathematical Modelling, 21-23 February 2018, Vienna, Austria.

2. **A. S. Nazmul Huda** and Rastko Živanović, Advanced computation method for value-based distribution systems reliability evaluation, 15th Symposium on Energy Innovation, 14-16 February 2018, Graz, Austria.

3. **A. S. N. Huda** and Rastko Živanović, Multilevel Monte Carlo method applied to distribution system reliability assessment, IEEE PES PowerTech, 18-22 June 2017, Manchester, UK, pp. 1-6.

4. **A.S.N. Huda** and Rastko Živanović, Distribution system reliability assessment using sequential multilevel Monte Carlo method, IEEE PES Innovative Smart Grid Technologies- Asia (ISGT-Asia), 28-01 December 2016, Melbourne, Australia, pp. 867-872.

5. **A. S. Nazmul Huda** and Rastko Živanović, Advanced simulation method for evaluation of interrupted energy assessment rates in distribution systems, Australasian Universities Power Engineering Conference, 27-30 November 2018, Auckland. Accepted.

6. **A. S. Nazmul Huda** & Rastko Živanović (2018) An efficient method for distribution system reliability evaluation incorporating weather dependent factors, 20th IEEE International Conference on Industrial Technology, February 13-15 2019, Melbourne. Accepted.

Acknowledgements

First of all, the author would like to thank the Almighty Allah for granting him the ability to complete his PhD study.

The author wishes to acknowledge the contribution of his supervisor Dr. Rastko Živanović for his valuable, constructive supervision and continuous support throughout his research and preparation of this thesis.

Thanks are also extended to Dr. Said Al-Sarawi and Dr. Wen Soong for their suggestion and support.

Financial support provided by The University of Adelaide is gratefully acknowledged.

Finally, the author would like to express his deepest gratitude to his parents, wife, daughter, sisters and their families, all the relatives and friends for their love, patience and support throughout his studies.

Chapter 1

Introduction

1.1. Background

In an electric power system, electricity is generated, transmitted and distributed to the end users through generation, transmission and distribution systems, respectively. Distribution system is the last portion which delivers electricity from the transmission system to the individual customers. A distribution system as shown in Figure 1 consists of several subsystems such as distribution substation, primary/main feeders, distribution transformers and secondary distribution circuits [1]. A primary feeder begins with a circuit breaker at the distribution substation and carries electricity to the customer load points through lateral section.

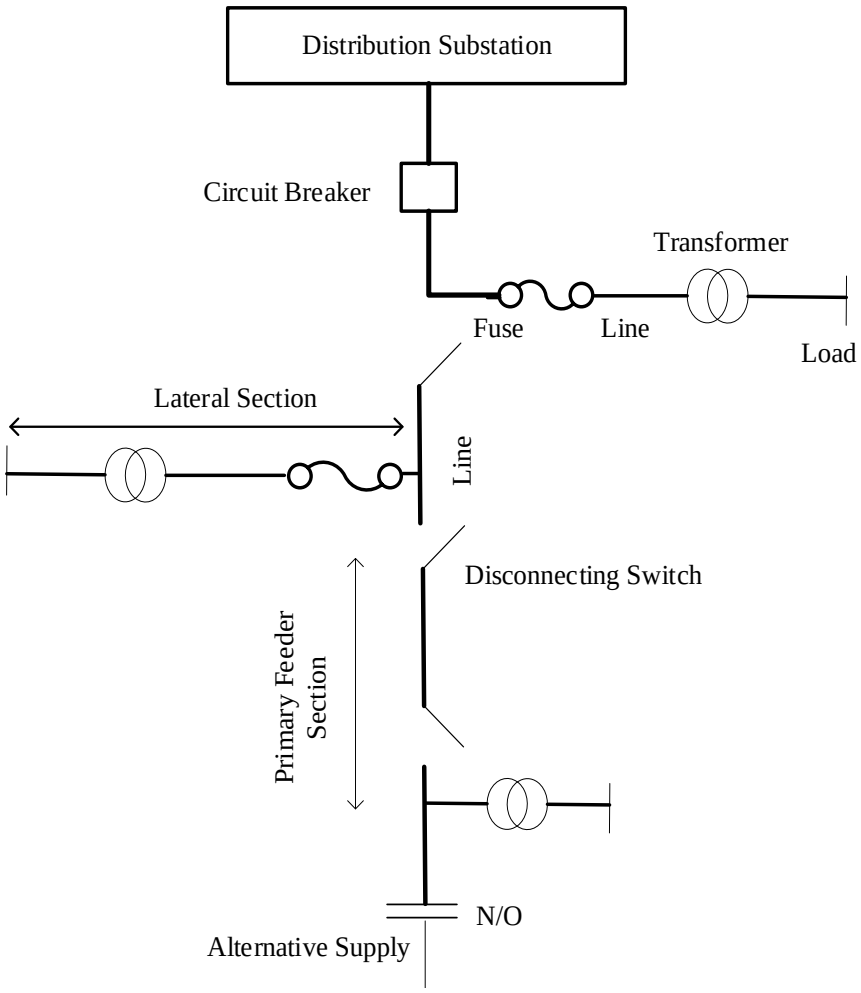

Fig. 1. Simple radial distribution system

The simplest distribution system consists of several primary feeders while each customer connected to a single feeder; this configuration is defined as radial distribution system. This type of system is very popular because of low cost and design simplicity. Since there is no feeder interconnection, a failure of any component in this system will interrupt all

downstream customers until it is cleared. There are a set of series components available between the substation and the customer load points as shown in Figure 1.

A general main section consists of disconnecting switches and a transmission line. Disconnecting switches can isolate the faulted part of the network by switching of sectionalizing equipment and supply power to the customers of unfaulty part if there is an availability of any alternative supply source, while the faulted component is being repaired. This reduces the outage duration and number of affected customers during failure. A general lateral section includes the basic components such as distribution transformer, transmission line and fuse. The availability of lateral fuse clears any fault on the lateral section or in the transformer and thus maintains the service of the primary feeder. If in any case, the fuse fails to restore the service, the circuit breaker or the back-up fuse on the primary feeder acts to isolate the faulted lateral section and the supply is then restored to the remaining system by closing the circuit breaker [2].

1.2. Distribution system reliability

The function of an electric distribution system is to deliver electricity to the customers without supply interruptions. The ability of a distribution system to fulfill the customer load requirement with continuity is usually defined as reliability. 100 percent reliable system delivers power to the customers without any interruption. Data on utility failure statistics show that distribution system failures are the causes of approximately 80 percent of the total customer interruptions which result from problems occurring between load points and distribution substations [3]. In a typical working condition, all components in a distribution system are energized. Therefore, customers are supplied power without any interruption. Scheduled and unscheduled events disrupt the regular operations and could lead to components failure and service interruption. The evaluation of reliability of a distribution system reveals the level of ability of system which depends on the components performance about how perfectly they perform their intended function. Through the evaluation, areas of high or low level of reliability can be recognized by identifying faulty equipment that degrades system reliability. The model can help to quantify the impact of design improvement options which includes [4]:

(a) New feeders and feeder expansion,
(b) Load transfer between feeders,
(c) New substation and substation expansion,
(d) New feeder tie points,

(e) Line reclosers,
(f) Sectionalizing switches,
(g) Feeder automation,
(h) Replacement of aging equipment and
(i) Replacing overhead circuits by underground cables.

In the evaluation, we measure or calculate some indices of interruption frequency and duration based on network configuration, connected components failure and restoration data and loading condition, etc. This evaluation can support a distribution system planner to access most of the required knowledge about expected frequency, duration, cost and energy loss of interruptions. The reliability measures are typically divided into measures of the impact of momentary and sustained interruptions to the supply [5]. Sustained interruption means an interruption to a distribution customer's electricity supply that has duration longer than three minutes [6]. Interruption duration is the time period starting from the initiation of interruption until supply has been provided or restored to the affected customers. The impact of a sustained interruption on customers is usually significantly more than that of a momentary interruption. Momentary interruption means an interruption to distribution customers' electricity supply with duration of three minutes or less. The impact of momentary interruptions on customers could be that their lights go off and return back on shortly. Some recommended indices for the sustained interruptions are System Average Interruption Frequency Index (SAIFI), System Average Interruption Duration Index (SAIDI) and Customer Average Interruption Duration Index (CAIDI), etc. [7] while the measures for momentary interruptions are Momentary Average Interruption Frequency Index (MAIFI) and Momentary Average Interruption Event Frequency Index (MAIFIE), etc. [6].

1.3. Reliability evaluation techniques

Two basic techniques are generally used to evaluate the reliability of a system: analytical and simulation techniques [8-10]. Analytical technique calculates only expected values of the reliability indices based on the historical data. Analytical techniques are mainly based on Failure Mode and Effect Analysis (FMEA) [11] [12], minimal path sets [13], minimal cut sets [14], Bayesian network methods [15], etc. The technique does not consider the random behavior of the reliability indices. However, the calculation of indices is based on two basic random parameters, i.e. time-to-failure and time-to-restoration and therefore the reliability indices are generally random in nature. Thus while estimating a reliability index;

it is important to consider the amount of deviation (i.e. upper and lower bounds) from an average value based on specified probability distribution for system expansion and future planning. Additionally, the need of analysis of different probabilistic factors in accurate reliability modelling is a very important task for complex modern distribution systems. Therefore, reliability analysts require the use of other technique which is accurate, efficient and can consider the random nature of reliability indices.

Monte Carlo (MC) method is the widely used simulation approach which allow the solution of mathematical and technical problems by means of system probabilistic models and simulation of random variables [16]. It is used to determine an estimate of the expected value of a parameter of interest and analyse systems whose variables follow various probability distributions such as binomial, exponential, Weibull, lognormal and gamma, etc. Therefore, it has been used for many years in different areas of science and engineering. Like other applications, MC simulation approach has been extensively used for many years in power system reliability evaluation applications [17-23]. It can be simulated in either a sequential or a non-sequential mode [24]. In the non-sequential mode, the states of all components are sampled and a non-chronological system state is obtained [25]. The sequential MCS is able to reproduce the chronological evolution of the system by sampling stochastic sequences of system states. These sequences are simulated based on the stochastic modeling of each system component failure and restoration cycles and overall system operating cycle is achieved by combining all the components cycles [25]. The sequential MC allows the consideration of the chronological matters and distributions of the reliability indices [26]. The state duration sampling approach is generally used to simulate chronological issues which can describe time-related reliability indices concerning frequency and duration of interruption [27]. The most attractive feature of MC simulation method is that the required number of samples for a target convergence criterion is not dependent on the number of number of buses in the power system [28]. However, a disadvantage of the sequential MC method is that it is very time-consuming when dealing with a highly reliable system with probabilities of very smaller occurrence. Therefore, the number of required samples increases with respect to the desired high accuracy level of the estimates and hence the practicability of this approach is decreased for a very reliable system.

In order to enhance the convergence speed of the MC method, variance reduction techniques (VRT) are generally used. Through VRT, the expected value of an output random variable can be obtained with reduced computation time by maintaining a pre-

defined level of accuracy. In power system reliability evaluation applications, various VRT have been proposed, such as control variates, antithetic variates [29] and state space pruning [30], etc. VRT based on importance sampling which are known as cross-entropy (CE) methods have been utilized extensively in power system reliability applications in order to speedup computation which are mainly carried out on the composite generation and transmission systems reliability evaluation [31-34]. CE methods were introduced [35] to estimate the rare events while sampling of abnormal states is increasingly difficult. For example, the CE method was successfully applied in generating capacity reliability problems [32] [36-38] and short-term reliability evaluation [33]. In the CE-based MC method, the state variables representing generation and transmission equipment are properly distorted according to a CE-based optimization process. Due to the optimal distortion applied to the generation model, the occurrence of failure events is more frequent and the convergence properties of the algorithm are thus greatly improved. This methodology was later used as the basis for developing more sophisticated MC based tools, such as quasi-sequential/CE [37], pseudo-chronological/CE [39], and sequential/CE [32]. In all cases, significant speed-ups were reported, especially when comparing each CE-based algorithm with its respective non-CE version [35]. However, these methods were unable to obtain probability distributions of indices. In one study, an improved importance sampling was applied to generation, transmission line and load states which reduced the required computational effort by orders of magnitude compared to previous efforts of similar nature [40]. Additionally, another VRT based on subset simulation has been successfully applied in power system reliability estimation [41] where a small failure probability is represented as the product of larger conditional probabilities.

1.4. Research gaps and objectives

From the review on the existing reliability evaluation techniques, it is seen that significant effort has been dedicated in the last few years for computationally efficient methods in the composite generation and transmission systems reliability evaluation applications. However, there has been a lack of research in the area of distribution systems reliability assessment particularly low voltage distribution systems which use computationally efficient methods when dealing with high level of accuracy i.e. very reliable systems [42-44]. However, the modernization of distribution system is a growing need within the electrical utility industry to refine the existing methods. This will save the evaluation time and help the distribution systems planners for taking fast reliability improvement actions.

The main objective of this thesis is therefore to present the computationally efficient estimation and accurate models. For this purpose, a novel Multilevel Monte Carlo (MLMC) method based reliability evaluation technique has been proposed. MLMC approach is a variance reduction technique for MC simulation which can reduce the computational burden of the MC method dramatically while both sampling and discretisation errors are considered for converging to a controllable accuracy level. Based on the proposed MLMC method, a number of reliability studies of distribution systems have been carried out in this thesis including customer interruption frequency and duration based reliability assessment, reliability cost/benefits estimation, reliability evaluation incorporating different time-varying factors such as weather-dependent failure rate and restoration time of components, time-varying load and cost models of supply points. The numerical results that demonstrate the computational performances of the proposed method are presented. The performances of the MLMC and MC methods are compared.

1.5. General overview of the thesis

This thesis contains a number of manuscripts which are submitted and accepted to internationally recognized journals. Each chapter of the thesis is presented in the form of a journal paper which is self-sufficient individually and do not need the accumulation of information from the previous chapters.

Chapter 2 presents the application of MLMC method which is implemented for reliability evaluation of a small distribution system. The Milstein path discretisation is used to approximate the numerical solution of stochastic equations. Case studies are carried to evaluate the basic system performance indices.

Chapter 3 presents a study on reliability evaluation of benchmark test distribution systems. The convergence characteristics of MLMC methods based on two discretisation schemes, i.e. Euler-Maruyama and Milstein discretisation schemes are investigated in this chapter. The Roy Billinton Test Systems are used as benchmark distribution systems.

Chapter 4 investigates the effect of basic protection components availability, failure and restoration parameters on reliability improvement. The effect of components availability on reliability indices for overall system, feeders and customer sector types are evaluated through the MLMC method. Additionally, sensitivity analyses are performed to show the impact of variation of the predefined reliability data and the MLMC parameters on computational performance.

Chapter 5 presents the MLMC based estimation results of system expected energy not supplied index by incorporating different time-varying load models. The Euler-Maruyama discretisation method is coupled with the MLMC method to develop a general framework for this estimation. The second objective is to explore the effect of various factors and criteria on computation performance such as failure starting time, failure duration, time-dependent load diversity factors, network complexity, systems reinforcement, target accuracy level and discretisation scheme. The outputs of the MLMC method are compared with the direct MCS from the accuracy and computational speed perspectives.

Chapter 6 investigates the application of MLMC method on estimating the system expected interruption cost. The performance of the proposed method is compared with the MC method in terms of computation accuracy and speed-up. The effect of different parameters on the MLMC computation method such as network configuration and load type, time-varying load and cost models, network reinforcement, transformer and line failure rate, drift and volatility values are investigated to provide insight into the variation of the interruption cost with different system factors.

Chapter 7 establishes a time sequential MLMC simulation for the reliability indices calculation of distribution systems in two different weather conditions. For modelling time-varying failure rate, weather dependent factors such as high wind speed and lightning are considered in reliability estimation. Different time-varying weight factors and a delay during adverse weather are considered in modelling of restoration time. Similarly, for load and cost modelling, different time-varying weight factors are incorporated in calculation. A comprehensive result showing the effects of different time-varying parameter models are presented while the computations are performed using MLMC method. The computation accuracy compared to the original MC method is also presented.

In terms of the improvement of reliability and efficiency, integration of distributed generation (DG) into distribution network has gained significant interest in recent years. However, existing distribution systems were not designed considering penetration of DG. **Chapter 8** reviews the required models of system components, the impacts of DG on system operation, mitigation of challenges, associated standards and regulations for the successful operation of distribution systems. The second objective is to make a summary of characteristics and features that an ideal computational tool should have to study increased DG penetration. A comparison study of two commonly used computational tools is also carried out in this paper.

References

[1] R. E. Brown, *Electric power distribution reliability*: CRC press, 2008.

[2] W. Li, *Reliability assessment of electric power systems using Monte Carlo methods*: Springer Science & Business Media, 2013.

[3] R. Billinton and J. Billinton, "Distribution system reliability indices," *IEEE Transactions on Power Delivery*, vol. 4, pp. 561-568, 1989.

[4] T. Gonen, *Electric power distribution engineering*: CRC press, 2016.

[5] T. H. Ortmeyer, J. A. Reeves, D. Hou, and P. McGrath, "Evaluation of sustained and momentary interruption impacts in reliability-based distribution system design," *IEEE Transactions on Power Delivery*, vol. 25, pp. 3133-3138, 2010.

[6] J. Nahman and D. Peric, "Distribution system performance evaluation accounting for data uncertainty," *IEEE Transactions on Power Delivery*, vol. 18, pp. 694-700, 2003.

[7] R. E. Brown and J. R. Ochoa, "Distribution system reliability: default data and model validation," *IEEE Transactions on Power Systems*, vol. 13, pp. 704-709, 1998.

[8] Y. Ou and L. Goel, "Using Monte Carlo simulation for overall distribution system reliability worth assessment," *IEE Proceedings-Generation, Transmission and Distribution*, vol. 146, pp. 535-540, 1999.

[9] R. Billinton and P. Wang, "Distribution system reliability cost/worth analysis using analytical and sequential simulation techniques," *IEEE Transactions on Power Systems*, vol. 13, pp. 1245-1250, 1998.

[10] A. Volkanovski, M. Čepin, and B. Mavko, "Application of the fault tree analysis for assessment of power system reliability," *Reliability Engineering & System Safety*, vol. 94, pp. 1116-1127, 2009.

[11] R. N. Allan, R. Billinton, I. Sjarief, L. Goel, and K. So, "A reliability test system for educational purposes-basic distribution system data and results," *IEEE Transactions on Power systems*, vol. 6, pp. 813-820, 1991.

[12] R. Billinton and P. Wang, "Reliability-network-equivalent approach to distribution-system-reliability evaluation," *IEE Proceedings-Generation, Transmission and Distribution*, vol. 145, pp. 149-153, 1998.

[13] K. Xie, J. Zhou, and R. Billinton, "Reliability evaluation algorithm for complex medium voltage electrical distribution networks based on the shortest path," *IEE Proceedings-Generation, Transmission and Distribution*, vol. 150, pp. 686-690, 2003.

[14] X. Xiang and Y. Hao, "Reliability Evaluation of Distribution Systems Based on the Minimum Cut Sets Method," *Journal of Electric Power*, vol. 21, pp. 149-153, 2006.

[15] D. C. Yu, T. C. Nguyen, and P. Haddawy, "Bayesian network model for reliability assessment of power systems," *IEEE Transactions on Power Systems*, vol. 14, pp. 426-432, 1999.

[16] C. P. Robert, *Monte carlo methods*: Wiley Online Library, 2004.

[17] Y. Ou and L. Goel, "Using Monte Carlo simulation for overall distribution system reliability worth assessment," *IEE Proceedings-Generation, Transmission and Distribution*, pp. 535-540, 1999.

[18] L. Goel and Y. Ou, "Reliability worth assessment in radial distribution systems using the Monte Carlo simulation technique," *Electric power systems research*, vol. 51, pp. 43-53, 1999.

[19] L. Goel, "Monte Carlo simulation-based reliability studies of a distribution test system," *Electric Power Systems Research*, vol. 54, pp. 55-65, 2000.

[20] R. Billinton and P. Wang, "Teaching distribution system reliability evaluation using Monte Carlo simulation," *IEEE Transactions on Power Systems*, vol. 14, pp. 397-403, 1999.

[21] Y. Hegazy, M. Salama, and A. Chikhani, "Adequacy assessment of distributed generation systems using Monte Carlo simulation," *IEEE Transactions on Power Systems*, vol. 18, pp. 48-52, 2003.

[22] R. Rocchetta, Y. Li, and E. Zio, "Risk assessment and risk-cost optimization of distributed power generation systems considering extreme weather conditions," *Reliability Engineering & System Safety*, vol. 136, pp. 47-61, 2015.

[23] L. Goel and Y. Ou, "Radial distribution system reliability worth evaluation utilizing the Monte Carlo simulation technique," *Computers & Electrical Engineering*, vol. 27, pp. 273-285, 2001.

[24] J. A. Momoh, *Electric power distribution, automation, protection, and control*: CRC press, 2007.

[25] W. Li, *Risk assessment of power systems: models, methods, and applications*: John Wiley & Sons, 2014.

[26] R. Billinton and A. Sankarakrishnan, "A comparison of Monte Carlo simulation techniques for composite power system reliability assessment," In: *IEEE Conference on Communications, Power, and Computing*, 1995, pp. 145-150.

[27] R. Billinton and W. Li, "Distribution System and Station Adequacy Assessment," in *Reliability assessment of electric power systems using Monte Carlo methods*, Springer, 1994, pp. 209-254.

[28] B. Zhaohong and W. Xifan, "Studies on variance reduction technique of Monte Carlo simulation in composite system reliability evaluation," *Electric Power Systems Research*, vol. 63, pp. 59-64, 2002.

[29] R. Billinton and A. Jonnavithula, "Composite system adequacy assessment using sequential Monte Carlo simulation with variance reduction techniques," *IEE Proceedings-Generation, Transmission and Distribution*, vol. 144, pp. 1-6, 1997.

[30] C. Singh and J. Mitra, "Composite system reliability evaluation using state space pruning," *IEEE Transactions on Power Systems*, vol. 12, pp. 471-479, 1997.

[31] K. Hou, H. Jia, X. Xu, Z. Liu, and Y. Jiang, "A continuous time Markov chain based sequential analytical approach for composite power system reliability assessment," *IEEE Transactions on Power Systems*, vol. 31, pp. 738-748, 2016.

[32] R. A. González-Fernández and A. M. L. da Silva, "Reliability assessment of time-dependent systems via sequential cross-entropy Monte Carlo simulation," *IEEE Transactions on Power Systems*, vol. 26, pp. 2381-2389, 2011.

[33] Y. Wang, C. Guo, and Q. Wu, "A cross-entropy-based three-stage sequential importance sampling for composite power system short-term reliability evaluation," *IEEE Transactions on Power Systems*, vol. 28, pp. 4254-4263, 2013.

[34] A. S. N. Huda and R. Zivanovic, "Accelerated Distribution Systems Reliability Evaluation by Multilevel Monte Carlo Simulation: Implementation of Two Discretisation Schemes," *IET Generation, Transmission & Distribution*, vol. 11, pp. 3397-3405, 2017.

[35] R. A. González-Fernández, A. M. L. da Silva, L. C. Resende, and M. T. Schilling, "Composite systems reliability evaluation based on Monte Carlo simulation and cross-entropy methods," *IEEE Transactions on Power Systems*, vol. 28, pp. 4598-4606, 2013.

[36] A. M. L. da Silva, R. A. Fernandez, and C. Singh, "Generating capacity reliability evaluation based on Monte Carlo simulation and cross-entropy methods," *IEEE Transactions on Power Systems*, vol. 25, pp. 129-137, 2010.

[37] A. M. L. da Silva, R. A. González-Fernández, W. S. Sales, and L. A. Manso, "Reliability assessment of time-dependent systems via quasi-sequential Monte Carlo simulation," In: *IEEE 11th International Conference on Probabilistic Methods Applied to Power Systems (PMAPS)*, 2010, pp. 697-702.

[38] R. González-Fernández and A. L. Da Silva, "Comparison between different cross-entropy based methods applied to generating capacity reliability," In: *IEEE 11th International Conference on Probabilistic Methods Applied to Power Systems (PMAPS)*, 2012, pp. 10-14.

[39] A. L. Da Silva, L. D. F. Manso, J. D. O. Mello, and R. Billinton, "Pseudo-chronological simulation for composite reliability analysis with time varying loads," *IEEE Transactions on Power Systems*, vol. 15, pp. 73-80, 2000.

[40] E. Tomasson and L. Söder, "Improved importance sampling for reliability evaluation of composite power systems," *IEEE Transactions on Power Systems*, vol. 32, pp. 2426-2434, 2017.

[41] B. Hua, Z. Bie, S.-K. Au, W. Li, and X. Wang, "Extracting rare failure events in composite system reliability evaluation via subset simulation," *IEEE Transactions on Power Systems*, vol. 30, pp. 753-762, 2015.

[42] G. T. Heydt and T. J. Graf, "Distribution system reliability evaluation using enhanced samples in a Monte Carlo approach," *IEEE Transactions on Power Systems*, vol. 25, pp. 2006-2008, 2010.

[43] F. Li, "A fast approach of Monte Carlo simulation based on linear contribution factors to distribution reliability indices," In: *IEEE PES Transmission and Distribution Conference and Exposition*, 2003, pp. 973-977.

[44] R. Arya, A. Tiwary, S. Choube, and L. Arya, "A smooth bootstrapping based technique for evaluating distribution system reliability indices neglecting random

interruption duration," *International Journal of Electrical Power & Energy Systems*, vol. 51, pp. 307-310, 2013.

Chapter 2

Simple Distribution System Reliability Evaluation

Statement of authorship

Title of Paper	Improving distribution system reliability calculation efficiency using multilevel Monte Carlo method
Publication Status	☑ Published ☐ Accepted for Publication ☐ Submitted for Publication ☐ Unpublished and Unsubmitted work written in manuscript style
Publication Details	A.S.N. Huda and Rastko Živanović (2017) Improving distribution system reliability calculation efficiency using multilevel Monte Carlo method, International Transactions on Electrical Energy Systems, 27(7), pp. 1-12. Link: https://onlinelibrary.wiley.com/doi/full/10.1002/etep.2333

Principal author

Name of Principal Author (Candidate)	A. S. Nazmul Huda		
Contribution to the Paper	Development of reliability evaluation model, performed simulation and numerical analysis, preparation of manuscript.		
Overall percentage (%)	80%		
Certification:	This paper reports on original research I conducted during the period of my Higher Degree by Research candidature and is not subject to any obligations or contractual agreements with a third party that would constrain its inclusion in this thesis. I am the primary author of this paper.		
Signature		Date	07.09.2018

Co-author contributions

By signing the Statement of Authorship, each author certifies that:

the candidate's stated contribution to the publication is accurate (as detailed above);

permission is granted for the candidate in include the publication in the thesis; and

the sum of all co-author contributions is equal to 100% less the candidate's stated contribution.

Name of Co-Author	Rastko Živanović		
Contribution to the Paper	Supervised for development of model, helped in data interpretation and manuscript evaluation		
Signature		Date	13.08.2018

Improving distribution system reliability calculation efficiency using multilevel Monte Carlo method

Summary- Power distribution system reliability is generally evaluated by sequential Monte Carlo simulation (MCS). To obtain a high accuracy, sequential MCS technique needs long execution time. In this paper, we show that reliability indices could be evaluated using a novel sequential multilevel Monte Carlo (MLMC) technique that improves the computational efficiency of MCS. The key idea behind the MLMC method is to use computationally cheaper low accuracy solutions of coarse grids as control variates for high accuracy solutions of fine grids. Therefore, the proposed method can construct multilevel estimators of reliability indices with lower variance. Reliability indices are modelled based on stochastic differential equations (SDE) and exponential probability distributions. The Milstein path discretisation is used to approximate the numerical solution of SDE. Case studies are carried out on a small distribution system. Numerical results are presented to demonstrate the computational cost-effectiveness of the proposed method in comparison to the sequential MCS.

Keywords—distribution system; reliability; multilevel Monte Carlo (MLMC); Milstein discretisation; computational efficiency

1. Introduction

Utility statistics show that more than 80 percent of the customer service interruptions occur due to the malfunction of distribution system components [1]. Therefore, electric utilities require improving the reliability of distribution system. Reliability assessment models of distribution systems could be useful to predict the system performance based on basic system topology and components reliability statistics. This assessment may help the system planners to develop necessary strategies [2, 3] for supplying power to the customers with the lowest possible interruptions and costs.

Methods for reliability assessment of distribution systems are generally divided into analytical and simulation categories. Analytical technique is basically based on component failure mode and effect analysis [4]. It can provide only the average values of the load point and system performance indices. This drawback of analytical approach can be overcome using the simulation approach which can provide both the average values and probability distributions of the load point and system indices. Time sequential Monte Carlo (MC) method based simulation techniques [5-14] have been extensively used in

distribution system reliability assessment. In a sequential simulation, artificial operating and restoration histories of system components are generated in chronological order using random number generators and components failure and restoration parameters. Using the operating and restoration histories of system components, the load point reliability indices and furthermore, overall system performance indices are determined. Since the calculations of the reliability indices are conducted using a large number of samples based on the desired accuracy, therefore it may require longer computation time to obtain a high accuracy.

The increased number of time-dependent random variables and system configurations complexities greatly increase the computation time of reliability assessment. The demand of reduction of computational complexity by maintaining the accuracy within an acceptable level is increasing day by day. By this way, the whole process will be faster and system planners can take necessary steps to speed up the process of reliability improvement. A lot of researches have been conducted to reduce the computation time in the planning problems [15-21]. In this study, a new variance reduction technique based on multilevel Monte Carlo (MLMC) method has been proposed to apply in distribution system reliability assessment.

The idea of MLMC method was first initiated by Heinrich [22] to improve the computational efficiency for high-dimensional parameter-dependent integrals. Then Brandt and Ilyin [23] used the method to speed up the statistical mechanical computations. The idea was later extended by Giles [24] to reduce the computational burden of estimating an expected value arising from stochastic differential equations (SDE) in mathematical finance. Since then, it has been applied in numerous areas [25-29] of solving SDE and stochastic partial differential equations (SPDE) with random variables. From these studies, the computational cost effectiveness of MLMC over MC method has been proved. In this study, we intend to apply the method in a new area which is electric distribution system to evaluate the uncertain random reliability indices.

In MC method, numerical models of reliability indices are simulated on the finest grid level. In the finest grid, simulation error is small but the computational cost of execution is very large. In MLMC method, same quantities are defined but using a geometric sequence of coarse grids, rather than only the finest grid. On a coarse grid, both the computational cost and simulation accuracy are reduced. Thus, the overall computational cost is reduced using this method. Since the method conducts the simulations on a sequence of coarse

grids, so less accurate approximation on the previous coarser grid can be sequentially corrected by evaluations on the following finer grids. Therefore, MLMC method can achieve the same accuracy as MC method. In this study, we explain how the computational cost is saved by MLMC in computing distribution system reliability indices.

In the current study, distribution system components are assumed to be represented by two-state models [30]. Time-to-failure (TTF) and time-to-repair (TTR) of a component are random variables [31] and these are simply approximations of the actual failure and repair time, respectively. Distribution system reliability is generally assessed with the useful life period of the component. The failure rate of a component is assumed as constant and exponential probability distribution is usually employed for modelling the uncertainty of TTF [32, 33]. Similarly, in this study, repair time is also assumed as constant and exponential distribution could be used for modelling TTR randomness. The MLMC method could be used in reliability evaluation by constructing the SDE based modelling of component TTF and TTR. Therefore, in the proposed method, a combination of SDE and exponential probability distributions [34, 35] based modelling of random variables is utilised for the approximation of the component's actual failure and repair time [31]. The Milstein path discretisation is used to approximate the numerical solution of SDE. Then, time sequential MLMC method is developed to determine the reliability indices.

The paper begins by discussing the basics of MC and MLMC methods. In this section, we summarise the difference between the two methods. Section 3 explains the methodology of reliability assessment based on the proposed method. Section 4 represents the case studies and associated simulation results to demonstrate the capability of MLMC method in distribution system reliability evaluation. Case studies are carried out on a simple distribution system to evaluate three basic system performance indices: system average interruption frequency index (SAIFI), system average interruption duration index (SAIDI) and customer average interruption duration index (CAIDI).

2. Detailed explanation of MC and MLMC methods

2.1. MC method

In this section, we will discuss the estimation of $E[Q]$ using MC simulations. For this study, we can define Q as follows:

$$Q = \begin{cases} SAIFI, & for\ SAIFI\ calculation, \\ SAIDI, & for\ SAIDI\ calculation, \\ CAIDI, & for\ CAIDI\ calculation. \end{cases} \quad (1)$$

In MCS, $E[Q]$ is estimated by using an expected value $E[Q_a]$ of a random variable. $E[Q_a]$ can be approximated by averaging over a large number of samples on a single fine level from the distribution of Q_a [36]. If $Q_a^{(i)}$ is the *i*th sample of Q_a and N_{MC} is the number of Monte Carlo samples. Then, the MCS estimator for $E[Q_a]$ is

$$Y_{MC} = \frac{1}{N_{MC}} \sum_{i=1}^{N_{MC}} Q_a^{(i)}. \quad (2)$$

Mean square error (MSE) is used to measure the accuracy of the MC estimator and is defined as follows [27]:

$$e(Q_a^{MC})^2 = N_{MC}^{-1} V[Q_a] + [E(Q_a - Q)]^2. \quad (3)$$

The first term of the MSE in (3) is the sampling error which is represented by the variance of the MC estimator. This error is small as $V[Q_a]$ is small and decays inversely with the number of samples N_{MC}. The second term is the square of the error in the mean value between Q_a and Q, which can be reduced by using a high accuracy fine grid. To achieve a root mean square error (RMSE) of ε with the MC estimator, we need to have $N_{MC}^{-1} V[Q_a] + [E(Q_a - Q)]^2 \leq \varepsilon^2$ i.e., both of the errors should be less than $\varepsilon^2/2$ [37]. To achieve this accuracy, we require $N_{MC} = O(\varepsilon^{-2})$ samples. Here, we simply expressed the complexity of Equation (3) through the relationship between the number of Monte Carlo samples and accuracy level using big O notation. Therefore, for the Y_{MC} estimator being a sufficiently accurate approximation of $E[Q]$ with a small ε, a large number of samples need to be simulated. This results in huge computational cost.

2.2. MLMC method

In MCS, all the samples are simulated on the finest level L using a specific timestep where we just sample one approximation Q_a of Q. In MLMC method, we use several approximations of Q. We estimate the approximations on different levels ℓ using a different timestep for each level. Starting from the coarsest level $\ell = 0$ to the finest level $\ell = L$, the proposed method uses a sequence of levels $\ell = 0,1, \ldots \ldots, L$. Mathematically, the idea of MLMC can be written as follows [24]:

$$E[Q_a] = E[Q_0] + \sum_{\ell=1}^{L} E[Q_\ell - Q_{\ell-1}], \quad (4)$$

In this method, the expectation on the finest level is equal to the expectation on the coarsest level plus a sum of corrections which give the difference in expectation between the simulations using different numbers of timesteps. Each of these expectations is independently estimated by standard MCS using a different number of samples on different levels in a way where the overall variance is minimised for a fixed computational cost.

Let $\hat{Y}_0$ be an unbiased MCS estimator for $E[Q_0]$ using N_0 samples and $\hat{Y}_\ell$ for $\ell \geq 1$ be the MCS estimator for $E[Q_\ell - Q_{\ell-1}]$ using N_ℓ samples. Then we have

$$\hat{Y}_0 = \frac{1}{N_0}\sum_{i=1}^{N_0} Q_0^{(i)}, \tag{5}$$

$$\text{and } \hat{Y}_\ell = \frac{1}{N_\ell}\sum_{i=1}^{N_\ell}\left(Q_\ell^{(i)} - Q_{\ell-1}^{(i)}\right), \tag{6}$$

Using (5) and (6), the overall estimator of MLMC method for each reliability index can be expressed as follows:

$$Y_{ML} = \sum_{\ell=0}^{L} \hat{Y}_\ell. \tag{7}$$

The estimator for $E[Q_\ell - Q_{\ell-1}]$ is computed in the form of $Q_\ell^f - Q_{\ell-1}^c$, where Q_ℓ^f is a fine-path estimator using timestep size [38]

$$h_f = 2^{-\ell}T, \tag{8}$$

and $Q_{\ell-1}^c$ is the corresponding coarse-path estimator using timestep size [38]

$$h_c = 2^{-(\ell-1)}T. \tag{9}$$

In the context of SDE simulation, the coarsest level ($\ell = 0$) has just one timestep for the whole time interval [0, T]. The simulations use 2^L uniform timesteps on the finest level ($\ell = L$). Each next level has twice more timesteps than the previous one. To avoid the introduction of an undesired bias, we require that

$$E\left[Q_\ell^f\right] = E[Q_\ell^c]. \tag{10}$$

Based on the expected solution computed on the coarsest level, the expected difference from this level to the next finer level $E[Q_\ell - Q_{\ell-1}]$ is added, until the finest level L is reached. As the level ℓ increases and the grid resolution becomes finer, the required time increases, but in the meantime the required number of samples decreases. This suggests

that MLMC runs most of the iterations on the cheaper lower levels and just a few on the computationally expensive higher levels. In this way, the total computational time is significantly saved compared to MCS which spends all its effort on the computationally most expensive finest grid. Since MLMC considers the estimations on a sequence of grids so that the less accurate approximation on the coarsest grid is sequentially corrected by the estimators on the following finer grids and thereby achieves the finest grid accuracy [24]. Thus MLMC can achieve the similar estimation as MCS with less computation time.

Like MCS, MSE of the MLMC estimator also consists of two terms: variance of the combined estimator $\sum_{\ell=0}^{L} N_\ell^{-1} V_\ell$, where V_ℓ is the estimated variance and approximation error $[E(Q_a - Q)]^2$.

$$e(Q_a^{ML})^2 = \sum_{\ell=0}^{L} N_\ell^{-1} V_\ell + [E(Q_a - Q)]^2. \tag{11}$$

In order to ensure the MSE of MLMC estimator in (11) is less than ε^2, it is sufficient to confirm that both $\sum_{\ell=0}^{L} N_\ell^{-1} V_\ell$ and $[E(Q_a - Q)]^2$ are less than $\varepsilon^2/2$. The value of N_ℓ on each level ℓ ensures that the estimated variance of the combined multilevel estimator is less than $\varepsilon^2/2$. Therefore, it is essential to choose N_ℓ optimally for obtaining the optimal MLMC convergence. To make $\sum_{\ell=0}^{L} N_\ell^{-1} V_\ell \leq \varepsilon^2/2$, the optimal N_ℓ is chosen as [24]

$$N_\ell = 2\varepsilon^{-2} \sqrt{V_\ell / C_\ell} \left(\sum_{\ell=0}^{L} \sqrt{V_\ell C_\ell} \right). \tag{12}$$

where C_ℓ is the cost of an individual sample on level ℓ [24]. The test for weak convergence tries to ensure that $[E(Q_a - Q)]^2 \leq \varepsilon^2/2$. If the convergence rate of $E(Q_a - Q)$ with ℓ for some constant c_1 is measured by a positive value α [24]. Then,

$$E[Q_\ell - Q_{\ell-1}] \leq c_1 2^{-\alpha \ell}, \tag{13}$$

and the remaining error is

$$E[Q_a - Q] = E[Q_L - Q_{L-1}]/(2^\alpha - 1), \tag{14}$$

This leads to the convergence test

$$E[Q_L - Q_{L-1}]/(2^\alpha - 1) < \varepsilon/\sqrt{2}. \tag{15}$$

3. Methodology of reliability assessment using MLMC method

The overall procedure for power distribution system reliability evaluation is briefly summed up in the following steps:

(1) At first, the failure rate and repair time of each component of the distribution system are defined from historical reliability data. For a component j connected to load point i (LPi), an average failure rate (failures/year) and an average repair or switching time (hour/failure) are considered as λ_{ij} and r_{ij}. We also define some MLMC simulation parameters:

a) Number of samples for convergence tests, N;

b) Initial number of samples on each level ℓ, N_a;

c) Desired accuracy, ε;

d) Rate of change of average value of stochastic process (drift value), μ and

e) Degree of variation of stochastic process over time (volatility), σ.

(2) Next, we will construct the SDE models of TTF and TTR. Let us consider, the randomness of variable, TTF of the component j is given by the Brownian motion, W on the time interval $[0, T]$ [39]. For both TTF and TTR, drift and volatility are considered as μ and σ, respectively. Then, the SDE model of TTF with given specific μ and σ parameters and an initial time-to-failure ($S_0 = 1/\lambda_{ij}$) can be expressed as follows [40]:

$$dS_t = \mu(S_t, t)dt + \sigma(S_t, t)dW \quad 0 < t < T \tag{16}$$

where S_t is the value of component random variable, TTF at a time t. Then, the solution to this SDE can be found by using a discretisation scheme. In this paper, Milstein discretisation is used for the approximate numerical solution of SDE [41]. An approximation S of the solution of SDE is obtained by linear interpolation of $S_0, \ldots\ldots, S_m$ [42]. The Milstein discretisation with number of timesteps n ($n = 2^\ell$ and ℓ is a nonnegative integer that is called the level), timestep size $h = T/n$ and Brownian increments ΔW_m is,

$$S_{m+1} = S_m + \mu(S_m, t_m)h + \sigma(S_m, t_m)\Delta W_m + \frac{1}{2}\sigma^2(S_m, t_m)(\Delta W_m^2 - h), \tag{17}$$

where $\Delta W_m = W_{m+1} - W_m$ with $m = 0, \ldots\ldots, n-1$ and $t_m = kh$ with $k = 0, \ldots\ldots, n$. $\Delta W_1, \Delta W_2, \ldots\ldots, \Delta W_{n-1}$ are independent and normally distributed random variables.

(3) For a component of average failure rate, λ_{ij}; consider $S_{m+1} = S_{\lambda ij(m+1)}$. SDE models of a random variable, TTF are constructed on levels $\ell = 0$ and $\ell > 0$ using (8) (9) and (17). For coarse and fine levels, SDE models are defined as follows:

$$S^c_{\lambda ij(m+1)} = S^c_{\lambda ij(m)} + \mu S^c_{\lambda ij(m)} h_c + \sigma S^c_{\lambda ij(m)} dW_{c(m)} + \frac{1}{2}\sigma^2 S^c_{\lambda ij(m)} [dW_{c(m)}{}^2 - h_c], \quad (18)$$

$$S^f_{\lambda ij(m+1)} = S^f_{\lambda ij(m)} + \mu S^f_{\lambda ij(m)} h_f + \sigma S^f_{\lambda ij(m)} dW_{f(m)} + \frac{1}{2}\sigma^2 S^f_{\lambda ij(m)} [dW_{f(m)}{}^2 - h_f], \quad (19)$$

(4) The artificial operating (T_{up}) and restoration (T_{dn}) histories of each component are defined on levels $\ell = 0$ and $\ell > 0$. For each component's time-to-failure, a random number between 0 and 1 is generated using uniform distribution. The artificial operating history, T_{up} is generated by converting the uniform distribution random variable into an exponential distribution using the inverse transform method [43]. Then, for component j, T_{up} using SDE model of component's time-to-failure $S_{\lambda ij(m+1)}$ can be expressed as follows:

$$T_{upij} = -S_{\lambda ij(m+1)} \times ln(U1), \quad (20)$$

where $U1$ is a uniformly distributed random variable between [0, 1]. Likewise, following the same procedure, the SDE model of another random variable, TTR can be determined. For TTR, both the drift, μ and volatility, σ values are considered equal as TTF stochastic process. If y_{ij} is a constant for component j connected to LPi and $y_{ij} = r_{ij} \times \lambda_{ij}$, then initial time-to-repair for component j connected to LPi is y_{ij}/λ_{ij}. Therefore, like (20), T_{dn} can be expressed as follows:

$$T_{dnij} = -y_{ij} \times S_{\lambda ij(m+1)} \times ln(U2), \quad (21)$$

where $U2$ is a uniformly distributed random variable between [0, 1].

(5) Then the values of average failure rate and average unavailability of load point caused by a component are calculated on levels $\ell = 0$ and $\ell > 0$. The values of average failure rate, Λ_{ij} and average unavailability, U_{ij} for a component j connected to LPi can be calculated using the following expressions:

$$\Lambda_{ij} = \frac{N_2}{\sum_{n=1}^{N} T_{upij(n)}}, \tag{22}$$

$$U_{ij} = \frac{\sum_{n=1}^{N} T_{dnij(n)}}{\sum_{n=1}^{N} T_{upij(n)} + \sum_{n=1}^{N} {T_{dnij(n)}}/{8760}}, \tag{23}$$

where N_2 is the number of times component j failures during total simulation period and N is the desired number of simulated periods. The load points affected by each component failure are found using the method in [44]. In a similar way, the values of average failure rate and unavailability for each component in the system are determined. The values of average load point failure rate, Λ_i (failures/yr) and average unavailability, U_i (hr/yr) are determined by accumulating the individual component value connected to the relevant load point. For LPi, average failure rate, Λ_i and average unavailability, U_i could be calculated as follows:

$$\Lambda_i = \sum_{j=1}^{n_j} \Lambda_{ij}, \tag{24}$$

$$U_i = \sum_{j=1}^{n_j} U_{ij}, \tag{25}$$

where n_j is the total number of components failures that affect the service of LPi. In a similar way, the values of average failure rate and unavailability for each load point in the system are determined. In the proposed study, system performance indices SAIFI, SAIDI and CAIDI will be calculated. Based on (24) and (25), other distribution reliability indices such as ASAI, EENS and AENS could be easily calculated [45, 46].

(6) The system performance indices SAIFI, SAIDI and CAIDI are determined on levels $\ell = 0$ and $\ell > 0$. SAIFI finds the average number of sustained interruptions in the distribution system per customer during a year. The unit of this index is interruptions/system customer.year. SAIDI is designed to provide information regarding the average duration of interruption for each customer during a year. This index is measured in the unit of hours/system customer.year. CAIDI gives the average outage duration or average restoration time that any given customers would experience. It is measured in the unit of hours/customer interruption. The reliability indices can be expressed as follows:

$$SAIFI = \frac{\sum_{i=1}^{n_i} \Lambda_i N_{C_i}}{N_T}, \tag{26}$$

$$SAIDI = \frac{\sum_{i=1}^{n_i} U_i N_{C_i}}{N_T}. \quad (27)$$

$$CAIDI = \frac{\sum_{i=1}^{n_i} U_i N_{C_i}}{\sum_{i=1}^{n_i} \Lambda_i N_{C_i}}. \quad (28)$$

where N_{C_i} is the number of customers at LPi; N_T is the total number of customers served and n_i is the number of load points in the distribution system. The sum of system performance indices values on levels $\ell = 0$ and $\ell > 0$ is calculated using (7). The whole process starting from step (2) is repeated until the number of samples is reached to *N*.

(7) After estimating the values of system performance indices on levels $\ell = 0$ and $\ell > 0$, the overall MLMC estimator for each of the reliability indices is determined in order to achieve the target accuracy. Initially, the minimum refinement level of MLMC method is set at $L = 2$. The number of samples N_s on each level $\ell = 0, 1, 2$ is determined using an initial number of samples N_a. At the same time, the sum of indices values is updated on each level $\ell = 0, 1, 2$. Then, the absolute value of average of system performance index, $m_\ell = |E[Y_\ell]|$ and variance $V_\ell = V[Y_\ell]$ are calculated on each level ℓ.

(8) The optimal number of samples N_ℓ on each level $\ell = 0, 1, \ldots\ldots, L$ is determined based on (12). The optimal N_ℓ is compared to the already calculated number of samples N_s on that level. If the optimal N_ℓ is larger, then additional samples on each level as needed are evaluated and the value of mean and variance on each level are then updated. The aim to determine the optimal N_ℓ is to keep the variance of the estimator $\sum_{\ell=0}^{L} N_\ell^{-1} V_\ell$ less than $\varepsilon^2/2$.

(9) The weak convergence of MLMC estimator is tested using (15). This ensures that the remaining bias error is less than $\varepsilon/\sqrt{2}$. If remaining bias error is greater than $\varepsilon/\sqrt{2}$, then $L = L + 1$ is set. The whole process is repeated starting from step (7) until the target accuracy level is found.

(10) Finally, the overall multilevel estimator for each system performance index is computed.

4. Case studies and numerical results

4.1. Test system

A simple radial distribution system [47] as shown in Figure 1 is chosen for case studies. For simplicity, the feeder breaker and fuses are assumed as 100% reliable. Disconnect switches S1 and S2 are normally closed and S3 is normally open. Average switching time for switches S1, S2 and S3 are considered as 0.5, 0.5 and 1 hour, respectively. For the main feeder and lateral section lines, the interruption rates are 0.1 and 0.25 interruptions/km/yr, respectively and the average time to repair are 3 hours and 1 hour, respectively. There are 250, 100 and 50 customers at the load points LP1, LP2 and LP3, respectively. In order to investigate the effect of different components on reliability assessment performance, three cases of different configurations are considered.

1. Case A: alternate power supply is unavailable.

2. Case B: alternate supply is available.

3. Case C: both alternate power supply and lateral fuses are unavailable.

The drift and volatility values for both failure and repair processes are assumed as $\mu = 0.01$ and $\sigma = 0.4$, respectively. These values are generally determined by using a time series of TTF and TTR values [34]. These time series data are not currently available. Therefore, the values of drift and volatility are determined by adjusting based on the accuracy levels for an index calculation and kept as constant for rest of the indices calculation. Using analytical technique, the system performance indices; SAIFI, SAIDI and CAIDI can be evaluated [47] which are considered as base case results.

Variance reduction technique is a process which is used to increase the precision of the output random variable from the simulation. If the variance is high, then the precision will be less (ε will be higher) and confidence intervals for the output random variable will be increased. Similarly, if the variance is reduced, then the precision will be higher (ε will be less) and confidence intervals for the output random variable will be smaller and the simulation will be more efficient. In this study, ε=0.0001, 0.0005 and 0.001 are predefined as test accuracy to check the simulation efficiency at different accuracy levels. The methodology was implemented using MATLAB and all computations were performed using an Intel Core i7-4790 3.60-GHz processor.

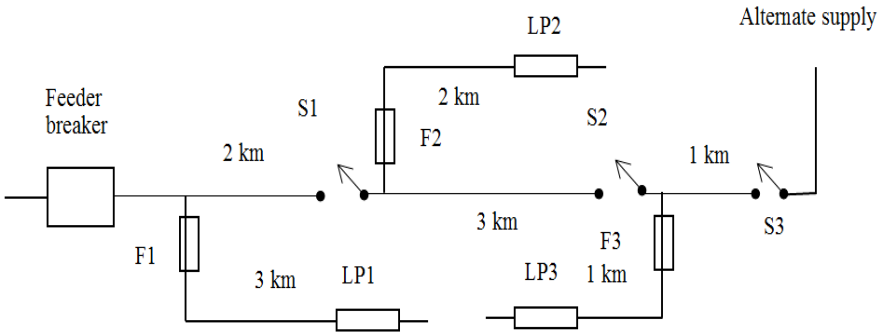

Figure 1. A simple radial distribution system

4.2. Test results

To describe the test results, comparisons among the analytical, MCS and proposed methods are conducted for three different cases. Tables I, III, and V show the accuracy levels of the sequential MCS and proposed method for cases A, B and C, respectively. Three different desired accuracies 0.0001, 0.0005 and 0.001 are set to calculate the system performance indices. DMC and DMLMC are the percentages of the absolute value of the difference of reliability indices values of sequential MCS and MLMC with respect to the base case values. From all these Tables, the results show that the differences in reliability indices values among three methods are very small. The maximum deviation of the results computed by the proposed approach is 1.69% which occurs in CAIDI calculation (ε=0.001). Such deviation is acceptable for distribution reliability evaluation which depends on uncertainty quantifications. This demonstrates the accuracy level of the proposed MLMC approach. From these three Tables, we can also find the effect of different network configurations with different components. For example, Table I and II show the effects of unavailability and availability of alternative power supply, respectively. It can be observed that the existence of the alternative supply in case B can decrease the value of SAIDI. Since the same components failures occur in cases A and B; therefore, in both cases the values of SAIFI are equal. In Table V, the effects of having no alternative supply and protective fuses are shown. Both the values of SAIFI and SAIDI increase in this case study.

The key benefit using the proposed method is to reduce the calculation time of system performance indices. Tables II, IV and VI present the calculation time of SAIFI, SAIDI and CAIDI for cases A, B and C, respectively. T_{MC} and T_{MLMC} are the calculation time in second (s), used by the MCS and MLMC methods, respectively to achieve the desired accuracy. T_{SAVE} is the percentage of calculation time saving using MLMC method over

MCS simulation. From all the Tables, it is clear that the calculation time required by MCS is significantly higher than that used by MLMC to achieve the same accuracy. The maximum calculation time in case of MLMC method is 15.1176s which requires for SAIDI calculation (ε=0.0001) in case C. Where MC method requires 448.9722s in this calculation which means MLMC is about 30 times faster than MC method. In case of time saving, the maximum value of T_{SAVE} using MLMC method is 97.9548% (ε=0.001) in SAIFI calculation of case C. On average, the sequential MLMC can reduce the reliability indices calculation time about 97% compared to the sequential MCS.

Table I. System performance indices values (case A)

ε	MCS	MLMC	DMC (%)	DMLMC (%)
SAIFI (interruptions/system customer/yr)				
0.0001	1.2129	1.2289	1.3902	0.0894
0.0005	1.2137	1.2279	1.3252	0.1707
0.001	1.2142	1.2286	1.2845	0.1138
SAIDI (hr/system customer/yr)				
0.0001	1.7374	1.7592	0.1494	1.1034
0.0005	1.7382	1.7561	0.1034	0.9252
0.001	1.7389	1.7589	0.0632	1.0862
CAIDI (hr/customer interruption)				
0.0001	1.4325	1.4327	0.8802	0.8943
0.0005	1.4326	1.4295	0.8873	0.6690
0.001	1.4335	1.4318	0.9507	0.8309

Table II. Computation time of system performance indices (case A)

ε	T_{MC} (s)	T_{MLMC} (s)	T_{SAVE} (%)
SAIFI			
0.0001	99.1410	2.2967	97.6844
0.0005	4.2883	0.1044	97.5654
0.001	1.3013	0.0334	97.4333
SAIDI			
0.0001	251.3491	9.2079	96.3366
0.0005	13.1915	0.3886	97.0541
0.001	4.2746	0.0924	97.8383
CAIDI			
0.0001	223.1117	8.4964	96.1942
0.0005	12.1456	0.3908	96.7823
0.001	4.1501	0.1156	97.2145

Table III. System performance indices values (case B)

ε	MCS	MLMC	DMC (%)	DMLMC (%)
SAIFI (interruptions/system customer/yr)				
0.0001	1.2129	1.2289	1.3902	0.0894
0.0005	1.2137	1.2279	1.3252	0.1707
0.001	1.2142	1.2286	1.2845	0.1138
SAIDI (hr/system customer/yr)				
0.0001	1.5126	1.5314	0.1721	1.4172
0.0005	1.5129	1.5322	0.1920	1.4702
0.001	1.5142	1.5314	0.2781	1.4172
CAIDI (hr/customer interruption)				
0.0001	1.2471	1.2468	1.3902	1.3658
0.0005	1.2470	1.2485	1.3821	1.5040
0.001	1.2478	1.2508	1.4471	1.6910

Table IV. Computation time of system performance indices (case B)

ε	T_{MC} (s)	T_{MLMC} (s)	T_{SAVE} (%)
SAIFI			
0.0001	99.1410	2.2967	97.6834
0.0005	4.2883	0.1044	97.5654
0.001	1.3013	0.0334	97.4333
SAIDI			
0.0001	235.4711	8.7544	96.2821
0.0005	12.1403	0.3676	96.9720
0.001	4.1848	0.0961	97.7035
CAIDI			
0.0001	186.0716	7.0544	96.2087
0.0005	10.7718	0.6008	94.4224
0.001	3.3303	0.0849	97.4506

Table V. System performance indices values (case C)

ε	MCS	MLMC	DMC (%)	DMLMC (%)
SAIFI (interruptions/system customer/yr)				
0.0001	2.0792	2.1075	0.9904	0.3571
0.0005	2.08	2.1039	0.9523	0.1857
0.001	2.0813	2.1207	0.8904	0.9857
SAIDI (hr/system customer/yr)				
0.0001	2.3469	2.3743	0.1319	1.0340
0.0005	2.3482	2.3763	0.0765	1.1191
0.001	2.3474	2.3854	0.1106	1.5063
CAIDI (hr/customer interruption)				
0.0001	1.1289	1.1288	0.7946	0.7857
0.0005	1.1283	1.1335	0.7410	1.2053
0.001	1.1297	1.1276	0.8660	0.6785

Table VI. Computation time of system performance indices (case C)

ε	T_{MC} (s)	T_{MLMC} (s)	T_{SAVE} (%)
SAIFI			
0.0001	287.8317	7.1235	97.5251
0.0005	13.5947	0.3008	97.7873
0.001	4.0143	0.0821	97.9548
SAIDI			
0.0001	448.9722	15.1176	96.6328
0.0005	24.1706	0.6412	97.3471
0.001	7.4004	0.1736	97.6541
CAIDI			
0.0001	154.2683	5.9225	96.1609
0.0005	10.8705	0.2683	97.5318
0.001	3.2587	0.1035	96.8238

The required numbers of samples N_ℓ on each level ℓ of MLMC for reliability indices assessment to achieve the desired accuracies are shown in Figures 2-4. Comparisons with the number of samples in MCS convergences are also displayed in these Figures. For the desired accuracy, the N_ℓ decreases as the level ℓ increases. As the level ℓ increases from the coarsest to the finest, the computational cost of each simulation increases. For example, in Figure 2(a1) when ε = 0.0001, levels ℓ=0, 1, 2 and 3 are required in SAIFI calculation. The numbers of samples on these levels are 1286451, 6522, 1918 and 928, respectively. This means most of the simulations are performed on the cheaper coarser levels rather than the most expensive finest level. In MCS, all the simulations are performed in the most expensive finest level. The number of required samples for MCS is 11302. This is how MLMC saves the calculation time of reliability indices.

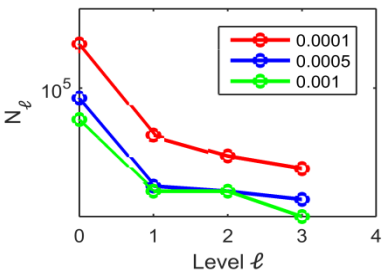

(A1) SAIFI [MLMC]

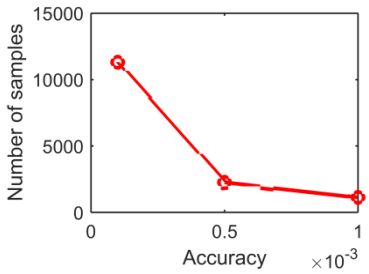

(A2) SAIFI [MC]

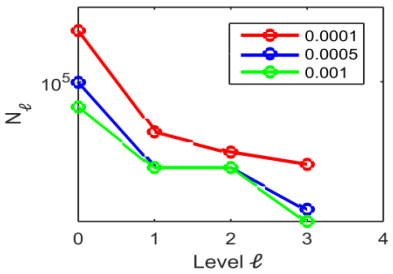

(B1) SAIDI [MLMC]

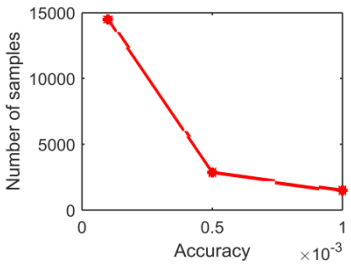

(B2) SAIDI [MC]

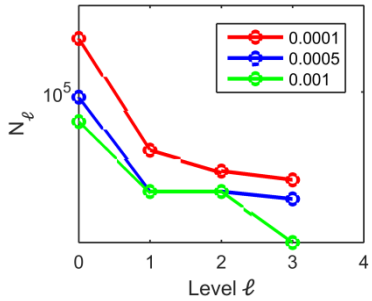

(C1) CAIDI [MLMC]

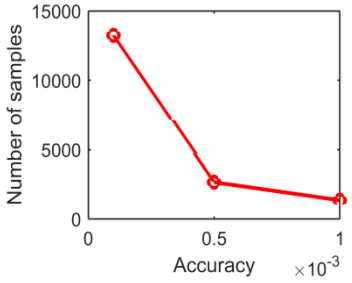

(C2) CAIDI [MC]

Figure 2. Required number of samples for convergence of MLMC and MCS (case A)

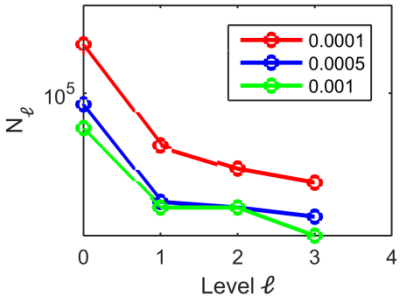

(A1) SAIFI [MLMC]

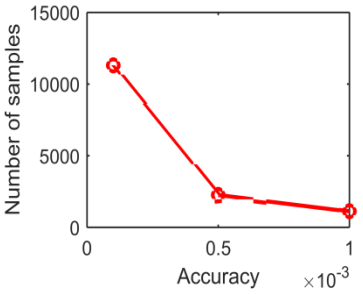

(A2) SAIFI [MC]

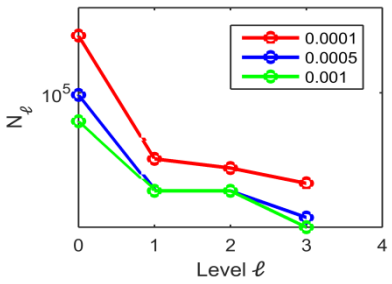

(B1) SAIDI [MLMC]

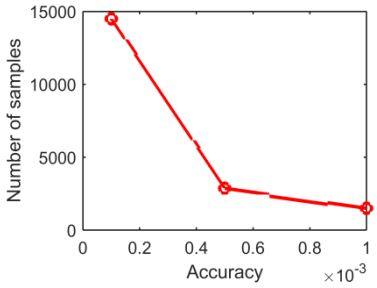

(B2) SAIDI [MC]

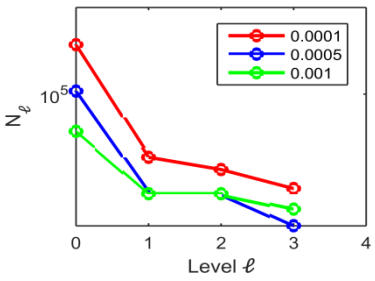

(C1) CAIDI [MLMC]

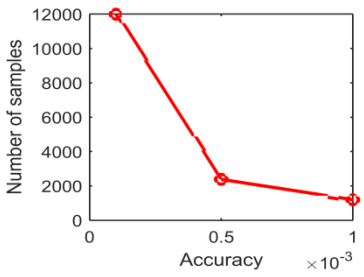

(C2) CAIDI [MC]

Figure 3. Required number of samples for convergence of MLMC and MCS (case B)

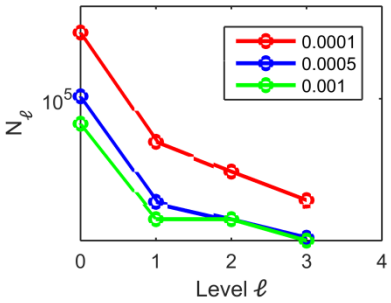

(A1) SAIFI [MLMC]

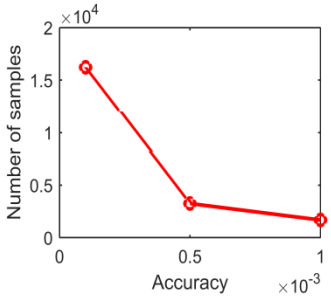

(A2) SAIFI [MC]

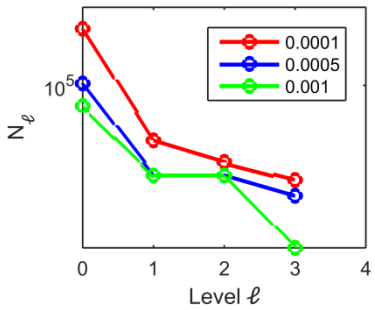

(B1) SAIDI [MLMC]

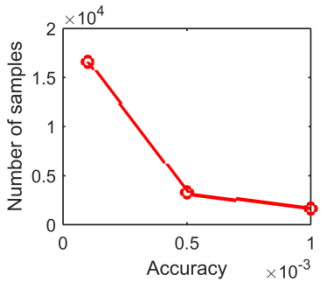

(B2) SAIDI [MC]

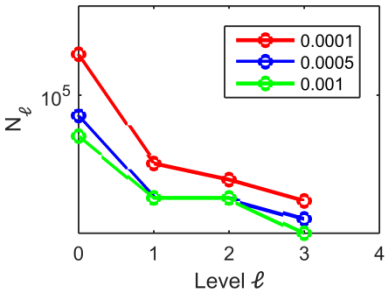

(C1) CAIDI [MLMC]

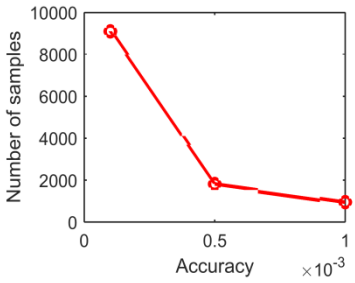

(C2) CAIDI [MC]

Figure 4. Required number of samples for convergence of MLMC and MCS (case C)

5. Conclusions

This paper illustrates the application of a new sequential multilevel Monte Carlo simulation technique using the Milstein discretisation for reliability indices calculation in radial distribution systems. The purpose of the proposed method over traditional sequential Monte Carlo technique is to reduce the reliability indices calculation time to achieve the defined accuracies. The saving in calculation time using MLMC is due to the fact that a lot of iterations are simulated on the computationally cheaper coarse discretisation grids and a few on the computationally expensive fine grids. So, the overall calculation time is reduced using MLMC method when compared to MCS which calculates the reliability indices only on the computationally most expensive finest discretisation grid. In MLMC, the calculations of reliability indices are performed on a geometric sequence of grids.

Therefore, the less accurate approximation on the coarsest grid is sequentially corrected by the estimators on the following finer grids. Thus, the finest grid accuracy is achieved by MLMC method.

Two basic random variables time-to-failure and time-to-repair of each component are modelled by jointly using stochastic differential equations and exponential probability distributions. The impacts of different system configurations with various components on three system performance indices (SAIFI, SAIDI and CAIDI) are discussed in this paper. Comparisons between the proposed approach and analytical method demonstrated the practicability of the method in a small scale distribution system. The differences in reliability indices calculated data using MLMC are within 1.5% of values using an analytical approach. In order to test the improvement in reliability indices calculation efficiency, the results of the proposed approach are compared to the MCS method. The results show that the proposed method can save the calculation time up to 97.95% compared to sequential MCS. In the future, the proposed MLMC method will be tested on the large distribution network. A method for probability distributions of these indices will be presented in the future paper.

6. List of symbols and abbreviations

λ_{ij}	An average failure rate for a component j connected to load point i (given)
r_{ij}	An average repair time for a component j connected to load point i (given)
$E[Q_a]$	An expected value of a random variable
Λ_i	Average failure rate for LPi
Λ_{ij}	Average failure rate for a component j connected to LPi (simulated)
U_{ij}	Average unavailability for a component j connected to LPi (simulated)
U_i	Average unavailability for LPi
T_{up}	Artificial operating histories
T_{dn}	Artificial restoration histories
ΔW_m	Brownian increments
W	Brownian motion
T_{MC}	Calculation time in second (s) used by MCS method
T_{MLMC}	Calculation time in second (s) used by MLMC method
CAIDI	Customer average interruption duration index
ε	Desired accuracy
μ	Drift value
$E[Q]$	Estimation of expectation
ℓ	Each grid level
L	Highest grid level
$Q_a^{(i)}$	ith sample of Q_a

N_a	Initial number of samples on each level ℓ
LPi	Load point i
MSE	Mean square error
MC	Monte Carlo
Y_{MC}	Monte Carlo estimator
MCS	Monte Carlo simulation
MLMC	Multilevel Monte Carlo
N_{C_i}	Number of customers at LPi
n_i	Number of load points in the distribution system
N_{MC}	Number of Monte Carlo samples
N	Number of samples for MLMC convergence tests
N_s	Number of samples N_s at levels $\ell = 0, 1, 2$ which are determined using N_i
N_2	Number of times component j failures during entire simulation period
DMC	Percentage of the absolute value of the difference of reliability indices values of sequential MCS with respect to the base case values
DMLMC	Percentage of the absolute value of the difference of reliability indices values of sequential MLMC with respect to the base case values
T_{SAVE}	Percentage of calculation time saving using MLMC method over MCS simulation
SAIDI	System average interruption duration index
SAIFI	System average interruption frequency index
SDE	stochastic differential equations
TTF	Time-to-failure
TTR	Time-to-repair
n_j	Total number of components fails that affect the service of LPi
N_T	Total number of customers served
Q	Random variable (system index in this study)
V_ℓ	Estimated variance
σ	Volatility value

References

1. Billinton R, Billinton JE. Distribution system reliability indices. *IEEE Transactions on Power Delivery* 1989; 4: .
2. Kavousi-Fard A, Akbari-Zadeh MR. Reliability enhancement using optimal distribution feeder reconfiguration. *Neurocomputing* 2013; 106: 1-11.
3. Park GP, Yoon YT. Application of ordinal optimization on reliability centered maintenance of distribution system. *European Transactions on Electrical Power* 2012; 22: 391-401.
4. Allan R. *Reliability evaluation of power systems*; Springer, 2013.

5. Sankarakrishnan A, Billinton R. Sequential Monte Carlo simulation for composite power system reliability analysis with time varying loads. *IEEE Transactions on Power Systems* 1995; 10: 1540-1545.

6. Billinton R, Chen H, Ghajar R. A sequential simulation technique for adequacy evaluation of generating systems including wind energy. *IEEE Transactions on Energy Conversion* 1996; 11: 728-734.

7. Billinton R, Fotuhi-Firuzabad M, Bertling L. Bibliography on the application of probability methods in power system reliability evaluation 1996-1999. *IEEE Transactions on Power Systems* 2001; 16: 595-602.

8. Wang P, Billinton R. Time sequential distribution system reliability worth analysis considering time varying load and cost models. *IEEE Transactions on Power Delivery* 1999; 14: 1046-1051.

9. Wang P, Billinton R. Reliability cost/worth assessment of distribution systems incorporating time-varying weather conditions and restoration resources. *IEEE Transactions on Power Delivery* 2002; 17: 260-265.

10. Hegazy Y, Salama M, Chikhani A. Adequacy assessment of distributed generation systems using Monte Carlo simulation. *IEEE Transactions on Power Systems* 2003; 18: 48-52.

11. Silva AM, Cassula AM, Nascimento LC, Freire Jr JC, Sacramento CE, Guimarães ACR. Chronological Monte Carlo-based assessment of distribution system reliability. *International Conference on Probabilistic Methods Applied to Power Systems*, 2006; 1-7.

12. Alvehag K, Söder L. A reliability model for distribution systems incorporating seasonal variations in severe weather. *IEEE Transactions on Power Delivery* 2011; 26: 910-919.

13. Celli G, Ghiani E, Pilo F, Soma GG. Reliability assessment in smart distribution networks. *Electric Power Systems Research* 2013; 104: 164-175.

14. Xudong W, Ling Q. Reliability evaluation for the distribution system with distributed generation. *European Transactions on Electrical Power* 2011; 21: 895-909.

15. González-Fernández RA, da Silva AML. Reliability assessment of time-dependent systems via sequential cross-entropy Monte Carlo simulation. *IEEE Transactions on Power Systems* 2011; 26:2381-2389.

16. Li F. A fast approach of Monte Carlo simulation based on linear contribution factors to distribution reliability indices. *IEEE PES Transmission and Distribution Conference and Exposition, 2003;*973-977.

17. Zhaohong B, Xifan W. Studies on variance reduction technique of Monte Carlo simulation in composite system reliability evaluation. *Electric Power Systems Research* 2002; 63: 59-64.

18. Naess A, Leira B, Batsevych O. System reliability analysis by enhanced Monte Carlo simulation. *Structural Safety 2009;*31: 349-355.

19. Hou K, Jia H, Xu X, Liu Z, Jiang Y. A continuous time Markov chain based sequential analytical approach for composite power system reliability assessment. *IEEE Transactions on Power Systems* 2016;31:738-748.

20. Oliveira GC, Pereira MV, Cunha SH. A technique for reducing computational effort in Monte-Carlo based composite reliability evaluation. *IEEE Transactions on Power Systems* 1989;4:1309-1315.

21. Miranda V, de Magalhaes Carvalho L, da Rosa MA, da Silva AML, Singh C. Improving power system reliability calculation efficiency with EPSO variants. *IEEE Transactions on Power Systems* 2009;24:1772-1779.

22. Heinrich S. Multilevel monte carlo methods. *in Large-scale scientific computing*; edn, Springer, 2001; 58-67.

23. Brandt A, Ilyin V. Multilevel Monte Carlo methods for studying large scale phenomena in fluids. *Journal of Molecular Liquids* 2003; 105: 245-248.

24. Giles MB. Multilevel monte carlo path simulation. *Operations Research* 2008; 56: 607-617.

25. Dereich S, Heidenreich F. A multilevel Monte Carlo algorithm for Lévy-driven stochastic differential equations. *Stochastic Processes and their Applications* 2011; 121: 1565-1587.

26. Kloeden PE, Neuenkirch A, Pavani R. Multilevel Monte Carlo for stochastic differential equations with additive fractional noise. *Annals of Operations Research* 2011; 189: 255-276.

27. Cliffe K, Giles MB, Scheichl R, Teckentrup AL. Multilevel Monte Carlo methods and applications to elliptic PDEs with random coefficients. *Computing and Visualization in Science* 2011; 14: 3-15.

28. Sanchez-Linares C, de la Asunción M, Castro M, Mishra S, Šukys J. Multi-level Monte Carlo finite volume method for shallow water equations with uncertain parameters applied to landslides-generated tsunamis. *Applied Mathematical Modelling* 2015; 39: 7211-7226.

29. Lu D, Zhang G, Webster C, Barbier C. Multilevel Monte Carlo method with application to uncertainty quantification in reservoir simulation, *AGU Fall Meeting Abstracts*, 2014; 3692.

30. Retterath B, Chowdhury AA, Venkata SS. Decoupled substation reliability assessment. *International Journal of Electrical Power & Energy* Systems 2005; 27: 662-668.

31. Retterath B, Venkata S, Chowdhury AA. Impact of time-varying failure rates on distribution reliability. *International Journal of Electrical Power & Energy* Systems 2005; 27: 682-688.

32. Moradkhani A, Haghifam MR, Mohammadzadeh M. Failure rate estimation of overhead electric distribution lines considering data deficiency and population variability. *International Transactions on Electrical Energy Systems* 2015; 25: 1452-1465.

33. Chowdhury A, Koval D. *Power distribution system reliability: practical methods and applications*; John Wiley & Sons: New Jersey, 2011.

34. Wang K, Crow ML. Fokker-Planck equation application to analysis of a simplified wind turbine model. *North American Power Symposium*, 2012; 1-5.

35. Zárate-Miñano R, Milano F. Construction of SDE-based wind speed models with exponentially decaying autocorrelation. *Renewable Energy* 2016; 94: 186-196.

36. Kalos MH, Whitlock PA. *Monte carlo methods*: John Wiley & Sons, 2008.

37. Elfverson D, Hellman F, Målqvist A. A multilevel Monte Carlo method for computing failure probabilities. *arXiv preprint arXiv:1408.6856*, 2014.

38. Giles M. Improved multilevel Monte Carlo convergence using the Milstein scheme. in *Monte Carlo and quasi-Monte Carlo methods 2006*; ed: Springer, 2008; 343-358.

39. Harrison JM. *Brownian motion and stochastic flow systems*; Wiley: New York, 1985.

40. Oksendal B. *Stochastic differential equations: an introduction with applications*; Springer, 2013.

41. Giles MB. Multilevel Monte Carlo for basket options. *Proceedings of the 2009 Winter Simulation Conference*, 2009; 1283-1290.

42. Kloeden PE, Platen E. Higher-order implicit strong numerical schemes for stochastic differential equations. *Journal of statistical physics* 1992; 66: 283-314.

43. Billinton R, Allan RN. *Reliability evaluation of engineering systems*; Springer, 1992.

44. Billinton R, Wang P. Teaching distribution system reliability evaluation using Monte Carlo simulation. *IEEE Transactions on Power Systems* 1999; 14: 397-403.

45. Goel L, Billinton R. Evaluation of interrupted energy assessment rates in distribution systems. *IEEE Transactions on Power Delivery* 1991; 6:1876-1882.

46. Sultana B, Sultana U, Bhatti AR. Review on reliability improvement and power loss reduction in distribution system via network reconfiguration. *Renewable and Sustainable Energy Reviews* 2016;66:297-310.

47. Billinton R, Li W. Distribution system and station adequacy assessment. in *Reliability assessment of electric power systems using Monte Carlo methods*; ed: Springer, 1994; 209-254.

Chapter 3

Comparative Reliability Study of Euler-Maruyama and Milstein Scheme Based Methods

Statement of authorship

Title of Paper	Accelerated distribution systems reliability evaluation by multilevel Monte Carlo simulation: Implementation of two discretisation schemes
Publication Status	☑ Published ☐ Accepted for Publication ☐ Submitted for Publication ☐ Unpublished and Unsubmitted work written in manuscript style
Publication Details	A. S. Nazmul Huda and Rastko Živanović (2017) Accelerated distribution systems reliability evaluation by multilevel Monte Carlo simulation: Implementation of two discretisation schemes, IET Generation, Transmission & Distribution, 11(13), 3397-3405. Link: https://ieeexplore.ieee.org/document/8063034/

Principal author

Name of Principal Author (Candidate)	A. S. Nazmul Huda		
Contribution to the Paper	Developed reliability evaluation model, performed simulation and numerical analysis, prepared manuscript.		
Overall percentage (%)	80%		
Certification:	This paper reports on original research I conducted during the period of my Higher Degree by Research candidature and is not subject to any obligations or contractual agreements with a third party that would constrain its inclusion in this thesis. I am the primary author of this paper.		
Signature		Date	07.09.2018

Co-author contributions

By signing the Statement of Authorship, each author certifies that:

the candidate's stated contribution to the publication is accurate (as detailed above);

permission is granted for the candidate in include the publication in the thesis; and

the sum of all co-author contributions is equal to 100% less the candidate's stated contribution.

Name of Co-Author	Rastko Živanović		
Contribution to the Paper	Supervised for development of model, helped in data interpretation and manuscript evaluation		
Signature		Date	13.08.2018

Accelerated distribution systems reliability evaluation by multilevel Monte Carlo simulation: Implementation of two discretisation schemes

Abstract- This article presents the performances of two discretisation schemes which are implemented in a novel multilevel Monte Carlo (MLMC) method for reliability calculation of power distribution systems. The motivation of using the proposed approach is to reduce the computational effort of standard Monte Carlo simulation (MCS) and accelerate the overall distribution system reliability evaluation process. The MLMC methods are implemented through solving the stochastic differential equations (SDE) of random variables related to the reliability indices. The SDE can be solved using different discretisation schemes. Two different discretisation schemes namely, Euler-Maruyama and Milstein are utilised in this paper. For this reason, the proposed MLMC methods are named as Euler-Maruyama MLMC (EM-MLMC) and Milstein MLMC (M-MLMC). The reliability evaluation efficiency of the methods is analysed and compared based on accuracy and computational time saving for basic reliability assessment of Roy Billinton Test System (RBTS). Numerical results show that both methods reduce the computational time required to estimate the reliability indices compared to the same discretisation schemes used in MCS and maintain satisfactory accuracy levels.

Keywords—multilevel Monte Carlo (MLMC); computational complexity; distribution system; reliability; discretisation schemes

1. Introduction

In power distribution systems planning, reliability analysis is an essential step for supplying the electricity with minimum customers' interruptions and cost. Reliability is generally measured by few indices related to the frequency and duration of the interruptions [1]. Component failure rate and unavailability are the fundamental reliability indices to measure the load point (LP), feeder as well as overall distribution system reliability. Failure rate and unavailability indices measure the expected number of failures and their duration for individual customers, respectively. Some reliability indices measure the feeder as well as overall system interruption frequency and duration related information. For example, System Average Interruption Frequency Index (SAIFI) and Customer Average Interruption Duration Index (CAIDI) calculate the average number of sustained interruptions that customers would experience in a year and average duration of each interruption, respectively. Two other common indices- System Average Interruption

Duration Index (SAIDI) and Expected Energy Not Supplied (EENS) measure the average interruption duration for each customer in a year and total amount of energy interruption in a year, respectively [2, 3].

The number of outages associated with a LP of a feeder and their restoration times vary randomly with time [4]. As a result, the values of reliability indices of the distribution systems also vary randomly. Approximations of reliability indices by considering the variability of the indices provide more accurate prediction of distribution systems performance. Commonly used approaches for reliability evaluation are analytical and Monte Carlo simulation (MCS) methods [5, 6]. Analytical approach evaluates the expected average value of a particular index without considering the variability of the index. On the other hand, MCS technique estimates the indices by simulating the components random failure and restoration behaviours over a time period. Therefore, MCS approach is extensively used in reliability evaluation applications. However, the main constraint of MCS is that its computational burden increases rapidly with the increased accuracy level for highly reliable systems. The presence of increased number of time-dependent random variables and system configurations complexities also greatly increase the computation time of reliability assessment. This motivates the development of a new technique which can reduce the computational effort of MCS in order to achieve the target convergence criteria without compromising the accuracy levels of the indices.

Several methods have been proposed to improve the computational efficiency of crude MCS in power system applications [7-10]. However, there is a lack of research to improve the computational efficiency of MCS applications in distribution system reliability evaluation by employing advanced MCS methods. Therefore, in this paper, we propose a novel multilevel Monte Carlo (MLMC) simulation technique that incorporates the idea of control variates in distribution systems reliability evaluation.

The MLMC method is an advanced MCS technique which has been recently developed for the estimation of expectations by constructing the stochastic differential equations (SDE) [11] of system random variables. In standard MCS method, all the samples are simulated on a single finest grid level at the highest accuracy and computational cost. On the other hand, proposed MLMC method uses a hierarchy of discretisation levels and simulations are carried out on multiple different grid levels, starting from the coarsest grid level. The simulation accuracy and computational burden using coarse levels are less than the simulation using fine levels. By using information on multiple levels, MLMC method

needs few samples on the expensive fine levels to achieve the target convergence criteria and thus the overall computational cost is dramatically reduced than MCS. The MLMC based methods are implemented by solving the SDE using different discretisation schemes. In this study, we propose Euler-Maruyama discretisation (EMD) and Milstein discretisation (MD) schemes for the approximations of the numerical solution of SDE. In our previous studies [12, 13], we have shown the effectiveness of the MLMC method on a simple distribution network. In this study, the proposed method is tested on three benchmark large and complex distribution networks.

In Section 2, we describe the basics of MLMC and its convergence criteria. In Section 3, we present the proposed methodology of the distribution system reliability evaluation. In this Section, firstly we develop the SDE modelling of component average time-to-failure and time-to-repair variables based on the proposed two discretisation schemes. The SDE models of LP, feeder and overall system reliability indices are constructed using these variables. Reliability indices SAIFI, SAIDI, CAIDI and EENS are considered for evaluation. In Section 4, we describe the test networks and numerical results. Simulation accuracy and running time are used to illustrate the effectiveness of the proposed methods. The results from the proposed methods are compared with the standard MCS and analytical techniques. Finally, Section 5 concludes the article.

2. Multilevel Monte Carlo simulation

2.1. Principles of MLMC

Suppose we want to estimate $\mathbb{E}[R]$. Let $\mathbb{E}[R_a]$ be the approximation of $\mathbb{E}[R]$. R is the target reliability index and R_a is a function of simulated random variables. In MCS method, an average value of R_a, $\mathbb{E}[R_a]$ is approximated by using a large number of simulations on a single fine grid level [14]. According to the MCS method, unbiased estimator for $\mathbb{E}[R_a]$ can be expressed as follows:

$$\widehat{\mathbb{E}}_{MC}[R_a] = \frac{1}{N_s}\sum_{i=1}^{N_s} R_a^{(i)}. \quad (1)$$

where $R_a^{(i)}$ is the ith sample of R_a and N_s is the total number of required samples on the finest grid level. The uncertainty around the approximation is measured by the variance of the estimator. The variance of this estimator is $N_s^{-1}V[R_a]$ and the root mean square error (RMSE) is $\mathcal{O}(1/\sqrt{N_s})$. Mathematically, $\mathcal{O}$ is introduced as big O notation, which is used to describe the complexity of a function by omitting constant factors and lower order terms.

Here, we simply express the relationship between the number of Monte Carlo samples and accuracy level using big O notation [13]. The convergence criterion in MCS method is based on the desired RMSE value. This RMSE value is often represented as simulation accuracy. To achieve an accuracy of β, it requires $N_s = \mathcal{O}(\beta^{-2})$ samples. This means for a high reliable system with smaller β, we need to simulate a large number of samples which results in high computational burden. To reduce the computational burden, variance reduction techniques are generally applied by maintaining the reasonable accuracy level.

For simplicity, standard MC method could be referred as single level MC simulation due to the estimation of $\mathbb{E}[R]$ by $\mathbb{E}[R_a]$ on a single fine level $\ell = L$. On the other hand, MLMC method uses multiple grid levels, $\ell = 0,1, \ldots \ldots, L$ with $\ell = 0$ (coarsest level) and $\ell = L$ (finest level). ℓ is a nonnegative integer.

For two-level version of MLMC, we can estimate $\mathbb{E}[R_a]$ by simulating R_0 which approximates R_a. R_0 denotes the samples or approximations on the computationally cheapest coarsest level $\ell = 0$. Therefore, the idea of two levels MLMC can be written by the following way:

$$\mathbb{E}[R_a] = \mathbb{E}[R_0] + \mathbb{E}[R_a - R_0] \tag{2}$$

In the above Equation (2), each expectation on the single level is individually assessed by the traditional MCS. Each level of the grid uses a different number of samples in a way which reduces the overall variance for a given convergence criteria. Mathematically, the general idea of MLMC for any number of grid levels can be formulated as follows:

$$\mathbb{E}[R_a] = \mathbb{E}[R_0] + \sum_{\ell=1}^{L} \mathbb{E}[R_\ell - R_{\ell-1}] \tag{3}$$

Let $\widehat{\mathbb{E}}[R_0]$ be an unbiased MCS estimator for $E[R_0]$ using N_0 samples for $\ell = 0$. Also, let $\widehat{\mathbb{E}}[R_\ell - R_{\ell-1}]$ be the MCS estimator for $\mathbb{E}[R_\ell - R_{\ell-1}]$ using N_ℓ samples for $\ell \geq 1$. Then we get

$$\widehat{\mathbb{E}}[R_0] = \frac{1}{N_0} \sum_{i=1}^{N_0} R_0^{(i)}, \tag{4}$$

$$\text{and } \widehat{\mathbb{E}}[R_\ell - R_{\ell-1}] = \frac{1}{N_\ell} \sum_{i=1}^{N_\ell} \left[R_\ell^{(i)} - R_{\ell-1}^{(i)} \right], \tag{5}$$

The overall estimator of MLMC method for each reliability index of distribution systems can be expressed by combining the Equations (4) and (5) as follows:

$$\widehat{\mathbb{E}}_{ML}[R_a] = \sum_{\ell=0}^{L} \frac{1}{N_\ell} \sum_{i=1}^{N_\ell} \left[R_\ell^{(i)} - R_{\ell-1}^{(i)} \right]. \quad (6)$$

In Equation (6), in order to avoid any unwanted bias, R_ℓ must have the same statistical properties, independent of whether they are used in the estimate $\mathbb{E}[R_\ell - R_{\ell-1}]$ from level $\ell - 1$ to ℓ or $\mathbb{E}[R_{\ell+1} - R_\ell]$ from ℓ to $\ell + 1$. This means that both $\mathbb{E}[R_\ell - R_{\ell-1}]$ and $\mathbb{E}[R_{\ell+1} - R_\ell]$ must have the same expectation. The estimator for $\mathbb{E}[R_\ell - R_{\ell-1}]$ is computed in the form of $\mathbb{E}[R_\ell^f - R_{\ell-1}^c]$. Based on the expected value computed on the coarsest level, the difference from one coarse level to the next fine level $\mathbb{E}[R_\ell^f - R_{\ell-1}^c]$ is added, until the finest level L is reached. The timesteps sizes for fine and coarse path estimators are [15]:

$$h_f = 2^{-\ell} T, \quad (7)$$

$$h_c = 2^{-(\ell-1)} T. \quad (8)$$

where h_f is the timestep size of the fine-path estimator $\mathbb{E}[R_\ell^f]$ and h_c is the timestep size of the corresponding coarse-path estimator $\mathbb{E}[R_{\ell-1}^c]$.

The simulations use just one timestep on the coarsest level ($\ell = 0$) and 2^L uniform timesteps on the finest level ($\ell = L$) for the whole time interval $[0, T]$. Each level has twice timesteps as the previous grid level. As the number of timesteps increases from the coarsest to finest level, the required computational effort also increases. In the meantime, the required number of samples on each level decreases with the variance reduction. The number of samples reduction from the coarsest to the finest level reveals that most of the samples are simulated on the computationally low-cost coarse levels and comparatively few samples are run on the expensive fine levels. By accumulating the overall calculation time, it is seen that the required time is considerably reduced when compared to MCS which runs all the simulations on the computationally most expensive finest grid level.

2.2. MLMC convergence criteria

The convergence criterion in the MLMC method is also based on the desired RMSE value which can be expressed as follows:

$$\beta^2 = \sum_{\ell=0}^{L} N_\ell^{-1} V_\ell + [\mathbb{E}(R_a - R)]^2. \quad (9)$$

In order to obtain the value of $MSE \leq \beta^2$, it is enough to ensure that both the estimated variance and approximation error are independently less than $\beta^2/2$. The different number of samples N_ℓ on each level ensures that the estimated variance of the MLMC estimator is less than $\beta^2/2$. As the level ℓ increases from the coarsest level and moves to finer levels, N_ℓ on each level decreases by setting the optimal N_ℓ. The optimal N_ℓ is determined using the following Equation [11]:

$$N_\ell = 2\beta^{-2}\sqrt{V_\ell/C_\ell}\left(\sum_{\ell=0}^{L}\sqrt{V_\ell C_\ell}\right). \tag{10}$$

where C_ℓ is the computational cost of an individual sample on the level ℓ. C_ℓ is measured as $C_\ell = c_3 2^{\gamma\ell}$ for a constant c_3 and some $\gamma > 0$. γ is the rate of computation cost increase with level ℓ and estimated by linear regression. In case of weak convergence, the test tries to confirm that $[\mathbb{E}(R_a - R)]^2 \leq \beta^2/2$. If the convergence rate of $\mathbb{E}(R_a - R)$ with ℓ for some constant c_1 is measured by a positive value α [11]. Then

$$|\mathbb{E}[R_\ell - R_{\ell-1}]| \leq c_1 2^{-\alpha\ell}, \tag{11}$$

and the remaining error is

$$\mathbb{E}(R_a - R) = \mathbb{E}[R_L - R_{L-1}]/(2^\alpha - 1), \tag{12}$$

This leads to the convergence test

$$\mathbb{E}[R_L - R_{L-1}]/(2^\alpha - 1) < \beta/\sqrt{2} \tag{13}$$

3. Reliability assessment methodology

3. 1. Modelling of reliability indices

In the distribution systems reliability calculation, an up-down state component model is usually used [16]. In the up state, the component works successfully. In the down state, component remains in the malfunction mode through repairing, replacing a component or switching activities. The average time during which a component is in the up and down state are called mean-time-to-failure ($MTTF$) and mean-time-to-repair ($MTTR$), respectively.

$$MTTF = 1/\lambda_j \tag{14}$$

$$MTTR = r_j \tag{15}$$

where λ_j and r_j are the average failure rate (failure/year) and the average repair or switching time (hour/failure) of a component *j*, respectively.

The behaviours of $MTTF$ and $MTTR$ of the distribution components are completely random. These are just the approximations of the historical $MTTF$ and $MTTR$ data and follow any probability distribution. In this paper, it is assumed that the failure rate and repair time of distribution components remain at a constant average rate. In this case, exponential probability distribution is employed for modelling the randomness of these variables. In a time sequential simulation, the artificial uptime (T_{UP}) and downtime (T_{DN}) histories of component *j* can be generated by simulating its failure and repair with respect to time using Equations (16) and (17), respectively.

$$T_{UPj} = -MTTF \times ln(U1), \tag{16}$$

$$T_{DNj} = -MTTR \times ln(U2), \tag{17}$$

where $U1$ and $U2$ are uniformly distributed random variables between [0, 1].

An important feature of the MLMC method is that the method is used for the approximation of reliability indices by constructing the SDE based random variables. Therefore, T_{UP} and T_{DN} of the component *j* are generated by approximating the SDE based modelling of component $MTTF$ and $MTTR$, respectively.

In this study, we assume that the uncertainty of $MTTF$ of component *j* is modelled by SDE driven by standard Brownian motion, B_t on the time interval $[0, T]$ [17]. Then, the SDE model of $MTTF$ with given specific μ, σ parameters and an initial given $MTTF$ [$S_{\lambda j(0)} = 1/\lambda_j$] can be expressed as [18]:

$$dS_{\lambda j(t)} = \mu[S_{\lambda j(t)}, t]dt + \sigma[S_{\lambda j(t)}, t]\, dB_t \quad 0 < t < T \tag{18}$$

where $S_{\lambda j(t)}$ is the value of $MTTF$ at a time t, μ is the rate of change of the average value of stochastic failure process (drift), and σ is the degree of variation of stochastic failure process over time (volatility).

The SDE model of $MTTF$ in Equation (18) is solved using a discretisation scheme. In this article, we use both EMD and MD in order to compare the performances for the numerical solution of SDE [19] and to find the effect on reliability evaluation method. An approximation $S_{\lambda j}$ of the solution of SDE is found by linear interpolation of

$S_{\lambda j(0)}, \ldots\ldots, S_{\lambda j(m)}$ [20]. The EMD and MD with n timesteps, timestep size $h = T/n$ and Brownian increments ΔB_m are expressed by [21]:

EMD:

$$S_{\lambda j(m+1)} = S_{\lambda j(m)} + \mu\left[S_{\lambda j(m)}, t_m\right]h + \sigma\left[S_{\lambda j(m)}, t_m\right]\Delta B_m, \tag{19}$$

and MD:

$$S_{\lambda j(m+1)} = S_{\lambda j(m)} + \mu\left[S_{\lambda j(m)}, t_m\right]h + \sigma\left[S_{\lambda j(m)}, t_m\right]\Delta B_m + \frac{1}{2}\sigma^2\left[S_{\lambda j(m)}, t_m\right](\Delta B_m^2 - h), \tag{20}$$

where $\Delta B_m = B_{m+1} - B_m$ with $m = 0, \ldots\ldots, n-1$ and $t_m = kh$ with $k = 0, \ldots\ldots, n$. ΔB_1, $\Delta B_2, \ldots\ldots$, ΔB_{n-1} are independent and normally distributed random variables.

Now Equation (16) can be rewritten as follows using SDE model of $MTTF$, $S_{\lambda j(m+1)}$:

$$T_{UPj} = -S_{\lambda j(m+1)} \times ln(U1), \tag{21}$$

Similarly, the SDE model of $MTTR$ can be determined. The values of drift, μ and volatility, σ are assumed same as for stochastic failure process. If a_j is a constant for component j and $a_j = r_j \times \lambda_j$. Then initial $MTTR$ for component j is a_j/λ_j. Like Equation (21), T_{DN} can be determined via $S_{\lambda j(m+1)}$ using Equation (17):

$$T_{DNj} = -a_j \times S_{\lambda j(m+1)} \times ln(U2), \tag{22}$$

The values of average failure rate, Φ_j and average unavailability, Ψ_j for a component j can be calculated using the following expressions:

$$\Phi_j = \frac{N_1}{\sum_{n=1}^{N} T_{UPj(n)}} \left(\frac{failure}{year}\right), \tag{23}$$

$$\Psi_j = \frac{\sum_{n=1}^{N} T_{DNj(n)}}{\sum_{n=1}^{N} T_{UPj(n)} + \sum_{n=1}^{N} {T_{DNj(n)}}/{8760}} \left(\frac{hour}{year}\right), \tag{24}$$

where N_1 is the number of times component j fails for entire simulation period and N is the desired number of simulated periods. Now, average failure rate, Λ_i and annual unavailability, U_i for LP i can be calculated as follows:

$$\Lambda_i = \sum_{j=1}^{n_j} \Phi_j, \tag{25}$$

$$U_i = \sum_{j=1}^{n_j} \Psi_j, \tag{26}$$

where n_j is the number of components failures that affect the service of LP *i*. Using the Equations (27) and (28), proposed reliability indices can be defined as follows:

$$SAIFI = \frac{\sum_{i=1}^{n_i} \Lambda_i N_{C_i}}{N_T} (int/syst\ cust.yr), \tag{27}$$

$$SAIDI = \frac{\sum_{i=1}^{n_i} U_i N_{C_i}}{N_T} (hr/syst\ cust.yr), \tag{28}$$

$$CAIDI = \frac{\sum_{i=1}^{n_i} U_i N_{C_i}}{\sum_{i=1}^{n_i} \Lambda_i N_{C_i}} (hr/cust\ int), \tag{29}$$

$$EENS = \sum_{i=1}^{n_i} U_i L_{AV_i} (MWhr/yr). \tag{30}$$

where N_{C_i} is the number of customers at LP *i*, N_T is the total number of customers served. On the other hand, n_i is the number of LPs in the distribution system and L_{AV_i} is the average load level at LP *i*.

3.2. MLMC simulation steps

The overall procedure for power distribution system reliability evaluation is briefly summed up in the following steps:

(1) Distribution components reliability data are defined at first i.e. component average failure rate and repair time. We also assume some MLMC simulation parameters as follows:

a) Number of samples for convergence tests, *N* [6000]

b) Initial number of samples on each level ℓ, N_a [500]

c) Desired accuracy, β [0.001]

d) Drift value, μ [0.02] and

e) Volatility value, σ [0.6].

(2) The SDE model of $MTTF$ is constructed using Equation (18) for a component of average failure rate, λ_j.

(3) The SDE models of $MTTF$ on levels $\ell = 0$ and $\ell > 0$ are solved by EMD and MD schemes using Equations (19) and (20), respectively. For coarse and fine levels, the solutions of SDE models are defined by Equations (31)-(34).

EMD:

$$S^c_{\lambda j(m+1)} = S^c_{\lambda j(m)} + \mu S^c_{\lambda j(m)} h_c + \sigma S^c_{\lambda j(m)} dB_{c(m),} \quad (31)$$

$$S^f_{\lambda j(m+1)} = S^f_{\lambda j(m)} + \mu S^f_{\lambda j(m)} h_f + \sigma S^f_{\lambda j(m)} dB_{f(m)}, \quad (32)$$

MD:

$$S^c_{\lambda j(m+1)} = S^c_{\lambda j(m)} + \mu S^c_{\lambda j(m)} h_c + \sigma S^c_{\lambda j(m)} dB_{c(m)} + \frac{1}{2}\sigma^2 S^c_{\lambda j(m)} [dB_{c(m)}{}^2 - h_c], \quad (33)$$

$$S^f_{\lambda j(m+1)} = S^f_{\lambda j(m)} + \mu S^f_{\lambda j(m)} h_f + \sigma S^f_{\lambda j(m)} dB_{f(m)} + \frac{1}{2}\sigma^2 S^f_{\lambda j(m)} [dB_{f(m)}{}^2 - h_f]. \quad (34)$$

(4) The following parameters are then computed on levels $\ell = 0$ and $\ell > 0$ using the Equations (31)-(34) depending on discretisation scheme used.

(a) T_{UP} and T_{DN} histories for each component are generated using Equations (21) and (22), respectively.

(b) The values of Φ_j and Ψ_j for each component are calculated using Equations (23) and (24), respectively.

(c) The values of Λ_i and U_i for each LP are calculated using Equations (25) and (26), respectively.

(d) SAIFI, SAIDI, CAIDI and EENS are determined using Equations (27)-(30), respectively.

(5) The sum of system performance indices values on levels $\ell = 0$ and $\ell > 0$ are calculated using Equation (3). The whole process starting from step (2) is repeated until the sample size is reached to is *N*.

(6) In order to achieve the target convergence criteria for each reliability index calculation by Equation (9), initially, the number of grid levels for MLMC simulation is set at $L = 2$.

(7) Using an initial number of samples N_a, the number of samples N_x on each level $\ell = 0, 1, 2$ is determined. At the same time, the sum of system performance indices values is updated on each level ℓ.

(8) The absolute value of average system performance index, $m_\ell = |\mathbb{E}[Y_\ell]|$ and variance $V_\ell = V[Y_\ell]$ are calculated on each level ℓ.

(9) The optimal number of samples N_ℓ on each level is determined using Equation (10). The optimal N_ℓ is compared to the already calculated N_x on that level. If N_ℓ is larger than N_x, then additional samples on each level are determined. In the same time, the mean reliability index value and variance on each level are also updated. The purpose of determining the optimal N_ℓ is to make the variance $\sum_{\ell=0}^{L} N_\ell^{-1} V_\ell$ less than $\beta^2/2$.

(10) The weak convergence criteria of Equation (9) ensures that the approximation error is less than $\beta/\sqrt{2}$. If remaining error is greater than $\beta/\sqrt{2}$, then a new level $L = L + 1$ is introduced. The whole process is repeated from step (7) until the target convergence criterion is met.

(11) Finally, the overall multilevel estimator for each system performance index is computed using Equation (6).

4. Case studies and numerical results

4.1. Test distribution networks

The Roy Billinton Test System (RBTS) is a 6 bus test system with five load buses (bus2-bus6). In this paper, three distributions networks with three different buses (buses 3, 5 and 6) are considered as test networks [22]. Figs. 1a, 1b and 1c show the buses 3, 5 and 6 test networks, respectively. RBTS bus 3 has 8 feeders and 42 LPs. RBTS bus 5 has 4 feeders and 26 LPs. RBTS bus 6 has 4 feeders and 40 LPs. The purpose of using three different networks is to find the effects on reliability computation by considering different networks sizes and the number of SDE. The number of SDE model in a distribution system reliability evacuation depends on the types of components varying their feeder length.

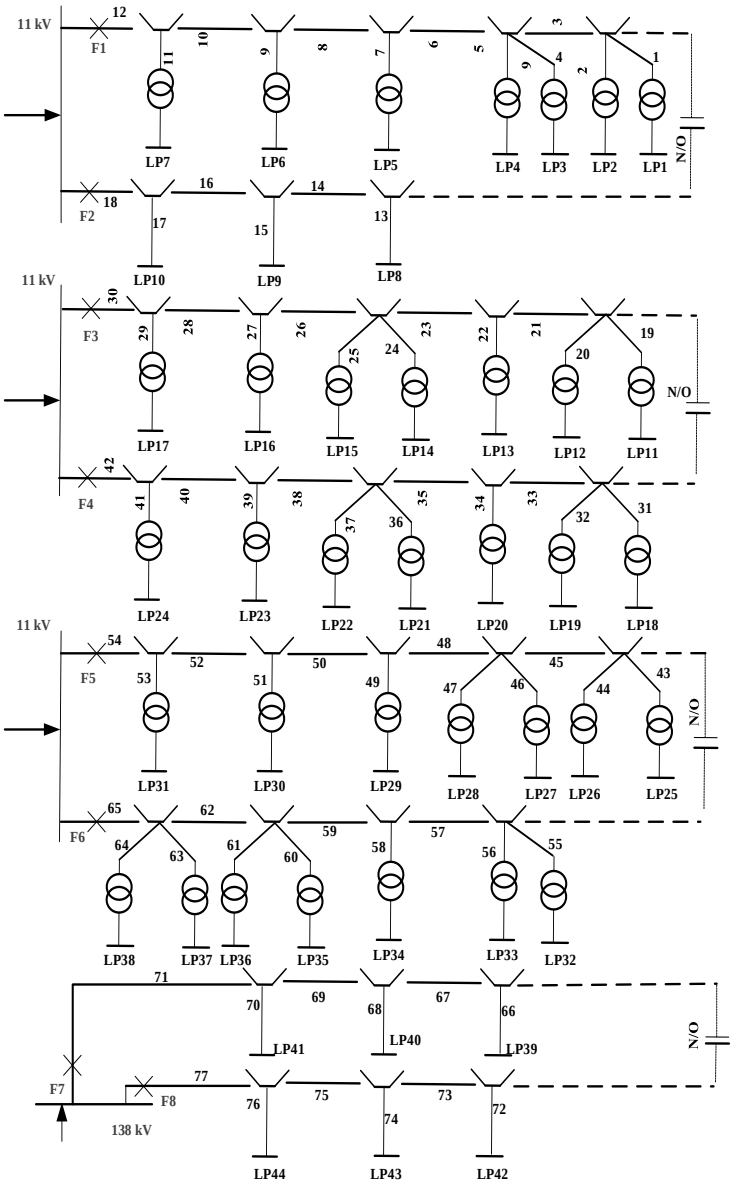
11 kV
F1
F2
F3
F4
F5
F6
F7
F8
138 kV
N/O
LP1
LP2
LP3
LP4
LP5
LP6
LP7
LP8
LP9
LP10
LP11
LP12
LP13
LP14
LP15
LP16
LP17
LP18
LP19
LP20
LP21
LP22
LP23
LP24
LP25
LP26
LP27
LP28
LP29
LP30
LP31
LP32
LP33
LP34
LP35
LP36
LP37
LP38
LP39
LP40
LP41
LP42
LP43
LP44

(a)

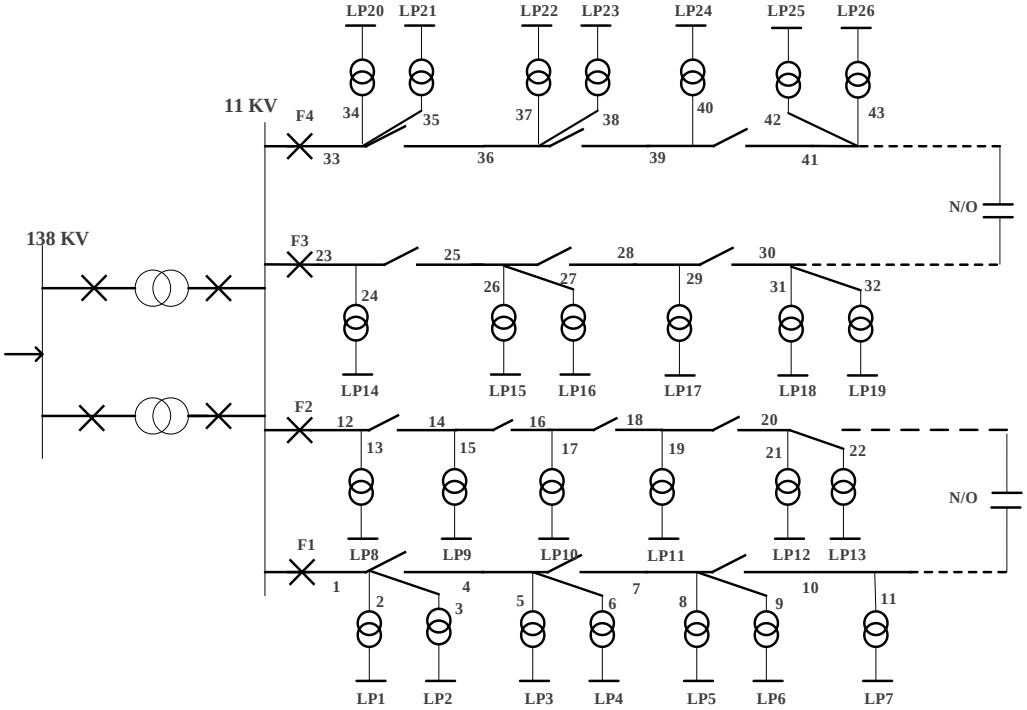

(b)

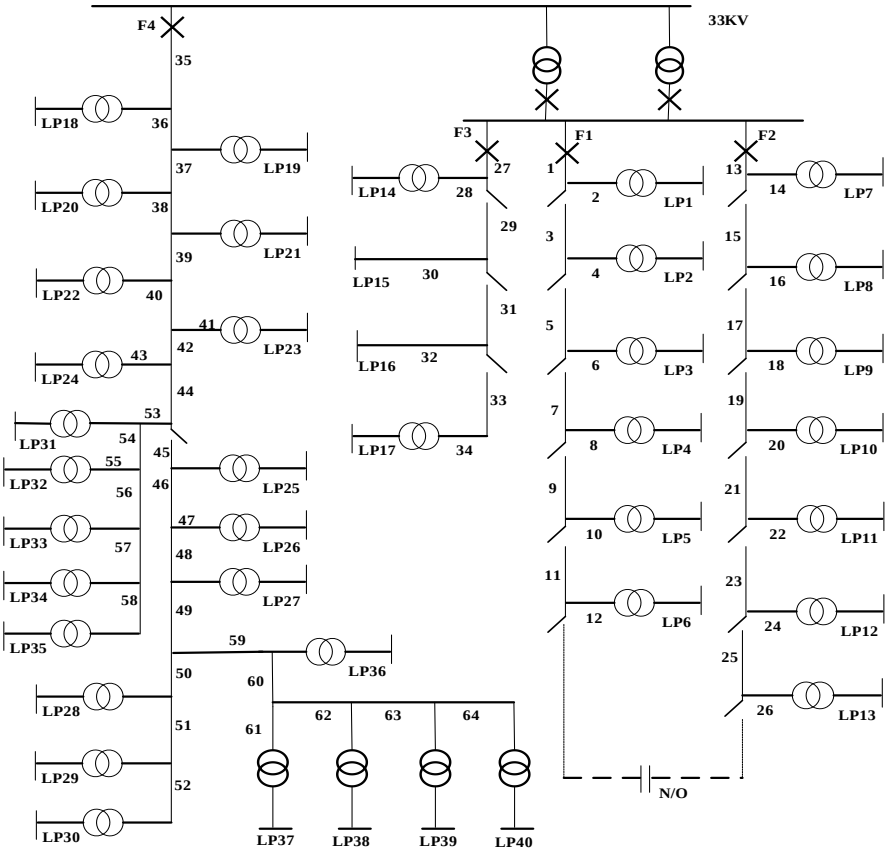

(c)

Fig. 1 Distribution systems for RBTS (a) Bus 3 (B) Bus 5 and (c) Bus 6

The network at bus 3 represents a typical industrial and large user network. The networks at bus 5 and 6 represent urban and rural types, respectively. These networks have several components between substation and LPs such as transmission lines, feeder breakers, transformers, fuses and disconnector switches. The failure of any component causes an outage of the LP(s). In this study, feeder breakers are assumed as 100% reliability. The failures of main and lateral section lines are considered with the availability of disconnectors, fuses, alternative supply and transformer. The alternative supply is used to supply power to that section of the main feeder which becomes disconnected from the main supply after the isolation of faulted section. Faults on a lateral distributor are normally automatically cleared by a fuse and therefore, service on the main feeder is maintained. The actions of transformers are restored by repairing. The reliability and system data of the components can be found in [23]. The lengths of the primary and lateral feeders, customers and loading data of the networks are taken from [22].

4.2. Numerical results

4.2.1. Calculation accuracy

The failure rate of a LP is affected by the numbers of components failures associated with the LP and length of feeders. The failure rates of LP with long feeders are higher than those with the short feeders. SAIFI value depends on the LPs failure rates and number of customers served. For example, in Fig. 2(a), the value of SAIFI for feeder 1 (F1) is higher than F2. For F1, each LP failure rate is affected by the failures of five main feeder sections, one lateral section and transformer. The reduced value of SAIFI for F2 is due to the reduced number of failures (three main feeder sections and one lateral section). The values of SAIDI and CAIDI depend on the components failure rate, repair time and number of customers served. In the current study, restoration of a component is performed either repairing or switching action. The average repair time of a component is longer than the switching time. The reduced values of SAIDI and CAIDI occur because of the fewer components failure as well as components less unavailability time. Similarly, EENS values vary with the components failure rates, repair times and average load level of the LPs.

In this section, we evaluate and compare the accuracy of different methods based on EMD and MD schemes i.e. Euler-Maruyama MLMC (EM-MLMC), Milstein MLMC (M-MLMC), Euler-Maruyama MC (EM-MC) and Milstein MC (M-MC) with respect to the base analytical value. The reliability indices values for different feeders of the test distribution networks are shown in Figs. 2, 3 and 4 [a, b, c and d]. From these Figs., it is

clear that the accuracy levels of the proposed methods are acceptable and very close to the true values.

For the network RBTS bus-3, the maximum deviation of the results from the analytical value computed by the proposed EM-MLMC and M-MLMC approaches are 2.9854% and 3.4102% which occur in the calculation of F7-SAIDI and F8-SAIDI, respectively. The maximum deviation using EM-MLMC and M-MLMC approaches for RBTS Bus-5 network are 2.4894% and 4.0980%, respectively where both occur in the calculation of F2-SAIFI. On the other hand, in the case of reliability indices calculation of RBTS bus-6 network, these deviations are 3.7399% and 4.0802%, whereas the indices F3-SAIFI and F4-SAIFI are computed, respectively.

Tables 1, 2 and 3 present the performances of the proposed methods to evaluate the overall system reliability indices. For the network RBTS bus-3, the maximum deviation of the results computed by the proposed EM-MLMC and M-MLMC approaches are 5.2234% and 3.9354% respectively where both occur in the calculation of SAIFI. The maximum deviation for RBTS bus-5 network using EM-MLMC and M-MLMC approaches are found 3.2339% and 2.2395% which occur in the calculation of SAIFI and CAIDI, respectively. On the other hand, in the case of reliability indices calculation of RBTS bus-6 network, these deviations are 2.0895% and 1.9853%, respectively where the index CAIDI is computed.

The accuracy levels of the indices values are basically influenced by the associated random variables and number of samples simulated on the grid levels. In MLMC methods, both coarse and fine levels are required where most of the samples are simulated on the coarse levels at low accuracy and relatively few samples are simulated on the fine levels at high accuracy. On the other hand, in MC methods, all the simulations are run on the finest level at the highest accuracy. Therefore, the accuracy levels of the indices computed by the MCS are generally higher than the results from MLMC methods. For example, in M-MLMC, levels ℓ=0, 1, 2 and 3 are required for CAIDI calculation. The numbers of samples on these levels are 13001866, 67343, 27537 and 10320, respectively. This means that most of the simulations are performed on the coarser levels rather than the finest level. In M-MC, the number of required samples is 32032 and all the simulations are performed on the finest level ℓ=3.

Table 1 Performance of system indices for RBTS Bus 3

Index	MC	E_{MC} (%)	T_{MC} (s)	MLMC	E_{MLMC} (%)	T_{MLMC} (s)	Saving (%)
Based on EMD							
SAIFI	0.2979	1.5857	0.0818	0.3186	5.2234	0.0019	97.6772
SAIDI	3.4717	0.0259	25.6715	3.5067	0.9806	1.2918	94.9679
CAIDI	11.6965	1.9832	364.7167	11.7275	2.2534	20.8212	94.2911
EENS	66.6645	0.0292	5396.6854	67.5675	1.3249	297.1727	94.4934
Based on MD							
SAIFI	0.2985	1.3875	0.0885	0.3147	3.9354	0.0046	94.8022
SAIDI	3.4728	0.0057	27.7406	3.5247	1.4990	1.6880	93.91
CAIDI	11.6969	1.9866	412.8202	11.7274	2.2526	20.6637	94.9945
EENS	66.6656	0.0275	5637.6037	67.5962	1.3679	289.5277	94.8643

$E_{MC}= \frac{|Base\ case-MC|}{Base\ case} \times 100\%$, $E_{MLMC}= \frac{|Base\ case-MLMC|}{Base\ case} \times 100\%$.
T_{MC} and T_{MLMC} are computation time in second (s), required by MCS and MLMC methods, respectively.
$Saving = \frac{T_{MC} - T_{MLMC}}{T_{MC}} \times 100\%$
Units: SAIFI - interruptions/system customer.yr, SAIDI - hr/system customer.yr
CAIDI - hr/customer interruption, ENS - MWhr/yr

Table 2 Performance of system indices for RBTS Bus 5

Index	MC	E_{MC} (%)	T_{MC} (s)	MLMC	E_{MLMC} (%)	T_{MLMC} (s)	Saving (%)
Based on EMD							
SAIFI	0.2272	2.2375	0.0513	0.2400	3.2339	0.0030	94.1520
SAIDI	3.5509	0.0056	24.9330	3.6022	1.4366	1.4924	94.0143
CAIDI	15.5795	1.9927	557.2309	15.6016	2.1373	33.4400	93.9988
EENS	40.1088	0.0264	2434.3770	40.6621	1.3527	154.2035	93.6655
Based on MD							
SAIFI	0.2287	1.5920	0.0522	0.2303	0.9384	0.0031	94.0613
SAIDI	3.5526	0.0422	28.2915	3.6028	1.4535	1.1629	94.8624
CAIDI	15.5786	1.9868	571.6676	15.6172	2.2395	32.8643	94.2511
EENS	40.1084	0.0274	2606.9451	40.6808	1.3993	150.5399	94.2254

Table 3 Performance of system indices for RBTS Bus 6

Index	MC	E_{MC} (%)	T_{MC} (s)	MLMC	E_{MLMC} (%)	T_{MLMC} (s)	Saving (%)
Based on EMD							
SAIFI	0.9869	1.9473	0.5952	1.0031	0.3475	0.0575	90.3393
SAIDI	6.6680	0.01170	94.2111	6.7650	1.4428	5.5803	94.0767
CAIDI	6.5267	1.4837	121.5628	6.7635	2.0895	9.1002	92.5139
EENS	72.6299	0.0163	11438.6979	73.63	1.3603	627.3600	94.5154
Based on MD							
SAIFI	0.9885	1.7883	0.6421	1.0094	0.2783	0.0451	92.9761
SAIDI	6.6683	0.0072	112.0105	6.7669	1.4713	5.2465	95.3160
CAIDI	6.5269	1.4807	137.2799	6.7566	1.9853	8.3901	93.8883
EENS	72.6300	0.0162	11557.5306	73.6604	1.4022	612.7943	94.6978

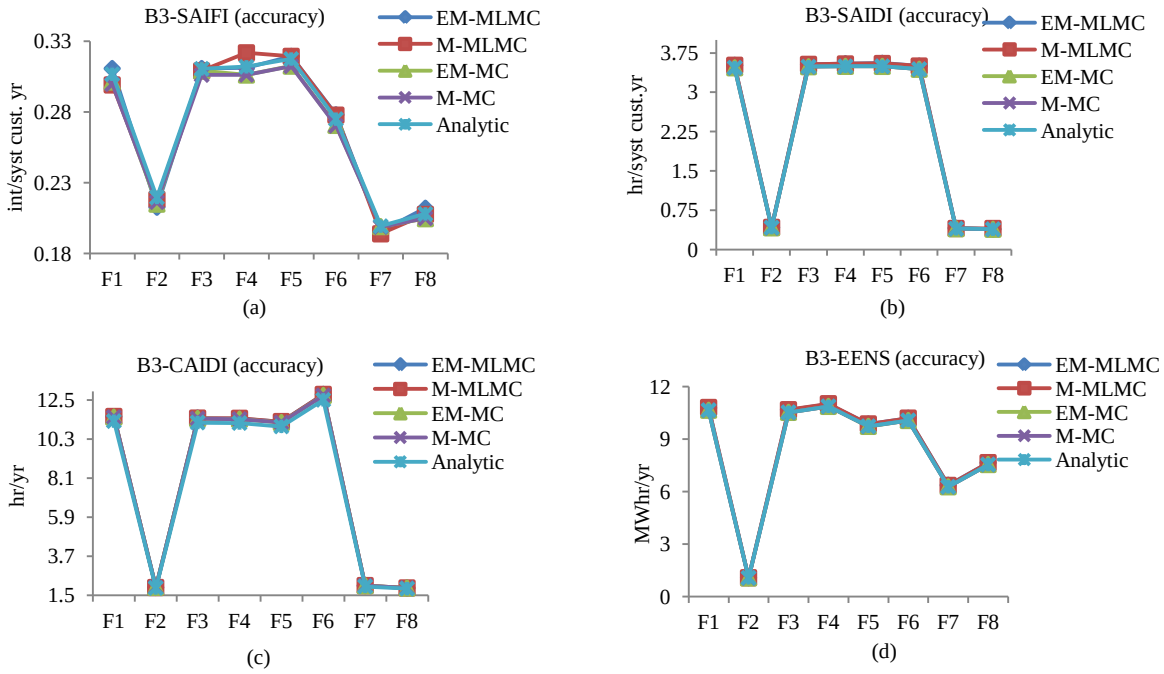

Fig. 2 Reliability indices calculation accuracy for various feeders of RBTS Bus 3[a) SAIFI b) SAIDI c) CAIDI d) EENS]

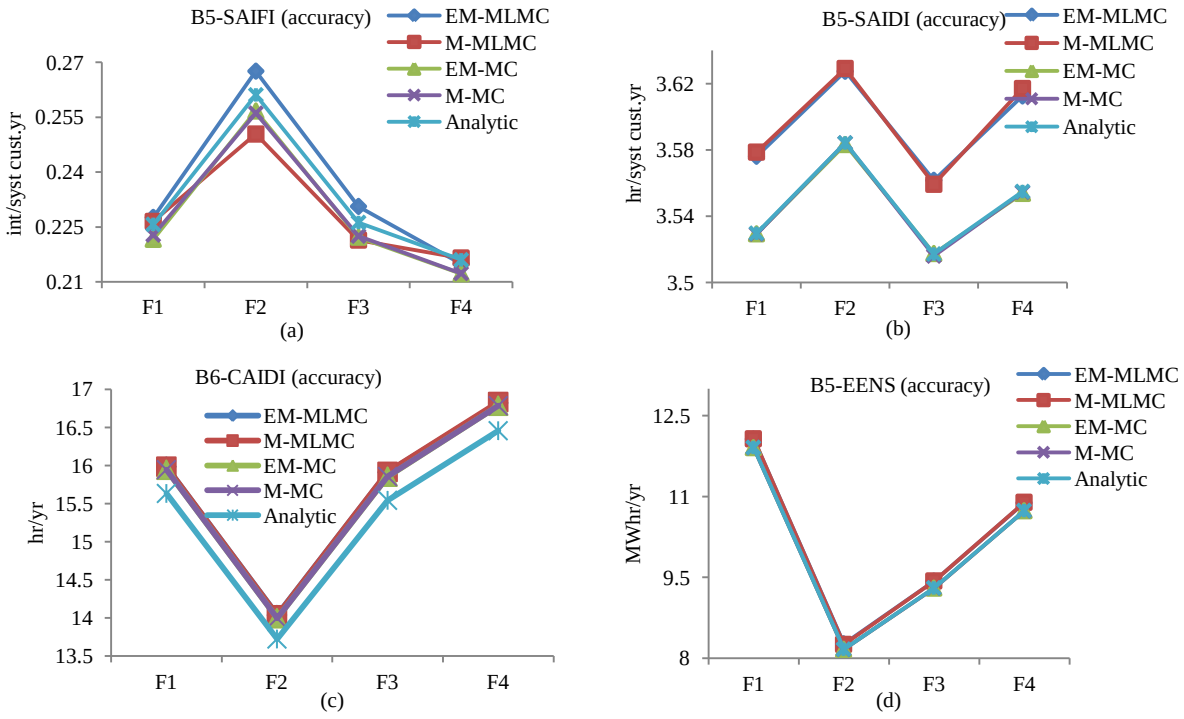

Fig. 3 Reliability indices calculation accuracy for various feeders of RBTS Bus 5 [a) SAIFI b) SAIDI c) CAIDI d) EENS]

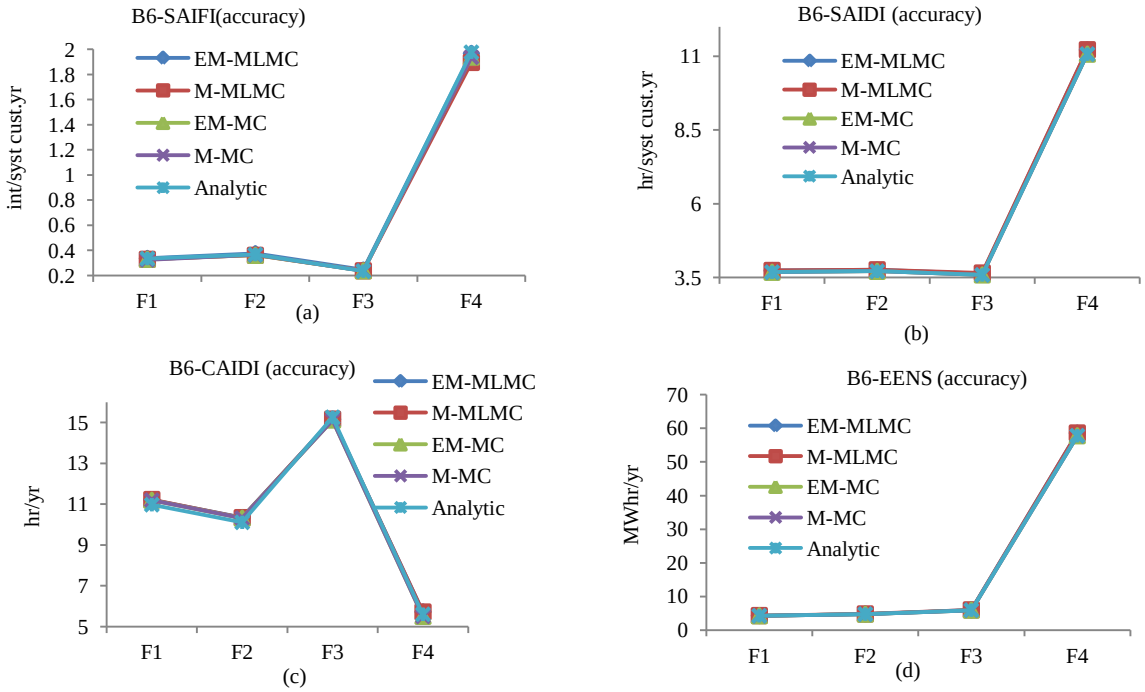

Fig. 4 Reliability indices calculation accuracy for various feeders of RBTS Bus 6 [a) SAIFI b) SAIDI c) CAIDI d) EENS]

4.2.2. Computational efficiency

The duration of computation time for numerical simulation of reliability evaluation depends on the number of SDE models and algebraic equations associated with the target index of distribution networks. Components failure rates and repair times are modelled using SDE. Reliability index of a feeder calculated by the higher number of SDE models and more algebraic equations needs long assessment time compared to other feeders. Figs. 5, 6 and 7 display the computational performances of different methods to evaluate the reliability indices of feeders. From these Figs, it could be seen that both the proposed methods increase the computational efficiency of the MC methods and save more than 90% calculation time for any feeder.

Tables 1, 2 and 3 also show the computational performances of the proposed methods to evaluate the overall system reliability indices. For the network RBTS bus-3, the maximum time saving by the proposed EM-MLMC and M-MLMC approaches are 97.6772% and 94.9945% respectively, which occur in the calculation of SAIFI and CAIDI, respectively. The maximum saving for RBTS bus-5 network using EM-MLMC and M-MLMC approaches are found 94.1520% and 94.8624% which occur in the calculation of SAIFI and SAIDI, respectively. On the other hand, in the time of reliability indices calculation of

RBTS bus-6 network, these savings are 94.5154% and 95.3160%, respectively while the indices EENS and SAIDI are computed. Numerical demonstrations of computational performance from Tables 1, 2 and 3 also describe that MC method based on EMD needs less simulation time than the computation based on MD scheme. On the other hand, reliability assessment using MLMC method based on EMD needs more simulation time than the computation based on MD scheme. Therefore, in most of the cases, there is more time-saving in M-MLMC method compared to the EM-MLMC method.

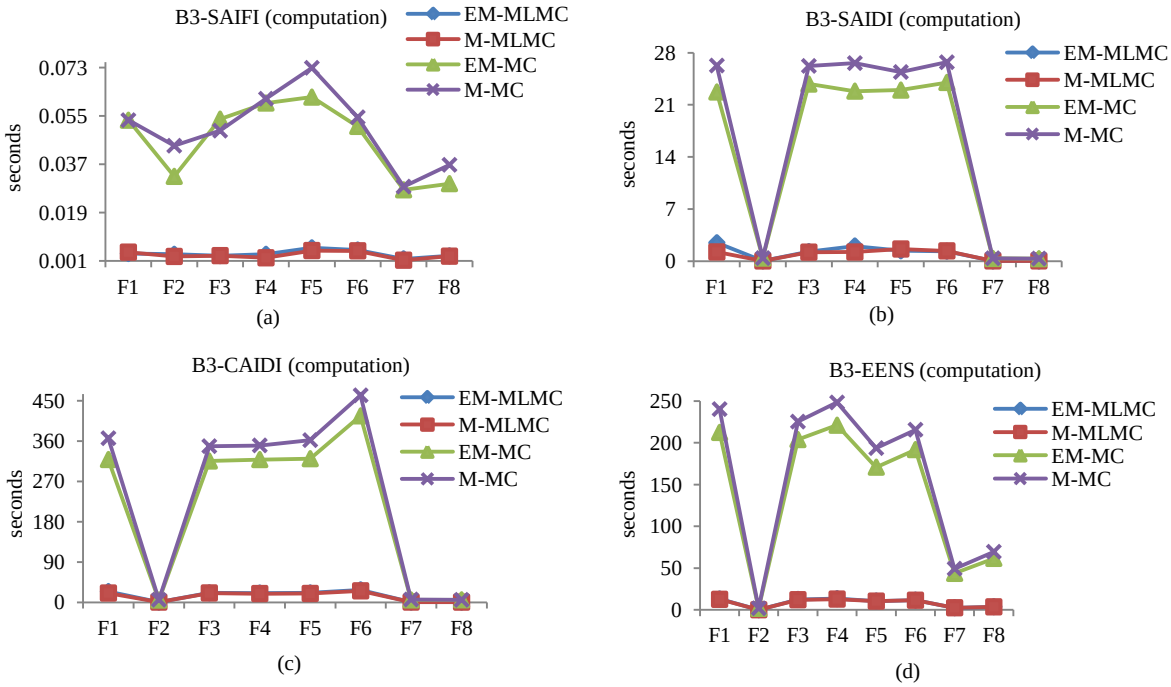

Fig. 5 Reliability indices computation time for various feeders of RBTS Bus 3 [a) SAIFI b) SAIDI c) CAIDI d) EENS]

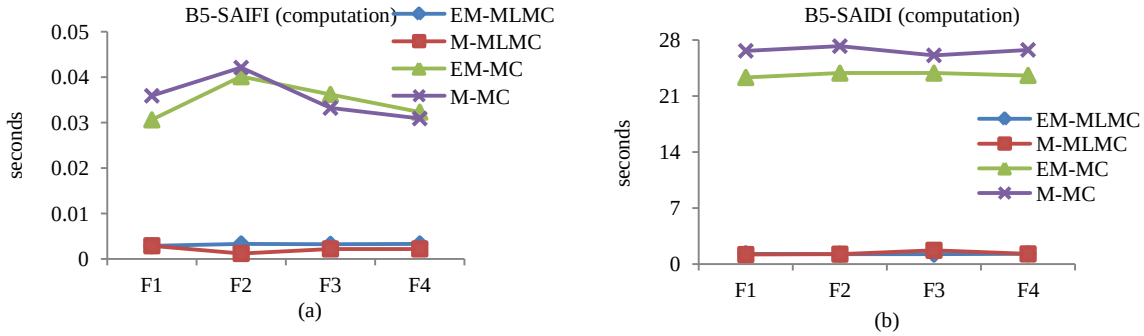

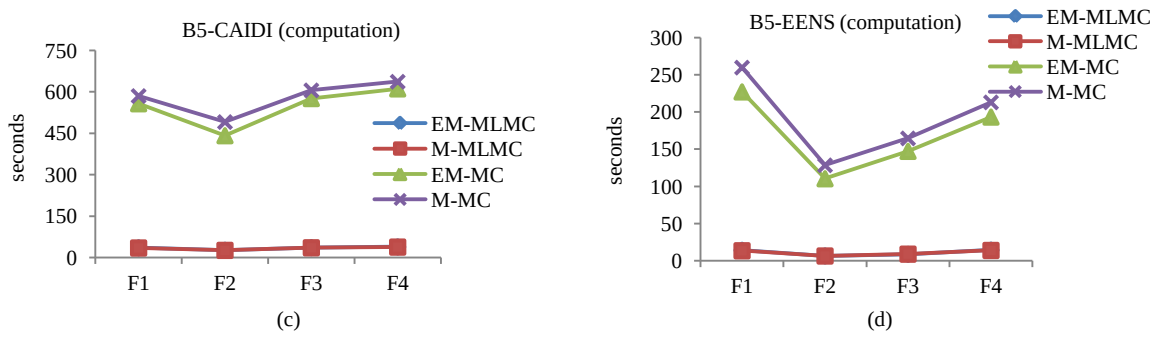

Fig. 6 Reliability indices computation time for various feeders of RBTS Bus 5 [a) SAIFI b) SAIDI c) CAIDI d) EENS]

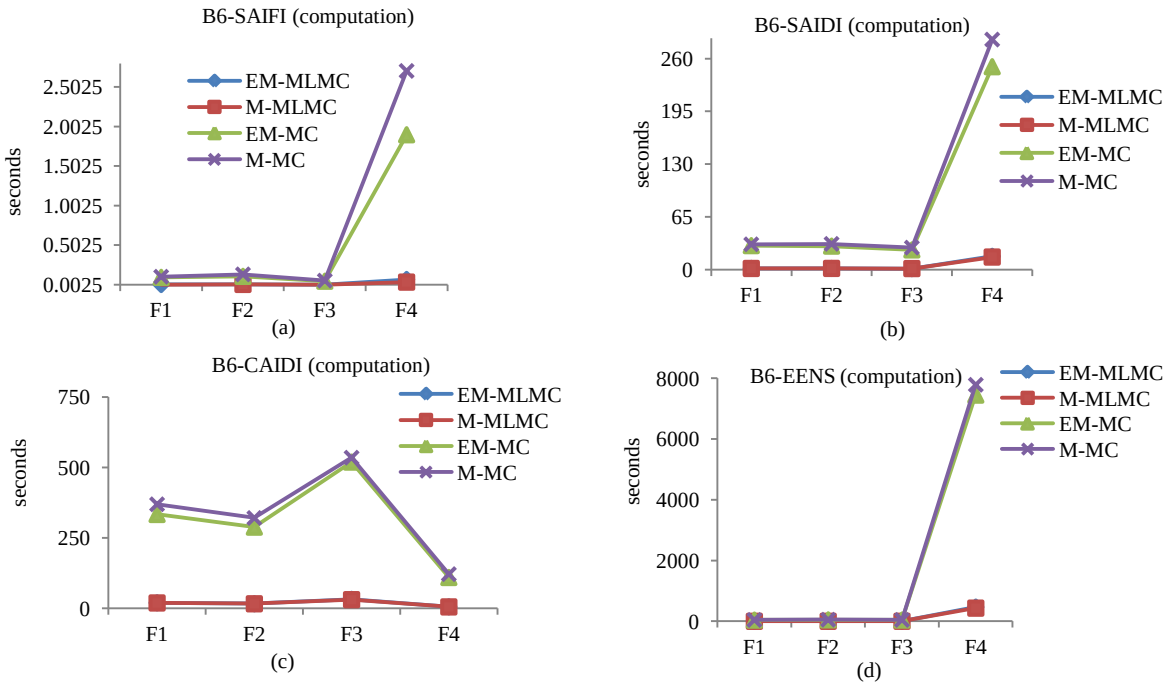

Fig. 7 Reliability indices computation time for various feeders of RBTS Bus 6 [a) SAIFI b) SAIDI c) CAIDI d) EENS]

The computational performance of MLMC is generally improved by controlling the number of samples simulated on the grid levels. In MLMC methods, both coarse and fine levels are utilised where most of the samples are simulated on the less expensive coarse levels and relatively few samples are simulated on the expensive fine levels. On the other hand, in MC methods, all the simulations are run on the most expensive finest level. Thus, the computational efficiency of the MLMC is improved over the MC methods. For example, as described in Section 4.2.1, 10320 samples are run on the most expensive finest level for CAIDI calculation based on M-MLMC and remaining large sample sets are simulated on the cheaper coarse levels. On the other hand, the number of required samples

for M-MC is 32032 and all the simulations are performed on the most expensive finest level ($L = 3$). Therefore, overall computation time is saved by MLMC method.

5. Conclusion

In this paper, we have applied new techniques based on multilevel Monte Carlo method for estimating the reliability of distribution systems. Two methods, Euler-Maruyama MLMC and Milstein MLMC have been proposed based on two discretisation schemes of SDE model solutions of reliability indices. The main objective of the methods is to reduce the calculation time of sequential Monte Carlo based reliability evaluation. The effectiveness of the proposed methods is validated on three test systems, RBTS-buses 3, 5 and 6.

From the results, we can conclude that both MLMC approaches based on discretisation schemes reduce the simulation running time and speed up the reliability evaluation process compared to MC method. Reasonably accurate reliability indices are found using these new methods.

In the future paper, we will concentrate on several issues. The current study only deals with the determination of reliability indices mean values while in the future, the proposed method for determining the probability distributions [24] of indices will be implemented and its capability will be compared with the MCS. The effects of varying pre-determined parameters (such as drift, volatility values) on reliability evaluation will be carried out. Finally, we will compare the performance of MLMC method with other advanced MC methods [25].

References

[1] Allan, R.: 'Reliability evaluation of power systems' (Springer Science & Business Media, 2013)

[2] Alkuhayli, A. A., Raghavan, S., Chowdhury, B. H.: 'Reliability evaluation of distribution systems containing renewable distributed generations', Proc. North American Power Symposium (NAPS), 2012, pp. 1-6

[3] Goel, L., Billinton, R.: 'Evaluation of interrupted energy assessment rates in distribution systems', IEEE Trans. Power Delivery, 1991, 6, pp. 1876-1882

[4] Billinton, R., Acharya, J.: 'Weather-based distribution system reliability evaluation', IEE Proc.- Gener. Transm. Distrib., 2006, 153, pp. 499-506

[5] Billinton, R., Wang, P.: 'Distribution system reliability cost/worth analysis using analytical and sequential simulation techniques', IEEE Trans. Power Syst., 1998, 13, pp. 1245-1250

[6] Martinez-Velasco, J. A., Guerra, G.: 'Parallel Monte Carlo approach for distribution reliability assessment', IET Gener. Transm. Distrib., 2014, 8, pp. 1810-1819

[7] González-Fernández, R. A., da Silva, A. M. L., Resende, L. C., Schilling, M. T.: 'Composite systems reliability evaluation based on Monte Carlo simulation and cross-entropy methods', IEEE Trans. Power Syst., 2013, 28, pp. 4598-4606

[8] Wang, Y.: 'Probabilistic spinning reserve adequacy evaluation for generating systems using an Markov chain Monte Carlo-integrated cross-entropy method', IET Gener. Transm. Distrib., 2015, 9, pp. 719-726

[9] Hou, K., Jia, H., Xu, X., Liu, Z., Jiang, Y.: 'A continuous time markov chain based sequential analytical approach for composite power system reliability assessment', IEEE Trans. Power Syst., 2016, 31, pp. 738-748

[10] da Silva, A. M. L., González-Fernández, R. A., Flávio, S. A., Manso, L. A.: 'Composite reliability evaluation with renewable sources based on quasi-sequential Monte Carlo and cross entropy methods', Proc. Int. Conf. Probabilistic Methods Applied to Power Systems (PMAPS), 2014, pp. 1-6

[11] Giles, M. B.: 'Multilevel monte carlo path simulation', Oper. Res., 2008, 56, pp. 607-617

[12] Huda, A. S. N., Živanović, R.: 'Distribution system reliability assessment using sequential multilevel Monte Carlo method', Proc. IEEE Innovative Smart Grid Technologies-Asia (ISGT-Asia) Conf., Melbourne, 2016, pp. 867-872

[13] Huda, A. S. N., Živanović, R.: 'Improving distribution system reliability calculation efficiency using multilevel Monte Carlo method', Int. Trans. Elect. Energy Syst., 2017

[14] Kalos, M. H., Whitlock, P. A.: 'Monte carlo methods' (John Wiley & Sons, 2008)

[15] Giles, M.: 'Improved multilevel Monte Carlo convergence using the Milstein scheme' (Monte Carlo and quasi-Monte Carlo methods 2006, ed: Springer, 2008, pp. 343-358)

[16] Retterath, B., Chowdhury, A.A., Venkata, S. S.: 'Decoupled substation reliability assessment', Int. J. Elect. Power Energy Syst., 2005, 27, pp. 662-668

[17] Harrison, J. M.: 'Brownian motion and stochastic flow systems' (Wiley New York, 1985)

[18] Oksendal, B.: 'Stochastic differential equations: an introduction with applications' (Springer Science & Business Media, 2013)

[19] Giles, M. B.: 'Multilevel Monte Carlo for basket options', Proc. Winter Simulation Conf., 2009, pp. 1283-1290

[20] Kloeden, P. E., Platen, E.: 'Higher-order implicit strong numerical schemes for stochastic differential equations', J. Stat. Phys., 1992, 66, pp. 283-314

[21] Platen, E.: 'An introduction to numerical methods for stochastic differential equations', Acta Numerica, 1999, 8, pp. 197-246

[22] Billinton, R., Jonnavithula, S.: 'A test system for teaching overall power system reliability assessment', IEEE Trans. Power Syst., 1996, 11, pp. 1670-1676

[23] Allan, R. N., Billinton, R. Sjarief, I.: 'A reliability test system for educational purposes-basic distribution system data and results', IEEE Trans. Power syst., 1991, 6, pp. 813-820

[24] Bierig, C., Chernov, A.: 'Approximation of probability density functions by the Multilevel Monte Carlo Maximum Entropy method', J. Comput. Phys., 2016, 314, pp. 661-681

[25] González-Fernández, R. A., da Silva, A. M. L.: 'Reliability assessment of time-dependent systems via sequential cross-entropy Monte Carlo simulation', IEEE Trans. Power Syst., 2011, 26, pp. 2381-2389

Chapter 4

Component Importance Analysis

Statement of authorship

Title of Paper	Study effect of components availability on distribution system reliability through Multilevel Monte Carlo method
Publication Status	☑ Published ☐ Accepted for Publication ☐ Submitted for Publication ☐ Unpublished and Unsubmitted w ork w ritten in manuscript style
Publication Details	A. S. Nazmul Huda and Rastko Živanović (2018) Study effect of components availability on distribution system reliability through Multilevel Monte Carlo method, IEEE Transactions on Industrial informatics. Published (Early access) Link: https://ieeexplore.ieee.org/document/8506413

Principal author

Name of Principal Author (Candidate)	A. S. Nazmul Huda		
Contribution to the Paper	Developed reliability evaluation model, performed simulation and numerical analysis, prepared manuscript.		
Overall percentage (%)	80%		
Certification:	This paper reports on original research I conducted during the period of my Higher Degree by Research candidature and is not subject to any obligations or contractual agreements with a third party that would constrain its inclusion in this thesis. I am the primary author of this paper.		
Signature		Date	07.09.2018

Co-author contributions

By signing the Statement of Authorship, each author certifies that:

the candidate's stated contribution to the publication is accurate (as detailed above);

permission is granted for the candidate in include the publication in the thesis; and

the sum of all co-author contributions is equal to 100% less the candidate's stated contribution.

Name of Co-Author	Rastko Živanović		
Contribution to the Paper	Supervised for development of model, helped in data interpretation and manuscript evaluation		
Signature		Date	13.08.2018

Study effect of components availability on distribution system reliability through Multilevel Monte Carlo method

***Abstract*—** Reliability model of a power distribution system is influenced by its components reliability and availability. The paper investigates the effect of some basic protection components availability on the distribution system reliability improvement. For this purpose, we use a new approach called Multilevel Monte Carlo to speed up the conventional Monte Carlo simulation based reliability assessment. The proposed method is implemented through solving stochastic differential equations of the system components random failure process using Milstein discretisation scheme. To illustrate the proposed method, two commonly used reliability indices are evaluated for a test distribution network.

***Index Terms*—** components importance, reliability, Multilevel Monte Carlo, distribution system, Milstein discretisation.

I. Introduction

Reliability is one of the key design considerations for an electric distribution system (EDS). A highly reliable EDS ensures a smaller number of supply interruptions and their short duration. Due to the simple design and comparatively low cost, radial distribution systems are usually popular [1]. In reliability evaluation, components availability effect or importance study investigates the comparative importance of individual components or groups of components to system performance improvement [2, 3]. An EDS consists of different components such as circuit breakers, fuses, main feeder sections, lateral sections, disconnecting switches and low voltage transformers, etc. The expansion of EDS by the inclusion of alternative supply source is also used to improve the network reliability level.

Any component failure could lead to interruption of a load point (LP) in a radial system. Three basic primary reliability indices (RI) of an EDS are mean values of Failure Time (FT), Repair Time (RT) and Annual Unavailability (AU) [4, 5]. The failure period and the number of customers affected due to a component failure can be reduced by making the availability of the protection components and alternative supply [6, 7]. Therefore, the level of reliability of an EDS primarily relies on the reliability of the basic components and the arrangement of these components in the EDS. In this paper, some case studies based on a benchmark radial distribution system is analyzed by considering different components configurations to show their importance in reliability improvement.

For reliability studies, generally computational tools utilize analytical methods or crude Monte Carlo (MC) method [5, 8]. MC method is usually preferred over the analytical techniques because the impact of uncertainties of RI variables can be incorporated. The importance of considering the uncertainties in EDS planning is widely recognised by the utility industries. The convergence of MC simulation is reached when the estimated variance lies within a specified tolerance level. Therefore, the efficiency of MC based method decreases when the system is very reliable and the estimation of the rare-event probability consumes a large time [9]. Hence one of the main issues in simple MC method or Markov Chain MC [10] is their slow convergence speed for achieving high simulation accuracy. The incorporation of stochastic uncertainties and reliability improvement by adding new components can significantly increase the system complexity and therefore, RI evaluation time by MC methods is prolonged.

In order to enhance the convergence speed of the MC method in power system reliability assessment applications, various variance reduction techniques (VRT) have been proposed, such as control variates, antithetic variates [11] and state space pruning [12] etc. Through VRT, the expected value of an output random variable can be obtained with reduced simulation time by maintaining an accuracy level. VRT based on importance sampling which are known as cross-entropy (CE) methods have been utilized extensively in power system reliability applications in order to speed up computation. The research studies are generally carried out for the reliability evaluation of the composite generation and transmission systems [13-16]. For example, CE method was successfully applied in generating capacity reliability problems [14] [17-19] and short-term reliability [15]. In the CE-based method, the state variables are properly distorted in accordance with an optimization process. Due to the optimal distortion, the rate of failure events is more frequent and the convergence rate of the algorithm is significantly enhanced. Later, this method was used for developing more advanced MC-based methods, such as quasi-sequential/CE [18], pseudo-chronological/CE [20], and sequential/CE [14]. In all methods using CE, significant simulation speed was accelerated compared to non-CE version [21]. However, these methods were unable to obtain probability distributions of indices. In one study, an improved importance sampling was applied to generation, transmission line and load states which reduced the computational effort [22]. Additionally, another VRT based on subset simulation has been successfully applied in reliability estimation [23] where a small failure probability is represented as the product of larger conditional probabilities.

From the above review, we find that significant effort has been dedicated in the last few years for developing efficient methods in the areas of composite generation and transmission systems reliability analysis. However, there has been a lack of research in the area of low voltage distribution systems when dealing with very reliable systems [24-26]. However, the modernization of the distribution system is a growing need within the electrical utility industry to refine the existing methods. Using the new method can save the evaluation time and help the distribution systems planners for taking fast reliability improvement actions. A recently developed approach called Multilevel Monte Carlo (MLMC) method [27] is therefore proposed in this research for investigating the components availability effect in reliability evaluation. The purpose of applying the proposed method is to reduce the computation cost for this investigation.

The main contributions are as follows. Firstly, the impact of some basic components availability on system reliability evaluation is investigated through the proposed method. For this purpose, six cases of a test system are considered. Two RI: System Average Interruption Duration Index (SAIDI) and Expected Energy Not Supplied (EENS) are determined [16]. This investigation shows the amount of overall system reliability improvement by analyzing the importance of each component. The benefits of using the proposed MLMC method regarding computation accuracy and time-saving are also demonstrated. The performance of MLMC and MC methods are compared. Secondly, the effect of components availability on the feeder and customer sector-wise reliability is analyzed through the MLMC method. These investigations show the impact of components availability in each feeder and customer-wise reliability improvement in an efficient way. Thirdly, some sensitivity analyses are performed to show the impact of variation of the failure rate and repair time of basic system components as well as the MLMC simulation parameters on the calculation accuracy and speed.

II. Overview of MLMC method

The MLMC method developed by Giles [27] is an advanced MC method, designed to enhance its computational efficiency. In MC method, an average expectation $E[X_a]$ from the distribution of X is estimated by simulating a large sample size on a single fine level. The estimator of MCS is then written as:

$$\hat{Z}_{MC} = \frac{1}{M}\sum_{i=1}^{M} X_a^{(i)}, \quad (1)$$

where X_a is the target reliability index and $X_a^{(i)}$ is the i^{th} sample of X_a, M is the MC sample size and $M^{-1}V[X_a]$ is the estimated variance. The root-mean-square-error (RMSE) value of the MC estimator is therefore, $\mathcal{O}(1/\sqrt{M})$. A sample size $M = \mathcal{O}(\varepsilon^{-2})$ is required to achieve an accuracy level of ε. This means a large sample size is required to be simulated on the finest level for a highly accurate model.

In the MC method, the calculation of an expectation is carried out on a single fine level $l = L$. l is a nonnegative integer. In this level, both the accuracy and computation cost of the expectation are high.

In the MLMC method, same expectation is approximated using multiple parts or levels instead of single-level L. The multiple levels can be divided as $l = 0, 1, \ldots\ldots, L$. Here $l = 0$ and $l = L$ are the coarsest and finest discretisation levels, respectively. On each level, expectations are estimated using different number of samples in a way which minimises the overall variance for a defined accuracy. Initially, a large number of samples are simulated on $l = 0$. The purpose of the next level $l = 1$ is to add a correction value that decreases the bias. Based on this correction value, the expected difference from one level to the next fine level is added, until level L is reached. By this way, the less correct estimation on the coarsest grid is successively corrected by the approximations on the subsequent fine grids and thus the finest grid accuracy is achieved. The MLMC expectation can be expressed as:

$$E[X_a] = E[X_0] + \sum_{l=1}^{L} E[X_l - X_{l-1}] = \sum_{l=0}^{L} E[Z_l], \tag{2}$$

Now the estimator for the above MLMC expectation is

$$\hat{Z}_{ML} = \hat{Z}_0 + \sum_{l=1}^{L} \hat{Z}_l = \sum_{l=0}^{L} \hat{Z}_l. \tag{3}$$

where $\hat{Z}_0$ is an unbiased estimator for $E[X_0]$ using sample N_0 and $\hat{Z}_l$ is the MCS estimator for $E[X_l - X_{l-1}]$ using N_l samples from $l \geq 1$.

$$\hat{Z}_0 = \frac{1}{N_0} \sum_{i=1}^{N_0} X_0^{(i)}, \text{ and} \tag{4}$$

$$\hat{Z}_l = \frac{1}{N_l} \sum_{i=1}^{N_l} \left(X_l^{(i)} - X_{l-1}^{(i)} \right), \tag{5}$$

$E[X_l - X_{l-1}]$ is approximated using the difference of expectation between coarse and fine level as $E[X_l^f - X_{l-1}^c]$. $E[X_l^f]$ and $E[X_{l-1}^c]$ are estimated using two different time-step sizes h_f and h_c, respectively [28]. where

$$h_f = 2^{-l}T, \tag{6}$$

$$h_c = 2^{-(l-1)}T. \tag{7}$$

On $l = 0$, a large and fixed value timestep is used to generate a large sample size N_0. This means that the coarsest level is the computationally cheapest level and the simulation time increases with the increase of level. The statistical properties of X_l are unchanged whether the estimation of $E[X_l - X_{l-1}]$ from level $(l-1)$ to l or $E[X_{l+1} - X_l]$ from l to $(l+1)$. This means that both $E[X_l - X_{l-1}]$ and $E[X_{l+1} - X_l]$ have the same expected value, i.e., $E[X_l^f] = E[X_l^c]$. The convergence criterion in the MLMC method depends on the desired RMSE value which can be expressed as follows:

$$\varepsilon^2 = \sum_{l=0}^{L} N_l^{-1} V_l + [E(X_a - X)]^2. \tag{8}$$

In order to obtain the value of $MSE \leq \varepsilon^2$, it is enough to ensure that both the estimated variance and approximation error are less than $\varepsilon^2/2$. The different number of samples N_l ensures that the variance of the MLMC estimator is less than $\varepsilon^2/2$. As the level l increases from the coarsest level and moves to finer level, number of samples on each level is decreased by setting an optimal N_l. The optimal N_l is chosen as [27]:

$$N_l = 2\varepsilon^{-2}\sqrt{V_l/C_l}\left(\sum_{l=0}^{L}\sqrt{V_l C_l}\right), \tag{9}$$

where the cost to compute one sample on the level l is $C_l = c_3 2^{\gamma l}$ for a constant c_3 and some $\gamma > 0$. γ is the rate of computation cost increase with level l.

In the case of weak convergence, the test tries to confirm that $[E(X_a - X)]^2 \leq \varepsilon^2/2$. Consider, the convergence rate of $E(X_a - X)$ with l for constant c_1 is measured by a positive value α, i.e., $|E[X_l - X_{l-1}]| \leq c_1 2^{-\alpha l}$ [27]. The remaining error is $E(X_a - X) = E[X_L - X_{L-1}]/(2^{\alpha} - 1)$ and the target convergence criterion is $E[X_L - X_{L-1}]/(2^{\alpha} - 1) < \varepsilon/\sqrt{2}$. β is assumed as the convergence rate of variance with l for a constant c_2 i.e., $V_\ell \leq c_2 2^{-\beta l}$. For a constant c_4, the computational complexity C of the MLMC estimator is bounded as follows [27]:

$$E[C] \leq \begin{cases} c_4\varepsilon^{-2}, & \beta > \gamma, \\ c_4\varepsilon^{-2}(log\varepsilon)^2, & \beta = \gamma, \\ c_4\varepsilon^{-2-(\gamma-\beta)/\alpha,} & \beta < \gamma. \end{cases} \quad (10)$$

III. Proposed methodology

The description of the proposed methodology can be presented as follows:

1. Read all the feeder length, failure and repair time data of components. Some simulation parameters are also defined: sample size for MLMC convergence (N), initial sample size (N_{in}), accuracy level (ε), drift (μ) and volatility (σ). μ is the rate of change of average value of stochastic process and σ is the degree of variation of stochastic process over time.

2. Generate artificial uptime and downtime histories of components. The variables FT and RT of each component are considered to be distributed using exponential probability function as (11) and (12), respectively.

$$T_{ui} = -1/\lambda_i \times ln(U), \quad (11)$$

$$T_{di} = -r_i \times ln(V), \quad (12)$$

where T_{ui} and T_{di} are the uptime and downtime histories of a component I (P_i), respectively. λ_i is the mean failure rate (FR) (failure/year) and r_i is mean RT (hour/failure) of P_i. U, V are uniformly distributed random variables between [0, 1].

3. Construct the stochastic differential equations (SDEs) of FT and RT on $l \geq 0$. We propose to model SDE by the Brownian motion due to its simplest form [29]. If $S_{\lambda i(t)}$ is the FT of P_i at a time t, then SDE model of FT with defined μ, σ and an initial FT [$S_{\lambda i(0)} = 1/\lambda_i$] can be written using the Brownian motion, W on the whole time interval $[0, T]$ [30] as:

$$dS_{\lambda i(t)} = \mu\left[S_{\lambda i(t)}, t\right]dt + \sigma\left[S_{\lambda i(t)}, t\right]d\mathrm{W} \quad (13)$$

4. Solve the SDE by Milstein discretisation which is proposed for this study [28]. The discretisation scheme with n timesteps, step size $h = T/n$ and Brownian increments ΔW_m can be written as:

$$S_{\lambda i(m+1)} = S_{\lambda i(m)} + \mu\left[S_{\lambda i(m)}, t_m\right]h + \sigma\left[S_{\lambda i(m)}, t_m\right]\Delta W_m + \frac{1}{2}\sigma^2\left[S_{\lambda i(m)}, t_m\right](\Delta W_m^2 - h), \quad (14)$$

where $\Delta W_m = W_{m+1} - W_m \ \ [m = 0, \dots\dots, n-1]$; $t_m = kh \ \ [k = 0, \dots\dots, n]$. ΔW_m are independent and normally distributed random variables.

5. Express the T_{ui} in (11) using the SDE model (14) of FT as:

$$T_{ui} = -S_{\lambda i(m+1)} \times ln(U), \tag{15}$$

Similarly, T_{di} can be determined using SDE model of RT. For RT modeling, μ and σ values are assumed equal as FT model. For simplification, we model the RT as a function of $S_{\lambda i}$. If q_i is a constant for P_i and $q_i = r_i \times \lambda_i$, then initial RT of P_i is q_i/λ_i. T_{di} can be therefore expressed as:

$$T_{di} = -q_i \times S_{\lambda i(m+1)} \times ln(V), \tag{16}$$

6. Calculate average AU (B_i) of P_i as follows

$$B_i = \frac{\sum_{n=1}^{N} T_{di(n)}}{\sum_{n=1}^{N} T_{ui(n)} + \sum_{n=1}^{N} {}^{T_{di(n)}}/_{8760}}, \tag{17}$$

where N is the desired number of simulated periods.

7. Repeat steps (2)-(6) for each component failure in the EDS.

8. Find the affected LPs by each component failure by the direct method [31] and determine LP AU (U_j) as:

$$U_j = \sum_{i=1}^{n_i} B_i, \tag{18}$$

where n_i is the total number of component failures that interrupt the service of LPj.

9. Repeat steps (2)-(8) for each LP in the EDS and evaluate the proposed system RI as (19) and (20):

$$SAIDI = \frac{\sum Customer\ Interruption\ Durations}{Total\ Number\ of\ Customer\ Served} = \frac{\sum_{j=1}^{n_j} U_j N_{C_j}}{N_T}, \tag{19}$$

$$EENS = \sum Unsupplied\ Energy = \sum_{j=1}^{n_j} U_j L_{AV_j}. \tag{20}$$

where N_{C_j} and L_{AV_j} are the number of customers and average load at LPj, respectively. N_T and n_j are the total numbers of customers served and LPs in the EDS, respectively.

10. Calculate the sum of the system RI values on levels $l \geq 0$. Repeat the whole process until the number of samples is reached to *N*.

11. To test the convergence criterion, set a minimum finest level of the MLMC method on $L = 2$. Generate the numbers of samples N_s on levels $l = 0, 1, 2$ using N_{in}. Also, update the sum of the RI values on each level.

12. Determine the absolute average value of reliability index $m_l = |E[Z_l]|$ and variance $V_l = V[Z_l]$ on each level *l*.

13. Determine the optimal number of samples N_l on each level $l = 0, 1, \ldots\ldots, L$ based on (9). Compare the optimal N_l with the calculated N_s on that level. If $N_l > N_s$, determine extra samples on each level as required.

14. Update the m_l and V_l on each level. The optimal N_l on each level keeps $\sum_{l=0}^{L} N_l^{-1} V_l < \varepsilon^2/2$.

15. Test the weak convergence as mentioned in Section 2, which confirms the remaining bias error is smaller than $\varepsilon/\sqrt{2}$.

16. Set $L = L + 1$, if the bias error is greater than $\varepsilon/\sqrt{2}$. Repeat the simulation from the step (11) until the target level of accuracy is reached. Finally, compute the overall multilevel estimator for each system reliability index using (3).

IV. Test system

A network connected to Bus 4 (B4) of the Roy Billinton Test system (RBTS) [32] is proposed to conduct the research. The single line diagram of the test system is provided in Appendix A. RBTS B4 is a typical urban EDS with seven (F1-F7) main feeders. A primary feeder begins with a circuit breaker at the distribution substation and carries electricity to the customer load points through lateral section. A lateral section consists of fuse, line and low voltage transformer. The feeders (types and lengths), customers and load data of the EDS are taken from [33]. For investigating components importance by MLMC method, six case studies are carried out by varying the availability of the components as shown in Table I. Case A is assumed as a base Case or ideal Case. For both MC and MLMC methods, a target ε of 0.001 was specified. All simulations are performed with an Intel Core i7-4790 3.60 GHz processor.

TABLE I. TEST CASES

Case	Disconnecting switches (DS)	Fuses (F)	Alternative supply (AS)	Transformer(T) [restoration]
A	Yes	Yes	Yes	Replacement
B	Yes	Yes	Yes	Repairing
C	No	Yes	No	Repairing
D	Yes	No	Yes	Repairing
E	Yes	No	No	Repairing
F	No	No	No	Repairing

V. Test results

A. Effect of EDS Components Availability on Reliability Improvement

In this section, the effect of components availability on reliability improvement is discussed. The indices are evaluated using the MLMC method. The RI- SAIDI and EENS measure the average interruption duration that a customer will experience and total unsupplied energy over the course of a year, respectively. From (19) and (20), it can be seen that the values of RI vary with the AU of the connected supply points. The unavailability of a LP service depends on both FR and RT of components. Therefore, for a fixed number of customers, the value of SAIDI can be reduced by decreasing the number of interruptions or by shortening the interruption hours. For a fixed average load level, EENS can be improved in the same ways. A reduction in SAIDI and EENS magnitude indicate an improvement in the reliability level.

Fig. 1 shows how the SAIDI and EENS values increase from Case A to F. RI values and the percentage of increment of RI value with respect to the base Case A are shown here. The replacement of transformer takes less time than repairing, therefore the RI values in Case A are less than B. The comparison of Case B and D shows the effect of fuses when switches and alternative supplies are available. A significant amount of SAIDI and EENS are increased in Case D where the fuses are unavailable. Similarly, the comparison of Case C and F reveals the effect of fuses when there are no disconnecting switch and alternative supply in the EDS. It is found that SAIDI and EENS are reduced greatly in C where there is no fuse.

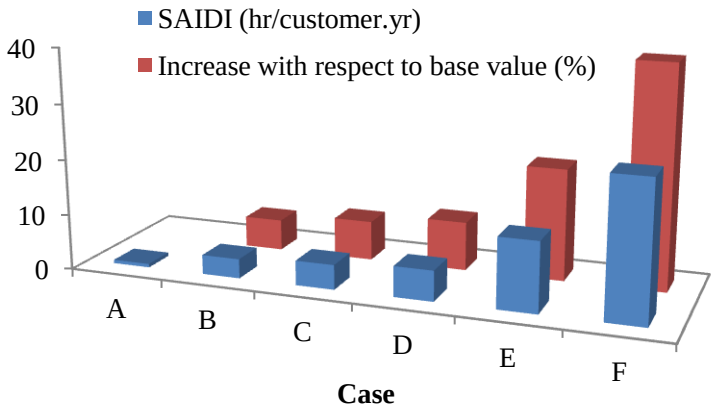

(a)

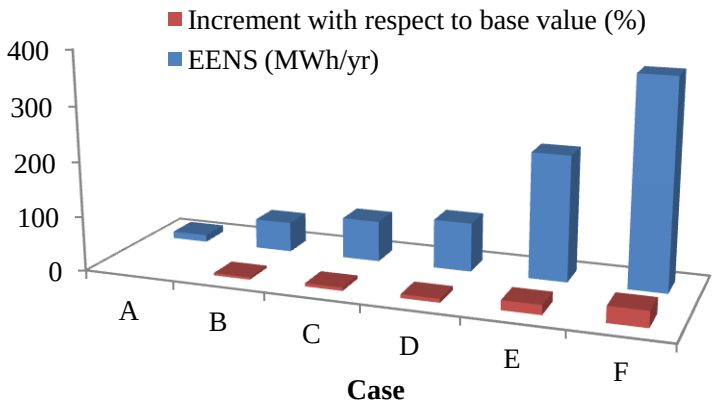

(b)

Fig. 1. Effect of components availability on system reliability indices magnitude (a) SAIDI and (b) EENS for the test cases and their respective percentage increase compared to base Case A value.

Case D and E present the effect of alternative supply when switches are available and the fuses are unavailable. The lack of alternative supply increases a large amount of SAIDI and EENS in Case E. Lastly, the comparative analysis of Case E and F present the effect of disconnecting switches when fuse and alternative supply are unavailable in the EDS. A reduction of SAIDI and EENS in Case E is noted by making available of switches.

TABLE II. EFFECT OF TRANSFORMER RESTORATION (DS, F & AS AVAILABLE)

Index	Case	MC	MLMC	C_{MC} [s]	C_{MLMC} [s]
SAIDI	A	0.6214 (0.1264)	0.6252 (0.7387)	0.7452	0.0228
	B	3.4648 (0.0124)	3.5054 (1.1592)	23.8602	0.8966
EENS	A	12.7401 (0.0018)	12.8683 (1.0044)	128.3440	7.5851
	B	54.2789 (0.0265)	54.8272 (0.9833)	3007.6355	180.5960
Units: SAIDI-hr/customer.yr and EENS- MWhr/yr for all calculations					

TABLE III. EFFECT OF LATERAL FUSES (DS & AS AVAILABLE)

Index	Case	MC	MLMC	C_{MC} [s]	C_{MLMC} [s]
SAIDI	B	3.4648	3.5054	23.8602	0.8966
	D	5.4417 (0.0536)	5.4986 (0.9914)	50.5225	2.4453
EENS	B	54.2789	54.8272	3007.6355	180.5960
	D	88.3791 (0.0453)	89.3202 (1.0190)	10113.6591	572.7638

TABLE IV. EFFECT OF LATERAL FUSES (DS & AS UNAVAILABLE)

Index	Case	MC	MLMC	C_{MC} [s]	C_{MLMC} [s]
SAIDI	C	4.4169 (0.0197)	4.4524 (0.7838)	25.1356	1.0281
	F	24.6349 (0.0446)	24.8734 (0.9231)	792.0293	48.0003
EENS	C	73.998 (0.0195)	74.7462 (0.9913)	6592.9041	244.5822
	F	373.9751 (0.0419)	377.7918 (0.9781)	200682.1171	13166.8712

TABLE V. EFFECT OF ALTERNATIVE SUPPLY (DS-AVAILABLE & F- UNAVAILABLE)

Index	Case	MC	MLMC	C_{MC} [s]	C_{MLMC} [s]
SAIDI	D	5.4417	5.4986	50.5225	2.4453
	E	12.4433 (0.05456)	12.5716 (0.9759)	246.1214	12.8689
EENS	D	88.3791	89.3202	10113.6591	572.7638
	E	225.9202 (0.0551)	228.3015 (0.9983)	75850.0544	3701.5146

TABLE VI. EFFECT OF DISCONNECTING SWITCHES (F & AS UNAVAILABLE)

Index	Case	MC	MLMC	C_{MC} [s]	C_{MLMC} [s]
SAIDI	E	12.4433	12.5716	246.1214	12.8689
	F	24.6349	24.8734	792.0293	48.0003
EENS	E	225.9202	228.3015	75850.0544	3701.5146
	F	373.9751	377.7918	200682.1171	13166.8712

B. Analysis of Components Availability Effect on System Reliability Evaluation through MLMC Method

The results showing the reliability evaluation accuracy and time for all the cases using both methods are shown in Tables II-VI. The values inside the first bracket are the percentage of absolute values of the evaluation errors by MC (E_{MC}) and MLMC (E_{MLMC}) which are computed by comparing with the analytical values. C_{MC} and C_{MLMC} are the required CPU time in second (s), by the MC and MLMC methods, respectively. Speedup rate of the MLMC based reliability evaluation is calculated as follows:

$$Speedup = \frac{C_{MC} - C_{MLMC}}{C_{MC}} \times 100\% \tag{23}$$

1) Case A

In Case A, we consider the availability of switches, fuses, alternative supply and replacement of transformers. The maximum E_{MLMC} value is 1.0044% [EENS]. As expected, the MC method needs the maximum CPU time of 2.1390 min for EENS calculation while MLMC needs only 7.5851 s. So, there is speedup around 90.6679% when compared with the MC.

2) Case B

The difference between Case A and B is transformer action restoration process. In Case B, transformer action is restored by repairing rather than replacing. The maximum E_{MLMC} in MLMC is 1.1592% [SAIDI]. The MC and MLMC methods spent the maximum CPU time of 50.1272 min and 3.0099 min [EENS] for this Case, respectively. Therefore, the computation speedup using MLMC is around 93.9954%.

3) Case C

In Case C, the unavailability of disconnecting switches and alternative supply is considered. The maximum E_{MLMC} value is 0.9913% [EENS]. For this Case, the MC and MLMC algorithms spent the maximum CPU time of 1.8313 hr and 4.0763 min, respectively. Therefore, the speedup of the proposed method in relation to the MC is around 96.2902%. As it could be expected, the system reliability is deteriorated in Case C and the CPU time increases.

4) Case D

The difference between Case B and D is the unavailability of fuses in Case D. The maximum E_{MLMC} value is 1.0190% [EENS]. The MC algorithm spent the maximum CPU time of 2.8093 hr. The MLMC method spent 9.5460 min and speedup is around 94.3367%.

5) Case E

In Case E, the unavailability of alternative supply is considered. The maximum E_{MLMC} value is 0.9983% [EENS]. The MC algorithm spent the maximum CPU time of 21.0694 hr [EENS]. The MLMC method spent 1.0281 hr and speedup is around 95.1199%.

6) Case F

The difference between Case B and F is the unavailability of disconnecting switches, fuses and alternative supply in Case F. The maximum E_{MLMC} value is 0.9781% [EENS]. The MC method spent the maximum CPU time of 55.7450 hr for this Case. The MLMC method spent 3.6574 hr and speedup in relation to the MC is around 93.4389%.

C. Analysis of Components Availability Effect on Feeder Reliability Evaluation through MLMC Method

By using MLMC method, the RI value for each feeder of the test system for all the cases and their CPU time is shown in Fig. 2. The specified feeder SAIDI and EENS increase gradually from Case A to F. The RI of a feeder depends on the reliability performance of the connected LPs. The low values of SAIDI and EENS of the feeders are due to the reduction of connected components outage times and the exclusion of LP transformers. For F2, F5 and F6, RI values are equal because of having the same connected components. Due to the effect of random variables, very small fractional difference among these is noticed. The analysis of components availability effect on feeder based reliability evaluation also takes less time through using MLMC method and the estimated RI values of feeders are very close to the true (analytical) values for all the cases.

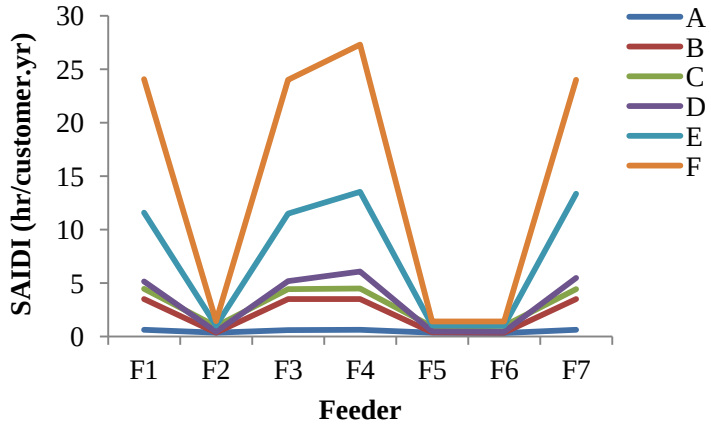
SAIDI (hr/customer.yr)
30
25
20
15
10
5
0
F1
F2
F3
F4
F5
F6
F7
Feeder
A
B
C
D
E
F

(a)

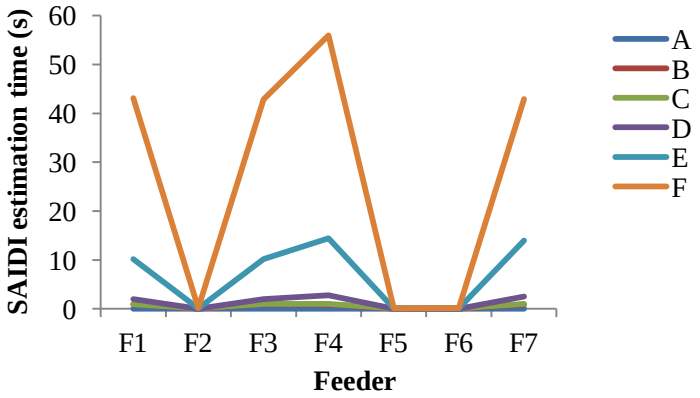
SAIDI estimation time (s)
60
50
40
30
20
10
0
F1
F2
F3
F4
F5
F6
F7
Feeder
A
B
C
D
E
F

(b)

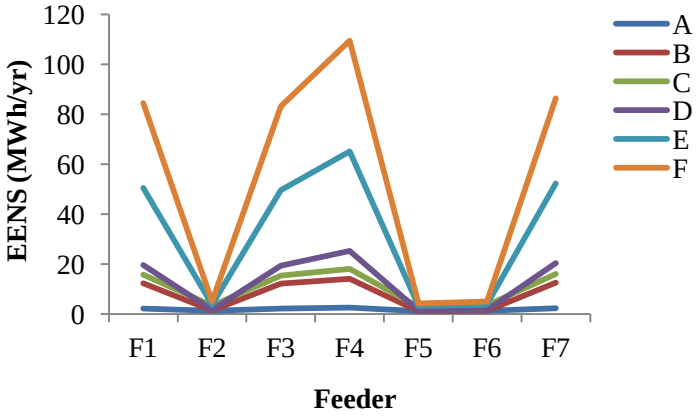
EENS (MWh/yr)
120
100
80
60
40
20
0
F1
F2
F3
F4
F5
F6
F7
Feeder
A
B
C
D
E
F

(c)

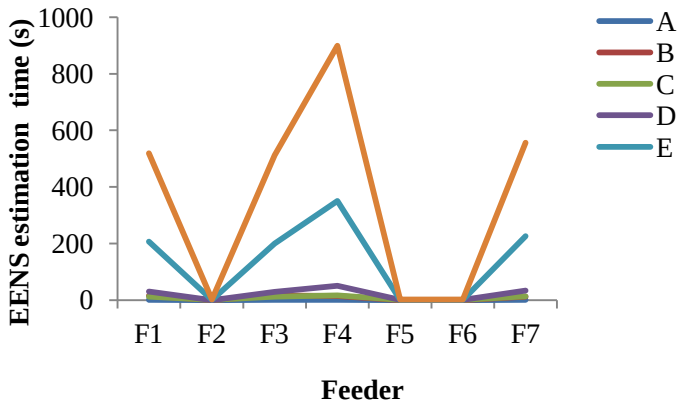

(d)

Fig. 2. Effect of components availability on the feeders reliability indices and their MLMC based computation performance (a) SAIDI and (b) its calculation time; (c) EENS and (d) its calculation time

D. Analysis of Components Availability Effect on Customer Sector Reliability Evaluation through MLMC Method

According to the customer sector, the RI values for the six cases and their CPU times are shown in Fig 3. Three types of customers are connected to the network: small user (SM), residential (RS) and commercial (CM). It can be seen that the specified sector SAIDI and EENS increase gradually from Case A to F. The reliability of a customer sector depends on the reliability performance of its connected LPs. The sequence of increasing SAIDI and EENS values for most of the cases of a specific case is according to SM<RS<CM. The low values of SAIDI and EENS in the SM sector are due to the reduction of connected components outage times and the exclusion of transformers serving at the SM users. From the results, it can be seen that the RI values calculated by the proposed method are very close to the actual values and computation cost is reasonable.

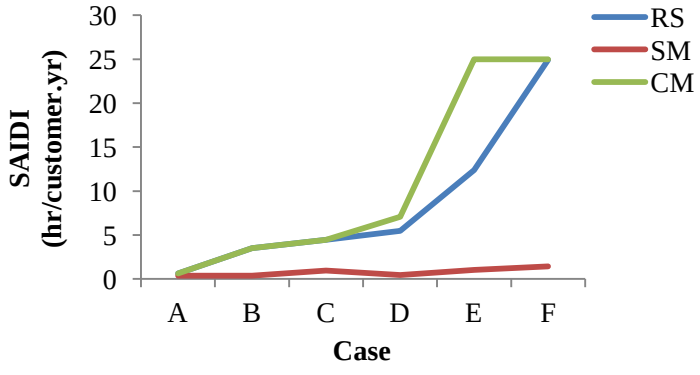

(a)

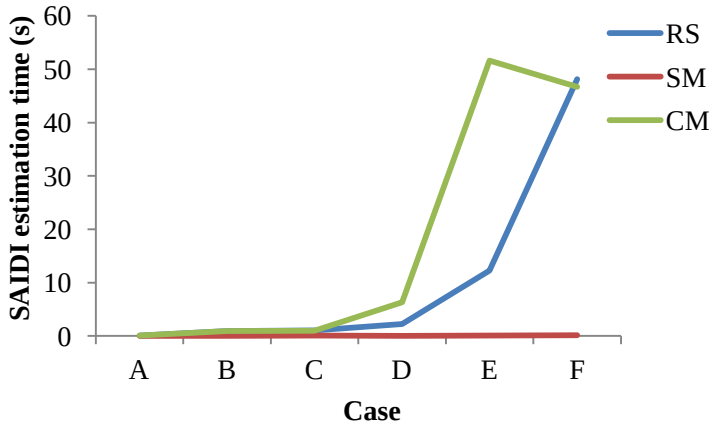

(b)

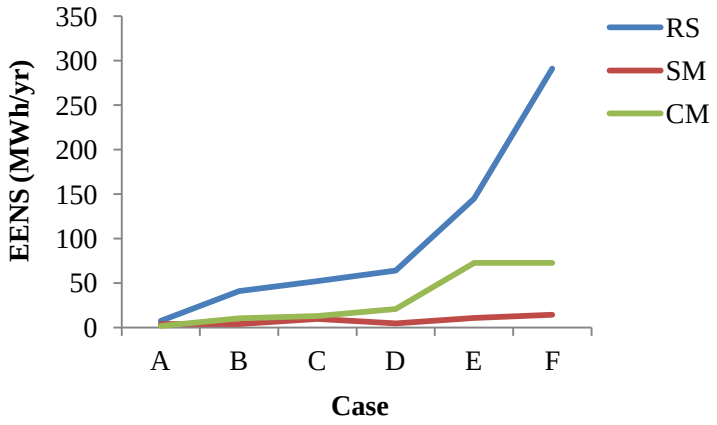

(c)

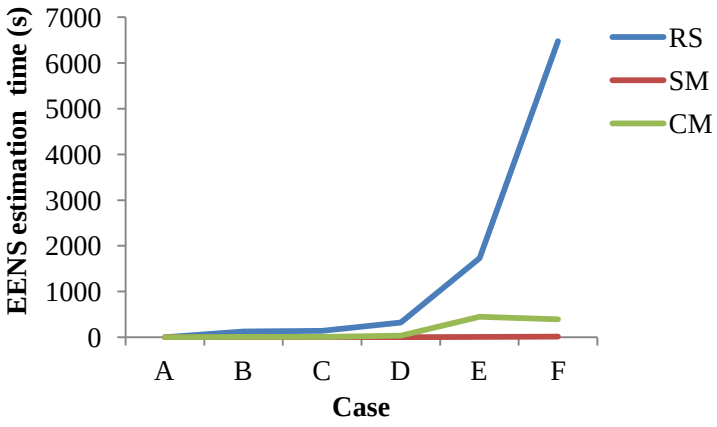

(d)

Fig. 3. Effect of components availability on the sector-wise reliability indices and their MLMC based computation performance (a) SAIDI and (b) its calculation time; (c) EENS and (d) its calculation time

V. Simulation time reduction by MLMC method

MLMC method controls the computational complexity in three ways [27]. In case of $\beta < \gamma$, the number of samples required by the estimator decays at a slower rate than the increase of the sampling cost at each level. Therefore, the overall cost is proportional to the cost of the finest grid level. When $\beta = \gamma$, the decay of the variance is balanced with the increase of the cost; therefore the contribution to the overall cost is the same from all the levels. Finally, when $\beta > \gamma$, the overall cost is dominated by the level $l = 0$, since consecutive levels will have a decaying contribution to the cost. In the proposed study- α, β and γ are not pre-defined and estimated by linear regression [27]. In all the cases of this study, the last criterion $\beta > \gamma$ is satisfied.

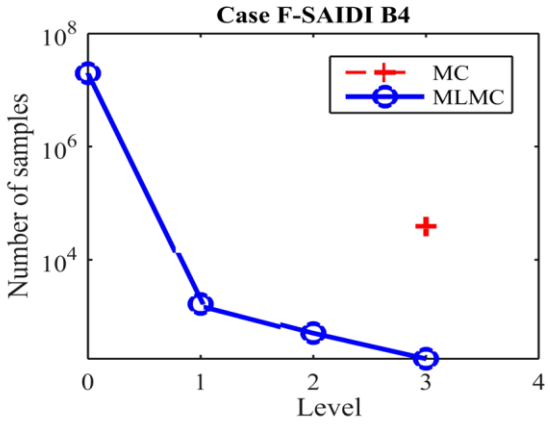

(a)

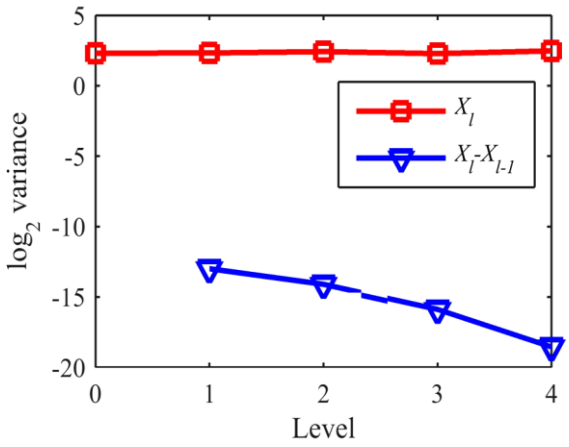

(b)

Fig. 4. (a) Number of required samples in MC and MLMC methods for Case F- SAIDI calculation and (b) variance reduction for this estimation while considering X_l and $X_l - X_{l-1}$.

Fig. 4(a) shows how MLMC saves CPU time compared to MC. In MLMC, the samples are executed from level $l = 0$ to $l = 3$. A total of 1.9919E+07 samples is required to achieve the convergence. From this total, about 1.9916E+07 samples are simulated on level $l = 0$, which is the computationally cheapest level. On the most expensive finest level $l = 3$, only 176 samples are executed. On the other hand, in MC, all the samples (38616) are simulated on the same finest grid level $l = 3$. In this way, MLMC method can reduce the samples on the finest grid level compared to MC method. Thus, MLMC requires less computation time than MC method.

Fig. 4(b) illustrates the benefits of using the difference of estimation $X_l - X_{l-1}$ rather than X_l only. As the grid level increases, the variance closes to the target convergence and therefore, the number of required samples on the next levels is decreased.

VI. Sensitivity analysis

A. Effect of Feeder Length on Computation

The length of a feeder is an important factor for calculating the RI. In an EDS, different types of feeders based on their length are used. Long length feeder decreases the reliability of EDS when compared to the short length feeder. For example, Table VII presents the results of system reliability of Case B by varying one feeder length in km. It can be seen that the system RI values and their calculation times increase gradually when the feeder length is increased.

TABLE VII. RELIABILITY PERFORMANCE BY VARYING FEEDER LENGTH

Length	**0.25**	**0.50**	**0.75**	**1.0**	**1.75**
SAIDI	3.4257	3.4751	3.5224	3.564	3.6608
T_{SAIDI} [s]	0.8549	0.8323	0.8797	0.8758	0.8847
EENS	53.1956	54.3704	55.5497	56.7259	59.0729
T_{EENS} [s]	179.4868	180.5613	181.6470	182.4712	186.2385
T_{SAIDI} and T_{EENS} are MLMC based estimation time of SAIDI and EENS					

B. Effect of Component Failure Rate on Computation

To illustrate the effect of component FR on reliability evaluation, the value of FR of a distribution line varied from 0.025 to 0.15 (interruption/yr). For instance, Table VIII shows the impact of the component FR on the system RI of Case B.

TABLE VIII. RELIABILITY PERFORMANCE BY VARYING FAILURE RATE

FR	**0.025**	**0.05**	**0.075**	**0.10**	**0.15**
SAIDI	3.4357	3.4655	3.5147	3.543	3.6355
T_{SAIDI}[s]	0.8484	0.8824	0.8763	0.8574	0.8731
EENS	53.1033	54.1905	55.2776	56.3637	58.5355
T_{EENS}[s]	179.7390	181.1427	183.4522	181.7587	184.3109

The system RI and their calculation time increase with the increase of component FR. The relationship between the component FR and system RI is almost linear for a specific case study.

C. Effect of Transformer Repair Time on Computation

In an EDS, restoration process of transformer action is an important factor to improve reliability. In order to examine the effect of transformer repair time (TRT), we varied TRT from 100 to 300 hours for Case B RI calculation. From Table IX, it is seen that the system RI and their calculation time increase at a fast rate as the TRT increases. The effect of TRT on reliability evaluation is high when compared to the FR and feeder length. This is due to the large value to TRT.

TABLE IX. RELIABILITY PERFORMANCE BY VARYING TRANSFORMER REPAIR TIME

TRT	**100**	**150**	**200**	**250**	**300**
SAIDI	1.9719	2.7446	3.5054	4.2589	5.0184
T_{SAIDI} [s]	0.2328	0.6785	0.8966	1.3209	1.9428
EENS	32.7519	43.7988	54.8272	65.8674	76.91
T_{EENS} [s]	48.5787	157.8696	180.5960	280.3414	401.2985

D. Effect of μ and σ Variation on Computation

In this section, we demonstrate the effects of μ and σ on RI evaluation accuracy and time. We evaluate the impacts of both parameters into three ways: 1) variation of μ, 2) variation of σ and 3) variation of both μ and σ simultaneously. For example, we consider the EENS evaluation of the Case A. The graphical representation of the effect of μ on parameters α, β, γ and EENS evaluation is shown in Fig. 5(a). From Fig., it is seen that initially the value of α is low with the decrease of μ, and after this the value of α increases and reaches a peak value. Then it continues decreasing with the increase of μ. The β value decreases gradually with μ increases. This suggests that the values of α and β are influenced by the selection of μ. Fig. 5(a) also shows that both the computation time and value of EENS decreases slowly with the increase of μ, but with acceptable value of the index.

Similarly, the effect of the σ on the parameters α, β, γ and EENS evaluation can be shown in Fig. 5(b). From Fig., it can be seen that, initially, the variance decay rate β decreases with the decrease of σ and after β reaches a peak value, it again starts to decrease with the increase of σ. Fig. also shows that the computation time and value of EENS increases gradually with the increase of σ. Fig. 5(c) shows the combined effect of μ and σ on EENS evaluation. It shows that the combined increasing values of μ and σ gradually decreases the value of β. Therefore, index value and its evaluation time also increase.

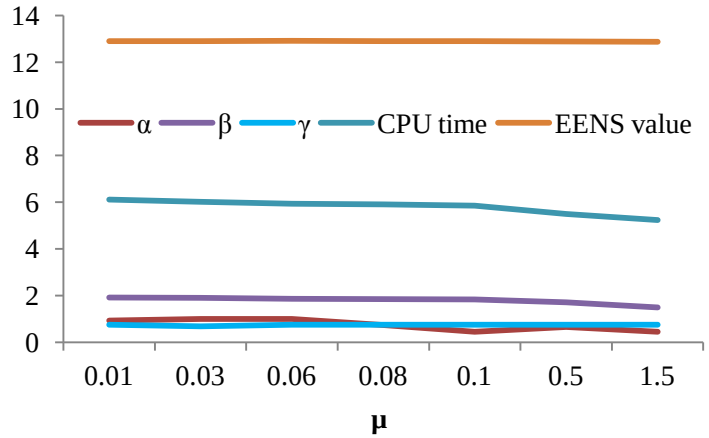

(a)

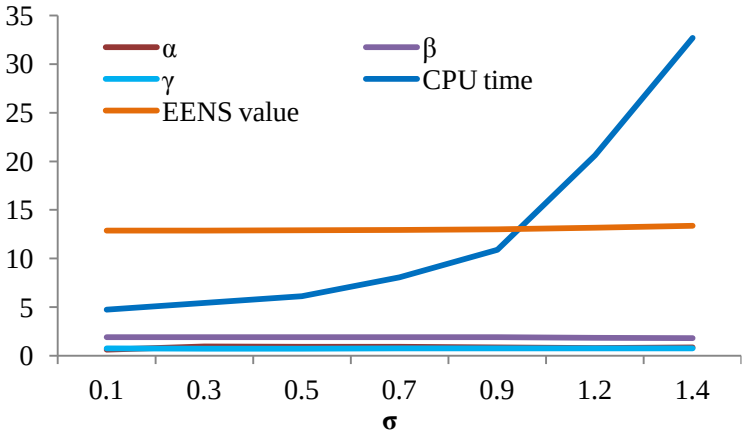

(b)

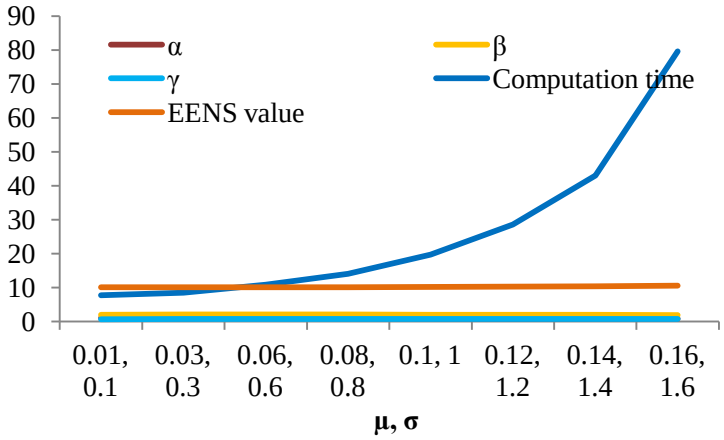

(c)

Fig. 5. An illustration of α, β, γ, EENS magnitude and computation time variation for given (a) μ (b) σ and (c) μ, σ.

E. Effect of ε and N_{in} on Computation

For higher accuracy with smaller ε values, each level needs a large number of samples than lower accuracy levels [32]. The value of N_l decreases as the level l increases for a desired accuracy level. The sample size N_l for each level decreases with the decreasing accuracy level ε. The decrease rate of N_l is about a constant independent of the accuracy level which relies on the variance decay rate β and the cost increase rate γ as indicated in Section 2. Fig. 6 shows the graphical representation of number of samples variation with level at different accuracy levels. The Fig. indicates that for higher accuracy with smaller ε values, each level needs a large number of samples. For example, when ε = 0.01, three levels are needed and the number of samples on the highest level ($l = L = 3$) is just 364; when accuracy level increases to ε = 0.0005, the number of samples on the highest level increases significantly to 200,000.

In addition, the accuracy of the estimate of V_l at each level depends on the size of the initial sample size N_{in}. The large the sample size, the more accurate the estimate and in the meantime the larger the computational cost. It is possible that for a large value of ε, the value of N_{in} at a higher level L may be larger than necessary and could cause a waste of computational time. So it is suggested to adjust the N_{in} based on the user specified ε.

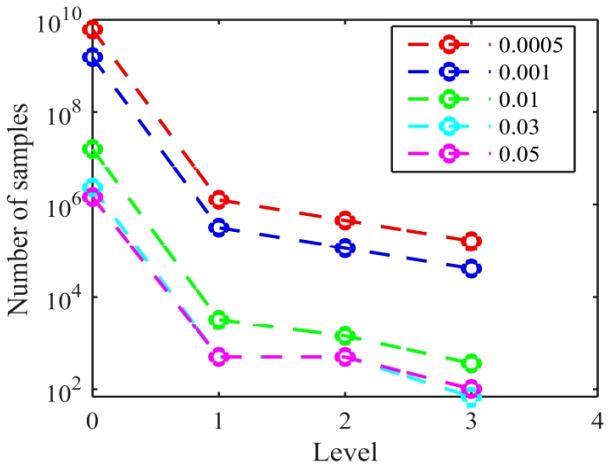

Fig. 6. Number of samples variation with level at different accuracy levels

VII. Conclusions

The paper presents a computation framework based on Multilevel Monte Carlo approach to show how the distribution networks topologies and components availability choices influence the distribution system, feeder and customer sectors reliability. For this purpose, the availability and unavailability of some protective equipment and alternative supply are considered. The RBTS B4 distribution system was used as a test system. Using the modification of this system, six different case studies were considered to compare the impact of components availability choices on reliability evaluation. The assessment results are based on the prediction of two commonly used reliability indices: SAIDI and EENS. The indices are chosen for the illustrative purpose. Usually, the same approach could be applied to evaluate the other indices.

Components availability has a great impact on system reliability. Higher availability reduces the interruptions. The results show that the addition of disconnecting switches, fuses and alternative supply source significantly improves the reliability of a system. Long duration of transformer repair has a great impact on customer interruption time.

Application of a novel MLMC method is proposed as an improvement over MC method. The performance of the proposed approach compared with MC method reveals that huge speed-ups are achieved in CPU time, with vast reductions in the number of samples in the fine grid levels required for convergence. Presented test results prove that the MLMC method could be effectively used for the proposed distribution system reliability study. In the future paper to finalize the proposed methodology, we will present a method on

probability density estimation in reliability studies using MLMC simulation based on Maximum Entropy method [34].

Appendix A

Single line diagram of the RBTS Bus 4 [32, 33]

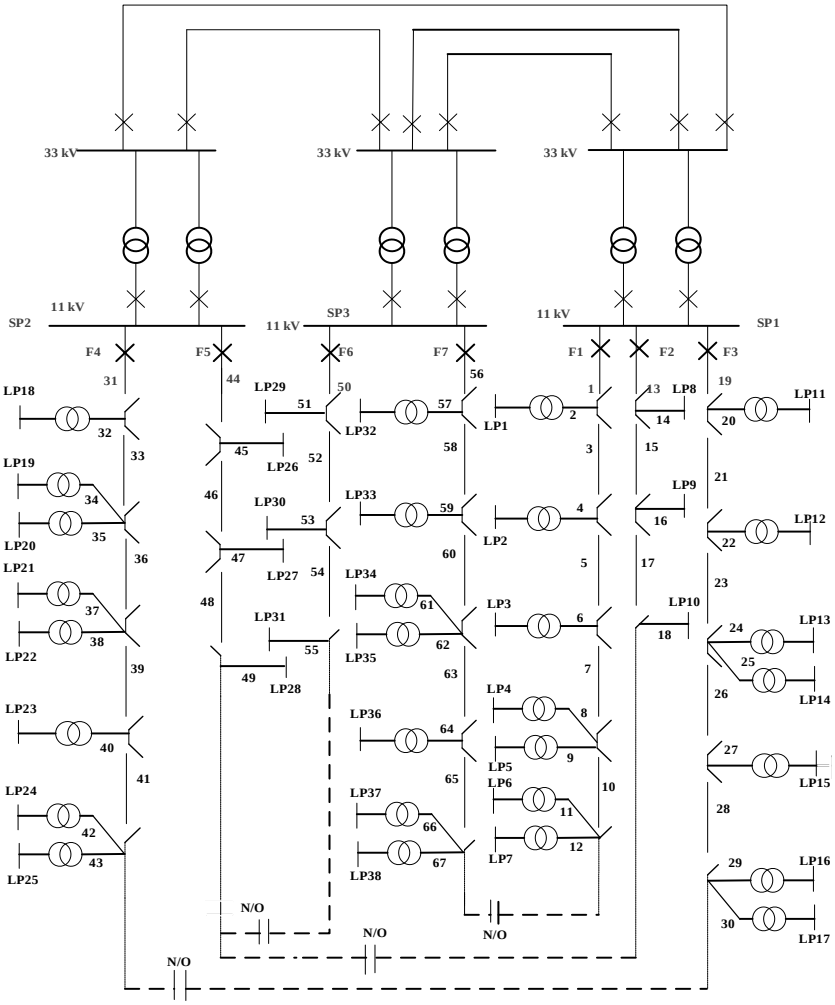

References

[1] H. L. Willis, Power distribution planning reference book: CRC press, 2004.

[2] W. Kuo and X. Zhu, "Relations and generalizations of importance measures in reliability," *IEEE Trans. Rel.*, vol. 61, pp. 659-674, 2012.

[3] J. Freixas and M. Pons, "Identifying optimal components in a reliability system," *IEEE Trans. Rel.*, vol. 57, pp. 163-170, 2008.

4] A. Heidari, Z. Dong, D. Zhang, P. Siano, and J. Aghaei, "Mixed-Integer Nonlinear Programming formulation for Distribution Networks Reliability Optimization," *IEEE Trans. on Ind. Informat.*, 2017.

[5] W. Li, Risk Assessment of Power Systems: Models, Methods, and Applications, 2005, IEEE Press/Wiley.

[6] H. Mirsaeedi, A. Fereidunian, S. M. Mohammadi-Hosseininejad, P. Dehghanian, and H. Lesani, "Long-Term Maintenance Scheduling and Budgeting in Electricity Distribution Systems Equipped with Automatic Switches," *IEEE Trans. on Ind. Informat.*, 2017.

[7] V. Calderaro, V. Lattarulo, A. Piccolo, and P. Siano, "Optimal switch placement by alliance algorithm for improving microgrids reliability," *IEEE Trans. on Ind. Informat.*, vol. 8, pp. 925-934, 2012.

[8] E. Zio, L. Podofillini, and G. Levitin, "Estimation of the importance measures of multi-state elements by Monte Carlo simulation," *Rel. Eng. Syst. Safety.*, vol. 86, pp. 191-204, 2004.

[9] P. Jirutitijaroen and C. Singh, "Comparison of simulation methods for power system reliability indexes and their distributions," *IEEE Trans. Power Syst.*, vol. 23, pp. 486-493, 2008.

[10] T. J. Dodwell, C. Ketelsen, R. Scheichl, and A. L. Teckentrup, "A hierarchical multilevel Markov chain Monte Carlo algorithm with applications to uncertainty quantification in subsurface flow," *SIAM/ASA J. Uncertainty Quantification*, vol. 3, pp. 1075-1108, 2015.

[11] R. Billinton and A. Jonnavithula, "Composite system adequacy assessment using sequential Monte Carlo simulation with variance reduction techniques," *IEE Proc.-Gener. Transm. Distrib.*, vol. 144, pp. 1-6, 1997.

[12] C. Singh and J. Mitra, "Composite system reliability evaluation using state space pruning," *IEEE Trans. Power Syst.*, vol. 12, pp. 471-479, 1997.

[13] K. Hou, H. Jia, X. Xu, Z. Liu, and Y. Jiang, "A continuous time Markov chain based sequential analytical approach for composite power system reliability assessment," *IEEE Trans. Power Syst.*, vol. 31, pp. 738-748, 2016.

[14] R. A. González-Fernández and A. M. L. da Silva, "Reliability assessment of time-dependent systems via sequential cross-entropy Monte Carlo simulation," *IEEE Trans. Power Syst.*, vol. 26, pp. 2381-2389, 2011.

[15] Y. Wang, C. Guo, and Q. Wu, "A cross-entropy-based three-stage sequential importance sampling for composite power system short-term reliability evaluation," *IEEE Trans. Power Syst.*, vol. 28, pp. 4254-4263, 2013.

[16] A. S. N. Huda and R. Zivanovic, "Accelerated distribution systems reliability evaluation by multilevel monte carlo simulation: implementation of two discretisation schemes," *IET Gener. Transm. Distrib.*, vol. 11, pp. 3397-3405, 2017.

[17] A. M. L. da Silva, R. A. Fernandez, and C. Singh, "Generating capacity reliability evaluation based on Monte Carlo simulation and cross-entropy methods," *IEEE Trans. Power Syst.*, vol. 25, pp. 129-137, 2010.

[18] A. M. L. da Silva, R. A. González-Fernández, W. S. Sales, and L. A. Manso, "Reliability assessment of time-dependent systems via quasi-sequential Monte Carlo simulation," in *Proc. IEEE 11th Int. Conf. Probabilistic Methods Applied to Power Systems (PMAPS), 2010*, pp. 697-702.

[19] R. González-Fernández and A. L. Da Silva, "Comparison between different cross-entropy based methods applied to generating capacity reliability," in *Proc. IEEE 12th Int. Conf. Probabilistic Methods Applied to Power Systems (PMAPS)*, 2012, pp. 10-14.

[20] A. L. Da Silva, L. D. F. Manso, J. D. O. Mello, and R. Billinton, "Pseudo-chronological simulation for composite reliability analysis with time varying loads," *IEEE Trans. Power Syst.*, vol. 15, pp. 73-80, 2000.

[21] R. A. González-Fernández, A. M. L. da Silva, L. C. Resende, and M. T. Schilling, "Composite systems reliability evaluation based on Monte Carlo simulation and cross-entropy methods," *IEEE Trans. Power Syst.*, vol. 28, pp. 4598-4606, 2013.

[22] E. Tómasson and L. Söder, "Improved Importance Sampling for Reliability Evaluation of Composite Power Systems," *IEEE Trans. Power Syst.*, vol. 32, pp. 2426-2434, 2017.

[23] B. Hua, Z. Bie, S.-K. Au, W. Li, and X. Wang, "Extracting rare failure events in composite system reliability evaluation via subset simulation," *IEEE Trans. Power Syst.*, vol. 30, pp. 753-762, 2015.

[24] G. T. Heydt and T. J. Graf, "Distribution system reliability evaluation using enhanced samples in a Monte Carlo approach," *IEEE Trans. Power Syst.*, vol. 25, pp. 2006-2008, 2010.

[25] F. Li, "A fast approach of Monte Carlo simulation based on linear contribution factors to distribution reliability indices," in *Proc. IEEE PES Transmission and Distribution Conf. and Exposition, 2003*, pp. 973-977.

[26] R. Arya, A. Tiwary, S. Choube, and L. Arya, "A smooth bootstrapping based technique for evaluating distribution system reliability indices neglecting random interruption duration," *Int. J Electr. Power Energy Syst.*, vol. 51, pp. 307-310, 2013.

[27] M. B. Giles, "Multilevel monte Carlo path simulation," *Oper. Res.*, vol. 56, pp. 607-617, 2008.

[28] M. Giles, "Improved multilevel Monte Carlo convergence using the Milstein scheme," in Monte Carlo and quasi-Monte Carlo methods 2006, Springer, 2008, pp. 343-358.

[29] J. M. Harrison, Brownian motion and stochastic flow systems, 1985, Wiley New York.

[30] B. Oksendal, Stochastic differential equations: an introduction with applications, 2013, Springer Science & Business Media.

[31] R. Billinton and P. Wang, "Teaching distribution system reliability evaluation using Monte Carlo simulation," *IEEE Trans. Power Syst.*, vol. 14, pp. 397-403, 1999.

[32] A. S. N. Huda and R. Živanović, "Multilevel Monte Carlo simulation applied to distribution systems reliability evaluation," in *Proc. IEEE Manchester PowerTech*, 2017, pp. 1-6.

[33] R. N. Allan, R. Billinton, I. Sjarief, L. Goel, and K. So, "A reliability test system for educational purposes-basic distribution system data and results," *IEEE Trans. Power Syst.*, vol. 6, pp. 813-820, 1991.

[34] C. Bierig and A. Chernov, "Approximation of probability density functions by the Multilevel Monte Carlo Maximum Entropy method, " *J. Comput. Phys.*, vol. 314, pp. 661-681, 2016.

Chapter 5

Interrupted Energy Estimation

Statement of authorship

Title of Paper	Estimation of Expected Energy Not Supplied considering Time-Varying Load Models by Multilevel Monte Carlo method: Effect of different factors on computation variation
Publication Status	☐ Published ☐ Accepted for Publication ☑ Submitted for Publication ☐ Unpublished and Unsubmitted w ork w ritten in manuscript style
Publication Details	A. S. Nazmul Huda and Rastko Živanović (2018) Estimation of Expected Energy Not Supplied considering Time-Varying Load Models by Multilevel Monte Carlo method: Effect of different factors on computation variation, Electric Power Components and Systems (Taylor & Francis). Revision submitted.

Principal author

Name of Principal Author (Candidate)	A. S. Nazmul Huda		
Contribution to the Paper	Developed reliability evaluation model, performed simulation and numerical analysis, prepared manuscript.		
Overall percentage (%)	80%		
Certification:	This paper reports on original research I conducted during the period of my Higher Degree by Research candidature and is not subject to any obligations or contractual agreements with a third party that would constrain its inclusion in this thesis. I am the primary author of this paper.		
Signature		Date	07.09.2018

Co-author contributions

By signing the Statement of Authorship, each author certifies that:

the candidate's stated contribution to the publication is accurate (as detailed above);

permission is granted for the candidate in include the publication in the thesis; and

the sum of all co-author contributions is equal to 100% less the candidate's stated contribution.

Name of Co-Author	Rastko Živanović		
Contribution to the Paper	Supervised for development of model, helped in data interpretation and manuscript evaluation		
Signature		Date	13.08.2018

Estimation of Expected Energy Not Supplied considering Time-Varying Load Models by Multilevel Monte Carlo method: Effect of different factors on computation variation

Abstract— The paper presents the estimation of power distribution systems Expected Energy Not Supplied (EENS) index by incorporating Time-Varying Load Models of different customer sectors. An application of a new and efficient advanced Monte Carlo simulation (MCS) with controllable accuracy called Multilevel Monte Carlo (MLMC) method is proposed for this estimation. The purpose of the proposed method is to increase the simulation speed of EENS estimation. The method could be easily replaced by the traditional MCS based estimation which requires huge computational effort for achieving high level of simulation accuracy.

Five distribution networks with seven different load models of Roy Billinton Test System are chosen as test distribution systems. To verify the effectiveness of the proposed method, computational time and estimated values of EENS using MLMC method are compared to the results from MCS. The computation performance of EENS estimation can be influenced by different factors and criteria which are also explored in this study. The results presented in the paper show that acceptable results can be obtained using the proposed method while substantial reduction of computational effort is also achieved.

Keywords— power distribution systems; Expected Energy Not Supplied; Time-Varying Load Models; Multilevel Monte Carlo simulation; Euler-Maruyama method.

1. Introduction

In distribution systems planning studies, customer expected interrupted energy is referred as the Expected Energy Not Supplied (EENS) index. Majority of the interruptions experienced by customers occur due to the distribution system components failures [1]. EENS index provides the information of the expected amount of energy shortage due to the failures in a specified time period [2, 3]. Based on the accurate estimation of the EENS index, appropriate planning and design initiatives could be implemented in the distribution systems for supplying cost-effective and reliable power to customers.

In reliability estimation including EENS estimation, two basic random variables are present i.e. Time-to-Failure (TTF) and Time-to-Repair (TTR) [4]. TTF is the expected time for a component to remain in the up state before it fails. TTR of a component is the

expected time required for a crew to repair an outage and restore the normal operation of the system. For accurate estimation, the uncertainties related to these variables are considered based on probability distribution. The accurate approximation of EENS also considers the Time-Varying Load Levels (TVLM) of different customer sectors such as residential, industrial and commercial, etc. Load level of a specific customer type usually fluctuates due to the discrepancy of the hourly load consumption level throughout a 24-hour period. In addition, seasonal inconsistency in the weather contributes prominently to loading level diversity [5].

For distribution system EENS estimation, two approaches are generally utilized, i.e. analytical and simulation approaches [6, 7]. Analytical approach calculates EENS by considering the constant specified values of random variables. On the other hand, simulation method mainly based on sequential Monte Carlo simulation (MCS) estimates the EENS by considering the probability distributions of these random variables which requires a large number of iterations depending on the target accuracy level, especially while dealing with the rare events [8]. Therefore, MCS is usually a time-consuming method. To increase the computational speed of MCS, numerous advanced MCS methods have been studied for power systems planning applications [9-12]. However, a small number of relevant studies have been conducted for distribution systems planning [13-15]. The review also shows that the result of system EENS estimation with the uncertainties of TTF and TTR through incorporating TVLM using any advanced MCS method has not been reported yet. For this reason, the novel application of an advanced MCS method called the Multilevel Monte Carlo (MLMC) simulation has been implemented and tested in this study in order to accelerate estimation process.

The MLMC method was first introduced by Heinrich for parametric integration [16] and then Giles extended the idea to the simulation of the stochastic process [17]. The fundamental improvement of the MLMC method is to utilize a hierarchy of discretisation levels and estimate expected value of a quantity of interest from a weighted sum of expectations over those levels. The optimized number of samples on each level is generated to run most of the simulations on the coarser levels with inexpensive forward computations. On the other hand, fewer samples are run on the more expensive finer resolution scales because of the smaller variances. By this approach, the MLMC method produces an unbiased estimator providing acceptable accuracy with considerably reduced computational effort than original MCS.

The first objective of this paper is to present the MLMC based estimation results of system EENS by incorporating different TVLM. We couple the Euler-Maruyama discretisation method with the MLMC method to develop a general framework for this estimation. The global load profiles of different customer sectors throughout a 24-hour period are taken into consideration for TVLM. The second objective is to explore the effect of various factors and criteria on computation performance such as failure starting time, failure duration, time-dependent load diversity factors, network complexity, systems reinforcement, target accuracy level and discretisation scheme. A benchmark Roy Billinton Test System (RBTS) of five different distribution systems connected to five load buses (B2-B6) [18] is selected to verify the efficiency of the suggested method. The purpose of testing the method on different systems is to find the effect of computation efficiency varying with the size and complexity of the systems as well as different TVLM. The outputs of the MLMC method are compared with the direct MCS from the accuracy and computational speed perspectives.

The outline of the remaining part of the paper is as follows. Section 2 describes the basic models to establish system EENS model. Section 3 presents proposed novel methods used in the EENS index estimation. Section 4 presents the simulation steps. Section 5 provides the description of the test systems and test results. In this section, effect of different factors on computation performance is analyzed. Finally, Section 6 concludes the paper.

2. Basic Models

2.1. Modelling of TTF

The uncertainty of EENS is basically characterized by two random variables in the estimation i.e., TTF and TTR. As described earlier, MLMC reduces the computational complexity of basic MCS through stochastic modelling of random variables. In this section, we represent the uncertainty of TTF using Stochastic Differential Equation (SDE). We consider the uncertainty of TTF of a component j (TTF_j) can be modelled by SDE which follows standard Brownian motion, B_t on the time interval $[0, T]$ [19]. The SDE of TTF_j with specified μ, σ parameters and an initial TTF_j can be expressed as [20]:

$$dS_{\lambda j(t)} = \mu[S_{\lambda j(t)}, t]dt + \sigma[S_{\lambda j(t)}, t]\, dB_t \quad 0 < t < T \tag{1}$$

where $S_{\lambda j(t)}$ is the mean value of TTF_j ($MTTF_j$) at a time t, μ is the rate of change of the average value of stochastic failure process (drift) and σ is the degree of variation of failure process over time (volatility).

In this study, we apply Euler-Maruyama discretisation method to solve the SDE in Eqn. (1). The method can approximate the numerical solution of the above SDE with a given initial value of $MTTF_j$. The solution of the above SDE using Euler-Maruyama method can be expressed as [21]:

$$S_{\lambda j(m+1)} = S_{\lambda j(m)} + \mu\left[S_{\lambda j(m)}, t_m\right]h + \sigma\left[S_{\lambda j(m)}, t_m\right]\Delta B_m \quad (2)$$

where n is the number of time-steps with size $h = T/n$ and ΔB_m are the Brownian increments. $\Delta B_m = B_{m+1} - B_m$ with $m = 0, \ldots\ldots, n-1$ and $t_m = kh$ with $k = 0, \ldots\ldots, n$. ΔB_m are independently and normally distributed random variables.

2.2. Time-Varying Load Models

Seven different loads connected to different test systems are considered in this study. In practice, most of the power industries accumulate load consumption data for a specified distribution zone depending on seasons and thus hourly load data for a selected customer sector are not available. Therefore, the global load profiles of different customer sectors are usually developed by taking into consideration of typical consumption cycles based on daily, weekly and annual load curves from the peak load demand of individual sector. This method is acceptable in the current study since it can present the difference between time-varying load model and constant load model based EENS estimation.

Let $L(t)$ be the load level of a load point (LP) at an hour t of a day. Then $L(t)$ can be modeled as follows [22]:

$$L(t) = L_{peak} \times W_l \times D_l \times H_l(t) \quad (3)$$

where L_{peak} is the annual peak load, W_l is the weekly peak load as a percentage of L_{peak}, D_l is the daily peak load as a percentage of weekly peak load and H_l is the hourly peak load as a percentage of daily peak load [23]. We consider three seasons in a year: summer, winter and fall/spring. Considering the conditions in Australia, the weeks represented by the seasons are summer weeks (1-8 & 48-52), winter weeks (20-36) and spring/fall weeks (9-19 & 37-47). Figs. 1(a) and 1(b) show the weekly and daily load curves, respectively.

Figs. 2(a)-(g) present the diversity of different load profiles throughout 24 hours on a weekday (Tuesday, week 27) of the winter season.

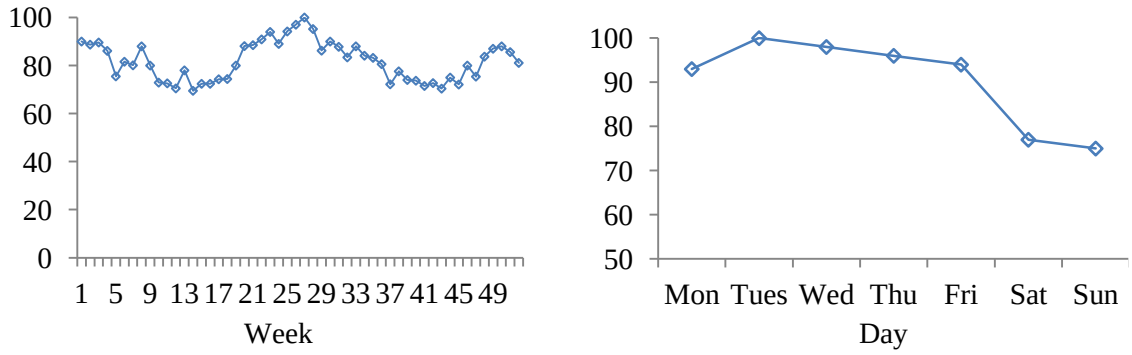

(a) (b)

Fig. 1 (a) Weekly load curve and (b) Daily load curve

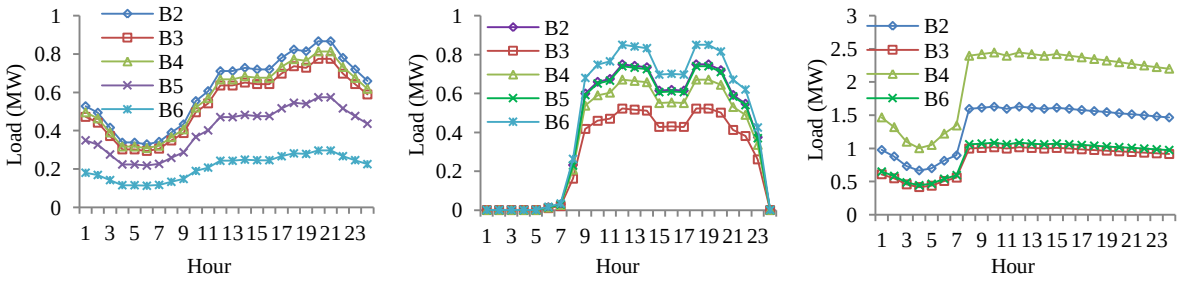

(a) Residential (b) Commercial (c) Industrial

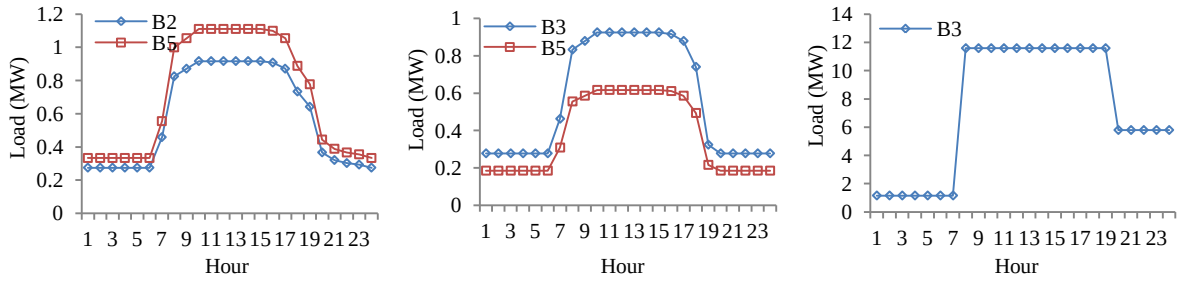

(d) Government and Institutional (e) Office buildings (f) Large users

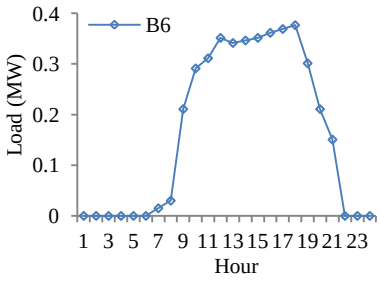

(g) Agricultural

Fig. 2. Daily load profile for different loads of distribution systems

3. MCS and MLMC method

3.1. MCS method

The standard MCS estimator using N_M number of independent samples is as follows [17]:

$$\hat{X}_{MC} = \frac{1}{N_M}\sum_{i=1}^{N_{MC}} Y_l^{(i)}. \tag{4}$$

where $Y_l^{(i)}$ is the *i*th sample of Y_l. Y is the EENS value of a distribution system. The expected value of the estimator is $\mathbb{E}[Y_l]$ and it is simulated on a finest level $l = L$. l is a nonnegative integer. The accuracy and computational burden of the estimation on this level are very high. The variance of the above estimator is $N_M^{-1}\mathbb{V}[Y_l]$. It requires $N_M = \mathbb{O}(\varepsilon^{-2})$ samples for an accuracy of ε (ε is the root mean square error) and computational burden is increased with the increase of target accuracy level.

3.2. MLMC method

The following sections describe how EENS evaluation estimators are constructed using MLMC method and then how the estimators satisfy the convergence condition.

3.2.1. Construct of MLMC estimator

The MLMC method is a variance reduction technique for the MCS. In this method, the system EENS is estimated using MCS with multiple time-step sizes defined as $h_l = 2^{-l}T$ as of Eqn. (2). Here $l = 0, 1, 2, \ldots\ldots, L$ with $l = 0$ being the computationally low-cost coarsest level and $l = L$ being the most expensive finest level. The fine $[Y_l^f]$ and coarse estimators $[Y_l^c]$ are calculated using time-step of $h_f = 2^{-l}T$ and $h_c = 2^{-(l-1)}T$,

respectively. The MLMC estimator is calculated as a sum of L level MCS estimator corrections as follows:

$$\hat{X}_{ML} = \sum_{l=0}^{L} \frac{1}{N_l} \sum_{i=1}^{N_l} \left(Y_l^{(i)} - Y_{l-1}^{(i)} \right). \quad (5)$$

where N_l is the number of samples on each level l.

The expected value of the MLMC estimator can be written as

$$\mathbb{E}[Y_L] = \mathbb{E}[Y_0] + \sum_{l=1}^{L} \mathbb{E}[Y_l - Y_{l-1}]. \quad (6)$$

The unbiased estimator of the term $\mathbb{E}[Y_0]$ is as follows:

$$\hat{X}_0 = \frac{1}{N_0} \sum_{i=1}^{N_0} Y_0^{(i)}, \quad (7)$$

The estimator for the $\mathbb{E}[Y_l - Y_{l-1}]$ can be calculated as:

$$\hat{X}_l = \frac{1}{N_l} \sum_{i=1}^{N_l} \left(Y_l^{(i)} - Y_{l-1}^{(i)} \right), \quad (8)$$

A geometric sequence of time-steps is used in the MLMC method as Eqn. (6) and therefore less accurate estimation on a level can be consecutively corrected by the subsequent fine levels estimations. This ensures the same value of EENS in the MLMC method as MCS. In addition, both coarse and fine estimators are calculated as $\mathbb{E}\left[Y_l^f\right] = \mathbb{E}[Y_l^c]$ to avoid undesired bias introduction and therefore,

$$\mathbb{E}\left[Y_L^f\right] = \mathbb{E}\left[Y_0^f\right] + \sum_{l=1}^{L} \mathbb{E}\left[Y_l^f - Y_{l-1}^c\right]. \quad (9)$$

3.2.2. Testing MLMC convergence

The accuracy of the MLMC estimator can be expressed as:

$$\varepsilon^2 = \mathbb{V}\left[\hat{X}_{ML}\right] + [\mathbb{E}(Y_L - Y)]^2, \quad (10)$$

where the variance of the MLMC estimator is $\mathbb{V}[\hat{X}_{ML}] = \sum_{l=0}^{L} N_l^{-1} \mathbb{V}[Y_l - Y_{l-1}]$.

The first and second terms in Eqn. (10) are the sampling error and bias error, respectively. In order to ensure accuracy of the MLMC estimator is less than ε^2, it is adequate to confirm that both sampling and bias errors are less than $\varepsilon^2/2$. If C_l is the computational cost of one sample of $[Y_l - Y_{l-1}]$, then the total expected cost of the MLMC estimator is

$C[\hat{X}_{ML}] = \sum_{l=0}^{L} N_l C_l$. To make sure the variance is smaller than $\varepsilon^2/2$, the optimal N_l is chosen as follows [17]:

$$N_l = 2\varepsilon^{-2}\sqrt{\mathbb{V}[Y_l - Y_{l-1}]/C_l}\left(\sum_{l=0}^{L}\sqrt{\mathbb{V}[Y_l - Y_{l-1}]C_l}\right). \quad (11)$$

If the convergence rate of $\mathbb{E}(Y_L - Y)$ with l for some constant c_1 is measured by a positive value α, then $|\mathbb{E}[Y_l - Y_{l-1}]| \leq c_1 2^{-\alpha l}$ [24]. The residual error is therefore $\mathbb{E}[Y - Y_L] = \mathbb{E}[Y_L - Y_{L-1}]/(2^{\alpha} - 1)$ and the weak convergence test satisfies the following condition.

$$|\mathbb{E}[Y_L - Y_{L-1}]|/(2^{\alpha} - 1) < \varepsilon/\sqrt{2}. \quad (12)$$

4. Simulation steps

The methodology for system EENS estimation considering TVLM is described in the following simulation steps. Steps (1) to (11) formulate the mathemical model of the estimation on the coarse and fine levels. From steps (12) to (17), the convergence test of the model is performed to meet the target accuracy level.

(1) Define the input data. The input data include failure rate, repair time of system component, peak load of each supply point L_{peak}, weekly (W_l), daily (D_l)and hourly (H_l) load diversity factors, number of samples for convergence test (N), initial number of samples on each level (N_a), drift value (μ), volatility (σ) and target accuracy level (ε).

(2) Construct SDE of $MTTF_j$ using Eqn. (1) and solve via Euler-Maruyama method on both coarse and fine level estimations as follows:

$$S^c_{\lambda j(m+1)} = S^c_{\lambda j(m)}\left[1 + \mu h_c + \sigma \Delta B_{c(m)}\right] \text{ and} \quad (13)$$

$$S^f_{\lambda j(m+1)} = S^f_{\lambda j(m)}\left[1 + \mu h_f + \sigma \Delta B_{f(m)}\right], \quad (14)$$

(3) Obtain artificial operating (T_{upj}) and restoration histories (T_{dnj}) of a component j using random number generators and exponential probability distribution as follows.

$$T_{upj} = -S_{\lambda j(m+1)} \times ln(u1), \quad (15)$$

$$T_{dnj} = -y_j \times S_{\lambda j(m+1)} \times ln(u2), \quad (16)$$

where y_j is a constant for component j and $y_j = r_j \times \lambda_j$. λ_j and r_j are the average failure rate and mean TTR of component j, respectively. u1 and u2 are uniformly distributed random variables between [0,1].

(4) Calculate annual unavailability, U_j (hr/yr) of component j on both levels as follows:

$$U_j = \frac{\sum_{n=1}^{N} T_{dnj(n)}}{\sum_{n=1}^{N} T_{upj(n)} + \sum_{n=1}^{N} {T_{dnj(n)}}/{8760}}, \tag{17}$$

where N is the desired number of simulated periods.

(5) Repeat the steps (2)-(4) for each distribution system component failure.

(6) Find the LPs affected by component j failure.

(7) Calculate annual unavailability, A_i of a load point i (LPi) on both levels by using sum of the unavailability values of all components connected to the LPi.

$$A_i = \sum_{j=1}^{n_j} U_j, \tag{18}$$

where n_j is the number of components failure that interrupt the service of LPi.

(8) Find the possible load profile for LPi based on Eqn. (3) during the outage period and calculate the average load level L_{ai} during this period.

$$L_{ai} = \frac{\sum_{t=ts}^{te} L(t)}{te+ts-1}, \tag{19}$$

where ts and te are failure start and end hour, respectively.

(9) Repeat the steps (2)-(8) for each LP in the system.

(10) Estimate the expected value of system EENS as follows.

$$EENS = \sum_{i=1}^{n_i} A_i L_{ai}, \tag{20}$$

where n_i is the number of LPs in the system.

(11) Calculate the sum of the system EENS values of levels $l = 0$ and $l > 0$. The simulation is repeated until the number of samples is reached to N.

(12) Set the initial finest level of MLMC simulation as $L = 2$.

(13) Generate number of samples N_x on each $l = 0, 1, 2$ using N_a and also update step (11).

(14) Calculate the absolute mean of EENS m_l and variance V_l on each level $l = 0, 1, 2$.

(15) Find out the optimal number of samples N_l on each level using Eqn. (11) and evaluate extra samples if needed by comparing with N_x. Moreover, update mean and variance on each level for confirming variance of the MLMC estimator $< \frac{\varepsilon^2}{2}$.

(16) Test weak convergence using Eqn. (12). If not converged, set $L = L + 1$ and repeat from step (13) until reached to the target accuracy level.

(17) Finally calculate the multilevel estimator by Eqn. (6).

5. Test systems and results

5.1. Test systems

Five radial distribution systems connected to five different load buses (bus 2-bus 6) of a benchmark RBTS are considered as test systems. The single line diagrams of the test systems are given in [18]. Table 1 shows the information of the load types, number of feeders and load points (LPs) in the distribution systems. The RBTS connected to B2-B5 represent the typical urban systems. The distribution system for B6 represents a typical rural type network. The amount of load consumption may differ from system to system due to the mix and dispersion of customer served. The peak load contribution of different loads in the test systems is also shown in Table 1. The large users and office building users sectors of RBTS B3 system have the highest and lowest percentage of peak load with 65.29% and 2.18%, respectively. The residential load type of all test systems except RBTS B3 contributes highest percentage of peak load. The agricultural load is only available in RBTS B6 system and makes contribution of 37% of total peak load. Some systems contain multiple kinds of the same load with dissimilar peak load connected to different LPs. For example, in RBTS B2 system, there are two types of residential load. Some residential LPs (1-3, 10, 11) have peak load of 0.8668 MW. On the other hand, few LPs (12, 17-19) have peak load of 0.7291 MW.

Table 1. Test systems load data

Distribution system	B2	B3	B4	B5	B6
Number of feeders and load points					
Feeders	4	8	7	4	4
Load points	22	42	38	26	40
Load type	% Peak load contribution				
Residential	36.25	23.41	47.50	44.50	39.25
Commercial	18.75	5.53	11.75	18.50	8.50
Industrial	17.50	3.59	40.75		15.25
Large users		65.29			
Govt./Inst.	27.50			27.75	
Office buildings		2.18		9.25	
Agricultural					37.00

The lengths of the main and lateral feeders, number of customers and the amount of load at each LP, components failure, repair and switching data in the systems are found in [18, 25]. The availability of breakers, fuses and disconnecting switches are considered to restore the service. Feeder breakers are assumed as 100% reliable for this study. The service of alternative supply sources is also considered for all systems. Additionally, assume that the action of a failed transformer is restored by time-consuming repair.

5.2 Test results

The simulated results obtained using the proposed MLMC and conventional sequential MCS methods are shown in Table 2. The results are estimated considering daily loads according to the winter season. Whereas consider the LPs interruptions start at 1 am. The parameters W_l and D_l are assumed as 100%. An accuracy of $\varepsilon = 1\%$ is targeted as convergence criterion for both methods. All computations are performed with an Intel Core i7-4790 3.60 GHz processor. The results are considered as base case results, where availability of breakers, fuses, disconnecting switches and alternative supply facilities are considered.

From the perspective of accuracy, it can be seen that the EENS values for different test systems agree with the results obtained from the sequential MCS method. The maximum relative difference with respect to MCS method is 1.19% for the distribution system connected to B4. Besides the load levels and their time-varying nature, the value of EENS estimation for a specific LP is mainly influenced by the number of interruptions and the interruption duration.

Table 2. Base case EENS estimation results

Distribution system	B2	B3	B4	B5	B6
EENS (MCS)	35.42	48.21	43.55	43.48	42.40
EENS (MLMC)	36.20	48.76	44.07	43.90	42.82
Relative Errors (%)	1.06	1.14	1.19	0.96	0.99
MCS time (s)	22.08	38.26	32.47	35.93	40.64
MLMC time (s)	1.08	1.91	1.52	1.73	1.96
Speedup (MCS/MLMC)	20.44	20.03	21.36	20.76	20.73

From the computational speed perspective, the proposed method saves a huge time for all the systems as shown in Table 2. For example, the sequential simulation approach utilizes 32.93 seconds (s) of CPU time for B4 system whereas the method with multilevel approach uses only 1.52 s, i.e., an increase of 20.44 times in the computational speed is attained. In all the cases, the percentage of computation speedup is above 90%. MLMC method reduces the computational effort of MCS method by reducing the number of samples on the finest level. For RBTS B4, the proposed method uses 1638 samples on the finest level and the MCS requires 10750 samples for convergence. Due to the utilization of many samples, MCS method estimates EENS with noticeably high accuracy compared to MLMC method.

The effects of different factors on EENS estimation performance are discussed in the following.

5.2.1. Effect of failure starting time

The starting time of a LP failure influences greatly the estimation of system EENS and its computation time. A very straightforward way to compute EENS is to use constant load level (Average) of a specific load point. Fig. 3 shows the difference between EENS results based on time-varying and constant load models (Avg) for different test systems. Three different starting times including peak and off-peak hours are considered to evaluate the effect of failure starting time (FST) on this estimation. It can be clearly seen that EENS values vary with the FST and there is a significant difference when compared to constant load model based EENS. At $ts = 8$ a.m., due to the high percentage of H_l for almost all load types during this period, test systems achieve overall maximum EENS than others except RBTS B6. In RBTS B6, there are four different types of LPs. From these, residential and agricultural load models contribute 39.25% and 37% of total peak load, respectively. From the Figs. 2(a) and 2(g), it is seen that both loads add high percentage of H_l during the failure period starting at FST= 4 p.m. which supplies maximum EENS for

B6 system. From the network complexity view, the maximum and minimum EENS values are provided by B6 and B2 systems, respectively. This occurs due to having more LPs and overall high percentage of H_l in B6 system compared to B2 system.

Figs. 3(b) and (c) show the effect of FST on TVLM based EENS computation time required in MLMC and MCS methods, respectively. The results obtained for the test systems show that EENS computation cost will be varied for different FST. It is possible to reduce the computation time of a system when used MLMC method. Overall, we can save more than 90% of estimation time compared to MCS method based estimation. The computation would be more time-consuming in the evaluation of high-value EENS of a complex system.

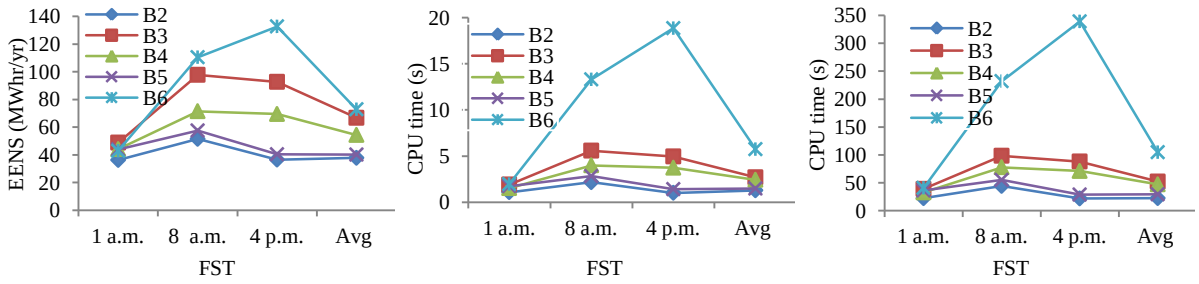

(a) (b) (c)

Fig. 3. Effect of FST on System EENS estimation (a) Variation of EENS values (b) MLMC based computation time variation (c) MCS based computation time variation

5.2.2. Effect of H_l and D_l

The load discrepancy within the days has a potential effect on the estimated time-varying system EENS. As shown in Fig. 1(b), it can be seen that Wednesday and Sunday need the highest and lowest percentage of weekly peak load, respectively. Following the difference in D_l, Fig. 4(a) shows the variation of system EENS with the day. As expected, the peak values of EENS for all the test systems occur in Wednesday and starts decreasing with the day ahead until Sunday.

Figs. 4 (b) and 4(c) present the computational performance of MLMC and MCS methods, respectively for EENS estimation considering the variation of D_l. A large amount of computational effort is reduced for all the test systems simulation. The minimum and maximum MLMC method based computation times are about 1.19 s and 13.30 s for B2 and B6 systems, respectively. To estimate EENS for these two cases, MCS method

requires 25.41 s and 232.07 s, respectively. Therefore, the proposed method speeds up these simulations about 21 and 17 times, respectively.

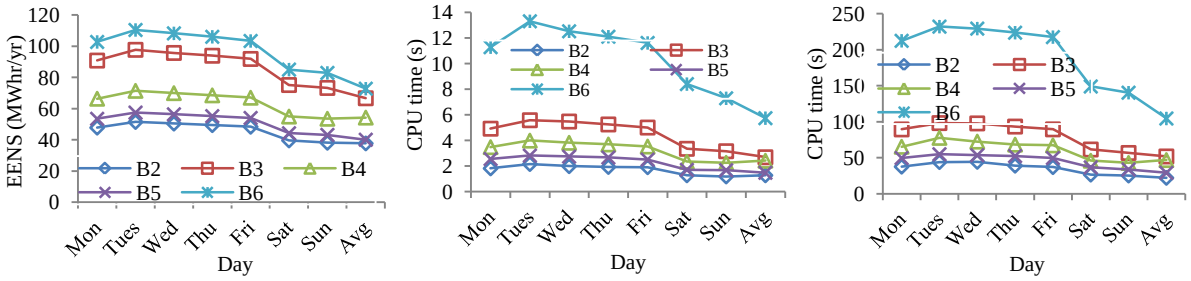

(a) (b) (c)

Fig.4. Effect of D_l on System EENS estimation (a) Variation of EENS values (b) MLMC based computation time variation (c) MCS based computation time variation

Additionally, the hourly load diversity factor (H_l) of different load models has also great impact on EENS estimation considering TVLM. The daily load profile pattern based on H_l is usually different in week and weekend days. In weekend days, there will be an average night time load for office buildings and institution loads. The commercial load profile is affected due to the reduced consumption of light and air conditioning loads. The industrial load profile is also affected by production processes and equipment. The fluctuation of residential loads may result through the effect of consumer availability and activity level. Generally, average load consumption level in daytime during workdays is typically lower than that in the weekends and in the workdays evening load consumption is higher than in weekend evenings. Because of these, the EENS estimation results could be changed. Due to data constraint, the loading diversity of different customer sectors between weekday and the weekend is ignored in this study. In future, we will include this part in EENS estimation.

5.2.3. Effect of W_l

The EENS is impacted not only by the daily and hourly peak load but also by the weekly peak load. Fig. 5(a) shows the variation of system EENS while considering the effect of W_l in the winter season. The highest and lowest values of EENS for test systems are found at week 27 and week 36, respectively. The deviation of EENS considering time-varying and constant load based estimation is strongly noticed while taking account of W_l.

Figs. 5(b) and 5(c) show the computational performance of the methods for EENS estimation considering the variation of W_l. As expected, a significant amount of computational time is saved in MLMC simulation. The minimum and maximum MLMC based estimation times are about 1.38 s and 13.14 s for RBTS B2 and B6 systems, respectively. To estimate these EENS, crude MCS requires 27.68 s and 235.26 s, respectively. Therefore, the proposed method accelerates the simulations about 20 and 18 times, respectively.

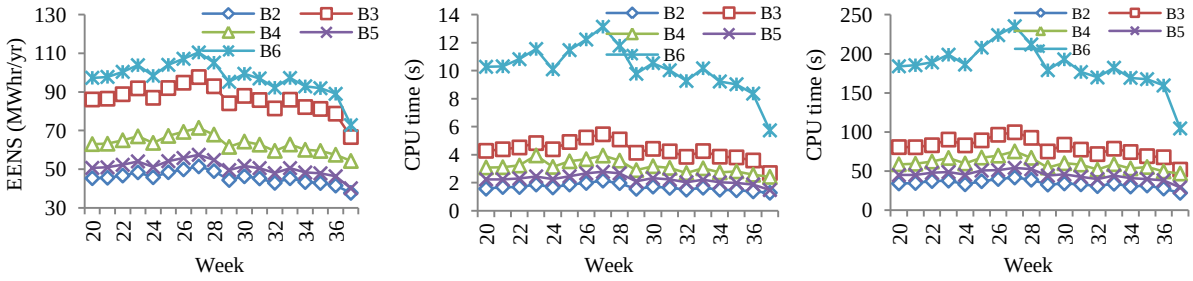

(a) (b) (c)

Fig. 5. Effect of W_l on System EENS estimation (a) Variation of EENS values (b) MLMC based computation time variation (c) MCS based computation time variation

Since the daily load pattern based on W_l is different in different seasons. Therefore, further variation of W_l depending on seasonal variation has potential impact on TVLM based estimation. In summer season, there would be low morning and evening peak loads than winter. Similarly, load pattern in spring could be changed noticeably due to the effect of cooling loads. Considering the change in load pattern, the EENS estimation results could be changed as well. Due to data constraint, we considered only winter season effect in this study.

5.2.4. Effect of customer load types

The load types of a test system affect the amount of EENS and its estimation time. Generally, the load consumption levels of large users and industrial customers are higher than other customers load levels. A test system with less number of LPs, but supplies to large users or industrial customers may increase the EENS value in the peak hours and also their estimation time could be increased.

5.2.5. Effect of network complexity

The EENS estimation of a distribution system could be more time-consuming with more complexity, where the failure of a LP affects a large number of components and stochastic failure models of more components need to be constructed as well as operating and restoration histories of these components are generated. For illustration, B3 system has 44 LPs and needs only four SDE models for EENS estimation of 48.76 MWhr/yr. On the other hand, B6 system supplies 42.82 MWhr/yr which consists of 40 LPs and needs SDE models for nine different components. Therefore, as shown in Table 2, due to the more network complexity, the EENS estimation time for B6 system is longer than B3.

5.2.6. Effect of network reinforcement

Distribution network reinforcement has a great impact on changing the amount of TVLM based EENS and its estimation time. The availability of fuses, feeder breakers, switches and alternative supply in the system play a vital role in reducing EENS. In this section, we consider four different cases of RBTS B2 system to find the systems reinforcement effects on TVLM based EENS. In all the cases, the action of low voltage transformer is restored by repairing.

Case A and B show the effect of fuses in the system where there are no disconnecting switch and alternative supply. As shown in Table 3, due to a large number of components outage, the unavailability of fuses in the case A increases the huge amount of EENS (189.33 MWhr/yr) and computation time (51.84 s). Base case in Table 2 and case C also show the effect of fuses where switches and alternative supply sources are available. The results show that system EENS increases from 36.20 to 54.04 MWhr/yr and computation time increase from 1.08 s to 2.68 s in case C where there is no fuse.

Table 3. EENS estimation results due to RBTS B2 system Reinforcement

Case	A	B	C	D
MCS: EENS (MWhr/yr)	231	44.08	53.35	139.37
MLMC: EENS (MWhr/yr)	233.90	44.57	54.04	141.10
Relative Errors (%)	1.25	1.11	1.29	0.70
MCS time (s)	831.76	26.74	51.48	344.59
MLMC time (s)	53.07	1.23	2.68	20.74
Speedup (MCS/MLMC)	15.67	21.73	19.20	16.61

The effect of availability of disconnecting switches and alternative supply with unavailability of fuses in the system can be evaluated from case C and D. Due to the

presence of alternative sources, a total EENS of 87.06 MWhr/yr and computation time of 18.06 s are decreased in case C when compared to case D. Similarly, the effect of disconnecting switches where there are no fuses and alternative supply sources in the system can be found from case A and D. The availability of switches in case D can reduce EENS from 233.90 to 139.37 MWhr/yr and simulation time from 53.07 s to 20.74 s.

5.2.7. Effect of target accuracy level

A higher level of expected accuracy increases the TVLM based estimation time of EENS as well as decreases the level of variance. Consequently, confidence intervals for the output EENS become narrower. By comparing with the base case from Table 2, it can be seen from Table 4 that the increased accuracy level ε= 0.1% increases huge computational effort for all test systems.

Table 4. EENS estimation results considering ε= 0.1%

Distribution system	B2	B3	B4	B5	B6
MCS: EENS (MWhr/yr)	35.81	48.20	43.55	43.47	42.39
MLMC: EENS (MWhr/yr)	36.27	48.80	44.09	44.01	42.92
Relative Errors (%)	1.28	1.24	1.23	1.24	1.25
MCS time (s)	27.79	47.67	38.81	42.44	47.97
MLMC time (s)	1.75	3.26	2.56	2.81	3.27
Speedup (MCS/MLMC)	15.88	14.62	15.16	15.10	14.66

5.2.8. Effect of discretisation scheme

The computational performance of TVLM based EENS estimation can also be affected by the selection of discretisation scheme for SDE solution. Table 5 shows the estimation results based on Milstein discretisation method [26]. By comparing between Table 2 and 5, it can be concluded that estimation based on Milstein method takes less CPU time than that used by Euler-Maruyama method. Also, the estimation is more accelerated using Milstein method than Euler-Maruyama method based estimation when compared to basic MCS method.

Table 5. EENS estimation results based on Milstein method

Distribution system	B2	B3	B4	B5	B6
EENS (MCS)	35.82	48.20	43.55	43.46	42.40
EENS (MLMC)	36.24	48.74	44.10	43.90	42.89
Relative Errors (%)	1.17	1.12	1.26	1.01	1.15
MCS time (s)	25.09	42.01	34.09	38.93	45.53
MLMC time (s)	1.00	1.88	1.58	1.64	1.94
Speedup (MCS/MLMC)	25.09	22.34	21.57	23.73	23.46

6. Conclusions

In this paper, a general framework for estimating distribution systems average Expected Energy Not Supplied (EENS) index considering Time-Varying Load Models has been proposed based on a novel Multilevel Monte Carlo (MLMC) method. The proposed method coupled with the Euler-Maruyama discretisation scheme can effectively estimate the EENS with acceptable accuracy and huge computational time saving compared to the standard Monte Carlo simulation. The simulation is based on computing the system EENS using a hierarchy of discretisation levels and estimating the final output by combining results from different levels. Mean square error considering both sampling and bias errors is used as the convergence criterion which can be reached by controlling the number of samples on each level and number of discretisation levels.

Using MLMC method, there is not much difference from the basic concept of EENS estimation based on constant load models except incorporating time-varying loads in the estimation. The global load profiles of different customer sectors throughout a 24-hour period are taken into consideration for this purpose. However, the effect of different parameters and criteria can significantly change the computation performance of the MLMC method. The effect of failure starting time, weekly, daily and hourly diversity factors show a considerable impact on the estimation. The effect of distribution systems reinforcement shows that unavailability of disconnecting switches, fuses and alternative supply sources in the systems can increase the amount of EENS and it has a huge impact on computation effort. Similarly, smaller target accuracy level can increase the estimation time. The discretisation scheme has also impact on computational performance and Milstein method can converge faster than Euler-Maruyama method for the EENS estimation.

In distribution system, integration of renewable energy sources is becoming widespread to increase the system reliability. Various loads and system random variables [27] could be modelled using probability distributions. As large numbers of uncertain variables are being incorporated, maintaining accuracy with reliable convergence speed will become more challenging in future. Computation method like MLMC can be used for improving system performance as well as for collecting information of probabilities [28].

List of symbols and abbreviations

λ_j	Average failure rate of a component j (given)
r_j	Average repair time of a component j (given)
L_{ai}	Average load level for load point i during failure period
L_{peak}	Annual peak load
U_j	Annual unavailability of component j (simulated)
A_i	Annual unavailability of a load point i (simulated)
T_{upj}	Artificial operating history of component j
T_{dnj}	Artificial restoration history of component j
$\mathbb{O}$	Big O notation
ΔB_m	Brownian increments
B_t	Brownian motion
Y_l^c	Coarse path estimator
C_l	Computational cost of one sample of $[Y_l - Y_{l-1}]$
D_l	Daily peak load as a percentage of weekly peak load
σ	Degree of variation of failure process over time
$\mathbb{E}[Y_l]$	Estimation of expectation on level l
l	Each grid level
Y	EENS value of a distribution system
Y_l	EENS value on level l
$C[\hat{X}_{ML}]$	Expected cost of the MLMC estimator
EENS	Expected Energy Not Supplied
$\mathbb{E}[Y_L]$	Expected value of the MLMC estimator
$\mathbb{E}[Y_0]$	Expected value of the MLMC estimator on level $l = 0$
$\mathbb{E}[Y_l^c]$	Expected value of the MLMC estimator on coarse level
$\mathbb{E}[Y_l^f]$	Expected value of the MLMC estimator on fine level
ts	Failure start hour
te	Failure end hour
FST	Failure starting time
Y_l^f	Fine path estimator
L	Finest level
H_l	Hourly peak load as a percentage of daily peak load
$Y_l^{(i)}$	ith sample of Y_l
N_a	Initial number of samples on each level l
LP	Load point
LPi	load point i
$L(t)$	Load level of a LP at an hour t
$S_{\lambda j(t)}$	Mean value of TTF_j at a time t
MCS	Monte Carlo simulation
MCS	Monte Carlo simulation
MLMC	Multilevel Monte Carlo
$\hat{X}_{ML}$	MLMC estimator
n_j	Number of components failure that interrupt the service of LPi
n_i	Number of load points in the distribution system
N_M	Number of Monte Carlo samples
N	Number of samples for MLMC convergence test
N_l	Number of samples on each level l
N_x	Number of samples on each level determined using N_a
n	Number of time-steps
μ	Rate of change of the average value of stochastic failure process
α	Rate of convergence
ε	Specified accuracy level

$\hat{X}_{MC}$	Standard Monte Carlo estimator
SDE	Stochastic Differential Equation
h	Time-step size
h_l	Time-step size on level l
h_f	Time-step size on fine level
h_c	Time-step size on coarse level
TTF	Time-to-Failure
TTF_j	TTF of a component j
TTR	Time-to-Repair
TVLM	Time-Varying Load Levels
T	Total time duration
$\hat{X}_0$	Unbiased estimator of the $\mathbb{E}[Y_0]$
$\hat{X}_l$	Unbiased estimator for the $\mathbb{E}[Y_l - Y_{l-1}]$
$\mathbb{V}[Y_l]$	Variance at a certain level l
W_l	Weekly peak load as a percentage of L_{peak}

References

[1] R. Billinton and Z. Feng, "Distribution system reliability risk assessment using historical utility data," *Electric Power Components and Systems*, vol. 35, pp. 693-713, 2007.

[2] X.-F. Wang, Y. Song and M. Irving, *Modern power systems analysis*: Springer Science & Business Media, 2010.

[3] G. Li, Y. Huang and Z. Bie, "Reliability evaluation of smart distribution systems considering load rebound characteristics," *IEEE Transactions on Sustainable Energy*, vol. 9, pp. 1713-1721, 2018.

[4] P. Mishra and J. Joshi, "Reliability estimation for components of photovoltaic systems," *Energy conversion and management*, vol. 37, pp. 1371-1382, 1996.

[5] R. P. Broadwater, A. H. Khan, H. E. Shaalan, and R. E. Lee, "Time varying load analysis to reduce distribution losses through reconfiguration," *IEEE Transactions on Power Delivery*, vol. 8, pp. 294-300, 1993.

[6] R. Billinton and P. Wang, "Distribution system reliability cost/worth analysis using analytical and sequential simulation techniques," *IEEE Transactions on Power Systems*, vol. 13, pp. 1245-1250, 1998.

[7] A. Escalera, B. Hayes and M. Prodanović, "A survey of reliability assessment techniques for modern distribution networks," *Renewable and Sustainable Energy Reviews*, vol. 91, pp. 344-357, 2018.

[8] A. Sankarakrishnan and R. Billinton, "Sequential Monte Carlo simulation for composite power system reliability analysis with time varying loads," *IEEE Transactions on Power Systems*, vol. 10, pp. 1540-1545, 1995.

[9] R. A. González-Fernández and A. M. L. da Silva, "Reliability assessment of time-dependent systems via sequential cross-entropy Monte Carlo simulation," *IEEE Transactions on Power Systems*, vol. 26, pp. 2381-2389, 2011.

[10] K. Hou, H. Jia, X. Xu, Z. Liu, and Y. Jiang, "A continuous time Markov chain based sequential analytical approach for composite power system reliability assessment," *IEEE Transactions on Power Systems*, vol. 31, pp. 738-748, 2016.

[11] R. Billinton, L. Cui, Z. Pan, and P. Wang, "Probability distribution development in distribution system reliability evaluation," *Electric Power Components and Systems*, vol. 30, pp. 907-916, 2002.

[12] E. Tomasson and L. Söder, "Improved importance sampling for reliability evaluation of composite power systems," *IEEE Transactions on Power Systems*, vol. 32, pp. 2426-2434, 2017.

[13] F. Li, "A fast approach of Monte Carlo simulation based on linear contribution factors to distribution reliability indices," in *Transmission and Distribution Conference and Exposition, 2003 IEEE PES*, 2003, pp. 973-977.

[14] G. T. Heydt and T. J. Graf, "Distribution system reliability evaluation using enhanced samples in a Monte Carlo approach," *IEEE Transactions on Power Systems*, vol. 25, pp. 2006-2008, 2010.

[15] A. S. N. Huda and R. Zivanovic, "Accelerated Distribution Systems Reliability Evaluation by Multilevel Monte Carlo Simulation: Implementation of Two Discretisation Schemes," *IET Generation, Transmission & Distribution*, 2017.

[16] S. Heinrich, "Multilevel Monte Carlo Methods," Berlin, Heidelberg, 2001, pp. 58-67.

[17] M. B. Giles, "Multilevel Monte Carlo methods," *Acta Numerica*, vol. 24, pp. 259-328, 2015.

[18] R. Billinton and S. Jonnavithula, "A test system for teaching overall power system reliability assessment," *IEEE Transactions on Power Systems*, vol. 11, pp. 1670-1676, 1996.

[19] J. M. Harrison, *Brownian motion and stochastic flow systems*: Wiley New York, 1985.

[20] B. Oksendal, *Stochastic differential equations: an introduction with applications*: Springer Science & Business Media, 2013.

[21] E. Platen, "An introduction to numerical methods for stochastic differential equations," *Acta numerica*, vol. 8, pp. 197-246, 1999.

[22] P. Wang and R. Billinton, "Time sequential distribution system reliability worth analysis considering time varying load and cost models," *IEEE Transactions on Power Delivery*, vol. 14, pp. 1046-1051, 1999.

[23] R. Allan, *Reliability evaluation of power systems*: Springer Science & Business Media, 2013.

[24] M. B. Giles, "Multilevel Monte Carlo path simulation," *Operations Research*, vol. 56, pp. 607-617, 2008.

[25] R. N. Allan, R. Billinton, I. Sjarief, L. Goel, and K. So, "A reliability test system for educational purposes-basic distribution system data and results," *IEEE Transactions on Power systems*, vol. 6, pp. 813-820, 1991.

[26] M. Giles, "Improved multilevel Monte Carlo convergence using the Milstein scheme," *Monte Carlo and quasi-Monte Carlo methods 2006*, pp. 343-358, 2008.

[27] A. Heshmati, H. R. Najafi, M. R. Aghaebrahimi, and M. Mehdizadeh, "Wind farm modeling for reliability assessment from the viewpoint of interconnected systems," *Electric Power Components and Systems*, vol. 40, pp. 257-272, 2012.

[28] C. Bierig and A. Chernov, "Approximation of probability density functions by the Multilevel Monte Carlo Maximum Entropy method," *Journal of Computational Physics*, vol. 314, pp. 661-681, 2016.

Chapter 6

Interruption Cost Estimation

Statement of authorship

Title of Paper	An efficient method with tunable accuracy for estimating expected interruption cost of distribution systems
Publication Status	☑ Published ☐ Accepted for Publication ☐ Submitted for Publication ☐ Unpublished and Unsubmitted work written in manuscript style
Publication Details	An efficient method with tunable accuracy for estimating expected interruption cost of distribution systems, International Journal of Electrical Power & Energy Systems, 105, 98-109. Link: https://www.sciencedirect.com/science/article/pii/S0142061518310469

Principal author

Name of Principal Author (Candidate)	A. S. Nazmul Huda		
Contribution to the Paper	Developed reliability evaluation model, performed simulation and numerical analysis, prepared manuscript.		
Overall percentage (%)	80%		
Certification:	This paper reports on original research I conducted during the period of my Higher Degree by Research candidature and is not subject to any obligations or contractual agreements with a third party that would constrain its inclusion in this thesis. I am the primary author of this paper.		
Signature		Date	07.09.2018

Co-author contributions

By signing the Statement of Authorship, each author certifies that:

the candidate's stated contribution to the publication is accurate (as detailed above);

permission is granted for the candidate in include the publication in the thesis; and

the sum of all co-author contributions is equal to 100% less the candidate's stated contribution.

Name of Co-Author	Rastko Živanović		
Contribution to the Paper	Supervised for development of model, helped in data interpretation and manuscript evaluation		
Signature		Date	13.08.2018

An efficient method with tunable accuracy for estimating expected interruption cost of distribution systems

Abstract— The paper presents a novel efficient method with tunable accuracy for estimating expected interruption cost (ECOST) of distribution systems. ECOST index quantifies the reliability of a distribution system in monetary basis. The performance of ECOST estimation could be influenced by various factors such as time-varying load and cost models, computational limitation and random nature of component failure and repair time. Generally, the interruption cost is estimated based on an analytical method which does not consider the input and parameter uncertainties that are represented as random variables. The simulation method based on Monte Carlo (MC) simulation could provide a more accurate approximation of ECOST due to consideration of stochastic factors. However, one basic challenge related to the MC method is the high computational cost in order to run a large number of iterations for a specified high accuracy. Speed up the accurate estimation process using fast computation method could be an important feature in distribution systems management software. An advancement of the MC method with controllable accuracy is the Multilevel Monte Carlo (MLMC) estimator which is proposed to estimate the system ECOST. The proposed method could reduce the huge computational cost needed for accurately estimating the index. To illustrate the performance of this method, five different size distribution systems of Roy Billinton Test System are utilized. The impacts of the network topology, customer load type, time-varying load and cost models, failure and repair statistics on the MLMC based system ECOST assessment performance are also investigated.

Keywords— Expected interruption cost (ECOST); Computation speedup; Multilevel Monte Carlo simulation; Milstein method.

1. Introduction

Expected interruption cost (ECOST) estimation is an important part of reliability analysis of distribution systems [1]. Knowing the value of a distribution system ECOST in monetary basis could play a significant role for making an optimal investment decision and for deciding the supply of which regions or sectors should be cut off during electricity shortage [2]. ECOST is a completely random variable [3] due to the dependency of random frequency and duration of interruption, time-varying load and cost levels of different customer sectors. In ECOST estimation, interruption frequency and duration are the

primary variables. Load level of a given customer sector varies through the duration of the failure period. Similarly, the interruption cost for a given type of customer which is found by analysing Sector Customer Damage Function (SCDF) [4, 5] and varies with the failure duration and starting time. Therefore, analytical method based on average interruption frequency, load and cost models could be replaced by simulation approach which could provide the more accurate result of ECOST estimation by considering random factors [6, 7]. Through the simulation method, information of probability distribution of ECOST index could be obtained which is necessary for distribution systems expansion and future planning.

Simulation approach generally used in distribution systems reliability evaluation [8-13] including ECOST estimation is based on standard Monte Carlo (MC) simulation. MC method generates the stochastic behavior of components outage and repair times. It can be simulated in either sequential or non-sequential mode [14]. In the non-sequential mode, the states of all components are sampled and a non-chronological system state is obtained [15]. On the other hand, the up and down cycles of all components are simulated in the sequential approach and overall system operating cycle is obtained by combining all the component cycles [15]. The sequential MC mode allows chronological issues to be considered [16]. The state duration sampling approach is generally used to simulate chronological issues which provide time-related reliability indices concerning frequency and duration of load point interruption [17]. However, the slow convergence rate of the sequential MC makes it very time consuming when a large number of samples are necessary to obtain a precise result depending on the accuracy level and a number of variables in the system; particularly it is not efficient at simulating rare events. It is mentioned that the estimation of a distribution system ECOST using any computationally inexpensive method with controllable accuracy has not been reported yet. Therefore, a new sequential Multilevel Monte Carlo (MLMC) simulation method has been applied in this study to overcome the MC based ECOST computational burden.

The MLMC estimator is an advanced MC estimator for performing stochastic simulations. In this method, the computational performance of the basic MC method is increased by maintaining the acceptable accuracy of the simulation. The idea of MLMC method is to use a hierarchy of computational meshes (levels) instead of using single time discretization level in MC method. By simulating on multiple levels, MLMC method runs most of the simulations on the computationally low-cost coarse levels and few simulations on the computationally expensive finest level. Where in MC method, all the samples are only

simulated on the finest level [18]. It is simple to understand that the computational cost on a fine level is higher than on coarse level [19]. Thus most of the computational effort in MLMC method is transferred from the finest level to the coarsest one, leading to substantial computational saving. As the whole simulation is are conducted using multiple approximations, therefore the less accurate estimate on the preceding coarse level can be sequentially corrected by averages of the differences of the estimations of two consecutive levels in the hierarchy. Detailed mathematical proofs of the MLMC method can be found in [20]. Initially, the method was introduced by Heinrich in the context of parametric integration [21]. The method has been extended further by Giles in the context of stochastic differential equations [18]. Since then the method is being applied for uncertainty quantification in various applications [22-28].

The objectives of this study are to investigate the application of MLMC method on estimating the system ECOST as well as to find the effect of different parameters on the computation performance. In the present study, components are represented by two-state model [29]. The operation history of each component is generated based on stochastic differential equation (SDE). Time-varying load and cost models are developed for each of the load points in the system. Milstein discretization scheme is used for the approximate numerical solution of the SDE. A benchmark Roy Billinton Test System (RBTS) [30] is used to apply the method. The performance of the proposed method is compared with the MC method in terms of computation accuracy and speed-up. The effect of different parameters on the MLMC computation method such as network configuration and load type, time-varying load and cost models, network reinforcement, transformer and line failure rate, drift and volatility values are investigated to provide insight into the variation of the ECOST with different system factors.

The remainder of this paper is organized as follows. Section 2 describes the mathematical explanation of the problem and the MLMC approach. In Section 3, ECOST evaluation methodology has been described. This Section consists of five subsections: generation of component operating history, modelling of load, modelling of per unit interruption cost, modelling of system ECOST, and simulation steps to evaluate the ECOST. In Section 4, we investigate the applicability of the proposed MLMC. We evaluate system ECOST considering different factors affecting the results to show how much the estimation results could be diversified from average value while these factors are considered. Finally, Section 5 concludes the paper.

2. Proposed approach

2.1. Problem statement

MC method is a straightforward way for the estimation of expectation arising from the stochastic simulation where ECOST is estimated by averaging over a large number of samples on a single fine grid level [31]. Let X be the ECOST for this study and $E[X]$ is the expectation or quantity of interest. Also, let $E[X_A]$ be the approximation to $E[X]$. $X_A^{(i)}$ is the ith sample of X_A and N_{MC} is the number of independent MC samples. Then, an unbiased MC estimator for $E[X_A]$ is

$$\hat{Z}_{MC} = \frac{1}{N_{MC}} \sum_{i=1}^{N_{MC}} X_A^{(i)}. \quad (1)$$

where $E[\hat{Z}_{MC}] = E[X_A]$, $N_{MC}^{-1} V[X_A]$ is the variance of this estimate and the rms error is $\mathcal{O}(1/\sqrt{N_{MC}})$.

To achieve an accuracy of ε, the simulation requires $N_{MC} = \mathcal{O}(\varepsilon^{-2})$ samples. For an increasing accuracy level, the number of samples also increases. As the samples are run on the finest level, the accuracy of evaluation is sufficiently accurate in MC method. However, the problem associated with the MC method is that huge computational burden is introduced due to large sample size. This motivates to find an alternative method which could speed up the system ECOST estimation in distribution systems planning application by maintaining an adequate level of accuracy. Hence the applicability of the proposed MLMC method is investigated in this study to perform this objective.

2.2. MLMC method

In the MC method, the calculation of system ECOST is carried out on a single fine grid level $l = L$. l is a nonnegative integer. In this level, both accuracy and estimation time of the expectation is very high.

In the MLMC method, same ECOST is evaluated but using multiple parts or levels instead of using only one level L. The multiple levels can be divided as $l = 0, 1, \ldots\ldots, L$. Here $l = 0$ and $l = L$ indicate the coarsest and finest discretisation levels, respectively. On each level, expectations are estimated using different sample size in a manner which could reduce the overall variance for a specified error tolerance. Initially, a large number of samples are run on $l = 0$. The purpose of the next level $l = 1$ is to add a correction value

that initiates to decrease the bias. Based on this correction value, the expected difference from one level to the next fine level is added, until level L is reached. By this way, the less correct estimate on the coarsest grid is successively corrected by the approximations on the subsequent fine grids and thus the finest grid accuracy is reached. The MLMC expectation can be expressed as:

$$E[X_A] = E[X_0] + \sum_{l=1}^{L} E[X_l - X_{l-1}] = \sum_{l=0}^{L} E[Z_l], \tag{2}$$

Now the estimator for the above MLMC expectation is

$$\hat{Z}_{ML} = \hat{Z}_0 + \sum_{l=1}^{L} \hat{Z}_l = \sum_{l=0}^{L} \hat{Z}_l. \tag{3}$$

where $\hat{Z}_0$ is an unbiased estimator for $E[X_0]$ using samples N_0 on $l = 0$ and $\hat{Z}_l$ is the estimator for $E[X_l - X_{l-1}]$ using N_l samples from $l \geq 1$.

$$\hat{Z}_0 = \frac{1}{N_0} \sum_{i=1}^{N_0} X_0^{(i)}, \tag{4}$$

$$\hat{Z}_l = \frac{1}{N_l} \sum_{i=1}^{N_l} \left(X_l^{(i)} - X_{l-1}^{(i)} \right), \tag{5}$$

$E[X_l - X_{l-1}]$ is approximated using the difference between the expectation of the coarse and fine level as $E[X_l^f - X_{l-1}^c]$. $E[X_l^f]$ and $E[X_{l-1}^c]$ are estimated using two different timestep sizes $h_f = 2^{-l}T$ and $h_c = 2^{-(l-1)}T$, respectively [32]. On level $l = 0$, a large and fixed value timestep is used to generate a large sample size N_0. This means that the coarsest level is the computationally cheapest level and the simulation time increases with the increase of level. The statistical properties of X_l are unchanged whether the estimation of $E[X_l - X_{l-1}]$ from level $(l-1)$ to l or $E[X_{l+1} - X_l]$ from l to $(l+1)$. This means that both $E[X_l - X_{l-1}]$ and $E[X_{l+1} - X_l]$ have the same expected value i.e. $E\left[X_l^f\right] = E[X_l^c]$. The convergence condition of the proposed method is the target rms error which could be written as follows:

$$\varepsilon^2 = \sum_{l=0}^{L} N_l^{-1} V_l + [E(X_A - X)]^2. \tag{6}$$

To obtain an overall mean square error $MSE \leq \varepsilon^2$, both the variance and weak error of the MLMC estimator could be reduced below $\varepsilon^2/2$. The variance could be reduced by setting a different number of samples N_l at different levels. As the level l moves from the initial coarsest level to next finer level, the choice of an optimal N_l is made as follows [18].

$$N_l = 2\varepsilon^{-2}\sqrt{V_l/C_l}\left(\sum_{l=0}^{L}\sqrt{V_l C_l}\right). \quad (7)$$

where the cost to compute one sample on the level l is $C_l = c_3 2^{\gamma l}$ for a constant c_3 and some $\gamma > 0$. γ is the rate of computation cost increase with the level l. For weak convergence, the test tries to confirm that $[E(X_A - X)]^2 \leq \varepsilon^2/2$. Consider, the convergence rate of $E(X_A - X)$ with l for constant c_1 is measured by a positive value α, i.e., $|E[X_l - X_{l-1}]| \leq c_1 2^{-\alpha l}$ [18]. The remaining error is $E(X_A - X) = E[X_L - X_{L-1}]/(2^{\alpha} - 1)$ and the target convergence criterion is $E[X_L - X_{L-1}]/(2^{\alpha} - 1) < \varepsilon/\sqrt{2}$. β is assumed as the convergence rate of variance with l for a constant c_2 i.e., $V_l \leq c_2 2^{-\beta l}$. For a constant c_4, computational complexity C of the MLMC estimator is bounded as [18]:

$$E[C] \leq \begin{cases} c_4\varepsilon^{-2}, & \beta > \gamma, \\ c_4\varepsilon^{-2}(log\varepsilon)^2, & \beta = \gamma, \\ c_4\varepsilon^{-2-(\gamma-\beta)/\alpha,} & \beta < \gamma. \end{cases} \quad (8)$$

3. Methodology

3.1. Generation of operating history

For generating the operating history of any component, the stochastic model of component Time-to-Failure (TTF) is first developed. Consider λ_i and r_i are the failure rate and repair time of a component i, respectively. Also, consider the SDE of TTF is driven by the Brownian motion [33]. If $S_{\lambda i(t)}$ is the TTF of an event i at a time t, then SDE of TTF with defined drift μ, volatility σ and initial TTF can be modelled using the Brownian motion W on the whole time interval $[0, T]$ [34] as follows:

$$dS_{\lambda i(t)} = \mu\left[S_{\lambda i(t)}, t\right]dt + \sigma\left[S_{\lambda i(t)}, t\right]dW, \quad (9)$$

In this paper, the SDE is solved by Milstein discretisation scheme [32]. The discretisation scheme with n time-steps, step size $h = T/n$ and Brownian increments ΔW_m could be written as:

$$S_{\lambda i(m+1)} = S_{\lambda i(m)} + \mu\left[S_{\lambda i(m)}, t_m\right]h + \sigma\left[S_{\lambda i(m)}, t_m\right]\Delta W_m + \frac{1}{2}\sigma^2\left[S_{\lambda i(m)}, t_m\right](\Delta W_m^2 - h), \quad (10)$$

where ΔW_m are the normally distributed independent random variables. $\Delta W_m = W_{m+1} - W_m$ $[m = 0, \dots\dots, n-1]$ and $t_m = kh$ $[k = 0, \dots\dots, n]$. Using Eqn. (10), the operating history of component i, T_{ui} could be generated as follows:

$$T_{ui} = -S_{\lambda i(m+1)}\, ln(U) \tag{11}$$

where U is a uniformly distributed random variable between [0, 1].

3.2. Modelling of load

Usually load level of a specific customer type fluctuates due to the discrepancy between the hourly consumption levels. In addition, seasonal inconsistency in the weather contributes prominently to loading level diversity [35]. Evaluation of interruption cost based on average load level without considering time-varying diversity factors does not reflect the time-varying nature of system ECOST. Thus accurate approximation of ECOST needs the consideration of modelling of loads throughout a 24-hour period depending on seasons. However, the most utilities collect load data for a specific distribution area only and also individual load point data throughout the daily 24 hours in a year are not usually available. The global behavior of each load type is therefore established by considering typical load consumption cycles which is found as an acceptable method in power systems reliability evaluation study performed by Billinton and Allan [36]. Complete load data of winter season in a weekday for modelling time-varying load models are displayed in Appendix A.

For modelling time-varying load $L_p(t)$ of a load point P at an hour t, annual peak load (L_{peak}), weekly peak load as a percentage of annual peak (W_p), daily peak load as a percentage of weekly peak (D_p) and hourly peak load as a percentage of daily peak (H_p) are formulated as [36]:

$$L_p(t) = L_{peak} \times W_p \times D_p \times H_p(t), \text{ MW} \tag{12}$$

Consider, the interruption of load point P starts and ends at ts and te hours, respectively. Then the average time-varying load level of this load point is evaluated as follows:

$$L_p = L_{peak} \times W_p \times D_p \times \frac{\sum_{t=ts}^{te} H_P(t)}{te-ts+1}, \text{ MW} \tag{13}$$

3.3. Modelling of per unit interruption cost

The interruption cost of a load point for any duration is found from SCDF [5]. The cost of a load point per unit interruption depends on the type of the customer connected in that point. The SCDF presents the customer interruption costs as a function of interruption duration. The SCDF for different types of customers are provided in Appendix A. It can be seen that per unit interruption costs for various customer sectors are different by depending on interruption duration. For example, when interruption lasts 1h, the maximum and minimum per unit cost are found for office buildings and residential customers, respectively. A linear interpolation of the cost data is used in this study where the interruption duration lies between two separate times.

Based on average cost model (C_{avg}) from SCDF, the interruption cost related to a load point P failure for a duration r_p can be expressed as: $C_p = C_{avg}(r_p)$. Here C_p is the customer interruption cost related to a load point P. From SCDF, only the average monetary losses of customer interruptions are found. On the other hand, for modelling interruption cost $C_p(t)$ at an hour t based on time-varying cost model, the multiplication of C_{avg} from SCDF and time-varying weight factor $W_p(t)$ is used, i.e. $C_p(t) = C_{avg} \times W_p(t)$. Then average time-varying cost level of a load point P for above failure period can be formulated as:

$$C_p = C_{avg} \times \frac{\sum_{t=ts}^{te} W_p}{te-ts+1}, (\$/\text{kW}) \quad (14)$$

3.4. Modelling of system ECOST

For a component failure i, the value of average outage rate B_i could be calculated using the following expression:

$$B_i = \frac{M}{\sum_{n=1}^{N} T_{ui}}, \text{ (f/yr)} \quad (15)$$

where M is the number of times component i fails during whole simulation period and N is the desired number of simulated periods.

For load point P, average outage rate F_p is evaluated as follows by accumulating the outage rate of all the failure events connected to this load point.

$$F_p = \sum_{i=1}^{n_i} B_i, (\text{f/yr}) \quad (16)$$

where n_i denotes the number of outage events interrupting the service of the load point P. Using Eqns. (13), (14) and (16), overall distribution system ECOST can be evaluated as follows.

$$ECOST = \sum_{p=1}^{n_p} F_p L_p \, C_p. \text{ (k\$/yr)} \tag{17}$$

where n_p is the total number of supply points in the system.

3.5. Simulation process

In the simulation, there are two phases. In the 1st phase, the stochastic model of ECOST is established on both coarse and fine levels. In the 2nd phase, overall MLMC estimator is calculated through satisfying the target convergence criteria of the simulation. In the 1st phase, initially, failure rate, repair/switching time of each distribution system component are defined. Additionally, the values of sample size for convergence test (N), initial sample size on each level (N_{in}), drift, volatility and target accuracy level are defined. The model of a component is represented by up-down states. The operating history of each component is generated according to the exponential probability distribution using Eqn. (11). Using Eqn. (13), time-varying load model of each load point during failure period is established based on peak load, hourly, daily and weekly load diversity factors. Similarly, time-varying cost model of each load point is established based on SCDF and cost weight factors by following Eqn. (14). After this, the value of each component average failure rate is calculated using Eqn. (15). The value of each load point average failure rate is calculated by accumulating the individual component value connected to the relevant load point by following Eqn. (16). System ECOST is then computed using Eqn. (17). A flowchart of the ECOST estimation on coarse and fine levels is shown in Fig. 1(a).

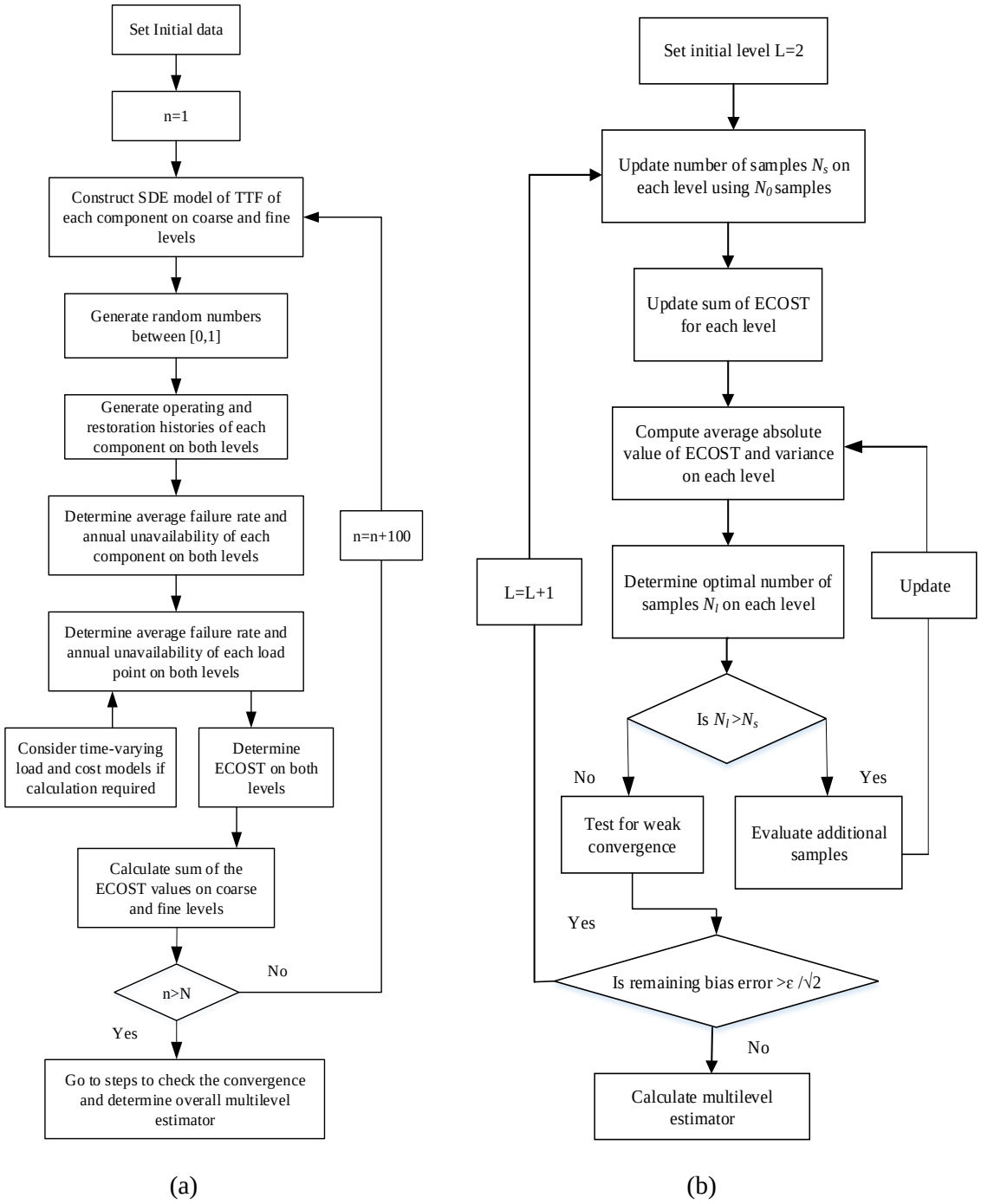

Fig. 1. Flowchart (a) ECOST estimation on coarse and fine levels (b) Convergence test

In the 2nd phase, overall MLMC estimator is calculated through satisfying the target convergence criteria of the simulation. Initially, the finest grid level of simulation is set at $L = 2$. The number of samples N_s on each level is then determined using initial sample size. The sum of ECOST values on coarse and fine levels is simultaneously updated. Then, the absolute average value of the index and variance are calculated on each level. The optimal sample size N_l on each level is determined based on Eqn. (7). Next, the optimal sample size on each level is compared to the already computed N_s on this level. If the N_l is

larger than N_s, then the additional samples on each level are evaluated and the values of mean, variance on each level are also updated. The purpose of determining the optimal N_l is to make the variance term of Eqn. (6) smaller than $\varepsilon^2/2$. The test for the weak convergence is then performed which ensures the remaining bias error < $\varepsilon/\sqrt{2}$. If the bias error remains greater than $\varepsilon/\sqrt{2}$, then the finest level is reset as $L = L + 1$. The entire process is repeated again until the target accuracy level is achieved. Finally, the combined multilevel estimator for system ECOST is computed using Eqn. (3). A flowchart for convergence test is presented in Fig. 1(b).

4. Test systems and simulation results

4.1. Test Systems

Five load busbars of a six-busbar test system-RBTS are used as test distribution systems. Detailed diagrams of the distribution systems at buses 2-6 of the RBTS are found in Appendix B. Basic data of the distribution systems is presented in Table 1. The customer data, load data and types, feeder section length data and component reliability data are taken from [30], [37]. The availability and reliability of breakers, fuses and disconnecting switches are considered as 100% in all the test systems. The availability of alternative supply source is also considered for all systems. The service of failed low voltage transformers is generally restored by repairing rather than replacing.

A target accuracy level of ε=3% is used to approximate the ECOST of the distribution systems. For all the systems, setting parameters for the MLMC simulation are: N=5000, N_{in}=500, μ=0.01 and σ=0.8. The methodology is implemented using MATLAB and all computations are performed using an Intel Core i7-4790 3.60-GHz processor.

Table 1. Basic data of test distribution systems

Distribution system	Typical type	Customers types	No of LPs	Average load (MW)
B2	Urban	R, GI, SI, C	22	12.291
B3	Large user	LU, SI, C, R, OB	44	52.63
B4	Complex urban	R, SI, C	38	24.58
B5	Urban	R, GI, OB, C	26	11.29
B6	Rural	A, SI, C, LU	40	10.7155

A-Agricultural, C-Commercial, GI-Government and Institutional, R-Residential, LU-Large users, OB-Office buildings, SI-Small industrial, LPs-Load points

4.2. Simulation results

4.2.1. Effect of network configuration and load type

Table 2 presents the effect of network configuration and load types in ECOST variation using MC and MLMC methods based computation. The RBTS distribution systems connected to five load buses (B2 to B6) are considered for this purpose [30]. By comparing different test systems, it is seen that the maximum and minimum system ECOST values are found in B3 and B6 systems, respectively. In Eqn. (17), we find that the amount of system ECOST depends on the failure rate, load level and interruption cost of the interrupted load points. In the B3 system, there are five types of loads such as residential, large users, small industrial, commercial and office building users and the total amount of average load for all 44 load points is 52.63 MW. On the other hand, in the B6 system, there are four types of loads such as residential, small industrial, commercial and agricultural and the total amount of average load for all 40 load points is 10.7155 MW. In most of the cases, average load level per load point in the B3 system is higher than the B6 system. Due to having load points with high interruption cost and duration in B3, it gives the large value of ECOST than the B6 system.

More specifically, the availability of commercial load highly increases interruption cost for all the systems except the B6 system, although the peak load level of this load type is not maximum. This happens due to the large amount of per unit interruption cost for commercial load type as displayed in SCDF [5]. In the B6 system, there are a large number of residential load points, where only two commercial load points are connected to the system.

The magnitude of ECOST also varies with the network topologies and loading types. Interruptions in different load connected systems have very different consequences. A test system with smaller number of load points, but having supplies to commercial customers (due to huge interruption cost) may increase the ECOST value in the peak period.

For validation, the results obtained from the proposed method should agree with the results from the analytical method. E[MC] and E[MLMC] are the percentages of the difference of ECOST values using MC and MLMC methods with respect to the analytical value. The results show that the ECOST values using MLMC method are very close to the values from MC and analytical methods. The absolute value of maximum E[MLMC] is 3.25% for

B2 system. These results are generally acceptable for an application with uncertainty quantifications. This proves the accuracy of the proposed MLMC approach.

As displayed in Table 2, the maximum and minimum computation times are required for the distribution systems connected to B3 and B6, respectively. In all cases, the percentage of computation speedup is above 90%. For example, the proposed and MC methods need 1.85 and 49.33 seconds, respectively for the B4 system. The MLMC method improves the calculation efficiency of the MC simulation by reducing the number of iterations on the finest level. For example, the proposed method requires 3293 iterations on the finest level and the MC method needs about 19000 iterations for target convergence of ECOST estimation. Due to a large number of required samples, MC method provides ECOST with noticeably high accuracy compared to the MLMC method as shown in Table 2.

Table 2. ECOST using average load and cost models

System	MC (k$/year)	MLMC (k$/year)	MC (s)	MLMC (s)	E[MC] (%)	E[MLMC] (%)	Speedup (%)
B2	185.51	190.18	35.23	1.14	-0.72	-3.25	96.76
B3	267.52	274.73	69.27	2.74	0.99	-1.67	94.73
B4	225.66	231.81	49.33	1.85	1.16	-1.52	96.24
B5	222.84	228.74	47.40	1.58	1.32	-1.29	96.67
B6	132.12	135.63	27.06	0.9	-0.03	-2.68	96.67

4.2.2. Effect of time-varying load and cost models

Table 2 shows the computation of ECOST of test systems while average load and interruption cost models are utilized. The complete simulated results for different test systems showing the variation of ECOST values due to the consideration of time-varying load, time-varying cost and their simultaneous effects are presented in Appendix C. Three different failure starting times depending on peak and off-peak hours are considered. For example, in Table 2, ECOST for the B2 system using MLMC method is 190.18 k$/yr which is calculated without time-varying load and cost models. On the other hand, if we consider the failure starting from 1:00, then this ECOST value according to the different time-varying models will be 167.21, 134.96 and 120.82 k$/yr, respectively as shown in Fig. 2. Depending on the failure starting time, ECOST values will be different. Additionally, Fig. 2 shows the effects of time-varying models in B2 system. There are four types of loads in B2 system i.e. residential, government/institutional, small industrial and commercial. As failure period mostly covers off-peak hours, therefore the hourly weighting levels associated with these loads and interruption costs are generally very low

during this period. For example, an interruption for residential customers at 8:00 interferes with recreation (e.g. television, internet); while at 1:00 an interruption has a much smaller effect because most people are asleep. This makes ECOST value lower compared to ECOST using average load and cost models. Conversely, failure period typically covering peak hours (i.e. working hours such as when failures start at 8:00) has the higher ECOST values. Furthermore, the season, the day of the week and the time of day influence the ECOST estimation.

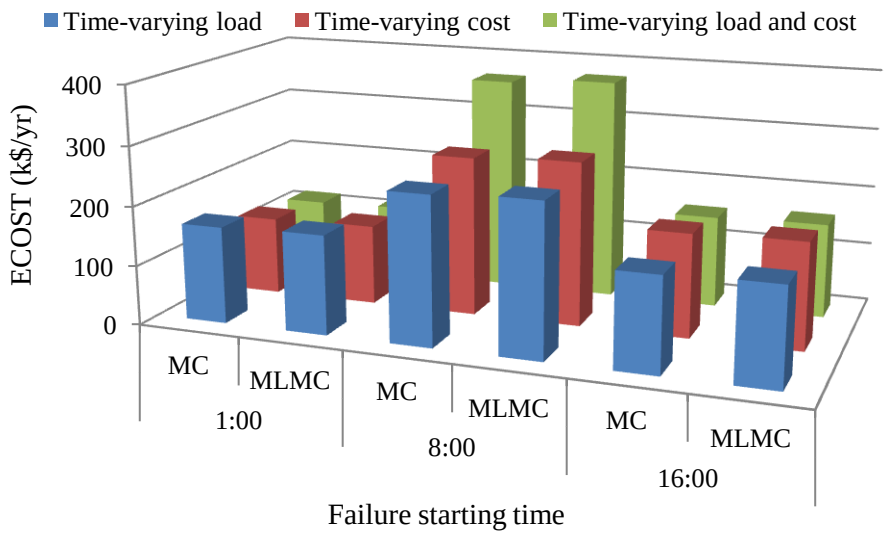

Fig. 2. ECOST magnitude variation for Bus 2 system with different failure starting times and different time-varying load and cost models

Fig. 3 presents the effect of failure starting time on time-varying ECOST computation time using MLMC and MC methods for B2 system. The results obtained for the test system show that ECOST computation cost will be varied for different starting times and different time-varying models. It is possible to reduce the computation time by using the MLMC method. Overall, we can save more than 90% of estimation time compared to MC based estimation. The computation would be more time-consuming in the evaluation of high-value ECOST of a system. The complete simulated results for different test systems showing the variation of ECOST computation times due to the consideration of time-varying load, time-varying cost and their simultaneous effects are presented in Appendix C.

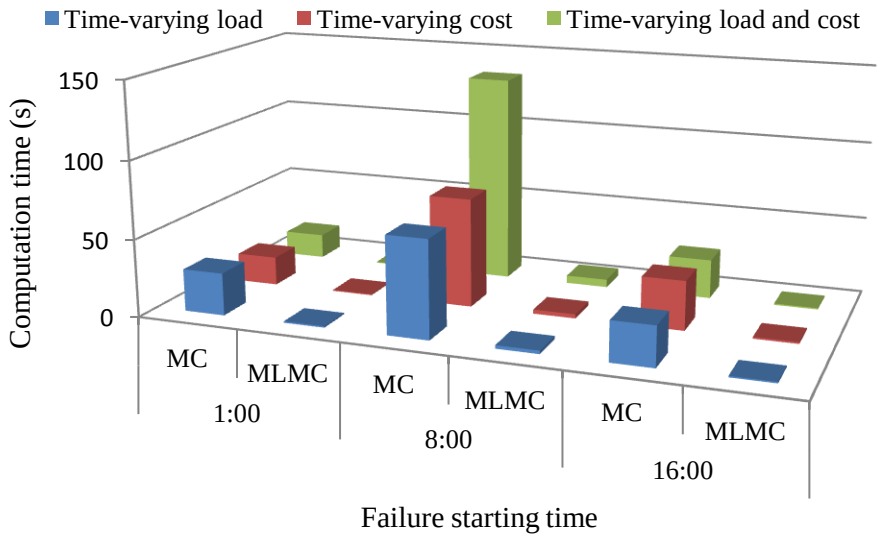

Fig. 3. ECOST computation time variation for Bus 2 system with different failure starting times and different time-varying load and cost models

4.2.3. Effect of network reinforcement

More than 80% of the customer interruptions happen due to the fault in the distribution systems. Availability of different protective and switching equipment could reduce the number and duration of these interruptions and increase the system reliability, i.e. more investment on utility could reduce the interruption cost. The variation of ECOST values and their estimation time demonstrate the effect of network reinforcement on cost value and estimation time. Six case studies are carried out as Table 3, where availability of protective devices and switches are considered in various combinations for the B2 system. The maximum and minimum ECOST values are found in case B and E, respectively. In case E, the availability of switches, fuses, alternative supply is considered with the restoration of low-voltage transformer action by replacement. On the other hand, in case B, all these protective equipment are unavailable with transformer action restoration by time-consuming repairing. In fact, the more investment in the protective equipment reduces the interruption effect and as a result, the value of ECOST is also reduced.

Table 4 shows the computational performance of the MC and MLMC methods for all case studies. By comparing with the MC based estimation, the proposed method can estimate ECOST with an acceptable accuracy and the proposed method is considerably more efficient than standard MC. The maximum and minimum simulation times are required for case B and E, respectively. In these cases, the percentages of time-saving using proposed

method are 95.66% and 96.52%, respectively. It can be concluded that the magnitude and computation time of ECOST are changed for both methods by the reinforcement.

Table 3. Cases for network reinforcement effect analysis

Case	Disconnecting Switches	Fuses	Alternative Supply	Transformer Action Restoration
A	Yes	Yes	Yes	Repairing
B	No	No	No	Repairing
C	No	Yes	No	Repairing
D	Yes	No	Yes	Repairing
E	Yes	Yes	Yes	Replacement
F	Yes	No	No	Repairing

Table 4. ECOST computation performance variation for network reinforcement

Case	ECOST (k$/year)		CPU time (s)	
	MC	MLMC	MC	MLMC
A	185.51	190.18	35.23	1.14
B	1253.90	1287.50	1110.13	48.19
C	220.16	225.95	49.67	1.71
D	299.28	307.37	80.19	2.76
E	28.60	29.33	0.9151	0.03228
F	907.76	931.79	317.25	25.15

4.2.4. Effect of transformer failure rate

Customer interruption cost could be reduced by decreasing the failure rate of the low-voltage distribution transformer (TFR). In order to examine the effect of this parameter, TFR is varied from 0.005 f/yr to 0.25 f/yr for ECOST calculation of B2 and B6 systems. From Fig. 4, it is seen that the system ECOST increases gradually with the increase of TFR. For the B2 system, the rate of ECOST increase is higher than the B6 system. This is mainly due to higher interruption cost of affected load points in the B2 system. From the computational perspective, the calculation time of ECOST increases also as TFR is increased and the proposed method could save a huge amount of CPU time compared with direct MC method as shown in Fig. 5.

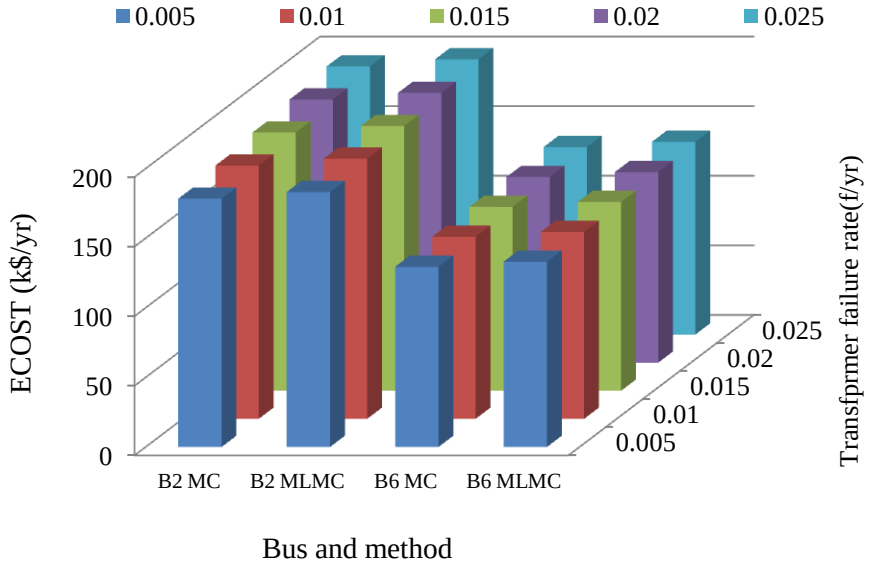

Fig. 4. ECOST magnitude variation for varying transformer failure rate

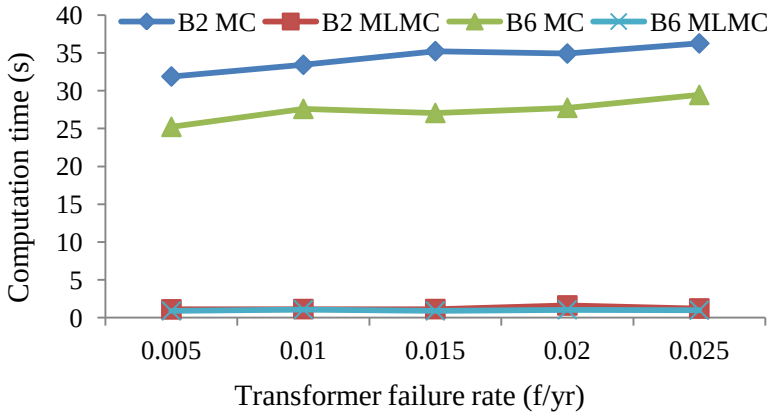

Fig. 5. ECOST computation time variation for varying transformer failure rate

4.2.5. Effect of line failure rate

The failure rate of overhead distribution line (LFR) has an impact of interruption cost estimation. For investigating the effect, a sensitivity analysis is carried out where LFR is varied from 0.025 f/yr to 0.15 f/yr for ECOST calculation of B2 and B6 systems. As shown in Fig. 6, the system ECOST increases at a higher rate with the increase of LFR. Overhead line is a very basic component of a feeder. In the radial system, any failure in a feeder line section could interrupt the function of all the connected supply points of the feeder. From the computational perspective in Fig. 7, the calculation time of ECOST increases also as LFR is increased and the proposed method could accelerate the computation process compared with MC method. Similarly, the length of a line section influences the ECOST

estimation since a long-length line increases the failure rate compared with the short-length line.

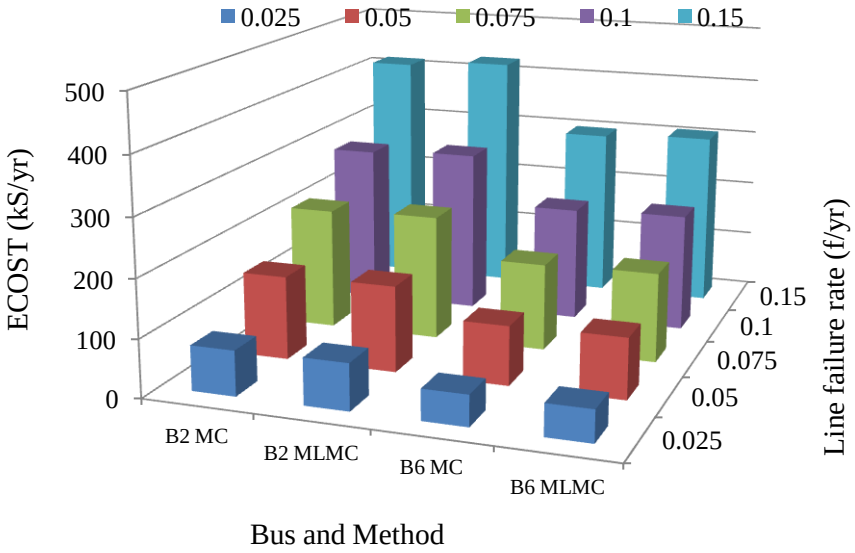

Fig. 6. ECOST variation for varying line failure rate

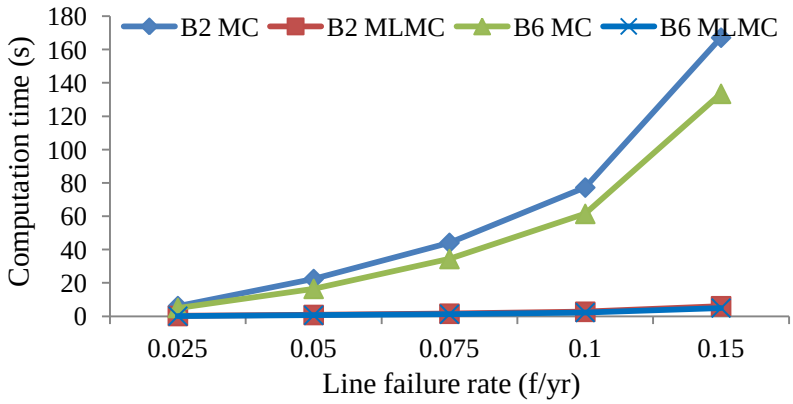

Fig. 7. ECOST computation time for varying line failure rate

4.2.6. Effect of drift and volatility values

The values of drift and volatility parameters of stochastic failure process could be found from time series of TTF [38]. However, due to the data constraint, the drift and volatility in this study are determined by adjusting based on the accuracy and assumed these values as constant for all case studies. Here the effect of both parameters on system ECOST evaluation accuracy and time are investigated. For example, Table 5 presents the variation of ECOST value and computation time of B4 system by varying μ while σ =0.8 is set as

constant. A gradual decrease of ECOST value and its computation time is noticed when μ is varied from 0.03 to 0.2. Similarly, Table 6 shows the variation of ECOST value and computation time of the same system by varying σ while μ =0.8 is set as constant. The results show that both the computation time and value of ECOST increase slowly with the increase of σ.

Table 5. ECOST variation for varying drift

μ	0.03	0.05	0.09	0.12	0.2
ECOST (k$/year)	227.11	222.72	214.14	208.23	193.85
CPU time (s)	1.73	1.65	1.40	1.30	1.02

Table 6. ECOST variation for varying volatility

σ	0.3	0.5	1.0	1.20	1.25
ECOST (k$/year)	228.80	228.90	234.81	239.47	240.90
CPU time (s)	0.58	0.85	3.25	5.84	6.72

4.2.7. Effect of accuracy level

The proposed method could be more efficient for estimating small probabilities, i.e., the probabilities of rare events, with a high accuracy when compared to MC method. For example, Table 7 presents the performance of B4 system ECOST at different accuracy levels. It is found that MLMC method greatly reduces the computation cost without compromising the accuracy of the index.

Table 7. ECOST computation at different accuracy levels

ε	MC (k$/year)	MLMC (k$/year)	MC (s)	MLMC (s)
0.001	225.67	231.68	38812.93	1641.74
0.01	225.69	231.73	359.43	16.83
0.03	225.66	231.81	49.33	1.85
0.05	225.72	231.44	18.64	0.68

5. Conclusions

This paper briefly illustrates the application of a novel Multilevel Monte Carlo (MLMC) method in distribution systems interruption cost estimation. MLMC is a variance reduction technique of Monte Carlo (MC) simulation. MLMC reduces the computational cost by performing most of the simulations with low accuracy at a correspondingly low cost on the coarse grids and relatively few simulations being performed on the computationally

expensive fine grids at high accuracy and high cost. Both accuracy and computational efficiency of the MLMC are considered to demonstrate the practicability of the proposed method. Comparisons of results obtained using the basic MC simulation are presented. The results show that the proposed method could estimate the average customer interruption cost accurately and also gives a significant speed-up over the MC based computation.

A number of sensitivity analyses have been carried out to show the effect of different parameters on the computation process. We found that network configuration and load type, time-varying load and cost models, network reinforcement, transformer and line failure rate, drift and volatility values parameters have a considerable effect of MLMC based system ECOST computation.

Due to the data constraint, the research on comparisons with other advanced MC methods and the probability distributions of MLMC [39] based ECOST estimations will be carried out in the future. For estimating MLMC Maximum Entropy method based PDF in the current study, the authors believe that more studies should be conducted where some additional algorithms, coding, methodology, sensitivity studies of some assumptions (such as number of moments in the Maximum Entropy method) need to be completed for ECOST analysis in order to publish the PDF. Therefore, in the present publication, we set our main focus to provide the MLMC based ECOST estimation to show its speed-up capability and also to present some sensitivity analysis which is necessary to analyse the large real-life systems. The computationally efficient algorithm and simulation examples presented in this paper would potentially help system planners to collect the useful information of reliability cost of their respective distribution systems. We believe that the proposed algorithm will be able to speed up the decision-making process in reliability improvement process.

References

[1] R. Billinton, S. Ali, G. Wacker, Rural distribution system reliability worth evaluation using individual customer outage cost characteristics, Int J Electr Power Energy Syst 26 (2004) 235-240.

[2] M. De Nooij, C. Koopmans, C. Bijvoet, The value of supply security: the costs of power interruptions: Economic input for damage reduction and investment in networks, Energy Econ 29 (2007) 277-295.

[3] O. Dzobo, C. Gaunt, R. Herman, Investigating the use of probability distribution functions in reliability-worth analysis of electric power systems, Int J Electr Power Energy Syst 37 (2012) 110-116.

[4] R. F. Ghajar, R. Billinton, Economic costs of power interruptions: a consistent model and methodology, Int J Electr Power Energy Syst 28 (2006) 29-35.

[5] P. Wang, R. Billinton, Time sequential distribution system reliability worth analysis considering time varying load and cost models, IEEE Trans Power Deliv 14 (1999) 1046-1051.

[6] R. Billinton, P. Wang, Distribution system reliability cost/worth analysis using analytical and sequential simulation techniques, IEEE Trans Power Syst 13 (1998) 1245-1250.

[7] A. Volkanovski, M. Čepin, B. Mavko, Application of the fault tree analysis for assessment of power system reliability, Reliab Eng Syst Saf 94 (2009) 1116-1127.

[8] Y. Ou, L. Goel, Using Monte Carlo simulation for overall distribution system reliability worth assessment. In: Generation, transmission and distribution, IEE proceedings-; 1999, p. 535-40.

[9] L. Goel, Y. Ou, Reliability worth assessment in radial distribution systems using the Monte Carlo simulation technique, Electr Power Syst Res 51 (1999) 43-53.

[10] L. Goel, Monte Carlo simulation-based reliability studies of a distribution test system, Electr Power Syst Res 54 (2000) 55-65.

[11] R. Billinton, P. Wang, Teaching distribution system reliability evaluation using Monte Carlo simulation, IEEE Trans Power Syst 14 (1999) 397-403.

[12] Y. Hegazy, M. Salama, A. Chikhani, Adequacy assessment of distributed generation systems using Monte Carlo simulation, IEEE Trans Power Syst 18 (2003) 48-52.

[13] R. Rocchetta, Y. Li, E. Zio, Risk assessment and risk-cost optimization of distributed power generation systems considering extreme weather conditions, Reliab Eng Syst Saf 136 (2015) 47-61.

[14] J. A. Momoh, Electric power distribution, automation, protection, and control, CRC press, 2007.

[15] W. Li, Risk assessment of power systems: models, methods, and applications, John Wiley & Sons, 2014.

[16] R. Billinton, A. Sankarakrishnan, A comparison of Monte Carlo simulation techniques for composite power system reliability assessment. In: WESCANEX 95. Communications, Power, and Computing Conference Proceedings., IEEE, 1995, p. 145-150.

[17] R. Billinton, W. Li, Distribution System and Station Adequacy Assessment, in Reliability assessment of electric power systems using Monte Carlo methods, ed: Springer; 1994. p. 209-54.

[18] M. B. Giles, Multilevel Monte Carlo path simulation, Ope Res 56 (2008) 607-617.

[19] K. Stuben, An introduction to algebraic multigrid, Multigrid; 2001. p. 413-532.

[20] M. B. Giles, Multilevel Monte Carlo methods, Acta Numer 24 (2015) 259-328.

[21] S. Heinrich, Multilevel Monte Carlo Methods. Berlin, Heidelberg; 2001, p. 58-67.

[22] G. Katsiolides, E. H. Müller, R. Scheichl, T. Shardlow, M. B. Giles, D. J. Thomson, Multilevel Monte Carlo and improved timestepping methods in atmospheric dispersion modelling, J Comput Phys 354 (2018) 320-343.

[23] S. E. Z. Soudjani, R. Majumdar, T. Nagapetyan, Multilevel Monte Carlo Method for Statistical Model Checking of Hybrid Systems. In: International Conference on Quantitative Evaluation of Systems; 2017. p. 351-367.

[24] S. Schultz, H. Handels, J. Ehrhardt, A multilevel Markov Chain Monte Carlo approach for uncertainty quantification in deformable registration. In: Medical Imaging 2018: Image Processing; 2018. p. 105740O.

[25] L. Szpruch, M. B. Giles, Multilevel Monte Carlo Methods for Applications in Finance. In: High-Performance Computing in Finance ed: Chapman and Hall/CRC; 2018. p. 197-247.

[26] A. Jasra, S. Jo, D. Nott, C. Shoemaker, R. Tempone, Multilevel Monte Carlo in approximate bayesian computation, arXiv preprint arXiv:1702.03628, 2017.

[27] A. S. N. Huda, R. Živanović, Accelerated distribution systems reliability evaluation by multilevel Monte Carlo simulation: implementation of two discretisation schemes, IET Gene Transm Distrib 11 (2017) 3397-3405.

[28] A. S. N. Huda, R. Živanović. Multilevel Monte Carlo simulation applied to distribution systems reliability evaluation. In: PowerTech, 2017 IEEE Manchester; 2017. p. 1-6.

[29] W. Li, Reliability assessment of electric power systems using Monte Carlo methods, Springer Science & Business Media, 2013.

[30] R. Billinton, S. Jonnavithula, A test system for teaching overall power system reliability assessment, IEEE Trans Power Syst 11 (1996) 1670-1676.

[31] C. de Schryver, P. Torruella, N. Wehn, A multi-level Monte Carlo FPGA accelerator for option pricing in the Heston model. In: Proceedings of the Conference on Design, Automation and Test in Europe; 2013. p. 248-53.

[32] M. Giles, Improved multilevel Monte Carlo convergence using the Milstein scheme, in Monte Carlo and quasi-Monte Carlo methods 2006, ed: Springer; 2008. p. 343-358.

[33] J. M. Harrison, Brownian motion and stochastic flow systems, Wiley, New York, 1985.

[34] B. Oksendal, Stochastic differential equations: an introduction with applications, Springer Science & Business Media, 2013.

[35] R. P. Broadwater, A. H. Khan, H. E. Shaalan, R. E. Lee, Time varying load analysis to reduce distribution losses through reconfiguration, IEEE Trans Power Deliv 8 (1993) 294-300.

[36] R. N. Allan, Reliability evaluation of power systems, Springer Science & Business Media, 2013.

[37] R. N. Allan, R. Billinton, I. Sjarief, L. Goel, K. So, A reliability test system for educational purposes-basic distribution system data and results, IEEE Trans Power Syst 6 (1991) 813-820.

[38] K. Wang, M. L. Crow, Fokker-Planck equation application to analysis of a simplified wind turbine model. In: North American Power Symposium (NAPS) 2012; 2012. p. 1-5.

[39] C. Bierig, A. Chernov, Approximation of probability density functions by the Multilevel Monte Carlo Maximum Entropy method, J Comput Phys 314 (2016) 661-681.

[40] A. S. N. Huda, R. Živanović, Efficient Estimation of Interrupted Energy with Time-Varying Load Models for Distribution Systems Planning Studies, IFAC-PapersOnLine 51 (2018) 208-213.

Appendix A

Load [5, 36, 40] and SCDF data [5]

Table A.1. Weekly peak load as a percentage of annual peak

Week	% Peak load	Week	% Peak load	Week	% Peak load	Week	% Peak load
1	90	14	69.5	27	100	40	73.7
2	88.7	15	72.4	28	95.2	41	71.5
3	89.6	16	72.4	29	86.2	42	72.7
4	86.1	17	74.3	30	90	43	70.4
5	75.5	18	74.4	31	87.8	44	75
6	81.6	19	80	32	83.4	45	72.1
7	80.1	20	88.1	33	88	46	80
8	88	21	88.5	34	84.1	47	75.4
9	80	22	90.9	35	83.2	48	83.7
10	72.9	23	94	36	80.6	49	87
11	72.6	24	89	37	72.2	50	88
12	70.5	25	94.2	38	77.6	51	85.6
13	78	26	97	39	74	52	81.1

Table A.2. Daily peak load as a percentage of weekly peak

Day	% Peak load
Mon	93
Tues	100
Wed	98
Thu	96
Fri	94
Sat	77
Sun	75

Table A.3. SCDF for different customer types

User sector	Interruption duration (Min.) & cost($/kW)				
	1 min.	20 min.	60 min.	240 min.	480 min.
Large user	1.005	1.508	2.225	3.968	8.240
Industrial	1.625	3.868	9.085	25.16	55.81
Commercial	0.381	2.969	8.552	31.32	83.01
Residential	0.001	0.093	0.482	4.914	15.69
Govt./Inst.	0.044	0.369	1.492	6.558	26.04
Office buildings	4.778	9.878	21.06	68.83	119.2
Agricultural	0.060	0.343	0.649	2.064	4.120

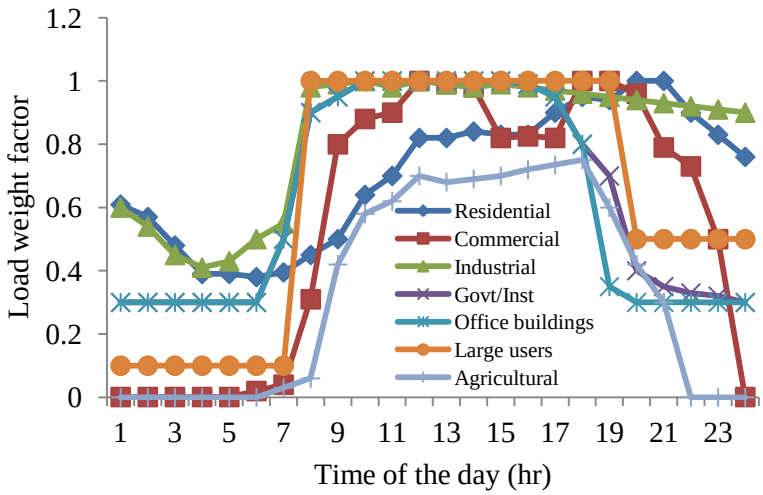

Fig. A.1. Hourly load weight factors for different customer sectors

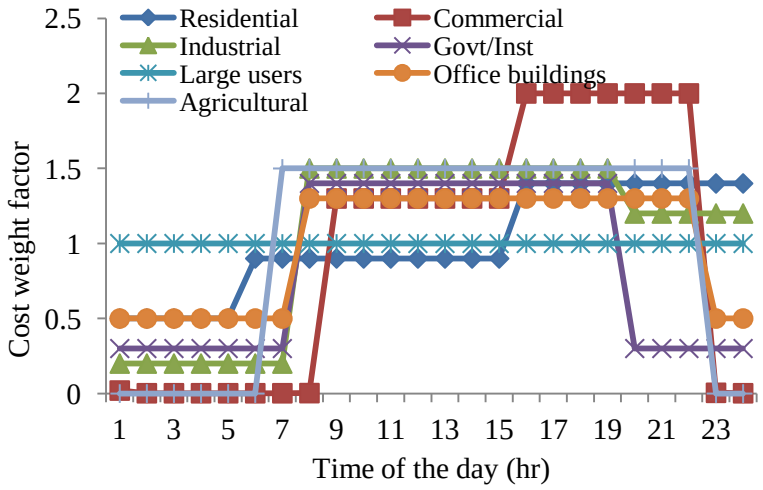

Fig. A.2. Hourly cost weight factors for different customer sectors

Appendix B

Single line diagrams of distribution systems [30]

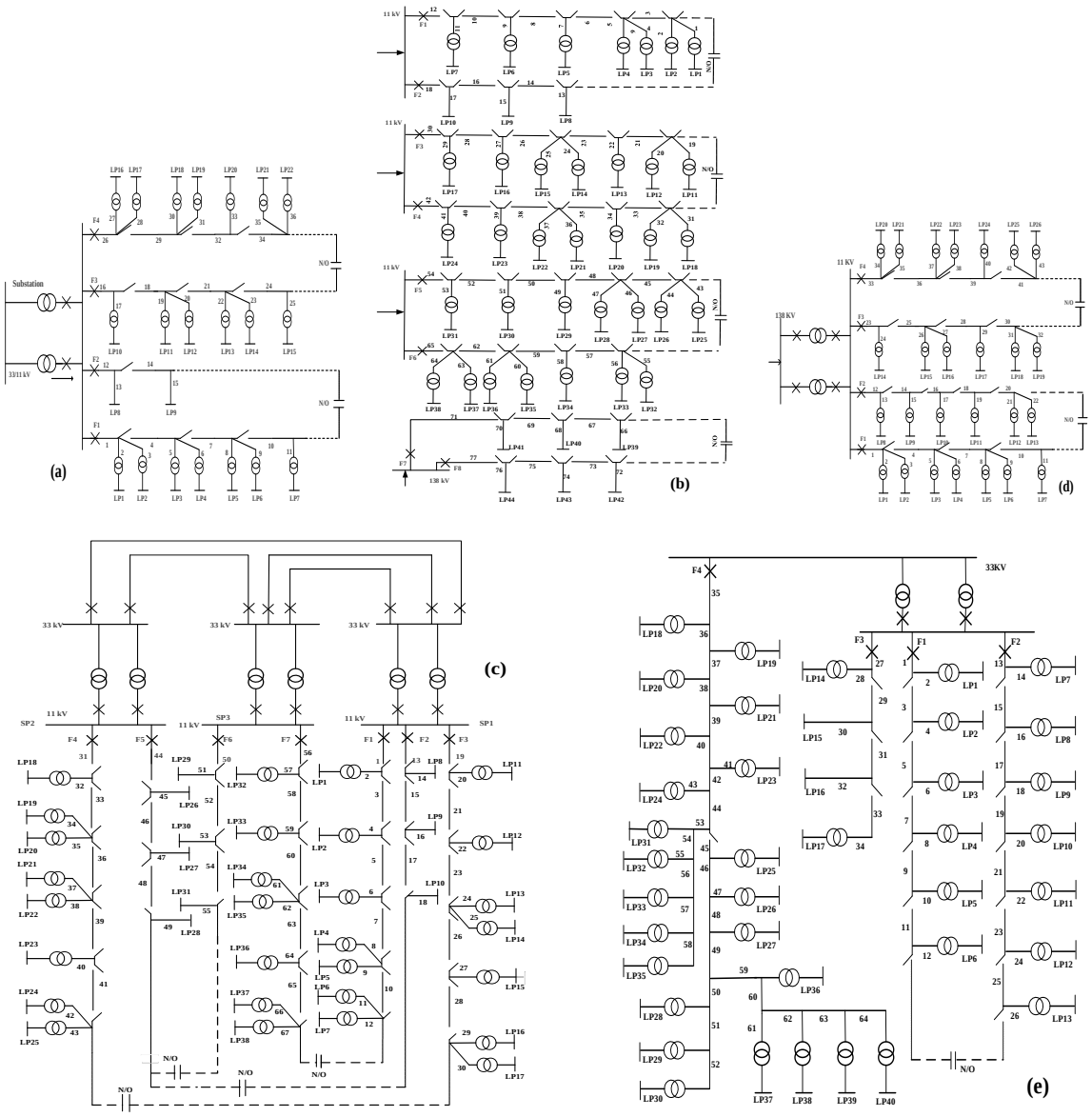

Fig. B.1. Distribution systems for RBTS (a) Bus 2 (b) Bus 3 (c) Bus 4 (d) Bus 5 and (e) Bus 6

Appendix C

Simulated results for different test systems showing the variation of ECOST estimation due to time-varying load, cost and their simultaneous effects

Table C.1. ECOST (k$/yr) variation with time-varying load

Failure starting time	1:00		8:00		16:00	
System	MC	MLMC	MC	MLMC	MC	MLMC
B2	163.07	167.21	249.67	256.35	159.12	163.59
B3	196.58	201.58	398.82	409.45	306.22	314.50
B4	159.41	163.61	307.48	315.61	258.10	265.17
B5	232.25	238.51	310.87	319.35	188.57	193.29
B6	112.78	115.79	201.07	206.29	205.04	210.53

Table C.2. ECOST (k$/yr) variation with time-varying cost

Failure starting time	1:00		8:00		16:00	
System	MC	MLMC	MC	MLMC	MC	MLMC
B2	131.18	134.96	268.07	275.45	174.36	178.76
B3	176.83	181.64	341.44	350.65	304.88	313.10
B4	121.65	124.73	298.70	306.87	272.96	280.37
B5	190.16	195.42	294.87	302.87	194.14	199.33
B6	73.50	75.56	164.10	168.49	161.01	165.23

Table C.3. ECOST (k$/yr) variation with time-varying load and cost

Failure starting time	1:00		8:00		16:00	
System	MC	MLMC	MC	MLMC	MC	MLMC
B2	117.81	120.82	364.03	373.61	154.78	159.01
B3	131.02	134.82	511.82	525.46	351.57	360.94
B4	91.65	94.40	411.02	422.21	316.23	324.63
B5	200.01	205.40	412.30	423.22	167.55	172.18
B6	71.66	73.62	242.95	249.48	268.59	275.91

Table C.4. ECOST computation time (s) variation with time-varying load

Failure starting time	1:00		8:00		16:00	
System	MC	MLMC	MC	MLMC	MC	MLMC
B2	27.35	0.90	63.13	2.18	25.79	0.89
B3	37.24	1.55	148.01	6.33	86.87	3.80
B4	23.93	0.94	87.21	3.53	64.55	2.50
B5	49.5	1.97	87.82	3.55	32.99	1.33
B6	20.02	0.75	56.62	2.69	57.25	2.23

Table C.5. ECOST computation time (s) variation with time-varying cost

Failure starting time	1:00		8:00		16:00	
System	MC	MLMC	MC	MLMC	MC	MLMC
B2	18.54	0.65	70.40	2.66	31.77	1.11
B3	30.5	1.25	110.72	5.31	87.02	3.85
B4	14.75	0.55	81.73	3.32	66.56	2.78
B5	32.94	1.32	80.17	3.14	34.70	1.42
B6	9.10	0.33	41.04	1.55	36.34	1.47

Table C.6. ECOST computation time (s) variation with time-varying load and cost

Failure starting time	1:00		8:00		16:00	
System	MC	MLMC	MC	MLMC	MC	MLMC
B2	15.87	0.51	134.38	5.04	25.44	0.87
B3	16.89	0.71	221.44	10.65	116.24	4.87
B4	8.68	0.34	154.38	6.31	92.48	3.78
B5	37.13	1.48	150.70	6.21	26.12	1.12
B6	8.62	0.32	82.85	3.40	101.24	4.49

Chapter 7

Effect of Weather Conditions on Computation

Statement of authorship

Title of Paper	Analysis effect of weather conditions on electric distribution system reliability evaluation through an efficient approach
Publication Status	☐ Published ☐ Accepted for Publication ☑ Submitted for Publication ☐ Unpublished and Unsubmitted w ork w ritten in manuscript style
Publication Details	A. S. Nazmul Huda, Rastko Živanović (2018) Analysis effect of weather conditions on electric distribution system reliability evaluation through an efficient approach, Quality and Reliability Engineering International. Wiley. Received feedback from reviewers

Principal author

Name of Principal Author (Candidate)	A. S. Nazmul Huda		
Contribution to the Paper	Developed reliability evaluation model, performed simulation and numerical analysis, prepared manuscript.		
Overall percentage (%)	80%		
Certification:	This paper reports on original research I conducted during the period of my Higher Degree by Research candidature and is not subject to any obligations or contractual agreements with a third party that would constrain its inclusion in this thesis. I am the primary author of this paper.		
Signature		Date	07.09.2018

Co-author contributions

By signing the Statement of Authorship, each author certifies that:

the candidate's stated contribution to the publication is accurate (as detailed above);

permission is granted for the candidate in include the publication in the thesis; and

the sum of all co-author contributions is equal to 100% less the candidate's stated contribution.

Name of Co-Author	Rastko Živanović		
Contribution to the Paper	Supervised for development of model, helped in data interpretation and manuscript evaluation		
Signature		Date	13.08.02018

Analysis effect of weather conditions on electric distribution system reliability evaluation through an efficient approach

Abstract- The objective of this paper is to evaluate the distribution system reliability indices under normal and adverse weather conditions while a new computationally efficient Multilevel Monte Carlo (MLMC) simulation approach is used as a computation tool. The evaluation of distribution system reliability in different weather conditions such as high winds, lightning can be characterized by incorporating time-varying failure rate and repair time of the failed components since these can be changed dramatically in adverse weather condition. Application of classic MC simulation is usually sufficient to evaluate the reliability accurately. However the increase of the computation speed of the time-consuming MC method based evaluation especially while dealing with the rare events could be an important contribution in modern power systems computation applications. MLMC method is a recently developed variance reduction technique for MC method which could reduce computation burden dramatically while both sampling and discretization errors are considered for converging to a controllable accuracy level. For validation purpose, applications of the implemented method are carried out on a benchmark test distribution system. The effects of the reliability estimation considering both normal and adverse weather effects on the computation performance are determined. The results are compared with those obtained by using typical MC simulation.

Keywords- Distribution system reliability; Simulation speedup; Multilevel Monte Carlo method; Weather effects.

1. Introduction

Reliability evaluation is an important prerequisite for designing and planning of power distribution systems. It reveals the ability of a system to meet the load requirement of customers in an economical way with minimal interruption [1]. About 20% of the load point interruptions happen due to the failures in generation and transmission systems and remaining 80% are caused by the problems in distribution systems [2]. The evaluation measures some indices of interruption frequency and duration based on network configuration and connected elements failure and repair information which supports a distribution system planner to access most of the required knowledge about expected frequency, duration, cost and energy loss of interruptions. The common indices concerning these are System Average Interruption Frequency Index (SAIFI) and System Average

Interruption Duration Index (SAIDI) [3, 4]. Additionally, the evaluation of Expected Cost of Interruption (ECOST) index related to economics assists utilities to establish a relationship between the importance of further improvement of reliability and the related economic challenge to system customers [5]. The index which describes the expected amount of interrupted energy is expressed by Expected Energy Not Supplied (EENS). By evaluating all these indices, the engineers can take necessary steps in designing and planning expansion of distribution systems according to the customer load reliability requirement.

Depending on the weather, the reliability indices can be assessed in two conditions: normal and adverse [6]. In the normal weather condition, usually the component failure rate and restoration time are considered non time-varying for simplification. However, adverse weather conditions could significantly affect the estimation of reliability through unexpected increasing the failure rate of components and their restoration time. In adverse condition, failure rate and restoration times are therefore modelled considering different time-varying weight factors for accurate estimation of reliability [7]. The adverse weather conditions: severe winds and lightning are the two primary sources of sustained interruptions in distribution systems [8, 9]. In this paper, we consider both these conditions which are extreme in nature [10]. The intensity level of each weather event greatly varies with time and reliability level of system is decreased with the increase of intensity level.

Two basic approaches are used to evaluate system reliability: analytical and simulation approaches [11-13]. Analytical method only evaluates an average value of the reliability indices based on the historical values without considering the random behavior of these indices. However, considering the deviation of reliability indices based on specified probability distribution is necessary for distribution system expansion and future planning. On the other hand, the complexity of modern distribution systems as well as the need of analysis of different probabilistic factors in accurate reliability modelling is a very important task. Therefore, reliability analysts require the use of other technique which is accurate, efficient and can consider the random nature of reliability indices. Monte Carlo (MC) simulation has been extensively used for many years in reliability evaluation applications [14-20] which can consider probability related to these indices. MC simulation generates the stochastic behavior of components outage and repair times. The method is divided into two modes: sequential and non-sequential [21]. In the non-sequential mode, the states of all components are sampled and a non-chronological system state is found [22]. On the other hand, the up and down cycles of all components are simulated in the

sequential form and overall system operating cycle is achieved by combining all the components cycles [22]. The sequential MC allows the consideration of the chronological matters and distributions of the reliability indices [23]. The state duration sampling approach is generally used to simulate chronological issues which can describe time-related reliability indices concerning frequency and duration of interruption [24]. However, the sequential MC simulation significantly decreases the computational efficiency and practicability when dealing with very reliable system with probabilities of very smaller occurrence (i.e. high accuracy).

Over the years, several advanced various variance reduction techniques (VRT) have been applied to enhance its convergence speed of the MC method. Through VRT, the expected value of an output random variable can be obtained with reduced computation time by maintaining a pre-defined level of accuracy. VRT based on cross-entropy method, importance sampling approach has been utilized extensively in power system reliability applications in order to speedup computation which are mainly carried out on the generation and transmission systems reliability evaluation [25-28]. There has been a lack of research in the area of distribution systems reliability assessment by applying these advanced MCS methods. Another issue is to incorporate weather condition which has an effect on the computation. It should be noted that the aim of this paper is not to develop new models of weather-dependent failure rate and restoration time. However the purpose of this paper is to demonstrate the practicality of the novel Multilevel Monte Carlo (MLMC) simulation technique in distribution system reliability evaluation under different weather conditions.

The MLMC simulation approach is an advanced MC method which has been recently developed by Giles [29]. In MC method, the accuracy of the output variable is high since a large number of iterations is run only on the finest grid level [30] which requires high computation time. In MLMC simulation, a series of coarse levels is used to achieve the finest level accuracy [31]. On each level, expectations are estimated using different sample size in a manner which could decrease the overall variance for a pre-defined error tolerance. Through performing simulations on multiple discretisation time-steps, less number of samples is required on the expensive finest level in MLMC than MC to achieve the same accuracy. Since a sequence of levels is used therefore less precise estimation on the previous coarse level can be sequentially corrected by estimation on the next fine levels [29].

The paper establishes a time sequential MLMC simulation for the reliability indices calculation of distribution systems in two different weather conditions. Two fundamental variables in the reliability evaluation, time to failure (TTF) and time to repair or restoration (TTR) have been modelled stochastically and solved using Milstein discretisation method. Four reliability measures: SAIFI, SAIDI, EENS and ECOST are evaluated. For modelling time-varying failure rate, weather dependent factors such as high wind speed and lightning are considered in reliability estimation. Different time-varying weight factors and a delay during adverse weather are considered in modelling of restoration time. Similarly, for load and cost modelling, different time-varying weight factors are incorporated in calculation. A comprehensive result showing the effects of different time-varying parameter models are presented while the computations are performed using MLMC method. The computation accuracy compared to the original MC method is also presented.

2. Multilevel Monte Carlo method

2.1. Monte Carlo method

Let P be the quantity of interest which is approximated as the expected value $E[P]$ of some random variable. In this study, P is the specified system reliability index. Using the direct MC method, a large number of independently and identically distributed samples of this random variable drawn and the mean value is computed to approximate the $E[P]$ numerically [32]. Consider $E[P_M]$ is the approximation of $E[P]$ and given the N number of samples ${P_M}^{(i)}$ $[i = 1, 2, \dots \dots, N]$. According to the MC method, the expected value of the P is approximately equal to the approximation of P, P_M which can be estimated by the mean of N samples of the random variable P_M and can be wrriten as follows:

$$E[P] \approx E[P_M] \approx \hat{P}_{MC} = \frac{1}{N_{MC}} \sum_{i=1}^{N_{MC}} P_M^{(i)}. \quad (1)$$

where $\hat{P}_{MC}$ is the standard MC estimator for $E[P_M]$. $P_M^{(1)}, \dots \dots P_M^{(N)}$ are independently and identically distributed copies of P_M. $E[P_M]$ is computed using the single approximation on the finest level $l = L$. Therefore, 2^L uniform time-steps are required over the interval $[0, T]$. The level is normally associated with a grid size or time-step length and we find the importance of time-step in computational cost variation from Eq. (17). On the finest level, both estimation accuracy and computation cost are very high.

The accuracy of this estimation can be quantified using the mean square error (MSE) of the estimator which is denoted by ε^2. Since all the simulations are carried out on the level $l = L$ therefore, it reduces the discretisation error but increases the simulation running time. The variance of the MC estimator is $V\left[\hat{P}_{MC}\right] = \frac{1}{N_{MC}} V[P_M]$. To achieve an accuracy level of ε, the simulation requires $N_{MC} = O(\varepsilon^{-2})$ samples which needs huge computation time. This is especially true when dealing with rare events. In term of computational complexity, the estimated cost related to this estimator can be written as:

$$C(\hat{P}_{MC}) = N_{MC} C_M \tag{2}$$

where C_M is the computation cost for one sample of P_M and estimated as $c_3 M^{\gamma}$ for a constant c_3 and some $\gamma > 0$. M is the cost refinement factor used to refine the time-step at each level [30]. For both MC and MLMC methods, $M = 2$ is considered which means each level has twice as many time-steps as the prior level. γ is the rate of cost increase with the increase of M. An effective numerical solver usually provides a small γ. The value of γ can be determined by fitting the curve of C_M with varies of M. The smaller values of N_{MC} and M reduce the cost of the estimator, but increase MSE. Therefore, in order to reduce the cost without altering the level of accuracy, an efficient estimator is required.

2.2. MLMC approach

2.2.1. Basics of MLMC method

MLMC approach is a VRT for the MC simulation. The basic idea of MLMC method is to use multigrid through a geometric order of levels starting from the coarsest grid to finest grid. Such as the target $E[P]$ is estimated through sum of multiple $E[P_l]$ which are run on a series of levels as $l = 0, 1, \ldots, L$. $l = 0$ and $l = L$ are the coarsest and finest levels, respectively. In stochastic modeling of reliability index using SDE, single time-step is used for simulations on $l = 0$. On the other hand, 2^L uniform time-steps are required on $l = L$. On the coarsest level, both accuracy and required computation time are least and on the finest level, both are highest. The cost is proportional to the total number of time-steps particularly the computation time increases greatly for large number of the finest level samples. Initially the expected value on $l = 0$, $E[P_0]$ is estimated using number of time-step $n = 2^0 = 1$ and then correction value of reliability estimation is estimated as $E[P_l - P_{l-1}]$ on levels $l = 1, \ldots, L$ using different number of time-steps $n = 2^1, \ldots\ldots, 2^L$,

respectively. By using the correction values, the finest grid accuracy of the estimation is achieved as follows:

$$E[P_M] = E\left[P_{M(0)}\right] + \sum_{l=1}^{L} E\left[P_{M(l)} - P_{M(l-1)}\right] = \sum_{l=0}^{L} E[Y_l], \quad (3)$$

In Eq. (3), most of the simulations are run using larger time-steps to decrease the variance in such a way that minimizes the overall simulation running time and also retains the accuracy associated with the smallest timestep on finest level [33]. $P_{M(0)}$ and $P_{M(l)}$ are the estimation of reliability on $l = 0$ and $l > 0$, respectively. Consider $\hat{Y}_0$ and $\hat{Y}_l$ are the estimators on $l = 0$ and $l > 0$ using N_0 and N_l samples, respectively.

$$\hat{Y}_0 = \frac{1}{N_0}\sum_{i=1}^{N_0} P_{M(0)}^{(i)};\ \hat{Y}_l = \frac{1}{N_l}\sum_{i=1}^{N_l}\left(P_{M(l)}^{(i)} - P_{M(l-1)}^{(i)}\right), \quad (4)$$

Overall reliability index estimator of MLMC simulation:

$$\hat{P}_{MLMC} = \sum_{l=0}^{L} \hat{Y}_l. \quad (5)$$

The estimator for $E\left[P_{M(l)} - P_{M(l-1)}\right]$ is calculated as $E\left[P_{M(l)}^{f} - P_{M(l-1)}^{c}\right]$ until level L is reached. Here $P_{M(l)}^{f}$is a fine level estimator using time-step size $h_f = 2^{-l}T$ and $P_{M(l-1)}^{c}$ is the corresponding coarse level estimator using time-step $h_c = 2^{-(l-1)}T$. The computation is performed as $E\left[P_{M(l)}^{f}\right] = E\left[P_{M(l)}^{c}\right]$ in order to remove the unwanted bias.

2.2.2. Computational cost of MLMC

The estimation of $E[P]$ causes two types of error: (1) sampling error due to the estimation of the exact solution $E[P]$ by a finite sample average and (2) discretization error due to the approximation of $E[P]$ by $E[P_M]$ which measures how closely the model simulates the true solution. The contribution of both errors could be analyzed through MSE which is used to quantity the accuracy of the MLMC estimator [34]:

$$e(\hat{P}_{MLMC})^2 = V\left[\hat{P}_{MLMC}\right] + [E(P_M - P)]^2 < \frac{\varepsilon^2}{2} + \frac{\varepsilon^2}{2} \quad (6)$$

The variance of the MLMC estimator in above Eqn. is the sampling error. $V[\hat{P}_{MLMC}]$ is estimated as $\sum_{l=0}^{L} N_l^{-1} V[\hat{Y}_l]$. This error declines inversely with the each level sample size N_l. The square of the error in mean between P_M and P in the Eqn. represents discretization/bias error and can be reduced by using a large fine grid size [34]. In terms of

computational complexity, the estimated cost related to this estimator can be written as follows:

$$C\left(\hat{P}_{MLMC}\right) = c_3 N_0 2^{\gamma(0)} + \sum_{l=1}^{L} c_3 N_l 2^{\gamma(l)}$$

$$= \sum_{l=0}^{L} C_l N_l \tag{7}$$

where C_l is the cost to compute one sample of Y_l and estimated as $c_3 2^{\gamma l}$. The expected computational complexity C can be defined with the following bound [29]:

$$E[C] \leq \begin{cases} c_4 \varepsilon^{-2}, & \beta > \gamma, \\ c_4 \varepsilon^{-2} (log\varepsilon)^2, & \beta = \gamma, \\ c_4 \varepsilon^{-2-(\gamma-\beta)/\alpha,} & \beta < \gamma. \end{cases} \tag{8}$$

$\alpha > 0$ is the weak convergence rate for a constant c_1i.e. $|E[P_l - P]| \leq c_1 2^{-\alpha l}$ and is related to the discretisation error. The discretisation error is controlled by choosing minimum level of grid. β>0 is assumed as the rate of decrease of multilevel variance with l for a constant c_2, i.e. $V_l \leq c_2 2^{-\beta l}$. In case of $\beta < \gamma$, the variance of the estimator reduces at a slower rate than the increase of the cost on each level. When $\beta = \gamma$, the decay of the variance is balanced with the increase of the cost; therefore the contribution to the overall cost is the same from all the levels. Finally, when $\beta > \gamma$, the total cost is controlled by the level $l = 0$ as successive levels will have a decaying impact to the cost [35]. In the proposed study, α, β and γ are not pre-defined and estimated by linear regression [29].

2.2.3. MLMC implementation

For MLMC method implementation, initially the simulation is started by choosing the coarsest level $l = 0$. After this, two basic optimal parameters are defined to achieve target accuracy i.e. optimal levels and the optimal samples on each level. In Eq. (6), an adequate circumstance to reach a RMSE of ε with the estimator is $V\left[\hat{P}_{MLMC}\right] + [E(P_M - P)]^2 < \varepsilon^2$ i.e. both of the errors should be less than $\frac{\varepsilon^2}{2}$. In order to make $V\left[\hat{P}_{MLMC}\right] \leq \frac{\varepsilon^2}{2}$, the samples on each level N_l is optimally controlled as [36]:

$$N_l = 2\varepsilon^{-2} \sqrt{V_l / C_l} \left(\sum_{l=0}^{L} \sqrt{V_l C_l} \right) \tag{9}$$

The optimal number of levels is confirmed by ensuring the weak error $[E(P_M - P)]^2 \leq \frac{\varepsilon^2}{2}$. The weak convergence rate is measured by a positive value α, i.e. $|E[P_l - P_{l-1}]| \leq c_1 2^{-\alpha l}$ [30]. The remaining error is $E(P_M - P) = E[P_L - P]/(2^{\alpha} - 1)$ and the target convergence criterion is $E[P_L - P_{L-1}]/(2^{\alpha} - 1) < \varepsilon/\sqrt{2}$.

3. Implementation for evaluating reliability in weather conditions

3.1. Basic modelling

3.1.1. Component modelling

In this study, the component modelling is represented by the two-state model as shown in Figure 1. The up and down states indicate the operating and restoration mode of the component, respectively. Figure 2 shows an example of component operating and restoration cycles. TTF and TTR are both random variables [37]. TTF is the expected time for a component to remain in the up-state before it fails. TTR of a component is the expected time required for a crew to repair an outage and restore the normal operation of the system. The switching from an up state to a down state is called the failure process. It can be caused by the failure of a component or by the removal of components for repairing.

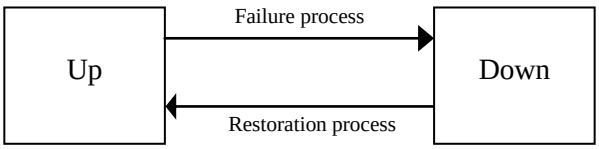

Fig. 1 State space diagram of component

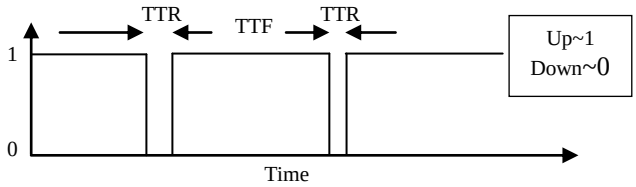

Fig. 2 Component operating and restoration cycles

3.1.2. Time-varying failure rate (TVFR) modelling

A model for TVFR, $\lambda(t)$ for the overhead line is considered in this study for more accurate estimation of the component failure rate in adverse weather conditions. The weather dependent failure rate is characterized by two conditions i.e. high wind and lightning. The

failure rate at an hour t for these two conditions can be calculated using the following equations [10]:

$$\lambda_{wind}(t) = \left(a_1 e^{a_2 w(t)} - a_3\right)\lambda \tag{10}$$

$$\lambda_{lighting}(t) = \left(b(N_g(t) + 1\right)\lambda \tag{11}$$

where $\lambda_{wind}(t)$ is the component failure rate at hour t. a_1, a_2 and a_3 are the scaling factors. $w(t)$ is the wind speed (m/s) at time t above the tolerance speed level which affects the component failure rate. λ is the failure rate ((failure/year) of component in normal weather condition. $N_g(t)$ is the ground flash density (flashes/km^2, hr) of greater than zero at time t and b is the scaling factor. All the parameters for estimating time-varying failure rate are found in Appendix.

3.1.3. Time-varying restoration time (TVRT) modelling

Restoration time of a component failure can be varied with the time of failure and weather condition. Based on failure time, restoration time could be different between working and after hours and also between weekday and weekend. Therefore, TVRT, $r(t)$ could be modelled by multiplying hourly (W_h) and weekly (W_d) varying weight factors with the constant restoration time (r)[hour/failure]. The weight factors are found from the past experience of TVRT. All the parameters for estimating time-varying restoration are found in Appendix. In case of adverse weather condition, an additional restoration time, r_a is added. r_a is the time duration of the severe weather after the starting of the interruption [6]. For switching time, r_a is equal to zero since the crew will try to isolate the fault as soon as it starts [38].

TVRT in normal weather:

$$r(t) = W_d \times W_h \times r \tag{12}$$

TVRT in severe weather:

$$r_{adverse}(t) = r(t) + r_a \tag{13}$$

3.1.4. Time-varying load (TVL) Modelling

The daily load curves have dissimilar shapes depending on the day type, month as well as seasonal variation. Due to the data constraint about information of the hourly load

consumption, the typical consumption cycles of each load is considered in this study which is developed using daily, weekly and annual load behavior. For a customer sector, the TVL $L(t)$ in an hour t of a day is modelled as follows:

$$L(t) = L_{peak} \times W_l \times D_l \times H_l(t) \tag{14}$$

where L_{peak} is the annual peak load, W_l is the weekly peak load as a percentage of L_{peak}, D_l is the daily peak load as a percentage of weekly peak and H_l is the hourly peak load as a percentage of daily peak. The seasons are represented through weeks as- summer: 1-8 & 48-52; winter: 20-36 and spring/fall: 9-19 & 37-47. Data for each load type can be found in [39].

3.1.5. Time-varying cost (TVC) modelling

The TVC model $C(t)$ at a time t in a day for a specific customer sector connected to a load point could be modeled as follows:

$$C(t) = C_j \times W_c(t) \tag{15}$$

where C_j is the average interruption cost in \$/kW of customers for a load point j. C_j is calculated for the duration of entire failure period using the Sector Customer Damage Function (SCDF) of the customer type at load point j. A linear interpolation cost data is used when the outage period lies between two distinct times. Data of SCDF for different customer types could be found in Appendix. W_c is the percentage of TVC weight factor as shown in the Figure 3.

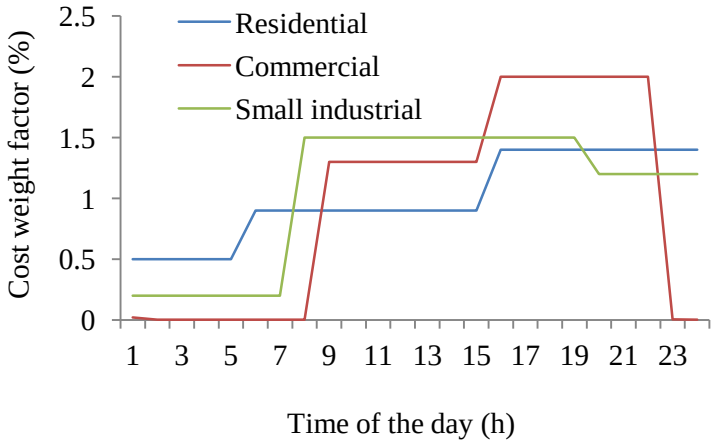

Fig. 3 Cost weight factors for different customer types

3.1.6. Modelling of time-varying system reliability

For modelling system reliability, two basic random variables of each component i.e. TTF and TTR are initially modelled. Note that the time of an outage event is absolutely random and there is no such guarantee that a component will follow the outage history of the similar elements. Therefore, TTF and TTR of an outage event are random variables and just approximations of the actual TTF and TTR, respectively. In this study, we model TTF and TTR using SDE which is driven by Brownian motion where the outputs are normally distributed random variables. Consider, λ_i and r_i represent constant failure rate and repair time of a component *i*, respectively. Then the SDE of TTF for this component on the time $[0, T]$ can be expressed as follows [40, 41]:

$$dX_{it} = \mu(X_{it}, t)dt + \sigma(X_{it}, t)dW, \qquad 0 < t < T \tag{16}$$

where X_{it} is the TTF at a time t with an initial TTF of $X_{i0} = 1/\lambda_i = 1/\lambda_{norm}$ in normal weather. For an adverse weather, initial TTF is defined by Eqs. (10) or (11) based on condition.

The rate of change of average value of stochastic process and the degree of variation of stochastic process over time are denoted as μ and σ, respectively. The SDE of TTF can be solved by using a discretisation scheme [42] and here we use Milstein discretisation [43]. The Milstein discretisation with n number of time-steps, step size $h = T/n$ and Brownian increments ΔW_m is [44]

$$X_{i(m+1)} = X_{im} + \mu(X_{im}, t_m)h + \sigma(X_{im}, t_m)\Delta W_m + +0.5\sigma^2(X_{im}, t_m)\left(\Delta W_m{}^2 - h\right), \tag{17}$$

where $\Delta W_m = W_{m+1} - W_m, m = 0, \dots\dots, n-1; t_m = kh,$
$k = 0, \dots\dots, n; \Delta W_1, \Delta W_2, \dots\dots, \Delta W_{n-1}$ are independently and normally distributed random variables.

Reliability of a distribution system is typically assessed with the useful life period of the component and the failure rate is assumed constant [45]. The operating history (T_{up}) of a component is generated in a sequential way based on random sampling method from the exponential probability distribution of component TTF [46, 47]. Now T_{up} of component i can be generated as:

$$T_{upi} = -X_{i(m+1)} \times \ln(V1), \tag{18}$$

where $V1$ is a uniformly distributed random variable between [0, 1].

Using the similar procedure, the artificial restoration history of each component is generated. For SDE of TTR, μ and σ are considered equal as TTF. The initial TVRT, $r_i(t)$ for component i during normal weather condition, y_i/λ_i. where y_i is a constant for component i and $y_i = r_i(t) \times \lambda_i$. For an adverse condition, $r_i(t)$ is replaced by $r_{adverse}(t)$ and λ_i is redefined based on Eqs. (10) or (11).

T_{dn} of component i can be generated as:

$$T_{dni} = -y_i \times X_{i(m+1)} \times \ln(V2), \tag{19}$$

where $V2$ is a uniformly distributed random variable between [0, 1].

The average failure rate, Λ_i and average unavailability, U_i for a component i can be calculated as:

$$\Lambda_i = \frac{NF}{\sum_{n=1}^{N} T_{upi(n)}}, \text{(outage/year)} \tag{20}$$

$$U_i = \frac{\sum_{n=1}^{N} T_{dni(n)}}{\sum_{n=1}^{N} T_{upi(n)} + \sum_{n=1}^{N} {T_{dni(n)}}/{8760}}, \text{(hour/year)} \tag{21}$$

where NF is the number of times component i fails during entire simulation time and N is the desired number of simulated periods. In Eq. (21), the denominator T_{dn} is divided by 8760 to convert its unit from hour to year. Average failure rate, A_j and annual unavailability, B_j for a load point j could be calculated as follows:

$$\mathrm{A}_j = \sum_{i=1}^{n_i} \Lambda_i, \text{(interruption/year)} \tag{22}$$

$$B_j = \sum_{i=1}^{n_i} U_i, \text{(hour/year)} \tag{23}$$

where n_i denotes the number of outage events affecting the service of load point j.

The reliability indices considering the time-varying parameter models can be modelled as follows:

$$SAIFI = \frac{\sum_{j=1}^{n_j} A_j N_{C_j}}{N_T} \text{(failure/system customer per year)} \tag{24}$$

$$SAIDI = \frac{\sum_{j=1}^{n_j} B_j N_{C_j}}{N_T} \text{ (hour/ system customer per year)} \quad (25)$$

$$ECOST = \sum_{j=1}^{n_j} A_j L_{t,j}\, C_{t,j} \text{ (k\$/year)} \quad (26)$$

$$EENS = \sum_{j=1}^{n_j} B_j L_{t,j} \text{ (MWh/year)} \quad (27)$$

where n_j is the total number of supply points. N_{C_i} is the number of customers at point j and N_T is the total number of customers served. $L_{t,j}$ and $C_{t,j}$ are the time-varying load and cost levels, respectively and estimated as follows:

$$L_{t,j} = \frac{\sum_{t=ts}^{te} L(t)}{te+ts-1};\ C_{t,j} = \frac{\sum_{t=ts}^{te} C(t)}{te+ts-1} \quad (28)$$

where ts and te are the failure start and end hours, respectively.

3.2. Summary of simulation procedure to estimate reliability

Using the proposed method, the reliability evaluation methodology consists by the following steps. Steps (1)-(8) describe the mathematical modelling of index on both coarse and fine grid levels and then steps (9)-(13) describe the convergence test process in the estimation.

(1) Define the input of reliability estimation. The input data include failure rate, repair time of each component failure event, sample size for convergence test (N), the initial sample size on each level (N_A) and the time-varying weight factors as described from section 3.1 to 3.4.

(2) Formulate the stochastic TTF models for a failed component i on the coarse and find levels using Milstein method as follows.

$$X^c_{i(m+1)} = X^c_{i(m)} + \mu\left[X^c_{i(m)}, t_m\right]h_c + \sigma\left[X^c_{i(m)}, t_m\right]\Delta W_{c(m)} + 0.5\sigma^2\left[X^c_{i(m)}, t_m\right]\left(\Delta W^2_{c(m)} - h_c\right) \quad (29)$$

$$X^f_{i(m+1)} = X^f_{i(m)} + \mu\left[X^f_{i(m)}, t_m\right]h_f + \sigma\left[X^f_{i(m)}, t_m\right]\Delta W_{f(m)} + 0.5\sigma^2\left[X^f_{i(m)}, t_m\right]\left(\Delta W^2_{f(m)} - h_f\right) \quad (30)$$

where h_c and h_f are the time-step sizes for coarse and fine path estimators which can be expressed as $h_c = 2^{-(l-1)}T$ and $h_f = 2^{-l}T$, respectively.

(3) Using the corresponding SDE of TTF, the operating (T_{upi}) and restoration histories (T_{dni}) of component i are generated on coarse and fine levels.

$$T_{upi}^{c} = -X_{i(m+1)}^{c}\, ln(V1);\; T_{upi}^{f} = -X_{i(m+1)}^{f}\, ln(V1) \tag{31}$$

$$T_{dni}^{c} = -y_i X_{i(m+1)}^{c}\, ln(V2);\; T_{dni}^{f} = -y_i X_{i(m+1)}^{f}\, ln(V2) \tag{32}$$

(4) Calculate component Λ_i and U_i on both levels using the corresponding operating and restoration histories as follows:

$$\Lambda_i^c = \frac{NF}{\sum_{n=1}^{N} T_{upi}^{c}};\; \Lambda_i^f = \frac{NF}{\sum_{n=1}^{N} T_{upi}^{f}}, \tag{33}$$

$$U_i^c = \frac{\sum_{n=1}^{N} T_{dni(n)}^{c}}{\sum_{n=1}^{N} T_{upi(n)}^{c} + \sum_{n=1}^{N} T_{dni(n)}^{c} \Big/ 8760};\; U_j^f = \frac{\sum_{n=1}^{N} T_{dni(n)}^{f}}{\sum_{n=1}^{N} T_{upi(n)}^{f} + \sum_{n=1}^{N} T_{dni(n)}^{f} \Big/ 8760}, \tag{34}$$

For each component failure, steps (2)-(4) are repeated.

(5) Find the load points interrupted by component i failure and calculate A_j and B_j on both levels using components indices.

$$A_j^c = \sum_{i=1}^{n_i} \Lambda_i^c;\; A_j^f = \sum_{j=1}^{n_i} \Lambda_i^f \tag{35}$$

$$B_j^c = \sum_{i=1}^{n_i} U_i^c;\; B_j^f = \sum_{i=1}^{n_i} U_i^f \tag{36}$$

(6) Repeat steps (2)-(5) for each load point in the system.

(7) Estimate the system reliability indices on both coarse and fine levels as follows:

$$SAIFI^c = \frac{\sum_{j=1}^{n_j} A_j^c N_{C_j}}{N_T};\; SAIDI^c = \frac{\sum_{j=1}^{n_j} B_j^c N_{C_j}}{N_T};\; ECOST^c = \sum_{j=1}^{n_j} A_j^c L_{t,j}\, C_{t,j};\; EENS^c = \sum_{j=1}^{n_j} B_j^c L_{t,j}. \tag{37}$$

$$SAIFI^f = \frac{\sum_{j=1}^{n_j} A_j^f N_{C_j}}{N_T};\; SAIDI^f = \frac{\sum_{j=1}^{n_j} B_j^f N_{C_j}}{N_T};\; ECOST^f = \sum_{j=1}^{n_j} A_j^f L_{t,j}\, C_{t,j};\; EENS^f = \sum_{j=1}^{n_j} B_j^f L_{t,j}. \tag{38}$$

(8) Using coarse and fine levels reliability index values, calculate the sum on levels $l = 0$ and $l > 0$. The simulation is repeated until the number of samples is reached to N.

(9) For convergence test, the initial value of the finest level is set at $L = 2$.

(10) Generate the number of samples N_s on $l = 0, 1, 2$ using N_A and also update the sum from step (8).

(11) Calculate the absolute mean m_l and variance V_l on each level $l = 0, 1, 2$.

(12) Find out the optimal number of samples N_l on each level using Eq. (9) and evaluate extra samples if needed by comparing with N_s. Moreover, update mean and variance on each level for confirming variance of the MLMC $< \frac{\varepsilon^2}{2}$.

(13) If not converged, set $L = L + 1$ and test convergence again until reached to the target accuracy level. Finally, calculate the multilevel estimator using Eq. (5).

3.3. Test System

A very well-known reliability test system called RBTS Bus 4 [48] as shown in Figure 4 is used as test distribution system. The test system is generally developed by considering all the actual complexities of a practical distribution system. It is a complex urban type network and consists of 38 supply points with commercial, residential and industrial customers. Component reliability data for the system are found in [49]. The customer data, load data and types, feeder and length data are provided in Appendix D. The availability and reliability of breakers, fuses and disconnecting switches are considered 100%. The availability of alternative supply source is also considered. The service of failed low voltage transformers is restored by repairing rather than replacing.

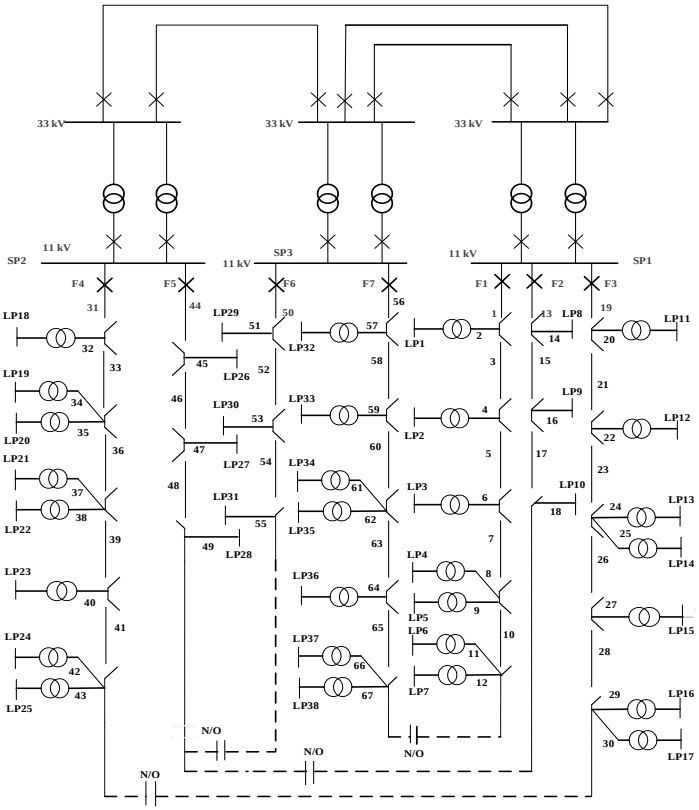

Fig. 4. Distribution system for RBTS bus 4

3.4. Simulation results

Four very common system reliability indices indicating interruption frequency, duration, energy and cost i.e. SAIFI, SAIDI, EENS and ECOST are evaluated using the proposed simulation method. In order to provide a comparative assessment, the results calculated using basic MC method is also presented. The indices values presented in the Tables 1-5 show the average value of each index through considering a large number of events. Here we only present the results assuming the failures occur at 1am in a weekday (Tuesday) of week 27. The target accuracy level is set as 5%. The reliability indices were computed on an Intel Core i7-4790 3.60 GHz processor.

3.4.1. Effect of normal weather condition

Tables 1-3 present the results of reliability evaluation under normal weather condition. I_{MC} and I_{MLMC} denote the specific index value based on MC and MLMC methods, respectively. R_{ID} is the percentage of the difference between I_{MC} and I_{MLMC} with respect to I_{MC}. Similarly, T_{MC} and T_{MLMC} represent the computation time in seconds based on MC and MLMC methods, respectively. R_{TD} is the percentage of the computation speedup using the proposed method with respect to MC method. In normal condition, component failure rate is not time-varying since it is assumed time-varying in adverse weather. Restoration time is

considered time-varying with the day and time of the day as mentioned in the Appendix. Here three cases are studied and compared considering TVRT case A) effect of TVRT incorporating not-TVFR, TVC and TVL; case B) effect of TVRT incorporating not-TVFR, not-TVL and TVC and case C) effect of TVRT incorporating not-TVFR, not-TVC and TVL. In case A, SAIFI will be as 0.2996 interruptions per year [50] since there is no effect of TVFR in SAIFI calculation. In case B, there is no effect of TVL on SAIDI estimation therefore EENS and ECOST are evaluated. Similarly, only ECOST is estimated in case C due to having TVC impact on it. In case A, incorporating TVL reduces EENS and ECOST values compared to the values of case B. Similarly, in case C, incorporating not-TVC increases high ECOST value than that of case A.

From the Tables it can be seen that the indices values using MLMC method are very close to the values using MC method. The maximum R_{ID} is found as 2.3186% for case A-SAIDI computation. These results are generally acceptable for a practical application where the stochastic process is involved. This proves the accuracy level of the proposed MLMC approach. Results also show that the time spent by the MC simulation is significantly higher than that used by MLMC. For example, the maximum T_{MC} is taken by 3.2055 s for case C- ECOST estimation. The proposed MLMC method takes only 0.1703 s for this estimation and saves 94.68% of simulation time. On average MLMC can reduce the simulation running time over 90% compared to the MC simulation.

Table 1. Effect of TVRT incorporating not-TVFR, TVC and TVL

Indices	I_{MC}	I_{MLMC}	R_{ID} (%)	T_{MC}	T_{MLMC}	R_{TD} (%)
SAIDI	3.4978	3.4167	2.3186	0.0311	0.0016	94.8553
EENS	44.5053	44.8213	-0.7100	2.3876	0.1753	92.6578
ECOST	91.6518	93.2163	-1.7070	1.2141	0.1041	91.4257

Table 2. Effect of TVRT incorporating not-TVFR, TVC and not-TVL

Indices	I_{MC}	I_{MLMC}	R_{ID} (%)	T_{MC}	T_{MLMC}	R_{TD} (%)
EENS	55.4307	56.1636	-1.3221	2.6799	0.1729	93.5482
ECOST	121.6464	123.3669	-1.4143	2.0195	0.1254	93.7905

Table 3. Effect of TVRT incorporating not-TVFR, not-TVC and TVL

Indices	I_{MC}	I_{MLMC}	R_{ID} (%)	T_{MC}	T_{MLMC}	R_{TD} (%)
ECOST	159.3804	162.0947	-1.7030	3.2055	0.1703	94.6872

3.4.2. Effect of adverse weather condition

Tables 4 and 5 show the results of reliability evaluation incorporating adverse weather condition. TVFR and TVRT with additional time are considered in indices calculation while compared to normal weather condition. For these conditions, TVFR and TVRT for overhead lines are modelled considering weather condition using Eqs. (10), (11) and (13). Table 4 shows the effect of high wind speed incorporating TVFR, TVRT, TVC and TVL. A wind speed of 12 m/s was assumed in calculation. Other variables used for this calculation are found from Appendix. An additional restoration time 1 hour is also considered. Comparing to the ideal condition in Table 1, all the indices values increase due to wind speed effect since the failure rate and repair time increase dramatically for the conditions based on Eqs. (10) and (13). Similarly, Table 5 presents the effect of lightning incorporating TVFR, TVRT, TVC and TVL on reliability evaluation. The required data for evaluating failure rate due to lightning effect are found in Appendix. Comparing to the wind speed effect in reliability evaluation; the lightning effect increases the reliability indices at the higher rate. The values of reliability indices increase with the values of wind speed and lightning flash density. It should be noted that the objective of this study is to show only the performance of MLMC method under different weather conditions. Therefore, the wind speed and lightning flash density values when failures occur are taken from previous study [10]. The maximum R_{ID} for wind speed and lightning effects are found at 3.049% and 1.4679%, respectively. The maximum T_{MLMC} is 1118.78 s (18.64 min) for ECOST computation with lightning effect while the MC simulation required 27781.41 s (7.72 h). From the computational view, the reliability indices with lightning effect need long calculation time than with wind effect.

Table 4. Effect of wind speed incorporating TVFR, TVRT, TVC and TVL

Indices	I_{MC}	I_{MLMC}	R_{ID} (%)	T_{MC}	T_{MLMC}	R_{TD} (%)
SAIFI	18.1033	18.6533	-3.049	0.0941	0.0015	98.4059
SAIDI	39.9462	40.4014	-1.1395	1.2447	0.0339	97.2764
EENS	736.0668	744.4176	-1.1345	167.8940	8.6744	94.8334
ECOST	5701.7	5770	-1.1978	3215.68	131.09	95.9234

Table 5 Effect of lightning incorporating TVFR, TVRT, TVC and TVL

Indices	I_{MC}	I_{MLMC}	R_{ID} (%)	T_{MC}	T_{MLMC}	R_{TD} (%)
SAIFI	52.5485	52.9127	-0.6930	0.6276	0.0180	97.1319
SAIDI	110.2557	111.8742	-1.4679	6.5111	0.3348	94.8580
EENS	2070.70	2093	-1.0769	1203.5883	70.3499	94.1549
ECOST	16587	16786	-1.1997	27781.41	1118.78	95.9729

4. Conclusion

An advanced Monte Carlo simulation called Multilevel Monte Carlo method that incorporates the high wind speed and lightning effects in distribution system reliability evaluation is presented in this paper. MC based simulation can quantify the variance coming from the random nature of failure events. The primary objective of the implemented method was to enhance the computation speed of MC method under such conditions through maintaining accuracy level. The proposed method was tested on a radial distribution system. In order to find the impacts of weather conditions on reliability evaluation, time-varying failure rate and repair time are used that accounts the increased failure rate and repair time for overhead lines in such weather conditions. Four system performance indices have been computed using the proposed technique. The effect of normal weather condition in several cases is studied to show the effect of adverse weather condition.

Both accuracy and computational efficiency of the MLMC were considered to demonstrate the practicability of the proposed method. The results indicate that the MLMC simulation method provides a realistic assessment under different weather conditions when compared to the usual MC simulation approach. The differences in reliability indices calculated data using MLMC are within 3% of values calculated using MC simulation. The MLMC approach may reduce the computation time up to 98% compared to the MC approach. Lightning effect increases both the reliability indices values and computation time extremely while compared to the wind effect. Computation time could be increased for ECOST and EENS calculation for time-varying load and cost models which account most of the peak hours when the interruption costs and load demands are higher.

Appendix: Time-varying parameters for estimating failure rate and restoration time, Sector Customer Damage Function data, network and customers data

See Tables 6, 7, 8, 9, 10 and 11

Table 6. Parameters for estimating time-varying failure rate [10]

Parameter	value
a_1	0.21
a_2	0.49
a_3	9.83
Critical speed	8
b	3100
$N_g(t)$	0.061

Table 7/ Hourly varying weight factors for TVRT [7]

Hour	Weight factor	Hour	Weight factor
1	1.2	13	1.0
2	1.2	14	1.0
3	1.2	15	1.0
4	1.2	16	1.0
5	1.2	17	1.0
6	1.2	18	1.0
7	1.2	19	1.1
8	1.0	20	1.1
9	1.0	21	1.1
10	1.0	22	1.1
11	1.0	23	1.1
12	1.0	24	1.1

Table 8. Daily varying weight factors for TVRT [10]

Daily	Weight factor
Weekday	0.92
Weekend	1.2

Table 9. SCDF for different customer types [51]

User sector	Interruption duration(Min.) & cost($/kW)				
	1 min.	20 min.	60 min.	240 min.	480 min.
Industrial	1.625	3.868	9.085	25.16	55.81
Commercial	0.381	2.969	8.552	31.32	83.01
Residential	0.001	0.093	0.482	4.914	15.69

Table 10. Feeder types and lengths [52]

Feeder type	Length (km)	Feeder section numbers
1	0.60	2 6 10 14 17 21 25 28 30 34 38 41 43 46 49 51 55 58 61 64 67
2	0.75	1 4 7 9 12 16 19 22 24 27 29 32 35 37 40 42 45 48 50 53 56 60 63 65
3	0.80	3 5 8 11 13 15 18 20 23 26 31 33 36 39 44 47 52 54 57 59 62 66

Table 11. Customer and loading data [52]

Number of load points	Load points	Customer type	Load level per load point, MW		Number of customers in each load point
			Average	Peak	
15	1-4, 11-13, 18-21, 32-35	Residential	0.545	0.8669	220
7	5, 14, 15, 22, 23, 36, 37	Residential	0.500	0.8137	200
7	8, 10, 26-30	Small user	1.00	1.63	1
2	9, 31	Small user	1.50	2.445	1
7	6, 7, 16, 17, 24, 35, 38	Commercial	0.415	0.6714	10
Totals			12.291	20.00	4779

References

1. Billinton R, Allan RN (1994) Reliability evaluation of power systems: Plenum Publishing (New York).
2. Billinton R, Billinton JE (1989) Distribution system reliability indices. IEEE Trans Power Del 4(1):561-568.
3. Goel L, Billinton R (1991) Evaluation of interrupted energy assessment rates in distribution systems. IEEE Trans Power Del 6(4):1876-1882.
4. Sultana B, Mustafa M, Sultana U, Bhatti AR (2016) Review on reliability improvement and power loss reduction in distribution system via network reconfiguration. Renew Sustain Energy Rev 66: 297-310.
5. Goel L (1998) Power system reliability cost/benefit assessment and application in perspective. Comput Electr Eng 24(5):315-324.
6. Alvehag K, L. Soder (2008) A stochastic weather dependent reliability model for distribution systems. In: Proceedings of the IEEE 10th international conference on probabilistic methods applied to power systems, pp 1-8.
7. Wang P, Billinton R (2002) Reliability cost/worth assessment of distribution systems incorporating time-varying weather conditions and restoration resources. IEEE Trans Power Del 17(1): 260-265.
8. Darveniza M, Arnold C, Holcombe B, Rainbird P (2007) The relationships between weather variables and reliability indices for a distribution system in South-East Queensland. In: Proceedings of international conference on electricity distribution, Vienna, Austria.
9. Pahwa A, Hopkins M, Gaunt T (2007) Evaluation of outages in overhead distribution systems of south africa and of Manhattan, Kansas, USA. In: Proceedings of international conference on power systems operation and planning, Cape Town, South Africa.
10. Alvehag K. Soder L (2011) A reliability model for distribution systems incorporating seasonal variations in severe weather. IEEE Trans Power Del 26(2): 910-919.
11. Ou Y, Goel L (1999) Using Monte Carlo simulation for overall distribution system reliability worth assessment. IET Gener. Transm. Distrib 146(5): 535-540.
12. Billinton R, Wang P (1998) Distribution system reliability cost/worth analysis using analytical and sequential simulation techniques. IEEE Trans Power Syst 13(4): 1245-1250.
13. Volkanovski A, Čepin M, Mavko B (2009) Application of the fault tree analysis for assessment of power system reliability. Reliab Eng Syst Safe 94(6): 1116-1127.

14. Ou Y, Goel L (1999) Using Monte Carlo simulation for overall distribution system reliability worth assessment. IET Gener. Transm. Distrib 146(5):535-540.
15. Goel L, Ou Y (1999) Reliability worth assessment in radial distribution systems using the Monte Carlo simulation technique. Electr Power Syst Res 51(1): 43-53.
16. Goel L (2000) Monte Carlo simulation-based reliability studies of a distribution test system. Electr Power Syst Res 54(1): 55-65.
17. Billinton R, Wang P (1999) Teaching distribution system reliability evaluation using Monte Carlo simulation. IEEE Trans Power Syst 14(2): 397-403.
18. Hegazy Y, Salama M, Chikhani A (2003) Adequacy assessment of distributed generation systems using Monte Carlo simulation. IEEE Trans Power Syst 18(1): 48-52.
19. Rocchetta R, Li Y, Zio E (2015) Risk assessment and risk-cost optimization of distributed power generation systems considering extreme weather conditions. Reliab Eng Syst Safe 136: 47-61.
20. Goel L, Ou Y (2001) Radial distribution system reliability worth evaluation utilizing the Monte Carlo simulation technique. Comput Electr Eng 27(3): 273-285.
21. Momoh JA (2007) Electric power distribution, automation, protection, and control: CRC press.
22. Li W (2014) Risk assessment of power systems: models, methods, and applications: John Wiley & Sons.
23. Billinton R, Sankarakrishnan A (1995). A comparison of Monte Carlo simulation techniques for composite power system reliability assessment. In: Proceedings of the IEEE communications, power, and computing. conference, vol 1, pp. 145-150.
24. Billinton R, Li W (1994) Distribution System and Station Adequacy Assessment, in Reliability assessment of electric power systems using Monte Carlo methods. Springer: 209-254.
25. Hou K, Jia H, Xu X, Liu Z, Jiang Y (2016) A continuous time Markov chain based sequential analytical approach for composite power system reliability assessment. IEEE Trans Power Syst 31(1): 738-748.
26. González-Fernández RA, da Silva AML (2011) Reliability assessment of time-dependent systems via sequential cross-entropy Monte Carlo simulation. IEEE Trans Power Syst 26(4): 2381-2389.
27. Wang Y, Guo C, Wu Q (2013) A cross-entropy-based three-stage sequential importance sampling for composite power system short-term reliability evaluation. IEEE Trans Power Syst 28(4): 4254-4263.

28. Huda ASN, Zivanovic R (2017) Accelerated Distribution Systems Reliability Evaluation by Multilevel Monte Carlo Simulation: Implementation of Two Discretisation Schemes. IET Gener. Transm. Distrib 11(13): 3397-3405.
29. Giles MB (2015). Multilevel Monte Carlo methods. Acta Numer 24: 259-328.
30. Giles MB (2008) Multilevel monte carlo path simulation. Oper. Res 56(3): p. 607-617.
31. Stuben K (2001) An introduction to algebraic multigrid. Multigrid: 413-532.
32. de Schryver C, Torruella P, When N (2013) A multi-level Monte Carlo FPGA accelerator for option pricing in the Heston model. In: Proceedings of the Conference on design, automation and test in Europe, pp. 248-253, EDA Consortium.
33. Giles M, Szpruch L (2013) Multilevel Monte Carlo methods for applications in finance. Recent Advances in Computational Finance, World Scientific.
34. Cliffe K, Giles,M, Scheichl R, Teckentrup AL (2011) Multilevel Monte Carlo methods and applications to elliptic PDEs with random coefficients. Computing and Visualization in Science 14(1): 3-15.
35. Aslett LJ, Nagapetyan T, Vollmer SJ (2017) Multilevel Monte Carlo for reliability theory. Reliab Eng Syst Safe 165: 188-196.
36. Elfverson D, Hellman F, Målqvist A (2014) A multilevel Monte Carlo method for computing failure probabilities. arXiv preprint arXiv:1408.6856.
37. Billinton R, Wang P (1999) Teaching distribution system reliability evaluation using Monte Carlo simulation. IEEE Trans Power Syst 14(2): p. 397-403.
38. Brown R, Gupta S, Christie R, Venkata S, Fletcher R (1997) Distribution system reliability assessment: momentary interruptions and storms. IEEE Trans Power Del 12(4): 1569-1575.
39. Huda ASN, Živanović R (2018) Efficient estimation of interrupted energy with time-varying load models for distribution systems planning studies. IFAC-PapersOnLine 51(2): p. 208-213.
40. Oksendal B (2013) Stochastic differential equations: an introduction with applications: Springer Science & Business Media.
41. Harrison JM (1985) Brownian motion and stochastic flow systems: Wiley New York.
42. Brugger C, de Schryver C, Wehn N, Omland S, Hefter M, Ritter K, Korn R (2014) Mixed precision multilevel Monte Carlo on hybrid computing systems. In: Proceedings of IEEE conference on computational intelligence for financial engineering & economics, pp. 215-222.
43. Giles MB (2009) Multilevel Monte Carlo for basket options. In: Proceedings of the IEEE Winter Simulation Conference (WSC), pp. 1283-1290.

44. Kloeden PE, Platen E (1992) Higher-order implicit strong numerical schemes for stochastic differential equations. J. Stat. Phys 66(1-2): 283-314.
45. Chowdhury A, Koval D (2011) Power distribution system reliability: practical methods and applications 48: John Wiley & Sons.
46. Wang P, Billinton R (2001) Time-sequential simulation technique for rural distribution system reliability cost/worth evaluation including wind generation as alternative supply. IET Gener. Transm. Distrib 148(4):355-360.
47. Billinton R, Allan RN (1992) Reliability evaluation of engineering systems: Springer.
48. Billinton R, Jonnavithula S (1996) A test system for teaching overall power system reliability assessment. IEEE Trans Power Syst 11(4): 1670-1676.
49. Goel L, Billinton R, Gupta R (1991) Basic data and evaluation of distribution system reliability worth. In: Proceedings of the IEEE Western Canada conference on computer, power and communications systems in a rural environment, pp. 271-277.
50. Huda ASN, Živanović R (2017) Multilevel Monte Carlo simulation applied to distribution systems reliability evaluation. In: Proceedings of the IEEE Manchester PowerTech, pp. 1-6.
51. Wang P, Billinton R (1999) Time sequential distribution system reliability worth analysis considering time varying load and cost models. IEEE Trans Power Del 14(3): 1046-1051.
52. Allan RN, Billinton R, Sjarief I, Goel L, So K (1991) A reliability test system for educational purposes-basic distribution system data and results. IEEE Trans Power Syst 6(2): 813-820.

Chapter 8

Study of Large-Scale DG Integration into Distribution Networks

Statement of authorship

Title of Paper	Large scale penetration of distributed generation into distribution networks: Study objectives, review of models and computational tools
Publication Status	☑ Published ☐ Accepted for Publication ☐ Submitted for Publication ☐ Unpublished and Unsubmitted w ork w ritten in manuscript style
Publication Details	A.S.N. Huda and R. Živanović (2017) Large-scale penetration of distributed generation into distribution networks: Study objectives, review of models and computational tools, Renewable and Sustainable Energy Reviews, 76, 974-988. Link: https://www.sciencedirect.com/science/article/pii/S1364032117303842

Principal author

Name of Principal Author (Candidate)	A. S. Nazmul Huda		
Contribution to the Paper	Study objectives, review of models and computational tools and preparation of manuscript.		
Overall percentage (%)	80%		
Certification:	This paper reports on original research I conducted during the period of my Higher Degree by Research candidature and is not subject to any obligations or contractual agreements with a third party that would constrain its inclusion in this thesis. I am the primary author of this paper.		
Signature		Date	07.09.2018

Co-author contributions

By signing the Statement of Authorship, each author certifies that:

the candidate's stated contribution to the publication is accurate (as detailed above);

permission is granted for the candidate in include the publication in the thesis; and

the sum of all co-author contributions is equal to 100% less the candidate's stated contribution.

Name of Co-Author	Rastko Živanović		
Contribution to the Paper	Provided guidelines for manuscript writing, helped in manuscript edit and evaluation		
Signature		Date	13.08.2018

Large-scale penetration of distributed generation into distribution networks: study objectives, review of models and computational tools

Abstract- In terms of the improvement of reliability and efficiency, integration of distributed generation (DG) into distribution network has gained significant interest in recent years. However, existing distribution systems were not designed considering large-scale penetration of DG. Due to the increasing penetration of DG, several technical challenges may arise which includes voltage control, power quality and protection issues, etc. Therefore, additional components need to be modelled together with conventional distribution system components in order to study the impact of DG on the distribution system. The first objective of this paper is to review the required models of system components, the impacts of DG on system operation, mitigation of challenges, associated standards and regulations for the successful operation of distribution systems. A number of commercial and open source tools are available for modelling and analysis of distribution systems. An ideal computational tool should include necessary functionalities to study the impacts of increased DG penetration as well as various options to overcome possible operational problems. Based on the first objective, the second objective is to make a summary of characteristics and features that an ideal computational tool should have to study increased DG penetration. A comparison study of two commonly used computational tools is also carried out in this paper.

Keywords: Distributed generation; distribution network; power quality; reliability; power system computational tools

1. Introduction

Distributed generation (DG) are relatively small power generation units that are connected to the distribution networks (DN) and close to the loads being served [1]. However, expansion of DN by integrating renewable based DG to electricity grid has attracted much attention worldwide due to their environmental benefits. This integration needs to provide a reliable and cost-effective service to customers while ensuring that voltage regulation, power quality and protection issues are within standard ranges.

Traditionally, DN are not designed considering the integration of a large number of DG units. High penetration of DG into DN affects the normal operation of the system in both positive and negative ways. Improved voltage profile, reliability, power loss reduction and support of ancillary services are major positive impacts [2], whereas negative ones include

malfunction of the protection system, poor power quality, reverse power flow and islanding, etc [3,4]. Various technical restrictions are being adopted worldwide in order to mitigate these negative impacts [5].

Currently, available distribution system analysis tools are insufficient to study the impacts of increased DG penetration due to the lack of required models and functionalities. Therefore, simulation tools must combine modelling and analysis capabilities of all required components related to DG and storage technologies together with traditional distribution components. This study aims to provide a comprehensive review of the negative impacts that increased DG penetration has on system operation, necessary mitigation studies, associated standards, required models of system components and computational tools.

The paper is organised as follows: Section 2 presents an overview of components that need to be modelled for conducting a study of large-scale penetration of DG. Section 3 provides an overview of the negative impacts of increased DG penetration on DN, operation standards and mitigation techniques of these impacts. Characteristics and functionalities that an ideal computational tool should have to model and analyse distribution systems with high penetration of DG have been discussed in Section 4. This section also provides a comparison between two commonly used computational tools. Finally, Section 5 concludes the paper.

2. Basic components of distribution system with DG penetration

2.1. Distribution networks

In an electric power system, power is generated in generation station and then it is transmitted through the transmission line. Finally, the electric distribution network is designed to deliver the electricity to the end users. Electric power can be distributed by overhead lines or underground cables. A distribution line is modelled by a 3×3 series impedance matrix which is expressed in per unit based on the nominal phase-to-ground voltages [6]. In most of the cases, distribution lines are placed underground due to high population density. Depending on the feeder arrangement, a distribution system can be divided into two fundamental ways: radial and loop systems [7].

2.2. Loads

An electrical load is an electrical appliance that consumes electric power. Loads can be modelled based on two different approaches. Firstly, static loads are modelled by following the behaviour of their active (P) and reactive power (Q) changes at any instant of time with respect to bus voltage and frequency at the same instant. Commonly used such load models are constant impedance, constant current, constant power, frequency dependent model, ZIP (polynomial) and exponential load models [8]. Secondly, dynamic loads are modelled by studying the P and Q at any instant based on the instantaneous and past histories of bus voltage and frequency [9]. A composite load combines both static and dynamic load models. Based on the types of consumers, the loads can be modelled in four different ways: commercial, industrial, agricultural and residential [10]. Commercial loads are typically air conditioning units and discharge lighting. Industrial loads are mostly induction motors (up to 95%). Likewise agricultural loads basically include induction motors for pumps. The residential loads include domestic appliances (e.g. refrigerators, washing machines etc. as well as heating and air conditioning units). These types of load models are usually represented by hourly load behaviour which is termed as load duration curve (LDC) [11]. LDC can be modelled using stochastic theory representing the uncertainty of weather and consumers types.

2.3. Voltage regulators

Change of distribution voltage depends on load variation and number of DG units penetration into DN. Voltage regulators (VR) are used for maintaining the voltage within standard limits [12-15] and consumers receive the steady state voltage. In the distribution system, VR are installed at a substation or along distribution lines. Different types of regulators are used such as on-load tap changer (OLTC) transformer, shunt capacitor and reactor, and flexible alternating current transmission system (FACTS) devices.

2.3.1. On-load tap changer transformer

On-load tap changing mechanism in transformers is generally used to avoid a supply interruption during a tap change [16]. The OLTC transformer equipped with automatic voltage control (AVC) relay and adjusts the transformer output to set the customer voltage within statutory limits [12]. OLTC voltage regulation is performed by changing the turn ratio of a transformer which is automatically controlled by AVC relay to increase or decrease the customer voltage level. Several voltage control techniques associated with

OLTC are available such as line drop compensation (LDC), time grading between series operating OLTCs and circulating current compensation techniques for parallel operating OLTCs [17].

2.3.2. FACTS devices

FACTS devices are power electronic based systems that control power flow in the transmission and distribution networks for enhancing controllability and increasing power transfer capability of the network. The key benefits of using FACTS include improvement in system stability, voltage regulation, reactive power balance, load sharing between parallel lines, and reduction in transmission losses [18]. FACTS can be connected in series, shunt or both in series and shunt configurations.

(a) Series compensation equipment

In series compensation, FACTS works as a controllable voltage source. The series compensation equipment can be modelled through variable impedance [19]. The static synchronous series compensator (SSSC) [20] and dynamic voltage restorer (DVR) [21] are examples of series compensators.

(b) Shunt compensation equipment

In shunt compensation, FACTS works as a controllable current source. A reactive current is injected into the line to regulate voltage by varying shunt impedance. There are two methods of shunt compensations: shunt capacitive compensation and shunt inductive compensation [22]. The static VAR compensator (SVC) [23] and static synchronous compensator (STATCOM) [24] are examples of such compensators.

(c) Series-shunt compensation equipment

Series-shunt compensation equipment can control both secondary side voltage and input Q at the same time. The unified power flow controller (UPFC) is an example of such equipment [25].

2.4. DG types

DG covers a wide range of renewable and non-renewable technologies such as gas turbine, internal combustion engine, micro turbine, wind turbine, photovoltaic generator, solar

thermal, biomass gasification, small and micro hydro turbines, fuel cell, geothermal, ocean energy and battery storage. Some of these are described below:

2.4.1. Internal combustion engine

Internal combustion (IC) engine converts chemical energy derived from liquid or gas fuels into mechanical energy. Then, it rotates a synchronous generator (SG) or an induction generator (IG) that is directly connected to the grid and converts mechanical energy into electrical form. Most often IC engines use diesel, gasoline and petroleum gas as fuels. IC engines include both intermittent (e.g., Reciprocating, Wankel and Bourkes engines) and continuous combustions (e.g., Jet engine, Rocket engine and Gas turbine) [26].

2.4.2. Gas turbine

A gas turbine consists of the compressor, the combustion chamber (or combustor) and the turbine [27]. Different types of fuels, including natural gas, fuel oils, and synthetic fuels can be used in a gas turbine. The potential energy from fuels is first converted to hot gases that spin a turbine to generate electric power. The turbine is interfaced with the utility grid through a SG.

2.4.3. Microturbine generator

The microturbine generator system consists of a high-speed (up to 120-*kilo revolutions per minute*) gas turbine unit and a permanent magnet synchronous generator (PMSG) [28]. The turbine unit includes a compressor, a combustion chamber and a turbine. Microturbine works like a gas turbine. The only difference is that this is interfaced with the utility grid through a PMSG.

2.4.4. Fuel cell

A fuel cell (FC) is a device that generates electricity by chemical reaction of hydrogen (H_2) and oxygen (O_2). Typically, FC is composed of reformer, stack and inverter [29]. Based on the electrolytic material, FC(s) are classified into five types [30]: alkaline, proton exchange membrane, phosphoric acid, molten carbonate and solid oxide FC(s). FC is connected to the distribution grid via an inverter and transformer. The output DC power of fuel cell is converted via an inverter to grid-compatible AC power.

2.4.5. Micro hydroelectric generator

A micro hydro (MH) power system generates electricity using the natural flow of water [31]. Generally, the MH plant produces electricity from 5 kW to 100 kW. The MH power project consists of a run-of-river hydraulic turbine coupled to a synchronous generator. The turbine converts the flow and pressure of the water to mechanical energy. The generator converts mechanical energy to electrical form which is supplied to the electrical loads.

2.4.6. Wind turbine generator

A wind turbine generator converts the wind power into electrical energy. A stochastic model of the wind turbine (WT) is established based on the distribution of wind speed over the year. WT generators can be configured as [32]: (a) fixed speed WT with direct grid-connected IG (b) variable speed WT with variable rotor resistance IG directly connected to the grid, (c) variable speed WT with direct grid-connected doubly-fed induction generator (DFIG) and DC/AC rotor converter and (d) synchronous machine and full scale AC/DC/AC converter.

2.4.7. PV generator

A photovoltaic (PV) system is composed of a number series/parallel connected solar cells to produce electricity from sunlight. The DC output power is converted via an inverter to grid-compatible AC power. The possible maximum output power can be achieved with a maximum power point tracking (MPPT) system. PV generator model is based on a current source converter. PV generators are modelled using PQ and PV control systems. Where the current set points can be found based on the desired P and Q and current measurements in the d-q reference frame [21].

2.5. Storage device

Storage devices such as flywheels and batteries are modelled as constant DC voltage sources. These devices act as controllable AC voltage sources and as a backup in the case of sudden loss of power generation. Storage devices are connected to the utility grid through AC/DC/AC converter and DC/AC inverter for flywheel and battery, respectively [33].

Table 1 displays the connection methods of various types of DGs to the utility grid as well as their suitable models for power flow studies.

Table 1. Models of DG [34]

DG type	Electrical machine	Grid interfacing	Suitable model
Internal combustion engine	Synchronous generator	Directly	PQ node Static voltage characteristic model (SVCM) PV node
	Squirrel cage induction generator	Directly	PQ node or SVCM
Gas turbine	Synchronous generator	Directly	PQ node SVCM PV node
Microturbine	Permanent magnet synchronous generator	Rectifier+inverter or AC/AC converter	PV node PQ node
	Squirrel cage induction generator	Directly	PQ node or SVCM
Wind	Doubly fed induction generator	Rectifier+inverter	PV node PQ node
	Conventional or permanent magnet synchronous generator	Rectifier+inverter	PV node PQ node
Photovoltaic	-	Inverter	PV node PQ node
Fuel cell	-	Inverter	PV node PQ node

3. Impacts of increased DG penetration into DN

DG interconnection into DN influences both steady state and dynamic (transient) stabilities of power system [35, 36]. The steady state impacts on the distribution system are voltage fluctuation, reverse power flow, high electrical losses, transformer and cable rating issues, poor power quality, poor power balancing, reactive power management, malfunction of protection scheme, the operation of OLTC, reliability and regulation issues [37-40]. Dynamic impacts include islanding effect and transients changes due to cloud cover in areas with PV. These impacts vary in severity as a function of the degree of DG penetration, the location of DG installation in the distribution feeder and the technology of distributed generators [41-43]. The categories of negative impacts caused by high penetration of DG on DN are discussed in the following sections including their standards and mitigation studies.

3.1. Voltage rise and reverse power flow

3.1.1. Impacts

DG system connected to distribution grid changes the loading conditions of the grid at the point of common coupling (PCC) [44, 45]. The normal direction of power flow in a radial distribution network is from the source (high voltage substation) towards the loads (low voltage customers). Due to the stochastic nature of the renewable DG resources, generation units are considered as uncontrollable sources (non-dispatchable) regarding active power [46]. The fluctuation of renewable energy generation in supplying power to the load causes overvoltage or undervoltage. The severity of such phenomenon is often influenced by weather conditions, geographical location of installed DG units and system topology [47].

During low load demand, the excess power generation from DG units flows back to the transmission system through the substations and thus produces reverse power flow in the feeder [48, 49]. Under this condition, normal behaviours of DN are changed and voltage profiles, substation protection schemes, capacitor bank and voltage regulator operations of the feeder are noticeably affected [1]. The associated reverse power flow tends to increase the voltage in the distribution feeder. Increased DG penetration further increases this voltage level. Hence, the network stability could be degraded [50] by exceeding the standard voltage boundaries defined by different standards, e.g. American National Standards Institute (ANSI C84.1) [51], International Electrotechnical Commission (IEC 60038) [14] and Australian Standard (AS 60038) [13]. Usually, the distributed generators produce power at unity power factor (PF) for optimal utilisation of resources. Therefore, the system only injects active power into the utility grid. The nearby buses may experience under/overvoltage due to the lack of reactive power [47]. Reactive power injection is required to maintain the local grid voltage within allowed limits [12]. If the grid still has to supply the reactive power, then it causes the system PF to decrease and thus implies inefficient transmission [52].

A certain level of DG penetration into the DN may be advantageous for improving distribution system performance, but beyond this level, it may cause degradation by feeder voltage deviation, feeder and substation loading and loss due to reverse power flow. A number of studies have been carried out to show the percentage of DG penetration on a distribution feeder without changing of the voltage level. A study from the UK [48] shows that the maximum allowable PV penetration level within standard voltage limit [15] is about 33%. In this study, a total of 629 PV systems is referred as ‘50% PV’. In [53], a

study in Japan indicated that tolerable PV penetration level ranges between 5% and 20%. In [46], the impact of DG penetration on rural feeders has been investigated considering PV penetration levels up to 11.25% and LV transformer capacity penetration level up to 75%. The study concluded that rural feeders may experience more voltage rise problems due to their long span, which increases the feeder impedance. In [41], tests are carried out to investigate the performance of commonly used voltage regulation schemes under DG penetration. [54, 55] provide the detailed studies on voltage variations and loss assessment of low and medium voltage networks with PV unit integration.

3.1.2. Voltage regulation standards

The primary task of the distribution system is to supply electricity to the customers while maintaining voltage level within the allowable limit. To ensure the perfect operation of devices connected to the utility grid, voltage range is defined in different standards [12-14]. For example, IEEE 1547-2003 [12] defines standards/guidelines that describe the requirements for DG connection to a distribution feeder. Generally, the requirements include the limits of harmonics, DC current injection, flicker, and PF [12]. The standards apply to the inverters with a rating of up to 10kVA per phase. As per standard, the generators are operated at unity PF and supply only active power. DG units are not allowed to regulate voltage actively at the PCC. Voltage regulators are used to maintain the constantly changing voltage within +10% and -5% of nominal voltage. The minimum and maximum RMS voltage limits are set at 0.9 and 1.1 p.u, respectively. AS 60038 sets voltage limits standard at customers' end in Australia which is 230 V (+10%/−6%) [13].

3.1.3. Mitigation studies

Traditionally, voltage regulation in a distribution feeder is performed using OLTC transformer equipped with an AVR. An AVR is used to measure the voltage and current at the load side of the transformer and then compares the measured voltage with a reference voltage of AVR. If the difference exceeds the tolerance setting of the AVR, the tap changer is initiated to adjust the voltage to a satisfactory level. With increased DG penetration into distribution grid, the AVR operation becomes more complicated and ineffective because of reverse power flow accompanying with high current and voltage in the network. Therefore, a proper voltage regulation approach is necessary in order to accommodate high penetration of DG into the network. Studies of voltage regulation approaches include active power curtailment, reactive power compensation, energy storage device approach, improved PV inverter controls, advanced control of OLTC, load control, reconfiguration of

network infrastructure and centralised control of voltage control equipment. Table 2 highlights the voltage rise control methods in the distribution system with DG units penetration.

Table 2. Voltage rise control methods in distribution system with DG penetration

References	Highlights of voltage rise control methods
	On-load tap changer (OLTC)
[56]	Fuzzy logic based control of OLTC
[57]	Using OLTC and line drop compensation in MV feeder
[58]	Using controller which coordinates the OLTC action in primary substation with the reactive production of DG plants (MV feeder)
[59]	Using OLTC voltage set-point reconfiguration approach in MV feeder
[60]	Multiple line drop compensation voltage regulation method that determines tap positions of under-load tap changer transformers
[61]	Area-based OLTC coordinated voltage control for embedded wind generation
[62]	A proper coordination among the OLTC, substation switched capacitors and feeder-switched capacitors and synchronous machine-based DG
[63]	Coordination technique based on the concepts of protection principles (magnitude grading and time grading) for controlling the operation of OLTC and single or multiple DG.
	Active power curtailment and reactive power control
[64]	Active power curtailment (APC) strategy utilising artificial neural network (ANN)
[65]	Use of droop-based active power curtailment technique
[66, 67]	Distributed reactive power regulation and active power curtailment strategies
[68]	Multi-objective probabilistic method Volt/Var control
[69]	Distributed multi-agent scheme reactive power management
[70]	Fuzzy logic supervisor based P/Q control
[71]	Conditional value-at-risk approach based real and reactive power optimisation
[72]	Reactive power control method with three aims (1) inverters coordination among each other (2) control most critical bus voltage inside the normal operation range (3) all the inverters on the same network should participate on the voltage support mechanism
[73]	Additional reactive power reserve of inverter-interfaced DGs is exploited to lower the grid voltage level by means of location adaptive Q(U) droop function
[74]	Local voltage control strategy based on PV generation curtailment as an alternative to “on/off” operation
	Reactive power compensation
[75,76]	Strategies for steady-state voltage and reactive power flow control of a wind farm equipped with STATCOM
[77]	Night time application of PV solar farm as STATCOM
[78]	Constant and variable power factor compensation for self-induced voltage variations regulation
	Energy storage system
[79]	Optimal management strategy for distributed storages
[80]	Inverter interface battery energy storage
[81]	Adaptive control of energy storage system

[82]	Control customer-side energy storage system
[83, 84]	Introducing limited local energy buffering at the location of power injection
	Inverter control
[85]	Voltage regulation using PV inverter
[86]	Use the voltage source inverters with DG
[87]	Voltage rise mitigation method by the grid interactive inverters of the PV systems with cooperating each other
[88]	Two techniques are proposed when inverter based DG is employed: (a) Voltage regulated power control (VR-PC) (b) Power tuned voltage regulated control (PT-VRC)
[89]	Overvoltage control scheme for multiple DG units having advantages of Plug-and-play compatibility, no need for communications, simple integration with existing constant power control schemes
	Centralised voltage control
[90]	Centralised voltage control approach that promptly reacts to suddenly burdensome events such as underload, overload and generators tripping
[91]	Intelligent centralized voltage control method
	Load control approach
[92]	Consumer load control approach
[93]	Real time voltage control model usable in emergency conditions that determine the required load reduction to control the voltage profile
	System planning, equipment coordination and DG location
[94]	Two voltage control techniques are proposed through system planning and equipment control. System planning for system design and equipment control techniques to regulate the bus voltages during real-time operation
[95]	Constrained multi-objective particle swarm optimisation for proper placement of DG
[96]	Controlling the target voltage of automatic voltage control relays at primary substations
[77]	Power conditioning subsystem overvoltage protection function to avoid the overvoltage in clustered PV systems
[98]	Coordinated voltage and reactive power control equipment
[97]	Coordinated voltage control for active network management
[99]	Coordination of the load ratio control transformer, step voltage regulator (SVR), shunt capacitor, shunt reactor, and static Var compensator
[100]	Voltage control of PV generator by inserting a series reactor in a service line
[101]	Control method requires over sizing of the PV inverters at the beginning and end of the feeder
[102]	Coordinated control of distributed energy storage system with OLTC and SVR
[103]	Coordinating the operation of multiple voltage regulating devices and DG units in a medium-voltage distribution system under structural changes and DG availability

3.2. Harmonic distortion

3.2.1. Impacts

In a distribution system, power is supplied to the loads by delivering current at the fundamental frequency. Harmonics are current and voltage waveform components having

frequencies which are integral multiples of the fundamental frequency. On the other hand, current and voltage components having frequencies which are not integral multiples of the fundamental frequency are referred as interharmonics. Harmonic distortion in an electrical system is the deviation of the voltage and current waveforms from a purely sinusoidal waveform. In a distribution system with DG, power electronic converters/inverters are used to convert the power from DG units to the correct voltage and frequency of the grid.

Harmonic distortion occurs when nonlinear loads draw non-sinusoidal current even connected through a sinusoidal voltage source. This non-sinusoidal current contains harmonic current that interacts with the impedance of distribution system and causes voltage harmonics. The connection of a new converter unit can also be a reason of increased total harmonic distortion (THD) at its PCC and in other buses. In a DG interconnected system, harmonic distortions depend on the power converter technology. Power electronics switching devices can inject high-frequency components rather than the desired current.

With increased PVDG penetration in the power grid, harmonic resonance is becoming a crucial issue in power systems [104]. In addition, PVDG placement also contributes to harmonic distortion in a power system. DG placement at the higher voltage network produces less harmonic distortion compared with a connection at the low voltage network [105]. Harmonic resonance can occur at the PCC of an individual or multiple DG units to the grid because of impedance mismatch between the grid and the inverter [106]. In a distribution network with increased penetration of DG, pulse width modulation (PWM) inverter harmonic currents can also be a cause of harmonic excitation for system resonance [107]. Large scale penetration of DG into DN, fluorescent lights with high-frequency ballast, computers equipped with active power-factor correction and adjustable-speed drives are the reasons of distortion at frequencies above 1 or 2 kHz [108, 109].

Harmonic distortion causes numerous impacts on distribution system equipment and loads connected to it. The impacts include high neutral currents, overheated main switchboards components, phase conductors, transformers, random tripping of circuit breakers, flickering lights, malfunction of sensitive equipment, fire hazards, reduced PF and system efficiency due to excessive heating and reduction of equipment lifespan [110, 111]. The effect of harmonic resonance presents severe power quality problems such as tripping of protection devices and damaging of sensitive equipment because of overvoltage or overcurrent [104].

The type and severity of harmonic problems depend on switching device technologies, harmonics characteristics, equipment ratings, and loading conditions of the host distribution feeder. This dependency decreases proportionally with reduced power converter rating [112]. Increased level of DG penetration into distribution system can also amplify harmonic distortion [113].

Several studies have been carried out regarding the maximum penetration level of DG unit considering the IEEE Std. 519 harmonics limit [114]. In [105], the maximum DG penetration level into DN for the centralised approach is determined considering harmonic effect caused by inverter-based DG units. The results show that maximum penetration is limited to 66.67% and 33.53% for 18 and 33 bus systems, respectively. In [115], the study shows that the penetration level can reach to 100% of the feeder capacity considering IEEE standard 519-1992 7th and 9th standard harmonic limits [114]. In [116], the effect of harmonic distortion in a utility owned inverter-based DG system is considered to find the maximum DG penetration level. The results found an optimal DG penetration level of 26.94% by placing DG units in an optimal location. In [117], the highest penetration of DG with harmonics within the allowable range [114] was found 72% of the total capacity of the transformer.

3.2.2. Standards

In the normal cases, studies on harmonic distortion are carried out considering frequency range up to about 1 or 2 kHz [118], where the existing standards apply. For example, in order to limit the harmonic injection in the network by the individual customers and the utility, IEEE 519-1992 standard has set limits for harmonics [114]. For customers at 69kV and below, harmonic voltage distortion limits are 3% on individual harmonic and 5% on the THD. Table 3 presents the IEEE 519 harmonic current limit for general distribution systems.

Table 3. IEEE 519 harmonic current limit for general distribution systems (120 V through 69KV) [114]

Maximum harmonic current distortion at PCC (in percent of fundamental)						
Individual harmonic order (Odd harmonics)						
I_{SC}/I_L	<11	11≤h<17	17≤h<23	23≤h<35	35≤h	THD_i
<20[a]	4.0	2.0	1.5	0.6	0.3	5.0
20<50	7.0	3.5	2.5	1.0	0.5	8.0
50<100	10.0	4.5	4.0	1.5	0.7	12.0
100<1000	12.0	5.5	5.0	2.0	1.0	15.0
>1000	15.0	7.0	6.0	2.5	1.4	20.0
Even harmonics are limited to 25% of the odd harmonic limits above.						
[a]All power generation equipment is limited to these values of current distortion, regardless of actual I_{SC}/I_L.						
I_{SC}= Maximum short-circuit current at PCC.						
I_L= Maximum demand load current (fundamental frequency component) at PCC						
THD_i =Limitation of harmonic current that a user can transmit/inject into the utility system.						

In Australia, for distribution voltage level up to 33 KV, harmonic voltage distortion limits are 4% on individual harmonic (odd), 2% on individual harmonic (even) and 5% on the THD [119]. In the standard of high-frequency distortion measurement, IEC 61000-4-7 (2002) has set a limit of harmonic distortion in the range from 2 to 9 kHz [120].

3.2.3. Harmonic mitigation studies

A number of research works have been done to compensate distribution system harmonic distortions using adjustable harmonics compensation methods, phase shifting techniques [121], active [122,123] and passive filters. In [124], an adjustable harmonics compensation method was used to mitigate voltage distortion at a load terminal for a grid connected PV system. In [125], active damping and grid synchronisation were utilised for mitigating harmonic resonance problems caused by impedance mismatch between a wind inverter and the grid. To mitigate voltage and current harmonics within microgrid, a traditional shunt active filter with energy storage (SAFES) is proposed in [126]. In a work [127], a double tuned filter has been designed for harmonic mitigation in grid-connected PV systems.

Installing additional filters for harmonic mitigation is not a cost-effective choice. Therefore, several studies have been proposed by using controller based harmonic mitigation techniques. In [128], distributed generator interface converter is proposed to compensate harmonic. Whereas in [129, 130], the ancillary harmonic compensation capability is integrated with the DG primary power generation function through modifying control references. In [131], a proportional-resonant-integral (PRI) controller is designed

for harmonic mitigation in a grid connected PV system. In [132], a double tuned PI-R based current controller was used to mitigate grid side harmonic current in a DFIG based wind power system. In [133], the virtual impedance method is suggested for harmonic compensation based on converter control.

3.3. Voltage sag/dip

3.3.1. Impacts

According to IEEE Std. 1159-1995, voltage sag in the distribution system is a reduction of RMS value of source voltage between 10 and 90 percent of nominal voltage for 10 milliseconds (ms) up to 60s (momentary interruption) [134]. Voltage sag could be introduced from both internal and external sources. The sudden lightning strike is one of the most common external causes. Internal causes include equipment failures, power line contacts (line to a ground fault), short circuit fault, sudden load changing, transformer energising (depending on transformer connection) and large motor start-ups (since starting draw large current).

Voltage sag may cause apparatus tripping, shut down electrical equipment and destroy the power electronic devices such as computers, industrial control systems, adjustable speed drives, programmable logic controllers (PLC) and thus leads to economic losses. The severity of voltage sag depends on the protection system design and coordination among protective devices.

The integration of DG affects the performance of the protection scheme of distribution system due to reverse power flow and therefore, the nature of voltage sags can be affected by increased DG penetration [135]. Faults in the power system cause voltage dip at the PCC. In a wind system, voltage dip may lead to the destruction of the converter by increasing the current in the stator windings of the WT. Voltage dips that lead to increase of currents can also occur when PMSG is connected to the grid via IGBT power electronic inverters. A study revealed that DG may have a positive impact on the voltage sag performance if the fault duration is no longer than 2s [135].

3.3.2. Voltage sag mitigations

Generally, voltage sag can be considerably mitigated by controlling the injected reactive power at the PCC. Reactive power could be injected using series-connected voltage source

converters such as DVR [136] and STATCOM [137]. Energy storage units in DVRs can also supply the active power component needed during voltage sag mitigation [138].

The use of grid-interfaces of distributed generators is an interesting approach to mitigate power quality issues, especially voltage dips [139]. Generally, DG units are connected to the utility grid via a voltage source converter (DC to AC) which could be utilised for voltage sag mitigation [140, 141]. During sustained utility outages, DG reduces voltage sags and acts as an instant backup [142]. In [136], DVR and distribution static compensator (DSTATCOM) are used for restoring the voltage at the wind farm terminals under fault conditions. Likewise, various DG-based schemes have been proposed for voltage dip mitigation including:

(a) application of converter-based DG, synchronous and asynchronous generators [143, 144];
(b) series and shunt compensation [145, 146];
(c) SAFES [126];
(d) DSTATCOM with DG [147, 148];
(e) fault decoupling device [149];
(f) optimal DG allocation and sizing [150] and
(g) DVR with artificial intelligence (AI) [151].

3.4. Voltage fluctuation/flicker

3.4.1. Impacts of voltage fluctuation

Voltage fluctuation is a systematic variation of the voltage envelope or a series of random voltage changes. It can be characterised by the fluctuations of two indices: amplitude and frequency. If the voltage fluctuation occurs with the frequency from 0.05 Hz to 42 Hz, then it is known as flicker which causes the luminance of incandescent lamps to fluctuate [152]. Rapid fluctuation of the power output of generators, load changes and induction motor starting are the potential reasons of voltage flicker. Moreover, flicker emission is also affected by the changes of the various grid conditions such as short-circuit ratio, type of loads, and grid impedance angle [152].

Voltage fluctuation is considered as a major power quality problem. It can affect motor starting, speed and causes disturbances to the applications driven by the affected motors which can lead to equipment temperature rise and motor overloading. Therefore, it affects

the production, machine service life and thus increases economic losses. In diode rectifiers, PF may be lowered and the harmonic currents will increase [152]. Also, it may reduce the service lifetime of the electronic, incandescent, fluorescent and CRT devices [153]. Flicker affects humans by causing light fluctuations that are irritating to the eyes.

In PV-DG system, voltage fluctuation occurs due to the stochastic nature of PV output. Moreover, switching of PV inverters, poorly designed MPPT systems are the reasons of unacceptable flicker emissions. DG units connected to weak supply networks can also cause flicker in the distribution system [154].

In grid-connected wind energy system, wind shear and tower shadow are sources of power fluctuation caused by wind speed variations. Voltage fluctuation depends on the penetration level of DG into the distribution grid. High penetration of DG will also increase the fluctuation [155]. Therefore, voltage fluctuation limits the penetration of DG unit into DN.

3.4.2. Voltage fluctuation due to cloud passages

The sudden change of cloud condition is another reason for flicker emission [156] in PV-DG system. In a study, the authors measure the rate of sunlight change caused by cloud passages is from 60 to 150 $W/m^2/s$ is [157]. Spatial distribution significantly reduces the transients caused by clouds [158]. During cloudy and foggy days, in a distribution system with increased penetration of PV units, cloud passages induce undesirable voltage fluctuations due to power generation fluctuations. This may lead to excessive operations of the OLTC and creates flicker [158-160]. Balancing of power and fast ramping are two ways to mitigate the effect of cloud passages and morning fog and to increase the overall system reliability and efficiency. PV power generation needs to be balanced with other very fast controllable sources such as gas, coal, other renewable energy sources or energy storage systems [161].

Several studies have been carried out to determine the maximum penetration levels of DG units into DN during cloud transients. Fast ramping using conventional generators could be a way to lessen the effect of cloud transients where PV is deployed as a central generation station. In a study [162], maximum tolerable PV penetration reached to 13.27%, where PV was used as a central generation station. In another study [163], it was found that PV penetration is limited to only 1.3% with ramping using coal-fired units installed at the same central station. However, due to the smoothing effect of geographic diversity, the

maximum penetration could be increased to 18% and 36%, if PV units are distributed over an area of 100 km^2 and 1000 km^2, respectively. In [159], cloud effect has been discussed also by considering PV distribution over a wide area. The results found that maximum integration of DG into the distribution network is 15% and above this level, clouds effects cause significant power swing.

3.4.3. Standards

According to IEEE Std. 1547.2-2008, voltage fluctuation at PCC is limited to ±5% as DG is paralleled to distribution system [12]. IEEE Std. 519-1992 [164] defines the maximum permissible voltage flicker levels with respect to frequency before it becomes objectionable to the customer (borderline to irritation). According to IEEE Std. 1547-2003 [12], DG systems will not create objectionable flicker for other customers in the area who might use different lighting systems including incandescent and fluorescent.

3.4.4. Mitigation studies

Traditionally, voltage flicker mitigation studies are performed using different ways such as current controlled PWM-based DSTATCOM [165], state-controlled, vacuum switched, shunt capacitors to reduce the effect of motor starting [166] or using SVC for reactive power control [167]. Several types of research have been carried out to control the voltage fluctuations from distributed generators. In [168], a cooperative control method using both SVR and UPFC considering interconnection of distributed generators is proposed to handle steep voltage fluctuations. In [169], a coordination of AVC and battery energy storage control was employed to mitigate the grid-side voltage fluctuations caused by environmental factors for a distribution system with high penetration of PV-DG. In [170], a novel fuzzy control based energy storage system consisted of a bidirectional inverter coupled with lead–acid batteries is proposed to mitigate the fluctuating voltage rises of low-voltage DN with PV systems under highly cloudy conditions. The system manipulates the flow of real power between the network and batteries. In [171], various techniques for mitigating output power fluctuation from PV sources have been presented.

Flicker mitigation by output reactive power control of a variable speed WT with DFIG has been carried out in few studies [172-174]. Various factors affect the flicker emission of wind farms including mean wind speed, turbulence intensity and short circuit capacity ratio [175] and grid impedance angle [172]. In [172], flicker mitigation approach based on grid impedance and power factor angle control using the grid-side converter of DFIG has been

proposed. In another study [173], a rotor-side converter based reactive power control scheme has been presented for flicker reduction during variable wind speed. In [174], the reactive power has been controlled using STATCOM to study flicker of grid-connected WT with DFIG. In a study [152], the combination of active power smoothening and reactive power compensation has been proposed to suppress flicker. In order to mitigate wind power fluctuations, an active current control of DFIG based technique is proposed in [176]. In [177], different flicker mitigation solutions have been investigated in distributed wind power. The solutions are based on the bandwidth of wind farm voltage controller, increased MV/HV transformer rating, using two parallel MV/HV transformers, series line compensation and changing of the wind farm connection point. The results show that these mitigation systems are less effective for a wind farm except changing of the wind farm connection point.

3.5. Voltage unbalance

3.5.1. Impacts

In a three-phase electric system, unequal line voltage magnitudes are defined as voltage unbalance [178]. Use of single-phase distributed generators and unbalanced phase loads in the electric system cause voltage unbalance. In a PV-DG system, increased penetration of residential rooftop PV into the grid with random installation across distribution system is also a reason for increasing or decreasing the network imbalance index [179].

Voltage unbalance creates negative effects on the distribution system which cause overheating of equipment such as induction motors, power electronic converters and adjustable speed drives, and power and energy losses in the distribution grid. Additionally, network problems such as the malfunction of relays and voltage regulators, and generation of non-characteristic harmonics from power electronic loads could be introduced. Therefore, maintaining a balanced voltage at the point of connection is necessary in order to mitigate voltage unbalance [180].

3.5.2. Standards

According to IEEE/ANSI C84.1-1995 standard, maximum voltage unbalance in a three phase distribution system is limited to 3% [51].

3.5.3. Mitigation studies

Several types of research have been carried out on voltage unbalance mitigation in distribution systems with increased DG penetration. In the previous studies, reactive power compensation, distributed energy storage technology, and DG unit connection topologies to the system have been studied to mitigate voltage unbalance. In [181], a DSTATCOM has been proposed to mitigate voltage unbalance problems by manipulating the reactive power flow between network and DSTATCOM. A unified power quality conditioner is used to compensate voltage unbalance, negative-sequence currents and harmonics [182]. In [183], an energy storage system using fuzzy control and Park's transformation is proposed to mitigate voltage unbalance in a highly intermittent PV interconnected distribution system. In [184], an energy storage approach is also proposed to be part of an intelligent active management solution for mitigating the voltage unbalance of a network with large-scale PV penetration. In [180], four different control strategies, which include a single-phase resistively behaving control strategy, a three-phase damping control strategy, a phase sinusoidal and a positive-sequence control strategy have been studied in DN with a three-phase inverter connected DG units. Both the negative-sequence and the zero sequence components are studied. The study concluded that the three-phase damping control strategy is the best to mitigate voltage unbalance which allows more integration of DG units in comparison with the other control strategies. The other control strategies lead to overvoltage in the network. Moreover, the use of a distributed generator has also been proposed in [185] for mitigation of voltage unbalance in low voltage DN.

3.6. Frequency deviation

3.6.1. Impacts

In a distribution system, frequency deviation from the nominal system frequency occurs when there is any imbalance between power generation and consumption. In a wind power interconnected distribution system, stored kinetic energy in the rotating parts of the generators works as a backup for a few seconds until governor's response. The generator inertia determines the time required to discharge a certain amount of its energy to modify the output power control signals. However, it leads to generator speed deceleration as well as frequency deviation. Moreover, the output power contains triple frequency components such as 3p, 6p, 9p, etc. as a result of wind shear and tower shadow effects [186]. Usually, the maximum allowable frequency deviation in a generator is 1%; otherwise, there could be a loss of synchronism [187].

When the load on a large grid is higher than the output power of an individual SG, multiple SG(s) are connected in parallel to the electrical grid to control the frequency deviation. Since frequency is directly proportional to the rotor speed, all the generators run at the same speed. However, the presence of non-synchronous PV and wind generators cannot provide satisfactory frequency control [188]. This frequency fluctuation is more severe in a distribution with large scale DG penetration than small scale DG interconnected systems.

Frequency deviation can change the electromotor winding speed and damage generators. Large scale inertia-less DG units reduce the capacity of the system to address frequency deviation during a major disturbance. The inertia of the rotating masses of SG(s) determines the immediate frequency response of the system during a major imbalance between generation and consumption. Replacement of large scale conventional power plants by DG systems can also affect the frequency stability of the system. This is because it decreases the number of generators participating in frequency control as well as reduces the overall inertia of the system [189].

3.6.2. Standards

DG must remain in synchronism with the network with respect to the frequency. For interconnected systems operating at 60 or 50 Hz AC supply, the frequency must be limited to a specified range. Outside of this range, the system must be disconnected within the time as indicated in Table 4.

Table 4. Frequency range and corresponding disconnection time

Frequency range (Hz)	Disconnection time (sec.)
IEEE 1547 [12]	
(DG ≤30 kW)	
59.3 <f<60.5	0.16
(DG >30 kW)	
> 60.5	0.16
< (59.8 to 57.0) (Adjustable set point)	Adjustable 0.16 to 300
<57.0	0.16
IEC 61727 [190]	
49.0 <f<51.0	0.2

3.6.3. Frequency control techniques

Power frequency disturbances are caused by a difference between generation and consumption of active power. Therefore, frequency disturbances could be mitigated by reducing the imbalance between generation and consumption. Automatic generation control (AGC) regulators are used to set system frequency at or very close to a specified nominal value of the power system [191]. Load–frequency control (LFC) is also employed to control frequency within allowable limits [192] and to keep tie-line power flows within some pre-defined tolerances by adjusting the MW outputs of the generators in order to balance fluctuating load demands [193]. A coordinated distributed model predictive control for the LFC of a power system that includes inherently variable wind-power generations is proposed in [194]. In [133], the virtual synchronous machine method is proposed as a promising future research direction for voltage and frequency control. The latest advancements in this area are the use of ANN, fuzzy logic and genetic algorithms to mitigate the challenges related to the design of AGC and LFC [191, 195].

3.7. Malfunction of protection system

3.7.1. Impacts

High penetration of DG into the existing DN may cause malfunctions of safety equipment, protection systems and decreases the reliability of the distribution system. The existing protection schemes are designed according to the unidirectional power flow. Bidirectional power flow may lead to overvoltage, increased fault current levels and misoperation of relays, reclosers, fuses, VR due to the lack of directional sensing and adequate sensitivity to detect the reverse faults [196]. Coordination of protective devices helps to isolate faulted equipment without bringing the complete power system down. Increased DG penetration into the DN may lead to wrong coordination due to the bidirectional flow of fault current [197].

Usually, the short circuit capacity level of a distribution system without DG integration is often close to its design value [198]. The design value is the maximum allowable fault current which is dependent on the switchgear, and thermal and mechanical withstand capabilities of the equipment and constructions [199]. Incorporating high penetration of DG into DN can change the direction and duration of short circuit currents depending on the DG unit location, rating, type and leads to malfunction of protection devices. Penetration of DG into the network also affects the fault clearing process of the system. In

a radial distribution system, there is only one power source and the opening of only one protective device acts for fault clearance. A combination of automatic recloser devices, circuit breakers, sectionalizers, and fuses is applied to clear the temporary single-phase to ground faults (about 80% of the network faults) and isolates the faulty part from the rest of the system [200]. Large scale integration of DG units contains multiple power sources which contribute to fault currents and the opening of only one protective device does not guarantee the fast clearance of the fault. This interrupts the operation of the conventional auto reclosing system and prevents temporary faults from being cleared. Therefore, it may damage the distributed SG(s) due to an out of phase reclosing during power restoration process. In order to maintain normal fault clearing processes, it is a requirement to disconnect DG from the system when a fault is suspected before the elapsed time of fast reclosing.

If a utility grid gets isolated, islanded operation occurs when only DG unit supplies power to the local loads. This can happen due to some emergency conditions associated with system safety, equipment protection and system control. The islanded could happen through intentionally (planned operation) or unintentionally (unplanned operation). Unintentional islanding may cause a hazardous effect on devices and to the public when a portion of DN becomes electrically isolated from the system but still, continues to be energised by the DG connection to the isolated subsystem. The main hazards and risks associated with the unintentional islanding are discussed as follows [201]:

- Exceeding the acceptable limits of power quality parameters which can lead to the failure of network and customer equipment;

- Uncleared faults (earth or phase faults) due to low short-circuit capacity or unearthed operation. Can cause possible damage to the network components, otherwise sustain the fault currents;

- Out of phase reclosing of protection device may damage protection equipment and causes high transient inrush currents which may lead to the failure of generator;

- Electric shock.

3.7.2. Necessary standards for protection

3.7.2.1. Reconnection

The reconnection of one or more generators particularly after an outage or fault needs a time delay after the system steady-state voltage and frequency are restored to the standard ranges [12]. IEEE Std. 1547 recommends that it requires at least 5 minutes of normal operation for a generator before reconnection [12].

3.7.2.2. Islanding detection

According to IEEE Std. 1547-2003, the unintentional island should be detected and isolated within 2 s [12].

3.7.3. Protection systems

3.7.3.1. Protection system for islanding detection

The effective detection of unintentional islanding is essential for avoiding unwanted hazardous effects. Remote and local detection techniques, signal processing and intelligent classifiers are utilised to detect islanding in the distribution system. Remote techniques require a communication scheme. These techniques are based on supervisory control and data acquisition (SCADA) system, transfer trip scheme and inter-tripping. Local techniques are developed based on local information and classified into active, passive and hybrid techniques. Impedance measurement and slip mode frequency shift are popular active methods. Passive techniques include under/over voltage monitoring, under/over frequency monitoring, voltage phase jump detection and harmonic measurement. A hybrid system is the combination of active and passive techniques. These techniques are: voltage unbalance and frequency set point reconfiguration approach [202], voltage and real power shift, voltage fluctuation injection and hybrid SFS and Q–f islanding technique [203, 204]. Wavelet-transform and S-transform are signal processing methods used for identification of island mode operation. Common AI classifiers used in islanding detection include the decision tree, rule-based techniques, ANN, probabilistic neural network, fuzzy logic, and support vector machines.

3.7.3.2. Protection coordination methods

Several studies have been carried out to solve the overcurrent relay coordination problem in distribution systems with increased penetration of DG units. These can be divided into

two main approaches. The first approach is to obtain a new relay coordination status and the second one is to limit fault current level. The details of these two approaches are found in [205, 206].

4. Computational tools for studying increased DG penetration

Several computational tools are available for studying increased DG penetration into DN. The tools differ in terms of capabilities, structures, application levels and programming codes. The list of tools include Open Distribution System Simulator (OpenDSS) [207], CymDist [208], PSS/Sincal [209], DigSilent Power Factory [210], GridLAB-D [211], PSAT [212], 4DIAC [213] and APREM [214], etc. In this paper, we will summarise the capabilities of two available tools, namely OpenDSS and GridLAB-D. OpenDSS is a widely used, freely available and user-friendly software, developed by Electrical Power Research Institute (EPRI) for carrying out research on DN analysis with penetration of DG resources. GridLAB-D is another open source advanced grid analysis tool, which has been developed by the U.S. Department of Energy (DOE) at the Pacific Northwest National Laboratory (PNNL) in collaboration with industry and academia.

The available software that the power companies use may be insufficient to analyse the distribution grid with increased penetration of DG resources. This is due to the modernization of the distributed generation technologies, switches and voltage controls, automation, and increasingly complex loads. In the following section, the characteristics of an ideal computational tool to study increased penetration of DG are described together with the capabilities of OpenDSS and GridLAB-D.

4.1. Load flow analysis

Power flow or load-flow studies are primarily carried out to determine (i) voltage magnitude and phase angle at each bus, (ii) power flow in each branch of DN (e.g., transformers and lines), (iii) power consumption and, (iv) system losses. The load flow analysis for studying increased DG penetration into the distribution grid should have the following features [215, 216]:

(a) modelling of basic components - line, transformer, capacitor, inductor, node, bus, DG components, inverter, reactor, voltage source (Vsource) and current source (Isource);

(b) reactive power and voltage control (Volt Var Control) - ability to model voltage regulators (i.e. OLTC, line drop compensator, FACTS devices), specifying the maximum

and minimum voltage limit, the tolerance on regulation settings; switching capacitor based on both time and electrical quantities (voltage, current, kVAr); also, options for automatic switching and reconfiguration as well as new localized and generation-based voltage regulation systems which have been discussed in Section 3.1.3 to study increased DG penetration into DN rather than usual voltage regulators;

(c) load flow modelling - for both balanced or unbalanced systems, single-phase/three-phase load flow;

(d) time series simulation - most distribution system analysis tools are commonly designed to study peak and off-peak loadings rather than different time-dependent loads based on LDC. Computational tool must handle hourly/daily/weekly/annual/seasonal loads, generation profiles and interruption rates to analyse the range of load demand and generation which depends on times;

(e) sensitivity studies - for losses, voltage profile, feeder reconfiguration and capacitor placement/size;

(f) modelling single or multiple distributed generators at the same load location of distribution network;

(g) automatically retrieve of environmental and weather data (e.g. solar irradiance, wind speed).

4.1.1. OpenDSS capabilities

OpenDSS includes a large number of circuit components to perform distribution system analysis with integration of DG systems. The circuit components are divided into four classes which are power delivery (PD), power conversion (PC), control and protection, and meter elements. The PD components are line, transformer, capacitor, and reactor. The PC components are load, generator, Vsource, Isource, PV system and storage. A total of six control elements can be modelled using OpenDSS which include capacitor control, voltage regulator, generator dispatcher, switch controller, storage controller and inverter controller. Energy meters, monitors and sensors are three-meter elements implemented in this software. The software can model n-phase, m-winding transformers rather than traditional two or three winding models. In OpenDSS, seven types of loads can be modelled: (a) conventional constant P, Q load model (b) constant Z load model (P and Q vary by the square of the voltage) (c) constant P but Q is modelled as a constant reactance (d) P and Q

variation defined by exponential models (e) constant current magnitude which is common in distribution system analysis (P and Q vary linearly with voltage magnitude) (f) constant P that can be modified by load shape multipliers, but Q is a fixed value independent of time (g) similar to (f), but Q is computed from a fixed reactance (varies with square of voltage).

OpenDSS enables sequential time simulations called ‘quasi-static solutions’. This feature makes OpenDSS suitable to study DG integration with DN since the availability of some DG resources varies with time. A few examples of time-varying models are: (a) electric vehicle charging (minutes, hours) (b) solar and wind generation (seconds) (c) dispatchable generation (minutes to hours) (d) storage (minutes to hours) (e) energy efficiency (hours) (f) distribution state estimation (seconds, minutes) (g) customers' load models (minutes to hours) (h) end-use thermal models (minutes to hours).

OpenDSS includes a lot of calculation modes for power flow studies including [207]

(a) Snapshot mode - This is a single snapshot power flow calculation mode in an iterative method. The global load multiplier (LoadMult) and the growth factor for the present year (Year) are used to modify the loads.

(b) Direct mode - This mode is also a single snapshot power flow studies mode that uses an admittance model of all loads. This is non-iterative and just a direct method using the currently specified voltage and current sources.

(c) Daily mode - The daily mode evaluates a series of power flow calculation following the daily load curves. The peak load is determined by the ‘LoadMult’ and the growth factor for the present year.

(d) Yearly mode - The yearly mode enables a series of power flow calculation following the yearly load curves.

(e) Peak day mode - It performs the power flow studies only for those days, where the peak exceeds a specified value.

(f) Duty cycle mode - The mode solves the power flow calculation following the duty cycle curves with the time increment specified.

4.1.2. GridLAB-D capabilities

GridLAB-D includes models of various distribution system components. The available models are overhead and underground lines, transformers, voltage regulators, shunt capacitor banks, distributed generators (including solar and wind) and energy storage, etc. Retail market modelling tools, SCADA and metering are also supported in this tool. Different types of load models are available such as constant Z, constant I, constant P, commercial, industrial and residential loads.

The tool supports time series simulations taking climate information into account and is capable of studying DN modelling and analysis ranging from a few seconds to decades. GridLAB-D offers capabilities that support Volt-Var management, load flow analysis, peak demand management, load control and loss calculation. The distribution module of GridLAB-D uses the traditional forward and backward sweep methods for studying power flow in a distribution network.

4.2. Fault and protection coordination analysis

A fault current analysis (FCA) provides the necessary information to design the fault protection scheme. FCA is performed by using a standard short circuit simulation. This type of analysis is used to determine appropriate coordination and setting of protection devices. However, increased penetration of DG into DN increases the time varying nature of the fault current and therefore, a more sophisticated tool is required. To study the large-scale penetration of DG into DN, FCA tool should have the following capabilities [215, 216]:

(a) modelling protective devices such as reclosers, fuses, relays, circuit breakers, and switches;

(b) modelling three phase, two-phase and single-phase overhead and underground lines;

(c) modelling of loads, DG/inverter; inverter internal impedance;

(d) balanced and unbalanced system analysis;

(e) provide a full range of transformer connections, and source flows;

(f) symmetrical fault analysis [217];

(g) asymmetrical fault analysis (single line to ground, double line to ground and line to line faults);

(h) modelling fault resistance;

(i) analysis fault current flow under different switching [218];

(j) identify and determine overvoltage during faults;

(k) protection device coordination analysis;

(l) interfacing capability with protection and reliability analysis software.

Generally, radial distribution network is protected by time overcurrent relays, circuit breakers, reclosers, fuses, and sectionalizers. Protection coordination among these devices is achieved through variable time delays in each protective device, where downstream devices operate faster than upstream devices at any specific current. The contribution of fault current from the DG must be quantified and considered in combination with load characteristics. Protection coordination needs to be recoordinated or redesigned in this situation. Moreover, software tools need to recognise the following two effects where protective approach may fail or may be degraded [215]: (a) where SG(s) and some inverters supply fault current which may cause malfunction of the time overcurrent protection system and (b) in intentionally islanded systems, where fault current is low and varies widely.

Both OpenDSS and GridLAB-D could be used for protection system simulation. In OpenDSS, fault study mode can implement FCA in DG connected distribution system. GridLAB-D also includes the studies of fault detection, device coordination, automation and feeder reconfiguration. Table 5 presents a comparison of fault and protection coordination analysis capabilities of these two tools.

Table 5. Fault and protection coordination analysis capabilities of OpenDSS and GridLAB-D

Type of study	OpenDSS	GridLAB-D
Modelling recloser, fuse, relay, circuit breaker, and switches	Yes	Yes
Modelling three phase, two phase and single phase lines	Yes	Yes
Modelling of three phase, two phase and single *phase* loads	Yes	Yes
Balanced and unbalanced system analysis	Yes	Yes
Single-phase or three-phase transformer configurations	Yes	Yes
Modelling of DGs	Yes	Yes
Investigation of symmetrical and unsymmetrical faults	Yes	Yes
Modelling fault resistance	Yes	-
Protection coordination	-	Yes
Fault analysis in DG connected distribution system	Yes	-

4.3. Dynamic analysis

Dynamic analysis investigates the system ability to maintain stability during faults and small signal fault conditions. It is recommended for a distribution system with high penetration of DG in order to maintain the system stability during voltage and frequency oscillations and rotor angle swing of distributed generators.

OpenDSS can perform basic electromechanical transient simulations. The capability has been expanding steadily due to needs in inverter modelling and other applications where machine dynamics are important. The built-in generator model has a simple single-mass model that is adequate for many DG studies for common distribution system fault conditions. In GridLAB-B, there is a dynamic mode, but the support is very limited.

4.4. Power quality analysis

In a distribution system equipped with DG through power electronic converters, power quality analysis tool must be able to cover the following areas [219]

(a) able to analyse impulsive and oscillatory transients [220];

(b) able to study high-frequency harmonic and interharmonic interferences;

(c) modelling three-phase as well as all phases harmonics independently for analysing multiple single phase DG applications;

(d) able to analyse voltage fluctuation. In a distribution system integrated with multiple DG systems, modelling of DG considering flicker could be a challenging task for some DG units, where there is no enough correlation between amount of output power fluctuation and distribution resource;

(e) able to analyse voltage sag with capabilities of short-circuit calculations;

(f) able to simulate temporary overvoltages due to phase-earth faults, load rejection, Ferranti rise, resonance, ferroresonance phenomena and lightening (see Ref [218] for details);

(g) calculation of power quality indices such as system average RMS variation frequency index, THD, PF, voltage distortion index, unbalance factor, transformer derating factor, and flicker factor [221, 222].

OpenDSS is a frequency domain tool which supports all RMS steady-state analyses (i.e., sinusoidal steady state, but not limited to fundamental frequency) [207]. This tool has been used for harmonic and interharmonic distortion analysis. Harmonics mode can implement harmonic analysis. In terms of harmonics analysis, OpenDSS is better than GridLAB-D. OpenDSS software can analyse voltage sag with capabilities of short-circuit calculations. Overvoltage study can also be carried out using this tool. In the case of short circuit calculation, GridLAB-D does not support short circuit contribution of DG sources.

4.5. Reliability analysis

Reliability primarily relates to DN components' failure and repair rates. The results could be used to evaluate the reliability indices of distribution system. The important features of the reliability analysis software are [223]:

(a) full three phase representations with the large-scale interconnection of DG units during various normal and abnormal conditions;

(b) integration of reliability tools with advanced metering systems and information for characterising and forecasting load profiles;

(c) databases of equipment reliability. Due to severe time constraints, most users currently use average or assumed typical values (failure rate, restoration time of system components);

(d) able to calculate distribution reliability measures for sustained and momentary interruptions;

(e) risk assessment approaches;

(f) economics of reliability evaluation;

(g) calculation of voltage sags and sustained interruptions as well as reliability indices such as SAIFI, SAIFI;

(h) considering the uncertainty modelling of DG parameters [224, 225].

In OpenDSS, the application of Monte Carlo method can be implemented for distribution system reliability analysis. The software can carry out risk-based distribution planning studies. The software should include reliability economics assessment methods.

GridLAB-D can assess the reliability of DN. The results include reliability indices and business metrics such as profitability, revenue rates of return and per customer or per line mile cost.

4.6. Object oriented, interfacing and co-simulation

The required tool should have the following co-simulation facilities:

(a) able to model new components and controls to support advanced analyses related to smart grid, grid modernization, increased DG penetration and renewable energy research;

(b) interfacing to other programming tools (e.g., MATLAB, Visual Basic) to facilitate post-processing of the simulation results which offers required plotting and calculation benefits;

(c) option for co-simulation with communication networks.

OpenDSS is an object oriented program and commands can be implemented both as standalone EXE program and component object model (COM) dynamic-link library (DLL) interface. DLLs can be written in most common programming languages such as MATLAB, Python, C++, R and other languages. However, the lack of a visual interface is the limitation of OpenDSS.

GridLAB-D software can be linked with various external programmes such as MATLAB, MySQL, Microsoft Excel and Access, and text-based tools. This is able to convert models from the SynerGEE [226] and the web integrated network for distributed management including logic (WINDMIL) [227] power distribution modelling systems.

5. Conclusions

Integration of distributed generation into the existing distribution networks is one of the widespread techniques for supplying the green energy to the customers. The objective of this paper is to review the required models, impacts, standards and mitigation of negative effects introduced by high DG integrated DN. Based on the literature review, the characteristics of an ideal simulation tool for studying increased DG penetration are listed.

It has been found that increased DG penetration is one of the influential factors for operation, design and modelling of the distribution systems. Some additional components are required to be modelled in this type of networks. The key additional components are DG based machines such as turbines (wind, hydropower), generators, fuel cell and also storage devices. These components are connected to the existing DN which causes various technological challenges.

Potential challenges include voltage regulation, power quality problems, malfunction of protection systems, and islanding. These challenges become more severe in distribution systems where there is high DG penetration, while there are low demand conditions. How to determine the maximum possible percentage of DG penetration is still unclear; it is studied by few researchers and depends on the regulations of each country [228, 229].

The mitigation studies of the above impacts are discussed briefly in this paper. Most of the studies about voltage regulation are PV oriented. The control technologies are developed based on specific network topology and DG installed. Control technologies for the integration of hybrid DG technology are not studied much. It could be a potential research field to expand the current control techniques for operating the hybrid DG integration. Relevant standards and regulatory requirements to ensure the successful operation of the DG integrated distribution systems are also reviewed for all the potential challenges.

The necessary features of an ideal computational tool required in studying increased DG penetration into distribution systems are presented. The main features are load flow analysis, fault analysis, protection coordination, power quality and reliability analysis,

dynamic stability analysis. Also, the computational tool could have the facility to interface with other programming tools. The comparison between two available tools has been studied by their main features and limitations. Most of the available tools have various specific features for particular topology and control techniques. But for an ideal tool, all the required features including modelling of all types of DG into DN should have been implemented in one platform. For reliability analysis, it is suggested that advanced Monte Carlo methods [230] considering the uncertainty parameters of DG could be included to reduce the computational complexity. It is expected that this review will be beneficial to the users, designers, manufacturers, researchers of distribution systems for developing the new computational tool by taking consideration of increased DG penetration.

References

[1] Ackermann T, Andersson G, Söder L. Distributed generation: a definition. Electr Power Syst Res 2001;57(3):195-204.

[2] Bayod-Rújula AA. Future development of the electricity systems with distributed generation. Energy 2009;34(3):377-83.

[3] Haque MM, Wolfs P. A review of high PV penetrations in LV distribution networks: Present status, impacts and mitigation measures. Renew Sustain Energy Rev 2016; 62:1195-1208.

[4] Petinrin J, Shaabanb M. Impact of renewable generation on voltage control in distribution systems. Renew Sustain Energy Rev 2016; 65:770-83.

[5] Marinopoulos AG, Alexiadis MC, Dokopoulos PS. Energy losses in a distribution line with distributed generation based on stochastic power flow. Electr Power Syst Res 2011;81(10):1986-94.

[6] Kersting WH, Phillips WH. Distribution feeder line models. In: Proceedings of 38th annual rural electric power conference;1994. p. A4/1-A4/8.

[7] Willis HL. Power distribution planning reference book: CRC press; 2004.

[8] Mota LTM, Mota AA. Load modeling at electric power distribution substations using dynamic load parameters estimation. Int J Electr Power Energy Syst 2004;26(10):805-11.

[9] Roy N, Hossain M, Pota H. Effects of load modeling in power distribution system with distributed wind generation. In: Proceedings of IEEE 21st Australasian universities power engineering conference (AUPEC); 2011. p. 1-6.

[10] Concordia C, Ihara S. Load representation in power system stability studies. IEEE Trans Power Appar Syst 1982:969-77.

[11] Al-Muhaini M, Heydt GT. Evaluating future power distribution system reliability including distributed generation. IEEE Trans Power Delivery 2013;28(4):2264-72.

[12] IEEE standard for interconnecting distributed resources with electric power systems. IEEE Std. 1547–2003:1-28.

[13] Standard voltages. Australian Std. 60038-2000.

[14] IEC standard voltages int electrotech comm. IEC 60038; 2002–07,6.2.

[15] BS EN 50160: Voltage characteristics of electricity supplied by public distribution systems. British standards institution; 2000.

[16] Sarimuthu CR, Ramachandaramurthy VK, Agileswari K, Mokhlis H. A review on voltage control methods using on-load tap changer transformers for networks with renewable energy sources. Renew Sustain Energy Rev 2016;62:1154-61.

[17] Gao C, Redfern MA. A review of voltage control techniques of networks with distributed generations using On-Load Tap Changer transformers. In: Proceedings of IEEE 45th international universities power engineering conference (UPEC); 2010. p. 1-6.

[18] Y.-H. Song and A. Johns, Flexible ac transmission systems (FACTS): IET, 1999.

[19] Oomori T, Genji T, Yura T, Watanabe T, Takayama S, Fukuyama Y. Development of equipment models for fast distribution three-phase unbalanced load flow calculation. Electr Eng Japan 2003;142(3):8-19.

[20] Sen KK. SSSC-static synchronous series compensator: theory, modeling, and application. Power Delivery, IEEE Transactions on 1998;13(1):241-6.

[21] Ghosh A, Ledwich G. Compensation of distribution system voltage using DVR. IEEE Trans Power Delivery 2002;17(4):1030-6.

[22] Mondal D, Chakrabarti A, Sengupta A. Power system small signal stability analysis and control: Academic press; 2014.

[23] Gyugyi L. Power electronics in electric utilities: static var compensators. In: Proceedings of the IEEE 1988;76(4):483-94.

[24] Rao P, Crow M, Yang Z. STATCOM control for power system voltage control applications. IEEE Trans Power Delivery 2000;15(4):1311-7.

[25] Sen KK, Stacey EJ. UPFC-unified power flow controller: theory, modeling, and applications. IEEE Trans Power Delivery 1998;13(4):1453-60.

[26] Mahmoud MS, AL-Sunni FM. Control and optimization of distributed generation systems. Springer; 2015.

[27] Pilavachi P. Power generation with gas turbine systems and combined heat and power. Appl Therm Eng 2000;20:1421-29.

[28] Saha A, Chowdhury S, Chowdhury S, Crossley P, Gaunt C. Microturbine based distributed generator in smart grid application. In: Proceedings of IET 20th international conference and exhibition on electricity distribution-part 1; 2009. p. 1-6.

[29] Azadani EN, Canizares C, Bhattacharya K. Modeling and stability analysis of distributed generation. In: Proceedings of IEEE power and energy society general meeting; 2012. p. 1-8.

[30] Das V, Padmanaban S, Venkitusamy K, Selvamuthukumaran R, Blaabjerg F, Siano P. Recent advances and challenges of fuel cell based power system architectures and control–A review. Renew Sustain Energy Rev 2017;73:10-18.

[31] Jawahar C, Michael PA. A review on turbines for micro hydro power plant. Renew Sustain Energy Rev 2017;72:882-7.

[32] Divya K, Rao PN. Models for wind turbine generating systems and their application in load flow studies. Electr Power Syst Res 2006;76(9):844-56.

[33] Lopes J, Moreira C, Madureira A. Defining control strategies for microgrids islanded operation. IEEE Trans Power Syst 2006;21(2):916-24.

[34] Moghaddas-Tafreshi S, Mashhour E. Distributed generation modeling for power flow studies and a three-phase unbalanced power flow solution for radial distribution systems considering distributed generation. Electr Power Syst Res 2009;79(4):680-6.

[35] Alam MJ, Muttaqi KM, Sutanto D, Elder L, Baitch A. Performance analysis of distribution networks under high penetration of solar PV. In: Proceedings of 44th international conference on large high voltage electric systems; 2012.

[36] Lopes JP, Hatziargyriou N, Mutale J, Djapic P, Jenkins N. Integrating distributed generation into electric power systems: A review of drivers, challenges and opportunities. Electr Power Syst Res 2007;77(9):1189-203.

[37] Baran M, Hooshyar H, Shen Z, Gajda J, Huq K. Impact of high penetration residential PV systems on distribution systems. In: Proceedings of IEEE power and energy society general meeting; 2011. p. 1-5.

[38] Dugan RC, Price SK. Issues for distributed generation in the US. In: Proceedings of IEEE power engineering society winter meeting; 2002. p. 121-6.

[39] Hoff T, Shugar DS. The value of grid-support photovoltaics in reducing distribution system losses. IEEE Trans Energy Convers 1995;10(3):569-76.

[40] Walling R, Saint R, Dugan RC, Burke J, Kojovic LA. Summary of distributed resources impact on power delivery systems. IEEE Trans Power Delivery 2008;23(3):1636-44.

[41] Liu Y, Bebic J, Kroposki B, De Bedout J, Ren W. Distribution system voltage performance analysis for high-penetration PV. In: Proceedings of IEEE energy 2030 conference; 2008. p. 1-8.

[42] Srisaen N, Sangswang A. Effects of PV grid-connected system location on a distribution system. 2006. In: Proceedings of IEEE Asia Pacific conference on circuits and systems (APCCAS); 2006. p. 852-5.

[43] Turitsyn K, Šulc P, Backhaus S, Chertkov M. Distributed control of reactive power flow in a radial distribution circuit with high photovoltaic penetration. In: Proceedings of IEEE power and energy society general meeting; 2010. p. 1-6.

[44] Enslin JHR. Dynamic reactive power and energy storage for integrating intermittent renewable energy. In: Proceedings of IEEE power and energy society general meeting; 2010. p. 1-4.

[45] Perera BK, Ciufo P, Perera S. Point of common coupling (PCC) voltage control of a grid-connected solar photovoltaic (PV) system. In: Proceedings of 39th annual conference of IEEE industrial electronics society (IECON); 2013. p. 7475-80.

[46] Tonkoski R, Turcotte D, El-Fouly TH. Impact of high PV penetration on voltage profiles in residential neighborhoods. IEEE Trans Sustain Energy 2012;3(3):518-27.

[47] Eltawil MA, Zhao Z. Grid-connected photovoltaic power systems: Technical and potential problems—A review. Renew Sustain Energy Rev 2010;14(1):112-29.

[48] Thomson M, Infield D. Impact of widespread photovoltaics generation on distribution systems. IET Renew Power Gener 2007;1(1):33-40.

[49] Ueda Y, Kurokawa K, Tanabe T, Kitamura K, Sugihara H. Analysis results of output power loss due to the grid voltage rise in grid-connected photovoltaic power generation systems. IEEE Trans Ind Electron 2008;55(7):2744-51.

[50] Widén J, Wäckelgård E, Paatero J, Lund P. Impacts of distributed photovoltaics on network voltages: stochastic simulations of three Swedish low-voltage distribution grids. Electr Power Syst Res 2010;80(12):1562-71.

[51] ANSI C84.1-1995, Electrical power systems and equipment - voltage ratings (60 Hz), American national standards institute, NY 10036, USA.

[52] Lewis S. Analysis and management of the impacts of a high penetration of photovoltaic systems in an electricity distribution network. In: Proceedings of IEEE PES innovative smart grid technologies asia (ISGT); 2011. p. 1-7.

[53] Kobayashi H, Takasaki M. Demonstration study of autonomous demand area power system. In: Proceedings of IEEE PES transmission and distribution conference and exhibition; 2006. p. 548-55. [54] Conti S, Raiti S, Tina G, Vagliasindi U. Study of the impact of PV generation on voltage profile in LV distribution networks. In: Proceedings of IEEE Porto Power Tech; 2001. p. 6.

[55] Hsieh W-L, Lin C-H, Chen C-S, Hsu C, Ku T-T, Tsai C-T, et al. Impact of PV generation to voltage variation and power losses of distribution systems. In: Proceedings of IEEE 4th international conference on electric utility deregulation and restructuring and power technologies (DRPT); 2011. p. 1474-8.

[56] Azzouz MA, Farag HE, El-Saadany EF. Fuzzy-based control of on-load tap changers under high penetration of distributed generators. In: Proceedings of IEEE 3rd international conference on electric power and energy conversion systems (EPECS); 2013. p. 1-6.

[57] Viawan FA, Sannino A, Daalder J. Voltage control with on-load tap changers in medium voltage feeders in presence of distributed generation. Electr Power Syst Res 2007;77(10):1314-22.

[58] Bignucolo F, Caldon R, Prandoni V. Radial MV networks voltage regulation with distribution management system coordinated controller. Electr Power Syst Res 2008;78(4):634-45.

[59] Casavola A, Franzè G, Menniti D, Sorrentino N. Voltage regulation in distribution networks in the presence of distributed generation: A voltage set-point reconfiguration approach. Electr Power Syst Res 2011;81(1):25-34.

[60] Choi J-H, Kim J-C. Advanced voltage regulation method of power distribution systems interconnected with dispersed storage and generation systems. IEEE Trans Power Delivery 2001;16(2):329-34.

[61] Liew S, Strbac G. Maximising penetration of wind generation in existing distribution networks. In: Proceedings of IET generation, transmission and distribution; 2002. p. 256-62.

[62] Viawan F, Karlsson D. Voltage and reactive power control in systems with synchronous machine-based distributed generation. IEEE Trans Power Delivery 2008;23(2):1079-87.

[63] Muttaqi KM, Le AD, Negnevitsky M, Ledwich G. A novel tuning method for advanced line drop compensator and its application to response coordination of distributed generation with voltage regulating devices. IEEE Trans Ind Appl 2016;52:1842-54.

[64] Yap WK, Havas L, Overend E, Karri V. Neural network-based active power curtailment for overvoltage prevention in low voltage feeders. Expert Syst Appl 2014;41(4):1063-70.

[65] Tonkoski R, Lopes LA, El-Fouly TH. Coordinated active power curtailment of grid connected PV inverters for overvoltage prevention. IEEE Trans Sustain Energy 2011;2(2):139-47.

[66] Tonkoski R, Lopes LA. Impact of active power curtailment on overvoltage prevention and energy production of PV inverters connected to low voltage residential feeders. Renew Energy 2011;36(12):3566-74.

[67] Demirok E, Sera D, Teodorescu R, Rodriguez P, Borup U. Evaluation of the voltage support strategies for the low voltage grid connected PV generators. In: Proceedings of IEEE energy conversion congress and exposition (ECCE); 2010. p. 710-7.

[68] Malekpour AR, Niknam T. A probabilistic multi-objective daily Volt/Var control at distribution networks including renewable energy sources. Energy 2011;36(5):3477-88.

[69] Rahman M, Mahmud M, Pota H, Hossain M. Distributed multi-agent scheme for reactive power management with renewable energy. Energy Convers Manag 2014;88:573-81.

[70] Rami G, Tran-Uoc T, Hadjsaid N. Fuzzy logic supervision and control of distributed generators. In: Proceedings of IET 18th international conference and exhibition on electricity distribution (CIRED); 2005. p. 1-5.

[71] Bazrafshan M, Gatsis N. Voltage regulation in electricity distribution networks using the conditional value-at-risk. In: Proceedings of IEEE global conference on signal and information processing (GlobalSIP); 2014. p. 909-13.

[72] Demirok E, Casado González P, Frederiksen KH, Sera D, Rodriguez P, Teodorescu R. Local reactive power control methods for overvoltage prevention of distributed solar inverters in low-voltage grids. IEEE J Photovolt 2011;1(2):174-82.

[73] Demirok E, Sera D, Rodriguez P, Teodorescu R. Enhanced local grid voltage support method for high penetration of distributed generators. In: Proceedings of IEEE 37th annual industrial electronics society conference; 2011. p. 2481-5.

[74] Conti S, Greco A, Messina N, Raiti S. Local voltage regulation in LV distribution networks with PV distributed generation. In: Proceedings of IEEE international symposium on power electronics, electrical drives, automation and motion; 2006. p. 519-24.

[75] Saad-Saoud Z, Lisboa M, Ekanayake J, Jenkins N, Strbac G. Application of STATCOMs to wind farms. IEE Proceedings- Generation, Transmission and Distribution 1998;145(5):511-6.

[76] Rahimi M, Assari H. Addressing and assessing the issues related to connection of the wind turbine generators to the distribution grid. Int J Elec Power 2017;86:138-53.

[77] Varma RK, Khadkikar V, Seethapathy R. Nighttime application of PV solar farm as STATCOM to regulate grid voltage. IEEE Trans Energy Convers 2009;24(4):983-5.

[78] Panosyan A, Walling R, Bärthlein E-M, Witzmann R. Reactive power compensation of self-induced voltage variations. 2012.

[79] Jayasekara N, Wolfs P, Masoum MA. An optimal management strategy for distributed storages in distribution networks with high penetrations of PV. Electr Power Syst Res 2014;116:147-57.

[80] Kashem M, Ledwich G. Energy requirement for distributed energy resources with battery energy storage for voltage support in three-phase distribution lines. Electr Power Syst Res 2007;77(1):10-23. [81] Shi D, Sharma RK. Adaptive control of energy storage for voltage regulation in distribution system. In: Proceedings of IEEE international conference on smart energy grid engineering (SEGE); 2013. p. 1-7.

[82] Sugihara H, Yokoyama K, Saeki O, Tsuji K, Funaki T. Economic and efficient voltage management using customer-owned energy storage systems in a distribution

network with high penetration of photovoltaic systems. IEEE Trans Power Syst 2013;28(1):102-11.

[83] Cappelle J, Vanalme J, Vispoel S, Van Maerhem T, Verhelst B, Debruyne C, et al. Introducing small storage capacity at residential PV installations to prevent overvoltages. In: Proceedings of IEEE international conference on smart grid communications (SmartGridComm); 2011. p. 534-9.

[84] Debruyne C, Vanalme J, Verhelst B, Desmet J, Capelle J, Vandevelde L. Preventing overvoltages in PV grids by integration of small storage capacity. In: Proceedings of IEEE PES international conference and exhibition on innovative smart grid technologies (ISGT Europe); 2011. p. 1-7.

[85] Patsalides M, Georghiou GE, Stavrou A, Efthymiou V. Voltage regulation via photovoltaic (PV) inverters in distribution grids with high PV penetration levels. In: Proceedings of IET 8th Mediterranean conference on power generation, transmission, distribution and energy conversion (MEDPOWER 2012); 2012. p. 1-6.

[86] Bollen M, Sannino A. Voltage control with inverter-based distributed generation. IEEE Trans Power Delivery 2005;20(1):519-20.

[87] Hojo M, Hatano H, Fuwa Y. Voltage rise suppression by reactive power control with cooperating photovoltaic generation systems. In: Proceedings of IET 20th international conference and exhibition on electricity distribution-part 1(CIRED); 2009. p. 1-4.

[88] Ahmed K, Massoud A, Finney S, Williams B. New voltage regulation techniques for low voltage radial feed PWM inverter based distributed networks. In: Proceedings of IEEE international symposium on industrial electronics (ISIE); 2010. p. 2241-6.

[89] Kennedy J, Ciufo P, Agalgaonkar A. Over-voltage mitigation within distribution networks with a high renewable distributed generation penetration. In: Proceedings of IEEE international energy conference; 2014. p. 1107-14.

[90] Cagnano A, De Tuglie E. Centralized voltage control for distribution networks with embedded PV systems. Renew Energy 2015;76:173-85.

[91] Vovos PN, Kiprakis AE, Harrison GP. Centralized and distributed voltage control: Impact on distributed generation penetration. IEEE Trans Power Syst 2007;22(1):476-83.

[92] Xu T, Taylor P. Voltage control techniques for electrical distribution networks including distributed generation. In: Proceedings of the 17th world congress the international federation of automatic control, Seoul; 2008.

[93] Zakariazadeh A, Homaee O, Jadid S, Siano P. A new approach for real time voltage control using demand response in an automated distribution system. Appl Energy 2014;117:157-66.

[94] Chen L, Qi S, Li H. Improved adaptive voltage controller for active distribution network operation with distributed generation. In: Proceedings of IEEE 47th international universities power engineering conference (UPEC); 2012. p. 1-5.

[95] Kayal P, Chanda C. Placement of wind and solar based DGs in distribution system for power loss minimization and voltage stability improvement. Int J Electr Power Energy Syst 2013;53:795-809.

[96] Hird C, Leite H, Jenkins N, Li H. Network voltage controller for distributed generation. IEE Proceedings-Generation, Transmission and Distribution 2004;151(2):150-6.

[97] Fila M, Reid D, Taylor G, Lang P, Irving M. Coordinated voltage control for active network management of distributed generation. In: Proceedings of IEEE power and energy society general meeting; 2009. p. 1-8.

[98] Viawan F, Karlsson D. Coordinated voltage and reactive power control in the presence of distributed generation. In: Proceedings of IEEE power and energy society general meeting-conversion and delivery of electrical energy in the 21st century; 2008. p. 1-6.

[99] Senjyu T, Miyazato Y, Yona A, Urasaki N, Funabashi T. Optimal distribution voltage control and coordination with distributed generation. IEEE Trans Power Delivery 2008;23(2):1236-42.

[100] Kakimoto N, Piao Q-Y, Ito H. Voltage control of photovoltaic generator in combination with series reactor. IEEE Trans Sustain Energy 2011;2(4):374-82.

[101] Vlachopoulos S, Demoulias C. Voltage regulation in low-voltage rural feeders with distributed PV systems. In: Proceedings of IEEE EUROCON international conference on computer as a tool; 2011. p. 1-4.

[102] Liu X, Aichhorn A, Liu L, Li H. Coordinated control of distributed energy storage system with tap changer transformers for voltage rise mitigation under high photovoltaic penetration. IEEE Trans Smart Grid 2012;3(2):897-906.

[103] Ranamuka D, Agalgaonkar AP, Muttaqi KM. Online coordinated voltage control in distribution systems subjected to structural changes and DG availability. IEEE Trans Smart Grid 2016;7:580-91.

[104] Azmy AM, Erlich I. Impact of distributed generation on the stability of electrical power system. In: Proceedings of IEEE power engineering society general meeting; 2005. p. 1056-63.

[105] Pandi VR, Zeineldin H, Xiao W, Zobaa AF. Optimal penetration levels for inverter-based distributed generation considering harmonic limits. Electr Power Syst Res 2013;97:68-75.

[106] Arrillaga J. Power system harmonic analysis: John Wiley & Sons; 1997.

[107] Enslin JH, Heskes PJ. Harmonic interaction between a large number of distributed power inverters and the distribution network. IEEE Trans Power Electron 2004;19(6):1586-93.

[108] Larsson E, Lundmark C, Bollen M. Measurement of current taken by fluorescent lights in the frequency range 2-150 kHz. In: Proceedings of IEEE power engineering society general meeting; 2006. p. 6 pp.

[109] Bollen M, Olofsson M, Larsson A, Ronnberg S, Lundmark M. Standards for supraharmonics (2 to 150 kHz). IEEE Electromagnetic Compatibility Magazine 2014;3(1):114-9.

[110] Farhoodnea M, Mohamed A, Shareef H, Zayandehroodi H. An enhanced method for contribution assessment of utility and customer harmonic distortions in radial and weakly meshed distribution systems. Int J Electr Power Energy Syst 2012;43(1):222-9.

[111] Chattopadhyay S, Mitra M, Sengupta S. Electric power quality: Springer; 2011.

[112] Sidrach-de-Cardona M, Carretero J. Analysis of the current total harmonic distortion for different single-phase inverters for grid-connected pv-systems. Sol. Energ. Mat. Sol. Cells 2005;87(1):529-40.

[113] Benhabib M, Myrzik J, Duarte J. Harmonic effects caused by large scale PV installations in LV network. In: Proceedings of IEEE 9th international conference on electrical power quality and utilisation; 2007. p. 1-6.

[114] IEEE recommended practices and requirements for harmonic control in electrical power systems. IEEE STD 1992:519-1992.

[115] Bhowmik A, Maitra A, Halpin SM, Schatz JE. Determination of allowable penetration levels of distributed generation resources based on harmonic limit considerations. IEEE Trans Power Delivery 2003;18(2):619-24.

[116] Pandi VR, Zeineldin H, Xiao W. Determining optimal location and size of distributed generation resources considering harmonic and protection coordination limits. IEEE Trans Power Syst 2013;28(2):1245-54.

[117] Papaioannou IT, Alexiadis MC, Demoulias CS, Labridis DP, Dokopoulos PS. Modeling and measurement of small Photovoltaic systems and penetration scenarios. In: Proceedings of IEEE Bucharest powertech; 2009. p. 1-7.

[118] Bollen MH, Ribeiro PF, Larsson EA, Lundmark CM. Limits for voltage distortion in the frequency range 2 to 9 kHz. IEEE Trans Power Delivery 2008;23(3):1481-7.

[119] Noone B. PV integration on Australian distribution networks. The Australian PV association, UNSW, Australia 2013.

[120] IEC 61000-4-7: Electromagnetic Compatibility (EMC) Part 4-7: Testing and measurement techniques general guide on harmonics and interharmonics measurements and instrumentation for power supply systems and equipment connected thereto. Technical norm 2002.

[121] Pachanapan P, Dysko A, Anaya-Lara O, Lo KL. Harmonic mitigation in distribution networks with high penetration of converter-connected DG. In: Proceedings of IEEE Trondheim power tech; 2011. p. 1-6.

[122] Qazi SH, Mustafa MW. Review on active filters and its performance with grid connected fixed and variable speed wind turbine generator. Renew Sustain Energy Rev 2016;57:420-38.

[123] Tareen WU, Mekhilef S, Seyedmahmoudian M, Horan B. Active power filter (APF) for mitigation of power quality issues in grid integration of wind and photovoltaic energy conversion system. Renew Sustain Energy Rev 2017;70:635-55.

[124] Hojo M, Ohnishi T. Adjustable harmonic mitigation for grid-connected photovoltaic system utilizing surplus capacity of utility interactive inverter. In: Proceedings of IEEE 37th power electronics specialists conference; 2006. p. 1-6.

[125] Céspedes M, Sun J. Modeling and mitigation of harmonic resonance between wind turbines and the grid. In: Proceedings of IEEE Energy conversion congress and exposition (ECCE); 2011. p. 2109-16.

[126] Carastro F, Sumner M, Zanchetta P. Mitigation of voltage dips and voltage harmonics within a micro-grid, using a single shunt active filter with energy storage. In: Proceedings of IEEE 32nd annual conference on industrial electronics; 2006. p. 2546-51.

[127] Yong B, Ramachandaramurthy V. Double Tuned filter design for harmonic mitigation in grid connected solar PV. In: Proceedings of IEEE international conference on power and energy (PECon); 2014. p. 293-7.

[128] Savaghebi M, Guerrero JM, Jalilian A, Vasquez JC. Mitigation of voltage and current harmonics in grid-connected microgrids. In: Proceedings of IEEE international symposium on industrial electronics (ISIE); 2012. p. 1610-5.

[129] Pogaku N, Green T. Harmonic mitigation throughout a distribution system: a distributed-generator-based solution. IEE Proceedings- Gener, Transm Distrib 2006;153(3):350-8.

[130] Moreno R, Pomilio J, Da Silva LP, Pimentel S. Mitigation of harmonic distortion by power electronic interface connecting distributed generation sources to a weak grid. In: Proceedings of IEEE Brazilian power electronics conference; 2009. p. 41-8.

[131] Kulkarni A, John V. Mitigation of lower order harmonics in a grid-connected single-phase PV inverter. IEEE Trans Power Electron 2013;28(11):5024-37.

[132] Hazrati A, Jalilian A. Grid side power quality enhancement in DFIG based grid connected wind plants. In: Proceedings of IEEE 17th conference on electrical power distribution networks; 2012. p. 1-7.

[133] Liang X, Emerging power quality challenges due to integration of renewable energy sources. IEEE Trans Ind Appl 2016.

[134] Bollen MH, Stockman K, Neumann R, Ethier G, Gordon JR, Van Reussel K, et al. Voltage dip immunity of equipment and installations-messages to stakeholders. In: Proceedings of IEEE15th international conference on harmonics and quality of power (ICHQP); 2012. p. 915-9.

[135] Martinez-Velasco J, Martin-Arnedo J. Distributed generation impact on voltage sags in distribution networks. In: Proceedings of IEEE 9th international conference on electrical power quality and utilisation; 2007. p. 1-6.

[136] Alvarez C, Amarís H, Samuelsson O. Voltage dip mitigation at wind farms. In: Proceedings of IEEE European wind energy conference; 2007.

[137] Eskander MN, Amer SI. Mitigation of voltage dips and swells in grid-connected wind energy conversion systems. IETE J Res 2011;57(6):515-24.

[138] Hossam-Eldin A, Elserougi A. Renewable energy fed inter-line dvr for voltage sag mitigation in distribution grids. 2013.

[139] Renders B, De Gussemé K, Ryckaert WR, Stockman K, Vandevelde L, Bollen MH. Distributed generation for mitigating voltage dips in low-voltage distribution grids. IEEE Trans Power Delivery 2008;23(3):1581-8.

[140] Trindade FC, do Nascimento KV, Vieira JC. Investigation on voltage sags caused by DG anti-islanding protection. IEEE Trans Power Delivery 2013;28(2):972-80.

[141] Jowder F. Design and analysis of dynamic voltage restorer for deep voltage sag and harmonic compensation. IET Gener, Transm Distrib 2009;3(6):547-60.

[142] Biswas S, Goswami SK, Chatterjee A. Optimum distributed generation placement with voltage sag effect minimization. Energy Convers Manag 2012;53(1):163-74.

[143] Kaddah SS, El-Saadawi MM, El-Hassanin DM. Influence of distributed generation on distribution networks during faults. Electr Power Compon Syst 2015; 43(16): 1781-1792.

[144] Ipinnimo O, Chowdhury S, Chowdhury S. Application of grid integrated wind energy conversion systems for mitigation of multiple voltage dips in a power network. In: Proceedings of IEEE 46th international universities power engineering conference (UPEC); 2011. p. 1-6.

[145] Macken KJ, Bollen MH, Belmans RJ. Mitigation of voltage dips through distributed generation systems. In: Proceedings of IEEE 38th annual meeting industry applications conference; 2003. p. 1068-74.

[146] Song-cen W, Kun-Shan Y, Guang-fu T. Mitigation of voltage sags by grid-connected distributed generation system in series and shunt configurations. In: Proceedings of IEEE joint international conference on power system technology and IEEE power India conference; 2008. p. 1-6.

[147] Wasiak I, Mienski R, Pawelek R, Gburczyk P. Application of DSTATCOM compensators for mitigation of power quality disturbances in low voltage grid with distributed generation. In: Proceedings of IEEE 9th international conference on electrical power quality and utilisation; 2007. p. 1-6.

[148] Magueed F, Awad H. Voltage compensation in weak grids using distributed generation with voltage source converter as a front end. In: Proceedings of IEEE international conference on power electronics and drives systems; 2005. p. 234-9.

[149] Cataliotti A, Cocchiara G, Ippolito MG, Morana G. Applications of the fault decoupling device to improve the operation of LV distribution networks. IEEE Trans Power Delivery 2008;23(1):328-37.

[150] Amanifar O, Golshan MEH. Optimal DG allocation and sizing for mitigating voltage sag in distribution systems with respect to economic consideration using Particle Swarm Optimization. In: Proceedings of IEEE 17th conference on electrical power distribution networks (EPDC); 2012. p. 1-8.

[151] Banaei M, Hosseini S, Khajee MD. Mitigation of voltage sag using adaptive neural network with dynamic voltage restorer. In: Proceedings of IEEE 5th international power electronics and motion control conference; 2006. p. 1-5.

[152] Van TL, Nguyen TH, Lee D-C. Flicker mitigation in DFIG wind turbine systems. In: Proceedings of IEEE 14th European conference on power electronics and applications; 2011. p. 1-10.

[153] Zheng T, Makram EB. Wavelet representation of voltage flicker. Electr Power Syst Res 1998;48(2):133-40.

[154] Hernández J, Ortega M, De la Cruz J, Vera D. Guidelines for the technical assessment of harmonic, flicker and unbalance emission limits for PV-distributed generation. Electr Power Syst Res 2011;81(7):1247-57.

[155] El-Samahy I, El-Saadany E. The effect of DG on power quality in a deregulated environment. In: Proceedings of IEEE power engineering society general meeting; 2005. p. 2969-76.

[156] Ding T, Kou Y, Yang Y, Zhang Y, Yan H, Blaabjerg F. Evaluating maximum photovoltaic integration in district distribution systems considering optimal inverter dispatch and cloud shading conditions. IET Renew Power Gener 2016.

[157] Gulachenski E, Kern Jr E, Feero W, Emanuel A. Photovoltaic generation effects on distribution feeders. Electric Power Research Inst., Palo Alto, CA (United States); New England Power Service Co., Westborough, MA (United States); Ascension Technology, Lincoln Center, MA (United States); Electric Research and Management, Inc., State College, PA (United States); Worcester Polytechnic Inst., MA (United States); 1991.

[158] Woyte A, Van Thong V, Belmans R, Nijs J. Voltage fluctuations on distribution level introduced by photovoltaic systems. IEEE Trans Energy Convers 2006;21(1):202-9.

[159] Ari G, Baghzouz Y. Impact of high PV penetration on voltage regulation in electrical distribution systems. In: Proceedings of IEEE international conference on clean electrical power (ICCEP); 2011. p. 744-8.

[160] Tan Y, Kirschen D, Jenkins N. Impact of a Large Penetration of Photovoltaic Generation on the PowerSystem. In: Proceedings of IEEE Barcelona 17th international conference on electricity distribution; 2003. p. 12-5.

[161] Borlase S. Smart grids: infrastructure, technology, and solutions: CRC Press; 2012.

[162] Jewell WT, Unruh TD. Limits on cloud-induced fluctuation in photovoltaic generation. IEEE Trans Energy Convers 1990;5(1):8-14.

[163] Jewell W, Ramakumar R. The effects of moving clouds on electric utilities with dispersed photovoltaic generation. IEEE Trans Energy Convers 1987(4):570-6.

[164] Blooming TM, Carnovale DJ. Application of IEEE Std 519-1992 harmonic limits. In: Proceedings of IEEE annual pulp and paper industry technical conference; 2006. p. 1-9.

[165] Sun J, Czarkowski D, Zabar Z. Voltage flicker mitigation using PWM-based distribution STATCOM. In: Proceedings of IEEE power engineering society summer meeting; 2002. p. 616-21.

[166] Jenner M, Brockhurst FC. Vacuum switched capacitors to reduce induction motor caused voltage flicker on a 12.47 kV rural distribution line. In: Proceedings of IEEE 34th annual rural electric power conference; 1990. p. B5/1-B5/.

[167] Virulkar VB, Aware MV. Voltage Flicker Mitigation Using STATCOM and ESS. In: Proceedings of IEEE joint international conference on power system technology and IEEE power India conference; 2008. p. 1-7.

[168] Naka S, Genji T, Yura T, Takayama S, Hayashi N, Tokuda H, et al. Cooperative control method for voltage control equipment considering interconnection of distributed generators. In: Proceedings of IEEE international conference on electrical engineering (ICEE), Xi'an, China;2001.

[169] Qi Y, Jia H. Research on a new voltage control strategy for photovoltaic grid-connected system. In: Proceedings of IEEE international conference on electrical machines and systems (ICEMS); 2011. p. 1-6.

[170] Wong J, Lim YS, Morris E. Novel fuzzy controlled energy storage for low-voltage distribution networks with photovoltaic systems under highly cloudy conditions. J Energy Eng 2014.

[171] Shivashankar S, Mekhilef S, Mokhlis M, Karimi M, Mitigating methods of power fluctuation of photovoltaic (PV) sources–A review. Renew Sustain Energy Rev 2016;59:1170-84.

[172] Machmoum M, Hatoum A, Bouaouiche T. Flicker mitigation in a doubly fed induction generator wind turbine system. Math Comput Simul 2010;81(2):433-45.

[173] Meegahapola L, Fox B, Flynn D. Flicker mitigation strategy for DFIGs during variable wind conditions. In: Proceedings of IEEE power and energy society general meeting; 2010. p. 1-8.

[174] Sun T. Power quality of grid-connected wind turbines with DFIG and their interaction with the grid: Institute of Energy Tecnology, Aalborg University; 2004.

[175] Sun T, Chen Z, Blaabjerg F. Flicker study on variable speed wind turbines with doubly fed induction generators. IEEE Trans Energy Convers 2005;20(4):896-905.

[176] Zhang Y, Hu W, Chen Z, Cheng M. Mitigation of wind power fluctuation by active current control of variable speed wind turbines. Int J Smart Grid Clean Energy 2013;2(2):252-7.

[177] Ammar M, Joos G. Flicker mitigation planning solutions in distributed wind power: A real-time simulation analysis. In: Proceedings of IEEE international conference on renewable energy research and application (ICRERA); 2014. p. 284-8.

[178] Von Jouanne A, Banerjee B. Assessment of voltage unbalance. IEEE Trans Power Delivery 2001;16(4):782-90.

[179] Shahnia F, Majumder R, Ghosh A, Ledwich G, Zare F. Voltage imbalance analysis in residential low voltage distribution networks with rooftop PVs. Electr Power Syst Res 2011;81(9):1805-14.

[180] Meersman B, Renders B, Degroote L, Vandoorn T, Vandevelde L. Three-phase inverter-connected DG-units and voltage unbalance. Electr Power Syst Res 2011;81(4):899-906.

[181] Hosseini SH, Nazarloo A. Voltage unbalance reduction by distribution static compensator in a case study network. In: Proceedings of IEEE 7th international conference on electrical and electronics engineering (ELECO); 2011. p. I-288-I-92.

[182] Graovac D, Katić V, Rufer A. Power quality problems compensation with universal power quality conditioning system. IEEE Trans Power Delivery 2007;22(2):968-76.

[183] Wong J, Seng Lim Y, Morris E. Distributed energy storage systems with an improved fuzzy controller for mitigating voltage unbalance on low-voltage networks. J Energy Eng 2014:04014058.

[184] Chua KH, Wong J, Lim YS, Taylor P, Morris E, Morris S. Mitigation of voltage unbalance in low voltage distribution network with high level of photovoltaic system. Energy Procedia 2011;12:495-501.

[185] Cziker A, Chindris M, Miron A. Voltage unbalance mitigation using a distributed generator. In: Proceedings of IEEE 11th International conference on optimization of electrical and electronic equipment; 2008. p. 221-6.

[186] Gerdes G, Santjer F. Power quality of wind turbines and their interaction with the grid. American wind energy association, Washington DC (United States); 1995.

[187] A Attya A, Hartkopf T. Control and quantification of kinetic energy released by wind farms during power system frequency drops. IET Renew Power Gener 2013;7(3):210-24.

[188] Yan R, Saha TK, Modi N, Masood N-A, Mosadeghy M. The combined effects of high penetration of wind and PV on power system frequency response. Appl Energy 2015;145:320-30.

[189] Rahmann C, Castillo A. Fast frequency response capability of photovoltaic power plants: The necessity of new grid requirements and definitions. Energies 2014;7(10):6306-22.

[190] International Electrotechnical Commission (IEC) 61727 - Photovoltaic (PV) systems - Characteristics of the utility interface. 2004.

[191] Kumar P, Kothari DP. Recent philosophies of automatic generation control strategies in power systems. IEEE Trans Power Syst 2005;20(1):346-57.

[192] Chang L, Kojabadi HM. Review of interconnection standards for distributed power generation. In: Proceedings of IEEE large engineering systems conference on power engineering (LESCOPE); 2002. p. 36-40.

[193] Pandey SK, Mohanty SR, Kishor N. A literature survey on load–frequency control for conventional and distribution generation power systems. Renew Sustain Energy Rev 2013; 25:318-34.

[194] Liu X, Zhang Y, Lee KY. Coordinated Distributed MPC for Load Frequency Control of Power System with Wind Farms. IEEE Trans Ind Electr 2016.

[195] Shayeghi H, Shayanfar H, Jalili A. Load frequency control strategies: A state-of-the-art survey for the researcher. Energy Convers Manag 2009;50(2):344-53.

[196] Conti S. Analysis of distribution network protection issues in presence of dispersed generation. Electr Power Syst Res 2009;79(1):49-56.

[197] Girgis A, Brahma S. Effect of distributed generation on protective device coordination in distribution system. In: Proceedings of IEEE large engineering systems conference on power engineering; 2001. p. 115-9.

[198] Boljevic S, Conlon MF. The contribution to distribution network short-circuit current level from the connection of distributed generation. In: Proceedings of IEEE 3rd international universities power engineering conference; 2008. p. 1-6.

[199] Boutsika TN, Papathanassiou SA. Short-circuit calculations in networks with distributed generation. Electr Power Syst Res 2008;78(7):1181-91.

[200] Tan S, Salman S. Investigation into the implementation of auto reclosing scheme in distribution networks with high penetration of DGs. In: Proceedings of IEEE 43rd international universities power engineering conference; 2008. p. 1-5.

[201] Bründlinger R, Bletterie B. Unintentional islanding in distribution grids with a high penetration of inverter-based DG: Probability for islanding and protection methods. In: Proceedings of IEEE Russia power tech; 2005. p. 1-7.

[202] Menon V, Nehrir MH. A hybrid islanding detection technique using voltage unbalance and frequency set point. IEEE Trans Power Syst 2007;22(1):442-8.

[203] Khamis A, Shareef H, Bizkevelci E, Khatib T. A review of islanding detection techniques for renewable distributed generation systems. Renew Sustain Energy Rev 2013;28:483-93.

[204] Chowdhury S, Chowdhury S, Crossley P. Islanding protection of active distribution networks with renewable distributed generators: A comprehensive survey. Electr Power Syst Res 2009;79(6):984-92.

[205] Zayandehroodi H, Mohamed A, Shareef H, Mohammadjafari M. A Comprehensive review of protection coordination methods in power distribution systems in the presence of DG. Electr Rev 2011(8):142-8.

[206] Kennedy J, Ciufo P, Agalgaonkar A. A review of protection systems for distribution networks embedded with renewable generation. Renew Sustain Energy Rev 2016;58:1308-17.

[207] Dugan RC. Reference guide: the open distribution system simulator (opendss). Electric Power Research Institute, Inc 2012.

[208] Tang Y, Mao X, Ayyanar R. Distribution system modeling using CYMDIST for study of high penetration of distributed solar photovoltaics. In: Proceedings of IEEE North American power symposium (NAPS); 2012. p. 1-6.

[209] Siemens A, PTI E. PSS® SINCAL Version 6.0. November; 2009.

[210] Manual DPF, PowerFactory D. Version 14.0. DIgSILENT GmbH, Gomaringen, Germany 2009.

[211] Chassin D, Schneider K, Gerkensmeyer C. GridLAB-D: An open-source power systems modeling and simulation environment. In: Proceedings of IEEE/PES transmission and distribution conference and exposition;2008.

[212] Milano F, Vanfretti L, Morataya JC. An open source power system virtual laboratory: The PSAT case and experience. IEEE Trans Edu 2008;51(1):17-23.

[213] Consortium D. 4DIAC–Framework for Distributed Industrial Automation and Control, Open Source Initiative. access date October 2007.

[214] Moffet M-A, Sirois F, Beauvais D. Review of open-source code power grid simulation tools for long-term parametic simulation. CanmetENERGY, TR–2011-137 (RP-TEC) 411-MODSIM 2011. [215] Ortmeyer T, Dugan R, Crudele D, Key T, Barker P. Renewable systems interconnection study: utility models, analysis, and simulation tools. Sandia NM: Sandia National Laboratory Report: SAND2008-0945 P, February 2008.

[216] Martinez J, De León F, Mehrizi-Sani A, Nehrir M, Wang C, Dinavahi V. Tools for analysis and design of distributed resources—Part II: Tools for planning, analysis and design of distribution networks with distributed resources. IEEE Trans Power Delivery 2011;26(3):1653-62.

[217] Gevorgian V, Singh M, Muljadi E. Symmetrical and unsymmetrical fault currents of a wind power plant. In: Proceedings of IEEE power and energy society general meeting; 2012. p. 1-8.

[218] Smeets R, Van der Sluis L, Kapetanovic M, Peelo DF, Janssen A. Switching in Electrical Transmission and Distribution Systems: John Wiley & Sons; 2014.

[219] Melhorn CJ, McGranaghan MF. Interpretation and analysis of power quality measurements. IEEE Trans Ind Appl 1995;31(6):1363-70.

[220] Dugan RC, McGranaghan MF, Beaty HW. Electrical power systems quality. New York, NY: McGraw-Hill, 1996.

[221] Beaulieu G, Bollen MH, Malgarotti S, Ball R. Power quality indices and objectives. Ongoing activities in CIGRE WG 36-07. In: Proceedings of IEEE power engineering society summer meeting; 2002. p. 789-94.

[222] Shin Y-J, Powers EJ, Grady M, Arapostathis A. Power quality indices for transient disturbances. IEEE Trans Power Delivery 2006;21(1):253-61.

[223] EPRI. Guideline for reliability assessment and reliability planning—evaluation of tools for reliability planning. 2006.

[224] Zubo RH, Mokryani G, Rajamani HS, Aghaei J, Niknam T, Pillai P. Operation and planning of distribution networks with integration of renewable distributed generators considering uncertainties: A review. Renew Sustain Energy Rev 2016.

[225] Balamurugan M, Sahoo SK, Sukchai S. Application of soft computing methods for grid connected PV system: A technological and status review. Renew Sustain Energy Rev 2016.

[226] SynerGEE Electric, information available: http://www.gl-group.com.

[227] WindMil, information available: http://www.milsoft.com.

[228] Obi M, Bass R. Trends and challenges of grid-connected photovoltaic systems–A review. Renew Sustain Energy Rev 2016;58:1082-94.

[229] Cabrera-Tobar A, Bullich-Massagué E, Aragüés-Peñalba M, Gomis-Bellmunt O. Review of advanced grid requirements for the integration of large scale photovoltaic power plants in the transmission system. Renew Sustain Energy Rev 2016;62:971-87.

[230] González-Fernández RA, da Silva AML. Reliability assessment of time-dependent systems via sequential cross-entropy Monte Carlo simulation. IEEE Trans power syst 2011;26:2381-2389.

Chapter 9

Conclusions and Future Work

In this dissertation, we presented a set of applications of an efficient method for electric distribution systems reliability evaluation. Quantitative reliability evaluation of distribution system plays an important role towards the decision-making process in planning and designing for future expansion of network or reinforcement. Use of standard Monte Carlo (MC) method for obtaining accurate estimate of the reliability can be computationally expensive particularly when dealing with the rare events (i.e. when high accuracy is required). A new efficient method based on Multilevel Monte Carlo (MLMC) method is therefore developed which saves huge computation time. The presented applications of the proposed method incorporate varying degrees uncertainty, reliability data and distribution system models to evaluate the reliability indices of the overall distribution system and their load points. We showed how the MLMC method can be implemented to improve the computational efficiency of the MC method when applied to reliability evaluation. The saving in calculation time using MLMC method is due to the fact that a lot of samples are simulated on the computationally cheaper coarse discretisation grids and a few on the computationally expensive fine grids. The calculations of reliability indices are performed on a geometric sequence of grids. Therefore, the less accurate approximation on the coarsest grid is sequentially corrected by the estimators on the following finer grids. Thus, the finest grid accuracy is achieved by the proposed MLMC method.

In summary, a number of reliability studies of distribution system have been carried out in this thesis including customer interruption frequency and duration based reliability assessment, reliability cost/benefits estimation, reliability evaluation incorporating different time-varying factors such as weather-dependent failure rate and restoration time of components, time-varying load and cost models of load points. The output results show that the proposed method can save huge computation time by maintaining acceptable accuracy level when compared to MC method. There is also a substantial effect of different parameters on the convergence rate of the proposed method.

9.1. Summary

Chapter 2 presents the application of the proposed technique for reliability evaluation of a small radial distribution system. Two basic random variables time-to-failure and time-to-repair of each component are modelled using stochastic differential equations following exponential probability distributions. Milstein discretisation scheme is proposed to solve the differential equation. The impacts of three different system configurations on three system performance indices (SAIFI, SAIDI and CAIDI) evaluation are discussed in this

chapter. Comparisons between the proposed approach and analytical method demonstrated the practicability of the MLMC method. It is found that the proposed method can reduce computational effort up to 97.95% compared to MC method by maintaining adequate accuracy level.

In **Chapter 3,** the performance comparisons of the convergence characteristics of MLMC methods based on two discretisation schemes, i.e. Euler-Maruyama and Milstein methods are investigated. The Roy Billinton Test Systems connected to RBTS-buses 3, 5 and 6 are used as benchmark distribution systems. It can be concluded that both MLMC approaches based on discretisation schemes reduce the computation time and speed up the reliability evaluation process compared to MC method. Reasonably accurate reliability indices are found using these methods. Reliability assessment based on Euler-Maruyama method requires more simulation time than Milstein method based computation. Therefore, in most of the cases, there is more time-saving in Milstein based MLMC method compared to the Euler-Maruyama based method.

In **Chapter 4,** a computation framework based on MLMC approach is presented to show how the distribution networks topologies and components availability choices influence the distribution system, feeder and customer sectors reliability. The RBTS B4 distribution system was used as a test system. Using the modification of this system, six different case studies were considered to compare the impact of components availability choices on reliability evaluation. Additionally, sensitivity analyses are performed to show the impact of variation of the predefined reliability data and the MLMC parameters on computational performance. Components availability has a great impact on system reliability. Higher availability reduces the interruptions. The results show that the addition of disconnecting switches, fuses and alternative supply source significantly improves the reliability of a system.

In **Chapter 5**, a general framework based on a novel Multilevel Monte Carlo (MLMC) method is proposed for estimating distribution systems average Expected Energy Not Supplied (EENS) index considering Time-Varying Load Models. The proposed method coupled with the Euler-Maruyama discretisation scheme can effectively estimate the EENS with acceptable accuracy and huge computational time saving compared to the standard Monte Carlo simulation. The effect of different parameters and criteria is also investigated to show the computation performance variation of the MLMC method. The effect of failure starting time, weekly, daily and hourly diversity factors show a considerable impact on the

estimation. The effect of distribution systems reinforcement shows that unavailability of disconnecting switches, fuses and alternative supply sources in the systems can increase the amount of EENS and it has a huge impact on computation effort. Similarly, smaller target accuracy level can increase the estimation time. The discretisation scheme has also impact on computational performance and Milstein method can converge faster than Euler-Maruyama method for the EENS estimation.

In **Chapter 6,** the application of MLMC method on estimating the system expected interruption cost is presented. Comparisons of results obtained using the basic MC simulation are presented. The results show that the proposed method could estimate the average customer interruption cost accurately and also gives a significant speed-up over the MC based computation. A number of sensitivity analyses have been carried out to show the effect of different parameters on the computation process. We found that network configuration and load type, time-varying load and cost models, network reinforcement, transformer and line failure rate, drift and volatility values parameters have a considerable effect of MLMC based system ECOST computation.

In **Chapter 7,** the reliability evaluation of distribution systems incorporating high wind speed and lightning effects is presented based on the proposed method. For modelling time-varying failure rate, weather dependent factors such as high wind speed and lightning are considered in reliability estimation. In order to find the impacts of weather conditions on reliability evaluation, time-varying failure rate and repair time are used that accounts the increased failure rate and repair time for overhead lines in such weather conditions. Four system performance indices have been computed using the proposed technique. The effect of normal weather condition in several cases is studied to show the effect of adverse weather condition. The results indicate that the MLMC simulation method provides a realistic assessment under different weather conditions when compared to the usual MC simulation approach. Lightning effect increases both the reliability indices values and computation time extremely while compared to the wind effect.

For reliability modelling and improvement of distributed generation (DG) integrated distribution network, several factors need to be considered in computational tool design. **Chapter 8** is provided to review the required models, impacts, standards and mitigation of negative effects introduced by high DG integrated DN. The characteristics of an ideal simulation tool for studying increased DG penetration are listed. Potential challenges include voltage regulation, power quality problems, malfunction of protection systems, and

islanding. The mitigation studies of the above impacts are discussed briefly in this chapter. Relevant standards and regulatory requirements to ensure the successful operation of the DG integrated distribution systems are also reviewed for all the potential challenges. The necessary features of an ideal computational tool required in studying increased DG penetration into distribution systems are presented. The main features are load flow analysis, fault analysis, protection coordination, power quality and reliability analysis, dynamic stability analysis. Also, the computational tool could have the facility to interface with other programming tools. For reliability analysis, it is suggested that advanced Monte Carlo methods considering the uncertainty parameters of DG could be included to reduce the computational complexity.

9.2. Future work

Further studies of the proposed method - In this thesis, we have conducted some basic studies on distribution system reliability evaluation using MLMC method and achieved acceptable outcomes. In the proposed project, we have three new objectives by using MLMC method-

a) To carry out the research in hybrid DG systems integrated into distribution networks

b) To determine the probability distributions in MLMC based estimation using Maximum Entropy method

c) To compared the results with other advanced MCS methods such as combination of MLMC and Importance Sampling, Subset Simulation, Quasi Monte Carlo method, etc.

Hybrid DG systems effects on reliability - In order to find the hybrid DG systems effects on reliability, it is important to study feasibility of different hybrid systems in reliability improvement. In the future project, we will study different hybrid DG systems combinations consisting of four different DG sources such as solar, wind, micro-hydro and storage. A comparison of the hybrid systems contribution in reliability improvement will be conducted to find the best combination of hybrid DG integrated distribution system.

Uncertainties modeling in reliability evaluation - In order to evaluate the accurate distribution systems reliability evaluation, it is important to consider all the uncertainties related to DG and basic reliability statistics in one platform. In literature review, it can be seen that very few uncertainties of DG and reliability data have been considered in reliability evaluation. In the proposed study, the target is to carry out research considering

all the uncertainties of hybrid DG integrated distribution system and find out the importance of each uncertainty.

Find differences between grid connected and islanded mode - For electrification in remote areas, it is important to develop hybrid DG systems in islanded mode. Therefore, in the proposed project, we will also study the reliability effects of DG systems in islanded mode and find the difference between grid-connected and islanded mode.